Final Technical Report

Air Force Laboratory Fellowship for Thomas R. Giallorenzi

Submitted to:

Warren D. Peele, Program Director
Southeastern Center for Electrical Engineering Education
Management Office, Central Florida Facility
11th & Massachusetts Avenue
St. Cloud, FL 34769

Submitted by:

Stephen G. Wilson
Professor of Electrical Engineering and Fellowship Supervisor

SEAS Report No. UVA/538341/EE94/102
March 1994

DEPARTMENT OF ELECTRICAL ENGINEERING

SCHOOL OF
ENGINEERING
& APPLIED SCIENCE

University of Virginia
Thornton Hall
Charlottesville, VA 22903

UNIVERSITY OF VIRGINIA
School of Engineering and Applied Science

The University of Virginia's School of Engineering and Applied Science has an undergraduate enrollment of approximately 1,500 students with a graduate enrollment of approximately 600. There are 160 faculty members, a majority of whom conduct research in addition to teaching.

Research is a vital part of the educational program and interests parallel academic specialties. These range from the classical engineering disciplines of Chemical, Civil, Electrical, and Mechanical and Aerospace to newer, more specialized fields of Applied Mechanics, Biomedical Engineering, Systems Engineering, Materials Science, Nuclear Engineering and Engineering Physics, Applied Mathematics and Computer Science. Within these disciplines there are well equipped laboratories for conducting highly specialized research. All departments offer the doctorate; Biomedical and Materials Science grant only graduate degrees. In addition, courses in the humanities are offered within the School.

The University of Virginia (which includes approximately 2,000 faculty and a total of full-time student enrollment of about 17,000), also offers professional degrees under the schools of Architecture, Law, Medicine, Nursing, Commerce, Business Administration, and Education. In addition, the College of Arts and Sciences houses departments of Mathematics, Physics, Chemistry and others relevant to the engineering research program. The School of Engineering and Applied Science is an integral part of this University community which provides opportunities for interdisciplinary work in pursuit of the basic goals of education, research, and public service.

REPORT DOCUMENTATION PAGE

AFRL-SR-BL-TR-98-
0739

athering
ction of
ay, Suite

1. AGENCY USE ONLY (Leave Blank)	2. REPORT DATE	3. REPORT TYPE AND DATES COVERED
	March, 1994	Final

4. TITLE AND SUBTITLE
Multiuser Receivers for Coded CDMA Systems

5. FUNDING NUMBERS

6. AUTHORS
Thomas R. Giallorenzi

7. PERFORMING ORGANIZATION NAME(S) AND ADDRESS(ES)
University of Virginia

8. PERFORMING ORGANIZATION REPORT NUMBER

9. SPONSORING/MONITORING AGENCY NAME(S) AND ADDRESS(ES)
AFOSR/NI
4040 Fairfax Dr, Suite 500
Arlington, VA 22203-1613

10. SPONSORING/MONITORING AGENCY REPORT NUMBER

11. SUPPLEMENTARY NOTES

12a. DISTRIBUTION AVAILABILITY STATEMENT
Approved for Public Release

12b. DISTRIBUTION CODE

13. ABSTRACT *(Maximum 200 words)*
See attachment

14. SUBJECT TERMS

15. NUMBER OF PAGES

16. PRICE CODE

17. SECURITY CLASSIFICATION OF REPORT	18. SECURITY CLASSIFICATION OF THIS PAGE	19. SECURITY CLASSIFICATION OF ABSTRACT	20. LIMITATION OF ABSTRACT
Unclassified	Unclassified	Unclassified	UL

Final Technical Report

Air Force Laboratory Fellowship for Thomas R. Giallorenzi

Submitted to:

Warren D. Peele, Program Director
Southeastern Center for Electrical Engineering Education
Management Office, Central Florida Facility
11th & Massachusetts Avenue
St. Cloud, FL 34769

Submitted by:

Stephen G. Wilson
Professor of Electrical Engineering and Fellowship Supervisor

Department of Electrical Engineering
UNIVERSITY OF VIRGINIA
SCHOOL OF ENGINEERING AND APPLIED SCIENCE
THORNTON HALL
CHARLOTTESVILLE, VA 22903-2442

Report No. UVA/538341/EE94/102
March 1994

Copy No._____

Multiuser Receivers for Coded CDMA Systems

A Dissertation
Presented to
the Faculty of the School of Engineering and Applied Science
University of Virginia

In Partial Fulfillment
of the requirements for the Degree
Doctor of Philosophy

by

Thomas R. Giallorenzi

May 1994

Approval Sheet

This dissertation is submitted in partial fulfillment of the

requirements for the degree of

Doctor of Philosophy

Author

This thesis has been read and approved by the examining committee:

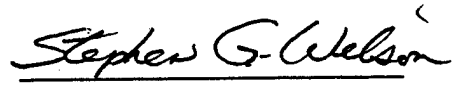

Dissertation Advisor

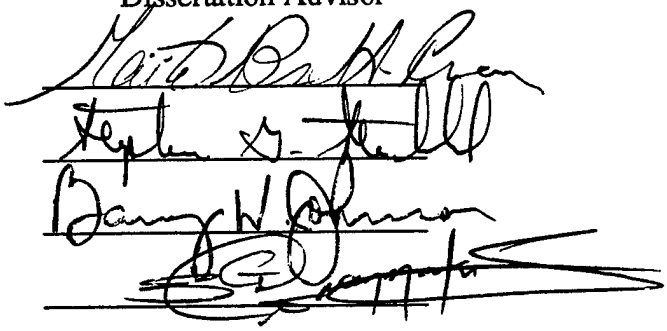

Accepted for the School of Engineering and Applied Science:

Dean, School of Engineering
and Applied Science

May, 1994

Abstract

In this dissertation, the asynchronous direct-sequence code division multiple access (CDMA) communication system is described and a number of multiuser detection approaches are proposed that improve upon the performance of the conventional basestation. Both coded and uncoded systems are studied for nondispersive, additive white Gaussian noise (AWGN) channels.

For the uncoded system case, the multiuser detection techniques that have already been proposed are first reviewed. Then, two decision feedback equalizers (DFE's) that have been proposed are combined to form a new hybrid DFE which outperforms the others in situations where the multiuser interference in the system is high.

Next, the case where each user in the system employs a convolutional code to improve its performance is studied. First, the optimal multiuser sequence estimator is formulated, and it is shown that this receiver may be implemented using a Viterbi algorithm which operates on a time-varying trellis with a number of states which is exponential in the product of the number of users in the system and the constraint length of the codes used (for the rate-1/2 code case). Because this optimal receiver has a very high complexity, a variety of suboptimum receivers are proposed which have a performance level near that of the optimal receiver's but have a more manageable complexity. All of the approaches are compared on the basis of their performance (through analysis and simulation), their complexity and their decoding delay.

Acknowledgements

It is not possible for me to thank every person who has helped me throughout the past three years of work that has led to this document. There are a few people whom I feel a need to express a special thanks to, however. First of all, I'd like to thank Professor Peele and everyone at SCEEE, as well as everyone at UVA, especially Gloria Reed and Clara Fortune, who handled the details of my fellowship over the years. I'd like to thank my fellowship mentor, John Patti, for all of his guidance over the past three years. Furthermore, I'd like to thank my doctoral committee members for all of their interest in the work that I have been doing. Thanks to Dr. Georgios Giannakis and Dr. Barry Johnson who have served as members of both my master's and doctoral committees. Thanks also to Dr. Steve Strickland, Dr. Steve Heppe and Dr. Maite Brandt-Pearce who all joined the committee more recently and have shown a great deal of interest in my work. I particularly appreciate the effort that Dr. Steve Heppe has put in over the past year in making many suggestions that have significantly strengthened what I have done. I also appreciate the many great discussions that I have had with Dr. Maite Brandt-Pearce and Karen Halford in the past few months. I'd also especially like to thank my office mate, David Matolak. Dave and I worked closely together to study for our comprehensive exams and to provide advice on research for each other throughout the past three years. Thanks very much, Dave!

Most of all, I'd like to thank Dr. Steve Wilson for all of the effort that he has poured into my education over the years. I did my senior thesis, masters thesis and finally my Ph.D. dissertation under his guidance for the simple reason that he is the finest educator that I have ever come across. His patience, perseverance, honesty and incredible ability to make complicated things seem simple all have been a real inspiration to me over the years. I will always appreciate everything that he has done for me.

I would also like to thank a few people who have made my personal life wonderful throughout graduate school. Angela Day has been a real source of strength and happiness for me throughout these past few years. She has been incredibly patient, understanding and supportive in my difficult times and a wonderful companion and friend in my good times. Thanks for everything Angie! I'd like to thank my family for all of their support, particularly my grandparents and my sister, Kathy. Finally, I'd like to thank my parents. I could not have been blessed with two more wonderful parents.

Table of Contents

Chapter 1: Introduction 1

Chapter 2: General Multiuser Detection 12

2.1: Possible Receiver Structures for the Uncoded Case 21

2.2: Possible Receiver Structures for the Coded Case 28

Chapter 3: A New Nonlinear Decision Feedback Equalizer 30

3.1: The Hybrid DFE 35

3.2: Simulation Results 37

3.3: Extensions 45

Chapter 4: The Multiuser ML Sequence Estimator for Convolutionally Coded CDMA Links 48

4.1: Optimum Sequence Estimator for Rate-1/2 Convolutional Codes 48

4.2: Performance of the Optimal Sequence Estimator 55

4.3: Simulation Results 67

Chapter 5: Suboptimum Multiuser Receivers for Convolutionally Coded CDMA Links 72

5.1: Hard-Decision Partitioned Approaches 74

5.2: Soft-Decision Partitioned Approaches 84

5.3: Combined Equalization and Decoding Approaches 101

5.4: Comparison of the Suboptimum Approaches 111

Chapter 6: Conclusions 115

6.1: Summary of Results 115

6.2: Future Research Possibilities 118

References 120

Chapter 1 Introduction

Multiple access communication systems are systems in which several (or many) users share a common communication channel of some kind. Generally, in these types of systems there are many more potential users than there are channel resources to accommodate them all at the same time. As a result, it is not possible to dedicate a fraction of the channel resource to every potential user. Fortunately, the users of this kind of system usually need to transmit bursty information messages. As a result, channel resources may be allocated to only those users which are active.

There are a number of methods that have been proposed over the years to allow the active users to share the channel resources, or available bandwidth. Some of these methods require that the users tightly coordinate their transmissions with each other in some fashion, while other methods require much less coordination. All may be interpreted as ways of having the active users coexist in the frequency and time space of the channel with an acceptable level of mutual interference. [68]

The least coordinated method of achieving multiple access communications is to have any user that needs to transmit do so using the entire channel while monitoring whether there was a message collision with any other user. This technique is often referred to as carrier sense multiple access with collision detection (CSMA/CD). If the transmitting user senses a collision, it will adhere to the rules of a well defined protocol to resolve the collision. This multiple access method requires no central controller to dictate when the users must transmit. With this method, if there are a significant number of active users, then there are many collisions and a great deal of the channel resources is wasted in resolving the collisions. This is a price paid for the lack of centralized control. CSMA/CD is most appropriate for systems which cannot tolerate any interference and throughput can be sacrificed for performance. CSMA/CD has traditionally found widespread application in computer networks which are bursty, are not overly congested,

and require that there are very few bit errors. For more congested systems which can tolerate higher error rates, such as a cellular telephone system in a city, CSMA/CD is not appropriate. Figure 1.1 illustrates a cellular communication system with basestations at the center of each cell and a number of mobile active users in the cell.

A more coordinated method of achieving multiple access is to have a central controller dictate which fraction of the time a particular active user may use. In this method, called time division multiple access (TDMA), each active user transmits its message during its assigned time slot in a round-robin fashion, thus the active users transmit at different times on the same frequency. When an active user finishes its message, it notifies the central controller and its time slot is reallocated to another active user.

A similar method is called frequency division multiple access (FDMA). In this method, the central controller dynamically allocates frequency slots to each of the active users. Thus, in FDMA, the active users transmit at the same time on different frequencies. When an active user completes its transmission, it notifies the central controller and its frequency slot is given away to another active user. One advantage of FDMA over TDMA is that the users do not need to be synchronized with each other in time. Both TDMA and FDMA can achieve a higher capacity than CSMA/CD, however, the prices paid for this capacity increase some interference between the active users which share the channel, the need for a central controller and the added delay associated with the process of requesting the channel resources from the central controller.

A fourth method for achieving multiple access is called **code division multiple access (CDMA).** In CDMA systems, the active users transmit at the same time on the same frequency and the way in which the users can be distinguished or addressed is through the use of a code which is impressed on each user's signal. In some CDMA systems, a central controller will allocate the codes to each user. In other CDMA systems, each user will be assigned a permanent code sequence and there will be no need for a central controller. This may be appropriate in a multipoint-to-multipoint system with a

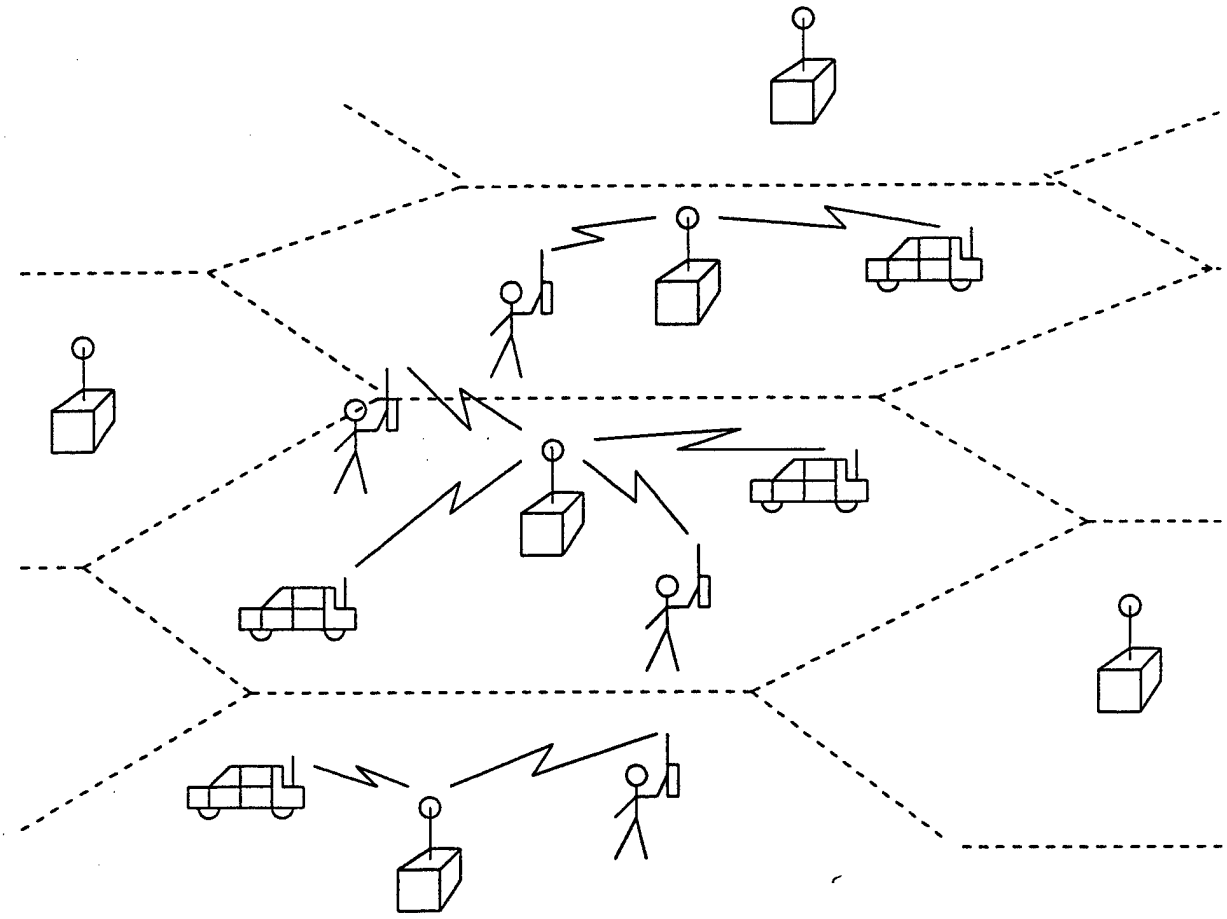

Figure 1.1 Illustration of a cellular communication system. Each basestation communicates with the users in its cell.

modest number of users. In this dissertation, we will primarily concern ourselves with cellular-type systems where the basestation of each cell acts as a central controller for its cell.

Because the active users transmit at the same time on the same frequency in CDMA, they are, in a sense, continuously colliding with each other. The key difference between the collisions of CDMA and CSMA/CD is that the codes which are impressed on the CDMA signals minimize the effect of the collisions, while in CSMA/CD the collisions are not tolerated at all. The higher that the quality of the codes is, the lower the mutual interference between the active users will be in a CDMA system.

A heated debate has erupted in the cellular communications industry over the past few years over the relative capacities of CDMA, TDMA and FDMA. Proponents of each method tend to distort the capacity calculations in favor of their favorite method. In this dissertation, we will not consider a comparison of the relative capacities, but will instead focus on CDMA and study methods of detection which ultimately lead to a large capacity increase for CDMA over the traditional methods of CDMA detection.

Two undisputed advantages of CDMA over TDMA and FDMA are its soft performance degradation with the number of users, and its lack of a need for any kind of time or frequency coordination between the active users. As the number of active users increases in a CDMA network, the interference for each of the active users increases. This results in a slow degradation of the performance of every user as the congestion in the network increases. In contrast, once all of the time or frequency slots are accounted for in TDMA or FDMA, the network is full. If slots are empty in TDMA or FDMA, then some of the channel resources are going to waste. Additionally, CDMA does not require that the active users coordinate their transmissions in time or frequency as in TDMA or FDMA. These uncoordinated CDMA networks are called asynchronous networks. Some other important advantages of CDMA over FDMA and TDMA are its robustness to narrowband fading and jammers, its ability to operate in the background noise of frequency

bands that are occupied by narrowband users and its inherent privacy.

The most common form of CDMA in commercial applications is direct sequence CDMA. In this form of CDMA, each active user is assigned a different code sequence, or *signature sequence*, and this high-rate sequence modulates the data for that user before it is transmitted. Because the signature sequence is a higher rate sequence than the data sequence, the effect of this modulation of the two signals is to spread the spectrum of the transmitted waveform to a bandwidth related to the signature sequence rate. Thus, the direct sequence modulation method is a form of *spread spectrum* communications.

The receiver operating in this environment receives a signal which is the sum of all of the active user's transmitted signals plus noise, and the receiver's job is to reliably decode the signal of interest from this received composite signal. The users are not synchronized in general, and in addition, the received signal strengths of each user are typically unequal. In an attempt to improve the performance of each link, error control coding may be used on each of the links as well. The receiver structures that will be studied in this dissertation are most appropriate for a basestation in a cellular telephone cell or personal communication network (PCN) cell. It is also possible, however, that the receiver architectures that will be discussed could be one of the user's receivers in a decentralized multiple access network.

The traditional method of coherently demodulating direct sequence CDMA signals is to synchronize a local code generator and oscillator to the signal of interest and then to make decisions on the received signal as though the desired signal is the only one present. The received signal usually consists of the desired signal, a multiuser interference (MUI) signal, thermal/shot noise, and may be further degraded by channel time-dispersion. The traditional decoder's structure is that of a correlator or matched filter which is matched to the desired signal followed by a decoder if coding is used on the link. Figure 1.2 illustrates this conventional receiver or basestation. (The notation used in this figure will be defined in Chapter 2.)

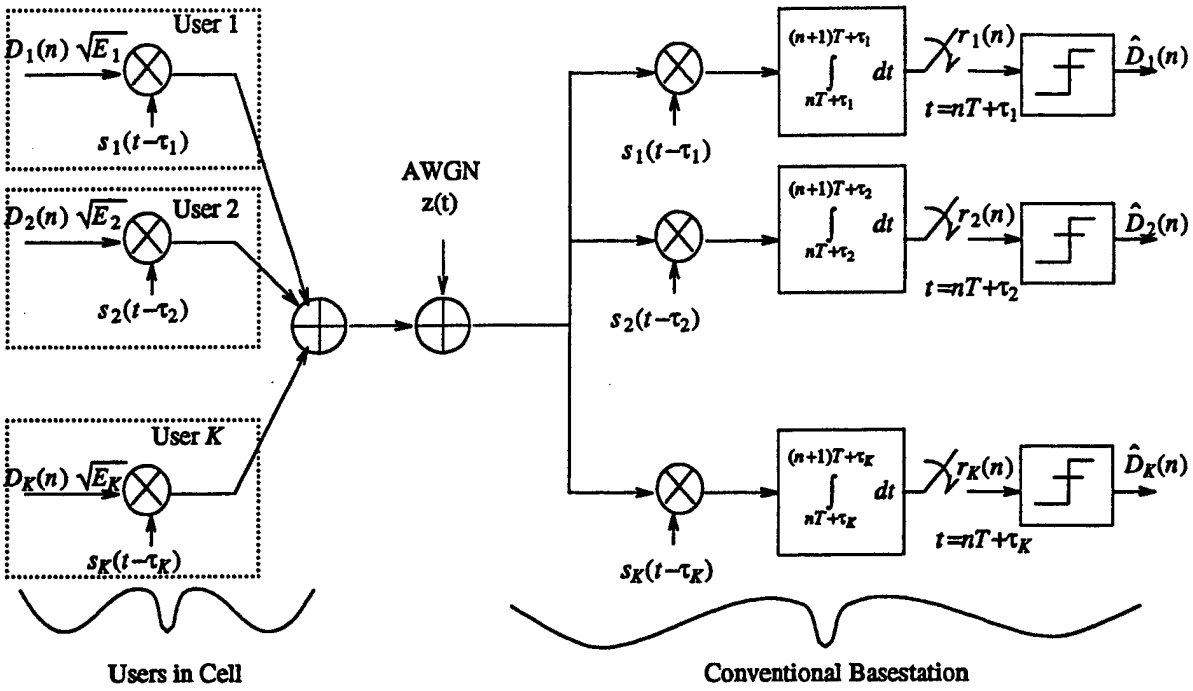

Figure 1.2 K-user asynchronous network with a conventional basestation that decodes each user independently.

The performance of the traditional decoder suffers for two major reasons. First, the signature sequences of the different users will usually not be orthogonal to each other, giving rise to the MUI, and second, in the common situation where all of the signals arriving at the receiver are of different strengths, the strong signals tend to overwhelm the weak signals, even with reasonably good signature sequences. This second problem is referred to as the *near–far* problem.

There are two traditional methods for improving the performance of the conventional receiver. The first is to find an improved set of signature sequences which have as high a degree of orthogonality as possible. The effectiveness of this approach is limited by the Welch inner product bound, which defines the lowest achievable maximum crosscorrelation between asynchronous signature sequences of a given length. The set of binary Kasami sequences achieves the Welch bound, although this set of sequences is unfortunately rather small. The set of binary Gold sequences is a much larger set, which comes close to the Welch bound. Thus there is not much to be gained by attacking the problem in this way. [64]

The second traditional method for improving the conventional receiver's performance is to implement a power control scheme, wherein each user's transmitted power is adjusted so that its received signal power at the basestation is the same as that of all of the other users' signals. It will be seen later in this dissertation that this approach is a solution to the near-far problem, but it is a conservative and somewhat inefficient solution.

A major improvement over the traditional receiver can be achieved by viewing the MUI not as a random noise signal, but instead as a structured interferer. Because all of the signals making up the MUI in a CDMA network are generally of the same structure as the signal of interest, and because their signature sequences are generally known to the receiving system, it is possible to augment the standard receiver structure and exploit this knowledge of the MUI. This can be done by estimating MUI and attempting to cancel it,

or by jointly estimating the entire message. Figure 1.3 illustrates this kind of receiver, which is generally referred to as a *multiuser receiver*. The augmentation required consists of some additional synchronization circuitry to lock into some or all of the interfering signals, and then a decoding algorithm which would use these additional statistics to estimate the MUI and cancel it.

The rationale for using this augmented receiver is that if it is successful in estimating the MUI, it will, in many situations, be able to eliminate the near-far problem and attendant error-rate floor, and its performance will be approximately that of a single-user link. The drawback of this approach is the complexity associated with the additional synchronization circuits and the algorithm for estimating and eliminating the MUI. It is important to note that in multipoint-to-point networks this additional synchronization circuitry must be a part of a conventional basestation anyway, as a basestation must lock to and demodulate the signals of all users in the cell served by that basestation. Thus, in certain applications, the additional complexity of jointly decoding the signals in the system will not be as great as in others, such as a single user's receiver in a multipoint-to-multipoint network.

It is important to note that this technique is not appropriate in a jamming environment where the interfering signal structure is not known. It is also worth keeping in mind that if the MUI becomes too severe, the main limitation of the CDMA system may be the synchronization of the basestation to each of the user's signal. If the MUI is strong enough to prevent the basestation from acquiring the component signals, then no form of coherent detection will be possible, conventional or otherwise. Finally, if the MUI is so weak that the users do not degrade each other's performance, then the performance of the conventional basestation will be essentially optimum. Thus the multiuser detection techniques described in this dissertation are aimed at the cases where at least some of the users in the system suffer in performance due to MUI, but the MUI is not so strong as to prevent acquisition of the signals at all.

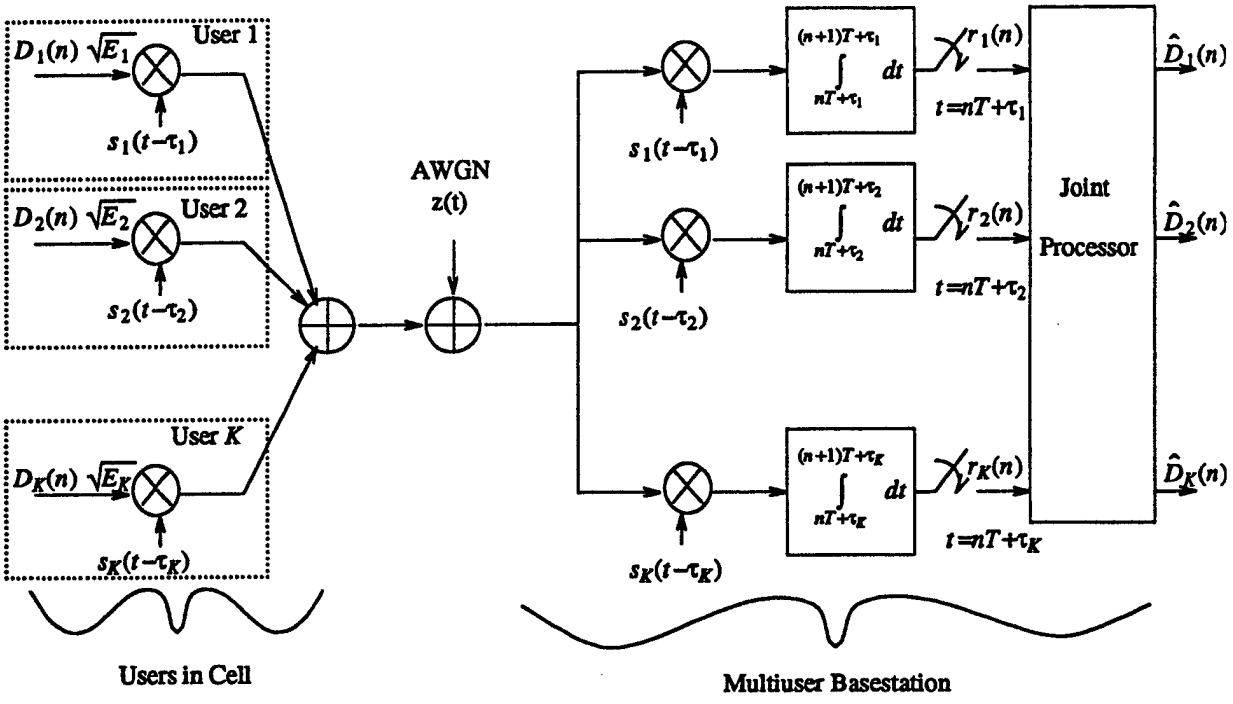

Figure 1.3 K-user asynchronous network with a multiuser receiver which jointly decodes all of the users in the system.

There has been a large amount of interest recently in the design of multiuser receivers for CDMA systems. Most of this work has centered on uncoded links, [1] - [44]. References [3] and [50] are particularly good tutorial papers on this subject. Only recently, [41], [43], [44] [53], has the problem of multiuser detection of coded links been considered.

In this dissertation, multiuser receivers will be examined for both coded and uncoded CDMA systems. We will begin by studying the notion of multiuser detection in Chapter 2 by examining some of the important multiuser receivers that have already been proposed. This theme will continue into Chapter 3 where we will take a detailed look at the decision feedback multiuser detection techniques for uncoded links which have already been proposed. This discussion will lead to a new hybrid decision feedback equalizer which provides superior performance to those that have already been proposed.

Error control coding is a traditional tool for improving the reliability of communication systems. As a result, Chapter 4 will begin our look at CDMA links where each user employs a convolutional code to improve performance. In this chapter, the optimal sequence estimator will be formulated and its performance will be analyzed both through an analytical analysis and through computer simulations. We will see that the optimal sequence estimator provides a benchmark for all other multiuser receivers, as it is the best we can achieve in terms of sequence error probability. The problem with this optimal receiver is that it has a prohibitively high complexity.

As a result of the optimal receiver's high complexity, in Chapter 5 we will examine a large number of suboptimum multiuser receiver architectures. The goal in studying the suboptimum approaches is to find a receiver that maintains most of the optimal receiver's high performance, while doing so with a much lower complexity. These receivers will be studied analytically, whenever possible, and using computer simulations when an analysis is not possible. A performance measure will be introduced called the asymptotic multiuser coding gain (AMCG), which will be used extensively to compare the various

receiver's performances. We will see from this performance analysis that many of the suboptimum approaches do achieve nearly-optimum performance with a low complexity.

In order to discuss the multiuser receivers in Chapters 3, 4 and 5, however, it is necessary to lay out the notation and to define the various approaches that have been proposed by other researchers in the past. This notation and background will be the subject of the next chapter.

Chapter 2 General Multiuser Detection

In this chapter, we will begin by outlining the notation which will be used throughout the dissertation. This will lead into a precise formulation of the problem which multiuser detection seeks to solve. A summary of the various multiuser receivers that have been proposed for uncoded links will then be given in order to provide the necessary background for the following chapters. Finally, a brief introduction to the topic of multiuser detection for coded links will be given to motivate the work in Chapters 4 and 5.

It will be assumed that the CDMA system has K users operating simultaneously on a common frequency in an asynchronous fashion. Furthermore, each user may employ binary convolutional coding on its link. While it is quite conceivable that block codes could be used effectively on a CDMA link, convolutional codes have the advantage that they operate in a sequential fashion. Because the decoders that will be studied in this work are sequential in nature, the convolutional codes are a much better match to the decoders than block codes. Also, in [38] it was shown that in CDMA systems, binary convolutional codes often outperform more general trellis codes which map information symbols onto M-level signals where M is larger than the alphabet size of the information symbols. In other words, there is no particular advantage to using nonbinary coding. This may be considered a further justification for the confinement in scope of this work to binary convolutional codes. One further assumption in this work is that each user employs the same convolutional code, although it is not at all difficult to generalize this work to the case where each user employs a different code.

At each time interval, n, of length T_s, the convolutional code is generated for user k by passing P binary information bits, $\overline{I}_k(n) = (I_k^{(1)}(n),..., I_k^{(P)}(n))$, through a shift register consisting of W stages with Q modulo-2 adders, as shown in Figure 2.1. The number of output bits for each P-bit input sequence is Q bits. The rate of the code is $R_c = P/Q$ and

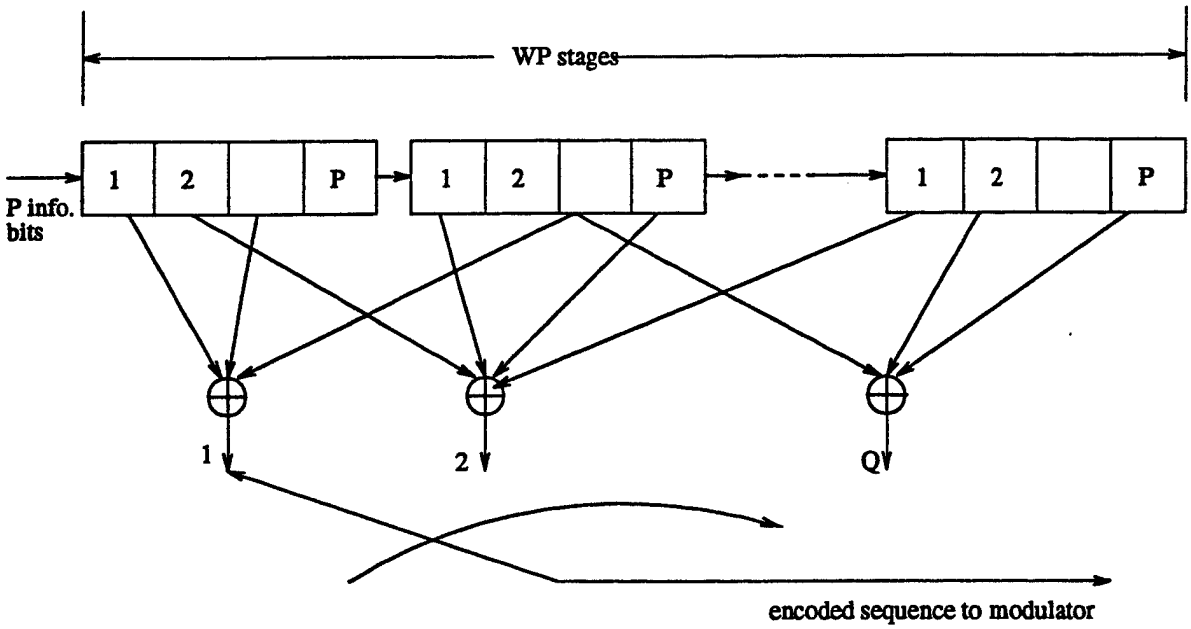

Figure 2.1 General convolutional encoder structure. [64]

the constraint length of the code is W. The output sequence of binary code bits for the interval corresponding to input bits $\bar{I}_k(n)$ is $(D_k^{(1)}(n),...,D_k^{(Q)}(n))$. Note that for $W = 1$ and $P = Q = 1$, we have the *uncoded* case, so in that case $D_k(n) = I_k(n)$.

In the time interval $[nT_s+(q-1)T+\tilde{\tau}_k, nT_s+qT+\tilde{\tau}_k)$, user k transmits data bit $D_k^{(q)}(n)$, where $\tilde{\tau}_k$ represents the time shift of the k^{th} user relative to some reference time, thus accounting for the asynchronism of the users relative to each other. T represents the code bit period and $T_b = T/R_c$ is the information bit duration, thus $T_s = QT = PT_b$. Let $\tilde{\tau}_k = m_kT+\tau_k$, $\tau_k \in [0,T)$, and $m_k \in \{0,...,Q-1\}$. Thus m_kT is a coarse time shift and τ_k is a fine time shift for user k.

Each user in the system is assigned a particular *signature sequence*, and it will be assumed that this signature sequence has a duration equal to the code bit interval, although this assumption can be relaxed with a change of the notation. We will combine the carrier and signature sequence into a single signal, thus the k^{th} carrier multiplied by the binary (± 1) signature sequence, $PN_k(t)$, will be denoted by

$$s_k(t) = \begin{cases} \sqrt{2/T}\, PN_k(t)\cos(\omega_c t) & 0 \le t \le T \\ 0 & otherwise \end{cases} \tag{2.1}$$

We will assume that $\omega_c T$ is an integer multiple of 2π to provide phase continuity at the code bit boundaries. Note that $s_k(t)$ is a unit-energy waveform. The energy of the k^{th} user's code bit measured at the receiver will be denoted by E_k. It will be assumed that all K users transmit their signals through a common additive white Gaussian noise channel with two-sided noise spectral density $N_0/2$, and so the received signal will have the following form

$$r(t) = \sum_{n=-\infty}^{\infty} \sum_{k=1}^{K} \sum_{q=1}^{Q} D_k^{(q)}(n)\sqrt{E_k}\, s_k(t-nT_s-(q-1)T-\tilde{\tau}_k) + z(t) \tag{2.2}$$

where $z(t)$ denotes the noise. If there is no coding on the link, $D_k(n) = I_k(n)$ and $T_s = T_b = T$, so (2.2) may be rewritten in a simpler form.

$$r(t) = \sum_{n=-\infty}^{\infty} \sum_{k=1}^{K} D_k(n)\sqrt{E_k}\, s_k(t-nT-\tau_k) + z(t) \ . \tag{2.3}$$

Because it is more notationally cumbersome to discuss the coded link case, we will use the uncoded link case for the remainder of this chapter and the next to introduce the system model and some of the receivers that have been proposed in the literature. As a result, for the remainder of this chapter and Chapter 3, we will use equation (2.3) to represent the received signal. In Chapters 4 and 5, where the coded link case will be discussed in detail, we will resort to the use of equation (2.2) to represent the received signal.

Next we define the *partial cross-correlation* of the known signature sequences of users j and k to be:

$$\rho_{jk}(l) = \int_{-\infty}^{\infty} s_j(t-\tau_j)\, s_k(t-lT-\tau_k)\, dt \ . \tag{2.4}$$

It is worth noting that $\rho_{jj}(0) = 1$ and $\rho_{jk}(l) = \rho_{kj}(-l)$.

We will assume that the front end of the receiver consists of a bank of K matched filters or correlators, each matched to one of the transmitted waveforms in the system. (Note that Figures 1.2 and 1.3 illustrate a correlator implementation of the matched filter bank.) It was shown in [1] that the complete set of matched filter outputs generates sufficient statistics for the demodulation of each user's data. In Chapter 4, we will not make this assumption about the front end, but will ultimately arrive at the result that the optimal sequence estimator may be implemented with the matched filter bank front end. The output of the filter matched to the k^{th} signal at time $(n+1)T+\tau_k$ is

$$r_k(n) = \int_{nT+\tau_k}^{(n+1)T+\tau_k} r(t)\, s_k(t-nT-\tau_k)\, dt \tag{2.5}$$

where perfect synchronization has been assumed here between the k^{th} component of the received signal and the local signature sequence generator at the receiver.

Substituting for $r(t)$ in equation (2.3) and integrating, we obtain

$$r_k(n) = \sum_{j=k+1}^{K} \rho_{kj}(-1) D_j(n-1)\sqrt{E_j} + \sum_{j=1}^{K} \rho_{kj}(0) D_j(n)\sqrt{E_j}$$

$$+ \sum_{j=1}^{k-1} \rho_{kj}(1) D_j(n+1)\sqrt{E_j} + z_k(n) \qquad (2.6)$$

Note that because the system is asynchronous, these matched filter outputs become available at different times for each user and interval. Figure 2.3 illustrates a time line for each user in the system. Without a loss in generality, we assume that the users are ordered according to increasing τ_k.

This set of K equations for the K received signals can be denoted in the following compact matrix form:

$$\bar{R}(n) = \bar{E}[\bar{\rho}(-1)\,\bar{D}(n-1) + \bar{\rho}(0)\,\bar{D}(n) + \bar{\rho}(1)\,\bar{D}(n+1)\,] + \bar{Z}(n) \qquad (2.7)$$

Here $\bar{\rho}(m)$ is the signature correlation matrix for lag m, which is $K \times K$. $\bar{E}$ is the $K \times K$ diagonal energy matrix with the k^{th} diagonal term being $\sqrt{E_k}$. $\bar{D}(n)$ is the $K \times 1$ data vector holding each user's independent and identically distributed data at time n, and $\bar{Z}(n)$ is a $K \times 1$ vector of noise variates which are Gaussian random variables colored both spatially and temporally as shown below. The noise variables have zero mean and covariance matrix

$$\bar{C}(m) = \frac{N_0}{2} \cdot \bar{\rho}(m) \qquad (2.8)$$

for the m^{th} time lag. These matrices are $K \times K$ at each time lag. $N_0/2$ is the two-sided noise spectral density.

For the case where there are two users in the system these matrix equations take the following form:

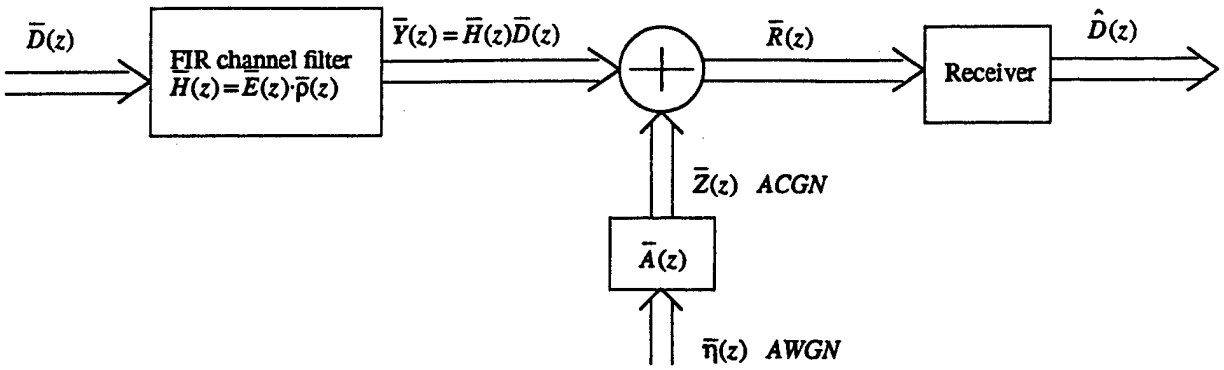

Figure 2.2 Discrete time vector model of the multiuser CDMA channel.

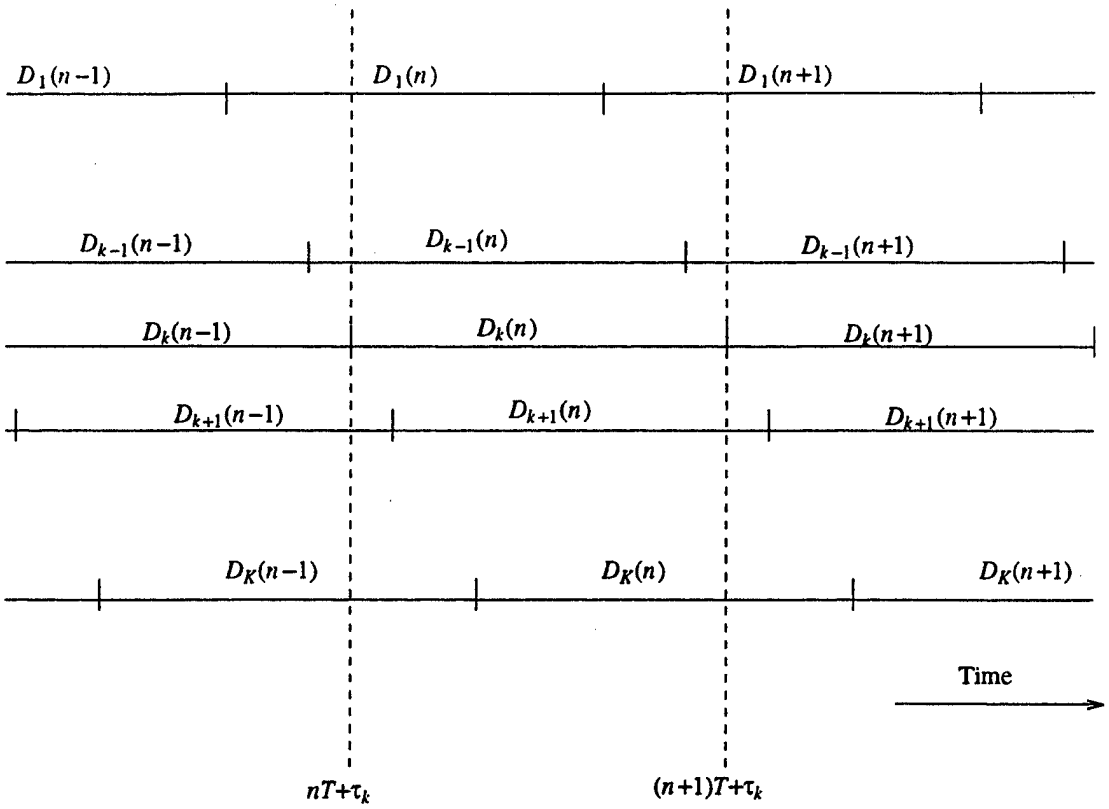

Figure 2.3 Time lines for each of the K users in an asynchronous CDMA system.

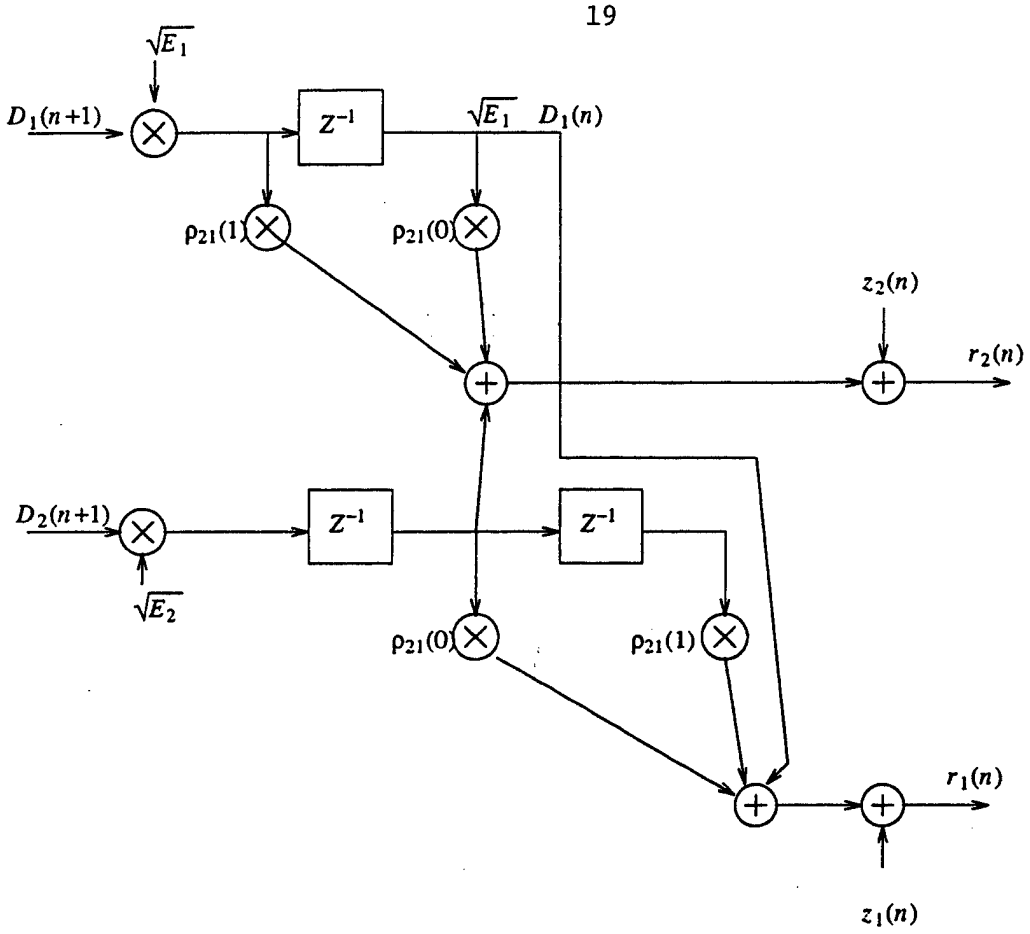

Figure 2.4 Discrete time model of a 2-user CDMA channel.

$$\begin{bmatrix} r_1(n) \\ r_2(n) \end{bmatrix} = \begin{bmatrix} 0 & \rho_{12}(-1) \\ 0 & 0 \end{bmatrix} \begin{bmatrix} \sqrt{E_1} & 0 \\ 0 & \sqrt{E_2} \end{bmatrix} \begin{bmatrix} D_1(n-1) \\ D_2(n-1) \end{bmatrix} + \begin{bmatrix} 1 & \rho_{12}(0) \\ \rho_{12}(0) & 1 \end{bmatrix} \begin{bmatrix} \sqrt{E_1} & 0 \\ 0 & \sqrt{E_2} \end{bmatrix} \begin{bmatrix} D_1(n) \\ D_2(n) \end{bmatrix}$$

$$+ \begin{bmatrix} 0 & 0 \\ \rho_{21}(1) & 0 \end{bmatrix} \begin{bmatrix} \sqrt{E_1} & 0 \\ 0 & \sqrt{E_2} \end{bmatrix} \begin{bmatrix} D_1(n+1) \\ D_2(n+1) \end{bmatrix} + \begin{bmatrix} z_1(n) \\ z_2(n) \end{bmatrix} \tag{2.9}$$

and the covariance matrix will be

$$\bar{C}(m) = \frac{N_0}{2} \begin{bmatrix} \delta(m) & \rho_{12}(-1)\delta(m-1) + \rho_{12}(0)\delta(m) \\ \rho_{12}(0)\delta(m) + \rho_{21}(1)\delta(m+1) & \delta(m) \end{bmatrix} \tag{2.10}$$

The matrix $\bar{\rho}(1)$ will be lower triangular in general, and the matrix $\bar{\rho}(-1)$ will be upper triangular in general.

As we noted from definition (2.4), $\rho_{12}(-1) = \rho_{21}(1)$. This implies that in the general K user case, $\bar{\rho}(-1) = \bar{\rho}^H(1)$ and furthermore that $\bar{\rho}(0)$ is a Hermitian matrix. Also, it is important to note that $\bar{\rho}(i) = \bar{0}$ when $|i| > 1$ due to the one symbol interval support of the waveform $s_k(t)$, and in addition, that the noise sequence within a given channel $\{z_k(n)\}_{n=-\infty}^{\infty}$ is temporally white.

At this point, the continuous-time CDMA waveform channel has been cast into the form of a discrete-time vector channel. The equivalent vector model is shown in Figure 2.2 in the z-domain for simplicity. In this figure, $\bar{H}(z)$ is the channel transfer function matrix, and $\bar{A}(z)$ is the transfer function matrix of a filter which properly colors the noise. The receiver's job might be to observe the sequence of matched filter outputs and to make an estimate of the entire data sequence $\bar{D}$ in the uncoded case and $\bar{I}$ in the coded case, or it might be to perform some form of symbol-by-symbol detection. $\bar{R}(n)$ consists of a filtered version of $\bar{D}(n)$ in noise which is both spatially and temporally colored according to $\bar{C}(m) = \bar{\rho}(m)N_0/2$. Due to the necessary synchronization circuits at the front end of the receiver, all of the signal cross-correlations can be generated at the receiver using at most $K(K+1)/2$ correlators, since we would need to dedicate at most one correlator to the computation of $\rho_{jk}(l)$ for each j and k pair. (If the channel transfer function matrix is not changing quickly, it may be possible to generate the signal cross-

correlations using a much smaller number of correlators in a time-sharing fashion.) As long as the receiver's synchronization circuits are locked to the appropriate component of the received signal, the normalized transfer function of the channel, $\bar{\rho}(z)$ will be measurable. In addition, if we assume that the receiver has gain estimation circuits built into the synchronization stage of the receiver, the energy matrix, $\overline{E}$ will also be known. Finally, the correlation matrix of the noise can be constructed easily from the locally generated signal cross-correlations. Throughout the rest of this work, we will make the assumption that the energies and cross-correlations of all of the users have been estimated perfectly, i.e. $\overline{H}$ is known.

2.1 Possible Receiver Structures for the Uncoded Case

The receiver's goal is to minimize the probability of error for the channel of interest. The traditional receiver for the k^{th} user will simply make a zero-threshold comparison on the observed statistic, $r_k(n)$, at each symbol interval, n. This detection strategy is optimal if the only available statistic is $r_k(n)$ and we have no knowledge of the structure of the interference, or if the signature sequences are mutually orthogonal, which is generally not the situation in the asynchronous case. If all of the other received statistics are available as well, in an augmented receiver or a basestation in a cellular network, then this knowledge may be used to perform a joint estimation of the sequences. (See Figure 1.3) This kind of augmented receiver is referred to in the literature as a *multiuser receiver*.

There are many multiuser receivers that have been proposed in the past decade. (See [1] - [44]) These approaches can be broadly grouped together in three main categories: **trellis and tree-based approaches, linear equalizer approaches** and **decision feedback approaches.** There are many many multiuser receivers that have been proposed in each of these categories. Furthermore, some of these receivers do not fit cleanly into one of these categories, but instead are hybrids of two of the approaches. Rather than discuss

each of the previously proposed receivers individually, we will discuss the three categories. In our discussion of each category, we will cite some of the key representatives of that approach.

2.1.1 Trellis/Tree-Based Approaches

The broad category of approaches which we refer to as trellis and tree-based include all decoders which operate by searching a either a trellis or a tree for the most likely sequence that was transmitted. As we will see, this search will result in the maximum likelihood sequence estimate of the transmitted data if the optimal metric is used and the search is performed with the Viterbi algorithm in a trellis with 2^{K-1} states for a K user system.

Due to the finite alphabet of the input data symbols to the known matrix FIR channel filter $\overline{H}(n)$, the multiuser detection problem may be considered to be one of estimating the inputs to a finite-state machine in colored Gaussian noise. The minimum probability of sequence error decoder for all of the users would then correspond to the maximum likelihood decoder if all of the input sequences were assumed to be equally likely. It was shown in [1] that the maximum likelihood sequence estimator (MLSE) can take the form of a Viterbi algorithm which traverses K stages of a 2^{K-1} state cyclically time-varying trellis in one bit period of the individual users in the system. The optimal metric at stage n of the trellis takes the form:

$$\Lambda_n(\overline{D}_n, \sigma_{n-1}) = \Lambda_{n-1}(\overline{D}_{n-1}, \sigma_{n-2}) + \lambda_n(D_n, \sigma_{n-1}) \tag{2.11}$$

where $\overline{D}_n$ represents all of the data bits for all of the users up to time interval n, σ_{n-1} represents the state at the end of stage $n-1$, and

$$\lambda_n(D_n, \sigma_{n-1}) = D_{\beta(n)}(\alpha(n))\sqrt{E_{\beta(n)}}\,[2r_{\beta(n)}(\alpha(n)) - D_{\beta(n)}(\alpha(n))\sqrt{E_{\beta(n)}}\,\rho_{\beta(n)\beta(n)}(0)$$
$$-2\sum_{j\le n-1} D_{\beta(j)}(\alpha(j))\sqrt{E_{\beta(j)}}\,\rho_{\beta(n)\beta(j)}(\alpha(j)-\alpha(n))\,] \tag{2.12}$$

where $\beta(n)$ and $\alpha(n)$ are the resulting components of a modulo-K decomposition of the

integer n, i.e. $n = \alpha(n)K + \beta(n)$ with $\beta(n) \leq K$

It is significant that the crosscorrelation $\rho_{\beta(n)\beta(j)}(\alpha(j)-\alpha(n))$ in the last term of equation (2.12) is zero for $|n-j| \geq K$. This implies that the limits of the sum can be reduced to the values over which $\rho_{\beta(n)\beta(j)}(\alpha(j)-\alpha(n))$ is nonzero, namely from $j = n-(K-1)$ to $j = n-1$. The number of terms in this sum of the final term and correspondingly, the number of past data bits that affect the stage metric is $K-1$. Because the state is defined as the past data bits affecting the stage metric, we see that the state of the system is given by

$$\sigma_{n-1} = [\, D_{\beta(n-1)}(\alpha(n-1)),\, D_{\beta(n-2)}(\alpha(n-2)),\, \ldots,\, D_{\beta(n-K+1)}(\alpha(n-K+1))\,] \quad (2.13)$$

and since each data bit is binary, we get the result that there are 2^{K-1} states that are possible for (2.13).

Because the metric must be computed for both of the paths that emanate from each of the 2^{K-1} states at each trellis stage, and because with each stage one bit is estimated, we may say that the time-complexity per estimated bit is $TCB = O(2 \times 2^{K-1}/1) = O(2^K)$, [1]. It is interesting that an earlier formulation of this problem used the philosophy that the system should be modeled as a vector state machine, [25]. This approach implies that the state is determined by the K bits from the previous interval, $n-1$, and the current input is the vector of the K bits, one for each user, in interval n. This approach had a time-complexity per estimated bit of $TCB = O([2^K 2^K]/K) = O(2^{2K}/K)$. The approach in [1] which does not view the problem as a vector problem is clearly less complex.

The obvious drawback of the Viterbi algorithm in this application is that the complexity of the state machine is exponential in K, the number of users in the system, and the receiver complexity will be excessive for a large system. It is therefore interesting to consider suboptimum solutions which are less complex than the optimal sequence estimator.

If the search is somehow performed on a trellis with fewer states and if a metric other than the optimal metric is used, the performance will be worse than that of the optimal MLSE by some amount. The goal of reduced state sequence estimation (RSSE) is to operate on a trellis with fewer states than the optimal MLSE, while still performing nearly as well as the optimal decoder. The key advantage of RSSE is that if the number of states is reduced significantly from 2^{K-1}, then the complexity savings for the decoder will be large. RSSE was introduced in [47] and [57] - [60] for the intersymbol interference (ISI) problem, and has also been studied for use with trellis codes and convolutional codes. [47] This idea has recently been applied to the simplification of the optimal sequence estimator of [1] in [8] and [56]. The complexity of the RSSE decoder will depend on how much the optimal trellis of 2^{K-1} states has been reduced. The performance is also a function of the degree of reduction that is performed.

It is also possible to view the problem as a search in a tree. Sequential decoding approaches are sparse tree search procedures which are useful for applications like decoding convolutional codes with very large constraint lengths and equalizing ISI when the channel's impulse response is long. As with RSSE, sequential decoding approaches provide a tradeoff of complexity versus performance. Naturally, these approaches can be an attractive way to reduce the optimal sequence estimator's high complexity. In [14], a modified Fano metric was used with the stack algorithm to simplify the decoding operation and still maintain a performance level near that of the MLSE.

2.1.2 Linear Approaches

The idea in these approaches is that decision statistics will be formed from linear combinations of the matched filter outputs, or more generally from linear operations on the received signal. Focusing, for now, on the first approach, we again consider the discrete time vector model of the channel from the input signals to the matched filter outputs as is illustrated in Figure 2.5. The Z-transform of the sequence of vector of matched

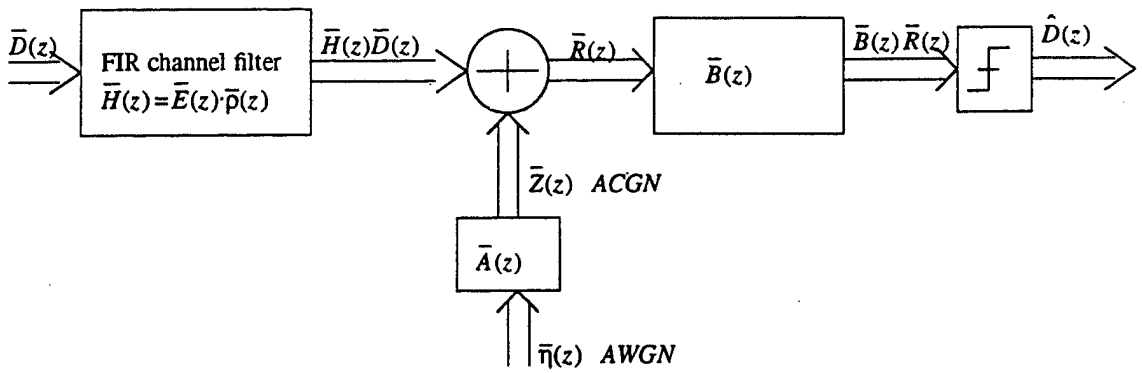

Figure 2.5 Discrete time vector model of the multiuser CDMA channel with a linear receiver.

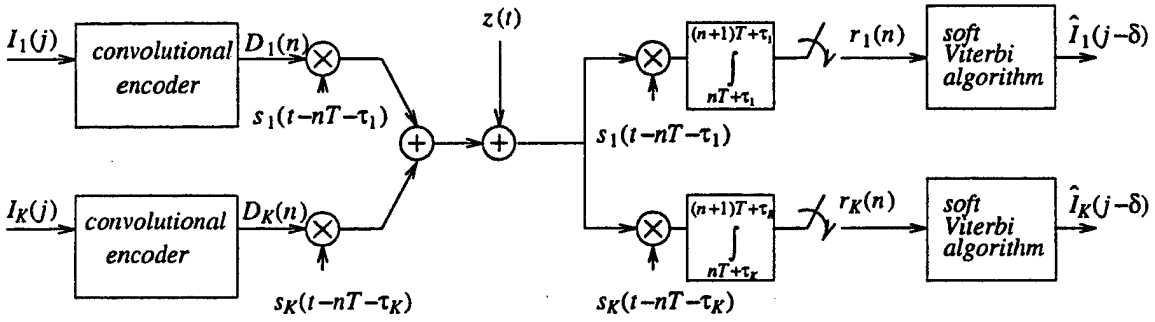

Figure 2.6 Convolutionally coded direct sequence CDMA link
with a conventional basestation architecture (case $E_j = 1$, $j \in \{1,...,K\}$ shown).

filter outputs is denoted by $\bar{R}(z)$. This sequence of received vectors is passed through a linear filter with transfer function matrix, $\bar{B}(z)$. The resulting decision statistics vectors are then compared with a threshold of zero, term by term, to produce the decision vector, $\hat{D}(n)$, in the n^{th} time interval. The Z-transform of the sequence of decision vectors is denoted in Figure 2.5 by $\hat{D}(z)$.

The obvious question which arises with this approach is what values should be used in the $\bar{B}$ matrix to minimize the error probability of the decisions. This problem, unfortunately, is not analytically tractable, and so alternate performance criteria must be adopted. The two most common criteria for solving this problem for linear equalizers for single-user systems which suffer from intersymbol interference (ISI) are the minimum mean squared error criterion (MMSE) and the zero-forcing criterion. Both of these criteria have been applied to the multiuser detection problem.

In [4] and also essentially in [17], the decorrelator receiver was proposed. This receiver is the multiuser analog of the zero-forcing linear equalizer for the ISI problem. The solution for the decorrelator is that $\bar{B}(z) = \bar{\rho}^{-1}(z)$, or in words, for the decorrelator the linear filter is chosen to invert the normalized channel transfer function matrix.

Because this receiver will form a portion of a multiuser receiver which will be proposed in Chapter 5, we will review the basic mathematics behind the decorrelator. Since the Z-transform of the sequence of received vectors is given by

$$\bar{R}(z) = \bar{\rho}(z)\bar{E}(z)\bar{D}(z) + \bar{Z}(z) \tag{2.14}$$

it follows that the decorrelator's decision statistic vector sequence will have Z-transform

$$\bar{B}(z)\bar{R}(z) = \bar{\rho}^{-1}(z)\bar{\rho}(z)\bar{E}(z)\bar{D}(z) + \bar{\rho}^{-1}(z)\bar{Z}(z) = \bar{E}(z)\bar{D}(z) + \bar{\rho}^{-1}(z)\bar{Z}(z) \tag{2.15}$$

Let the decorrelator's output noise vector sequence have Z-transform

$$\tilde{Z}(z) = \bar{\rho}^{-1}(z)\bar{Z}(z) \tag{2.16}$$

Equation (2.15) shows that the decorrelator has eliminated the multiuser interference

caused by $\bar{\rho}(z)$, however, in general, the variance of $\tilde{z}_k(n)$ will be larger than that of $z_k(n)$. ($\tilde{z}_k(n)$ represents the noise on the k^{th} user's n^{th} decision statistic.) Let the covariance matrix of this noise be denoted by

$$\Phi_{jk}(l) = E[\tilde{z}_j(n)\tilde{z}_k(n-l)] \tag{2.17}$$

The Z-transform of the covariance matrix sequence may be written as

$$ZT[\bar{\Phi}(n)] = E[\tilde{Z}(z)\tilde{Z}^T(z)] = E[\bar{\rho}^{-1}(z)\bar{Z}(z)\bar{Z}^T(z)\bar{\rho}^{-T}(z)] = \bar{\rho}^{-1}(z)N_0/2 \tag{2.18}$$

since $E[\bar{Z}(z)\bar{Z}^T(z)] = \bar{\rho}(z)N_0/2$. This is obtained from taking the Z-transform of equation (2.8). Finally, it is not difficult to show that $E[\tilde{z}_k(n)] = 0$, and $Var[\tilde{z}_k(n)] = \Phi_{kk}(0)\cdot N_0/2$. Because $\Phi_{kk}(0)$ will be greater than one, the noise variance is enhanced by some amount. Thus, the decorrelator linearly combines the matched filter outputs in such a way so as to eliminate the MUI, but in doing so, the noise variance is increased. This is the same effect which is observed for the zero-forcing linear equalizer for the ISI problem.

The MMSE linear receiver that was discussed in [13], [21] and [24]. The transfer function of the MMSE receiver turns out to be

$$\bar{B}(z) = (\bar{\rho}(z) + \bar{I}\cdot N_0/2)^{-1} \tag{2.19}$$

From this equation, it is easy to see that this receiver reduces to the decorrelator when the background noise in the multiuser system goes to zero, $N_0/2 \rightarrow 0$. In the case where there is background noise, the MMSE receiver can outperform the decorrelator because it minimizes the variance of both the MUI and the noise.

Other linear receivers have also been introduced in the literature, see for example [4], however we will not review these approaches in this work. The interested reader is referred to the references.

One final thing to note about the linear approaches is that they generally have a linear complexity in K. The size of the receiver's matrix filter, $\bar{B}(n)$ is $K \times K$, so $2K+1$

new FIR filters must be added to the matrix filter when user $K+1$ enters the system. The ideal decorrelator and MMSE FIR matrix filters can not be realized with a finite number of taps, however the filter impulse response would inevitably be truncated at some depth, δ. It therefore follows that the number of multiplications which are necessary for each bit decoded is roughly $O(\delta K^2/K) = O(\delta K)$. The complexity associated with the tap computation is a "one time" cost, as the taps only need to be computed once as long as the channel conditions do not change. However, if new users enter and leave the system often or if $\bar{\rho}(z)$ changes with time, the new filter taps have to be recomputed often and this would make the complexity of these approaches much higher. Furthermore, taking the inverse of a polynomial matrix is not an easy task.

2.1.3 Decision Feedback Approaches

The decision feedback approach to the equalization problem is not linear, but instead involves feeding back tentative decisions in some fashion to attempt to cancel the multiuser interference. DFE structures were studied in [6], [7], [12], [13], [20], [22] - [24]. In the literature, some of these approaches are called multistage receivers, some are called successive cancellation receivers and some are simply called DFE's. Chapter 3 will present a number of the various approaches in a unified way to illustrate their commonality and we will use the term DFE to refer to this class. The decision feedback approach will be discussed in detail in that chapter and a hybrid DFE will be developed which outperforms the nonlinear DFE's proposed to this point. These DFE approaches will also turn out to have a linear complexity with K.

2.2 Possible Receiver Structures for the Coded Case

After we discuss DFE's in Chapter 3, we will move on to consider multiuser detection for coded links. Consider for a moment CDMA links where each user employs a convolutional code. The basestation that will be referred to as the *conventional*

basestation on this coded link attempts to estimate the k^{th} user's data using only the matched filter outputs for the k^{th} user, (see Figure 2.6). It will be assumed that the Viterbi algorithm operating on each user's observed code symbols is a soft-decision Viterbi algorithm having a decoding delay which generally will be several times the constraint length, W, of the code. The time complexity per decoded bit for this receiver may be estimated by considering the number of metric computations per information bit decided. If we define the binary memory order of the encoder to be $\kappa = \log_2 S$, where S is the number of states of each user's encoder, then there are $2^{\kappa+P}$ metrics computed for every P bits decided, so $TCB = O(2^{\kappa+P}/P)$.

As in the uncoded case, there are a number of ways that a multiuser receiver can operate to improve upon the performance of the conventional basestation. In the Chapter 4, the optimum sequence estimator will be derived for this problem and analyzed. Because this receiver has a very high complexity, in Chapter 5 a broad range of suboptimum receivers will be introduced which have a lower complexity than the optimal sequence estimator and still maintain high performance levels in many cases. The only work that has appeared in the literature on this topic at this time are [44], [53], [41] and [43]. These approaches will all be unified in Chapter 5 and their performance will be analyzed whenever possible.

Before moving on to the coded case, however, we will consider DFE's for the uncoded case in the next chapter. These DFE's which will be examined in Chapter 3 will form the foundation for a number of the suboptimum low-complexity receivers of Chapter 5.

Chapter 3 A New Nonlinear Decision Feedback Equalizer

To begin our discussion of the possible DFE structures, we will focus on two nonlinear multistage-style DFE algorithms that have already been proposed. By comparing them, we will be led to the hybrid structure which is the real focus of this chapter. We will see that the new hybrid structure greatly outperforms the previous DFE's in most situations.

The multistage algorithm proposed by Varanasi and Aazhang in [6] can be viewed as a form of a DFE that is appropriate for the multiuser problem, although it has a different structure from the DFE's used in the ISI problem. In [6], it was assumed that the matched filter outputs were delayed appropriately so that they all became available to the multistage algorithm at the same time. In this discussion, we will present the algorithm in an equivalent sequential fashion because it will lead naturally to the DFE proposed in [13] and the hybrid DFE to be proposed in Section 3.1. For the purposes of this discussion, this algorithm will be referred to as Varanasi's DFE or as Varanasi's algorithm.

In Varanasi's multistage algorithm, a hard decision is made on each matched filter output and the output is stored in a buffer as is illustrated in Figure 3.1. This buffer has an output which is available to the multistage algorithms operating on the other sequences of matched filter outputs. This hard decision and storage forms what is referred to as the first-stage of the algorithm. The second-stage uses a delayed matched filter output and the tentative first-stage estimates of each user's bits to obtain a better second-stage estimate of the appropriate user's bit. Because the actual MUI for user j at time interval n is given by

$$MUI_j(n) = \sum_{l=1}^{j-1} \rho_{jl}(1) D_l(n+1)\sqrt{E_l} + \sum_{l \neq j} \rho_{jl}(0) D_l(n)\sqrt{E_l} + \sum_{l=j+1}^{K} \rho_{jl}(-1) D_l(n-1)\sqrt{E_l} \qquad (3.1)$$

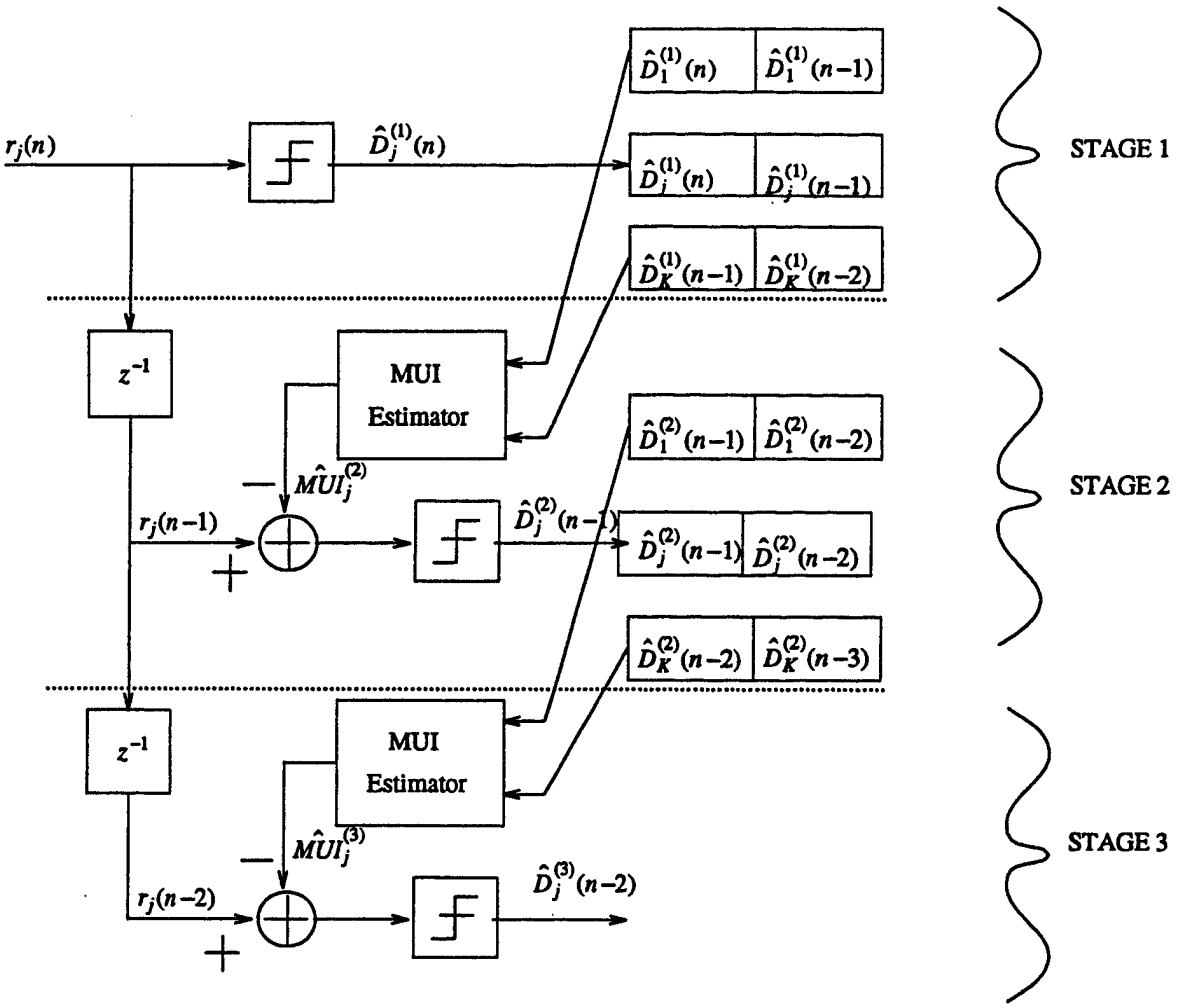

Figure 3.1 A 3-stage version of the multistage algorithm proposed by Varanasi and Aazhang in [6]. Iterative estimation of user j's bit sequence shown.

the idea is to use first-stage estimates of each of the $D_i(k)$ values in (3.1) to estimate this MUI. The values of $\rho_{jl}(k)$ are again obtained by cross-correlating the local signal generators at the front end of the receiver which are synchronized to the actual signal of interest, and the values of $\sqrt{E_l}$ are obtained by estimating the signal strength of each user.

In the second-stage, the estimated MUI is subtracted from the delayed matched filter output and the resulting real number is compared with a zero threshold. The result is placed into the appropriate position in the second-stage buffer and again this buffer position is accessible for each of the other multistage algorithms which operate on the other users matched filter output sequences. This procedure can be performed as many times as is desired, but there is a number of stages beyond which very little additional gain is achieved by adding stages. [12]

A second DFE structure was proposed by Xie, Short and Rushforth in [13], and for the purposes of this discussion, this structure will be referred to as Xie's DFE or Xie's algorithm. Xie's DFE was not proposed as a multistage algorithm, but instead as a variant of the more traditional ISI-style DFE structure. This algorithm can also be viewed as a two-stage multistage algorithm, however. It is in this spirit that it is presented in Figure 3.2 so that it can be easily compared with the multistage algorithm of Figure 3.1.

The first-stage of this DFE is again a conventional detector which simply makes hard decisions on the matched filter outputs and stores the estimated bits in a buffer. This section of the DFE was viewed by Xie et al as a nonlinear feedforward portion and the second-stage was viewed as a nonlinear feedback portion. This view connects it with the ISI equalizers which have linear feedforward portions followed by nonlinear feedback portion.

The MUI which corrupts each matched filter output is described by equation (3.1) and may be broken up into two parts. One part consists of bits which trail the bit being decided in time and have already been estimated at the second-stage level. This portion is

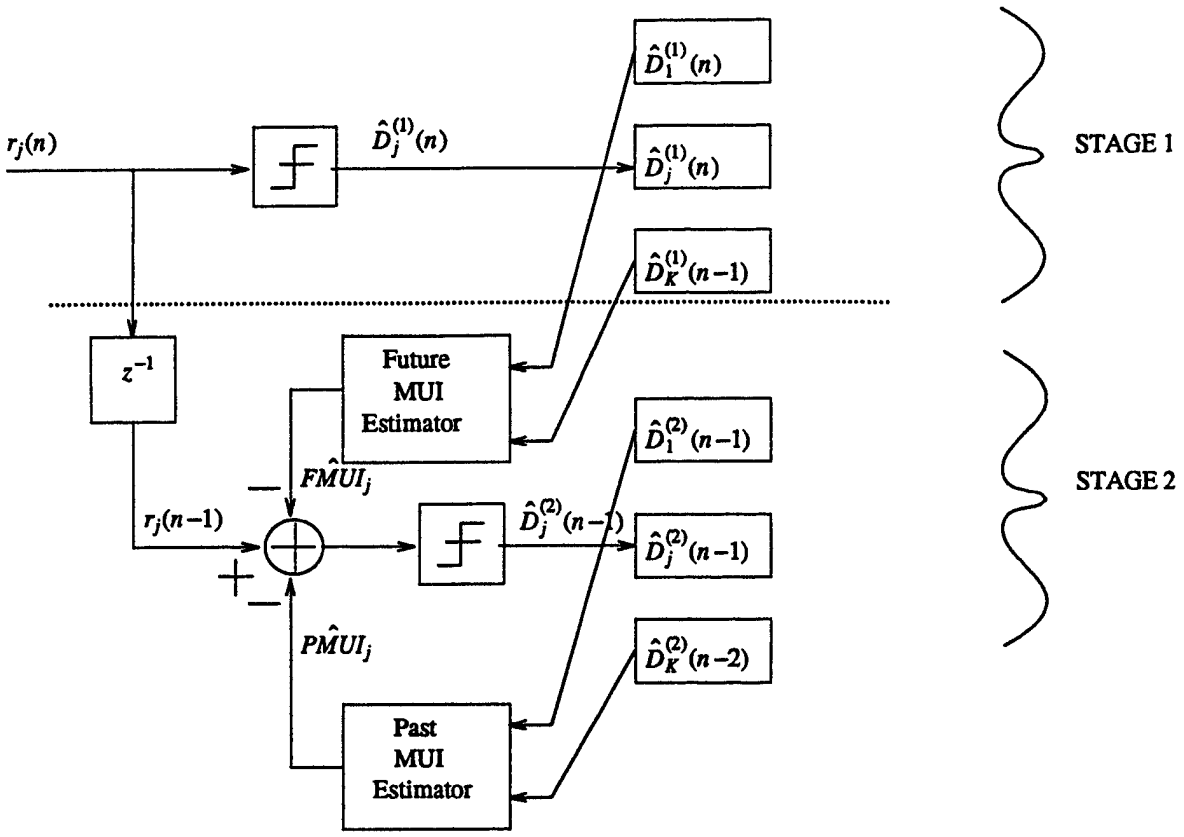

Figure 3.2 The decision feedback equalizer proposed by Xie, Short and Rushforth in [13] shown in the form of a 2-stage multistage algorithm. Estimation of user j's bit sequence is shown.

called the *past portion* of the MUI, and for user j at time interval $n-1$ it can be written as

$$PMUI_j(n-1) = \sum_{l=1}^{j-1} \rho_{jl}(0) D_l(n-1)\sqrt{E_l} + \sum_{l=j+1}^{K} \rho_{jl}(-1) D_l(n-2)\sqrt{E_l} \qquad (3.2)$$

The second portion of the MUI consists of bits which have not yet been estimated by the second-stage and so first-stage estimates of these bits must be used. The *future portion* of the MUI for user j at time interval $n-1$ can be expressed as

$$FMUI_j(n-1) = \sum_{l=1}^{j-1} \rho_{jl}(1) D_l(n)\sqrt{E_l} + \sum_{l=j+1}^{K} \rho_{jl}(0) D_l(n-1)\sqrt{E_l} \qquad (3.3)$$

which is the portion of (3.1) which is not included in (3.2).

It should be apparent at this point that the process carried out by this DFE can be extended easily to more stages by using the second-stage estimates of the data as bits in the future portion of a third-stage MUI estimate. This may in some cases provide better data estimates than are available from a two-stage equalizer.

A major difference between the two multistage algorithms is that Varanasi's DFE uses exclusively first-stage data estimates in its second-stage MUI estimate, while Xie's DFE uses as many of the more reliable second-stage data estimates as are available at the decision time for the j^{th} user's data. It is thus expected that Xie's DFE will typically outperform Varanasi's two-stage multistage algorithm.

A major drawback of both algorithms, however, is that they both rely upon a conventional detector as their first-stage. It will be shown in the next section, that in a severe MUI environment where either the cross-correlation between adjacent users is very high, or there are enough moderately cross-correlated users to produce the situation where the MUI term is larger than the desired signal term, this conventional first-stage badly limits the performance of these equalizers. It is for this reason that we propose a hybrid equalizer which does not use a conventional first-stage. This hybrid decoder will be shown to perform better in the severe MUI environment than the other DFE's examined so far because it will use a better first-stage. This decoder and a variety of simulation results

comparing all of these DFE structures are the subjects of the next two sections.

3.1 The Hybrid DFE

Figure 3.3 illustrates two stages of an alternative multistage DFE. The first-stage is not a conventional detector which simply makes hard decisions on the matched filter outputs, but is instead a nonlinear decision feedback equalizer itself. Due to the need for causality of the equalizer, however, not all of the MUI can be estimated at the first-stage, and so only the past portion of the MUI can be reconstructed. In this way, the first-stage makes an attempt to estimate the past half of the MUI in the first-stage and subtracts the influence of those data bits from the appropriate matched filter output. Thus the first-stage data estimate for the j^{th} user's n^{th} data bit will be the following:

$$\hat{D}_j^{(1)}(n) = sgn[\, r_j(n) - \hat{PMUI}_j^{(1)}(n) \,] \tag{3.4}$$

where $sgn\,[\cdot]$ is the signum function which performs the zero-threshold comparison and

$$\hat{PMUI}_j^{(1)}(n) = \sum_{l=1}^{j-1} \rho_{jl}(0)\, \hat{D}_l^{(1)}(n)\, \sqrt{E_l} + \sum_{l=j+1}^{K} \rho_{jl}(-1)\, \hat{D}_l^{(1)}(n-1)\, \sqrt{E_l} \tag{3.5}$$

The subsequent stages operate in the same way as the second-stage of Xie's DFE. Here because of the delay imposed, the $n-1^{st}$ data bit will be estimated at time n by:

$$\hat{D}_j^{(2)}(n-1) = sgn[\, r_j(n-1) - \hat{PMUI}_j^{(2)}(n-1) - \hat{FMUI}_j^{(2)}(n-1) \,] \tag{3.6}$$

where

$$\hat{PMUI}_j^{(2)}(n-1) = \sum_{l=1}^{j-1} \rho_{jl}(0)\, \hat{D}_l^{(2)}(n-1)\, \sqrt{E_l} + \sum_{l=j+1}^{K} \rho_{jl}(-1)\, \hat{D}_l^{(2)}(n-2)\, \sqrt{E_l} \tag{3.7}$$

$$\hat{FMUI}_j^{(2)}(n-1) = \sum_{l=1}^{j-1} \rho_{jl}(1)\, \hat{D}_l^{(1)}(n)\, \sqrt{E_l} + \sum_{l=j+1}^{K} \rho_{jl}(0)\, \hat{D}_l^{(1)}(n-1)\, \sqrt{E_l} \tag{3.8}$$

Note that if the feedback is correct and the energies and crosscorrelations are perfectly estimated, the MUI will be perfectly cancelled. If the feedback is incorrect for a particular bit, then that bit's contribution to the interference will effectively be doubled.

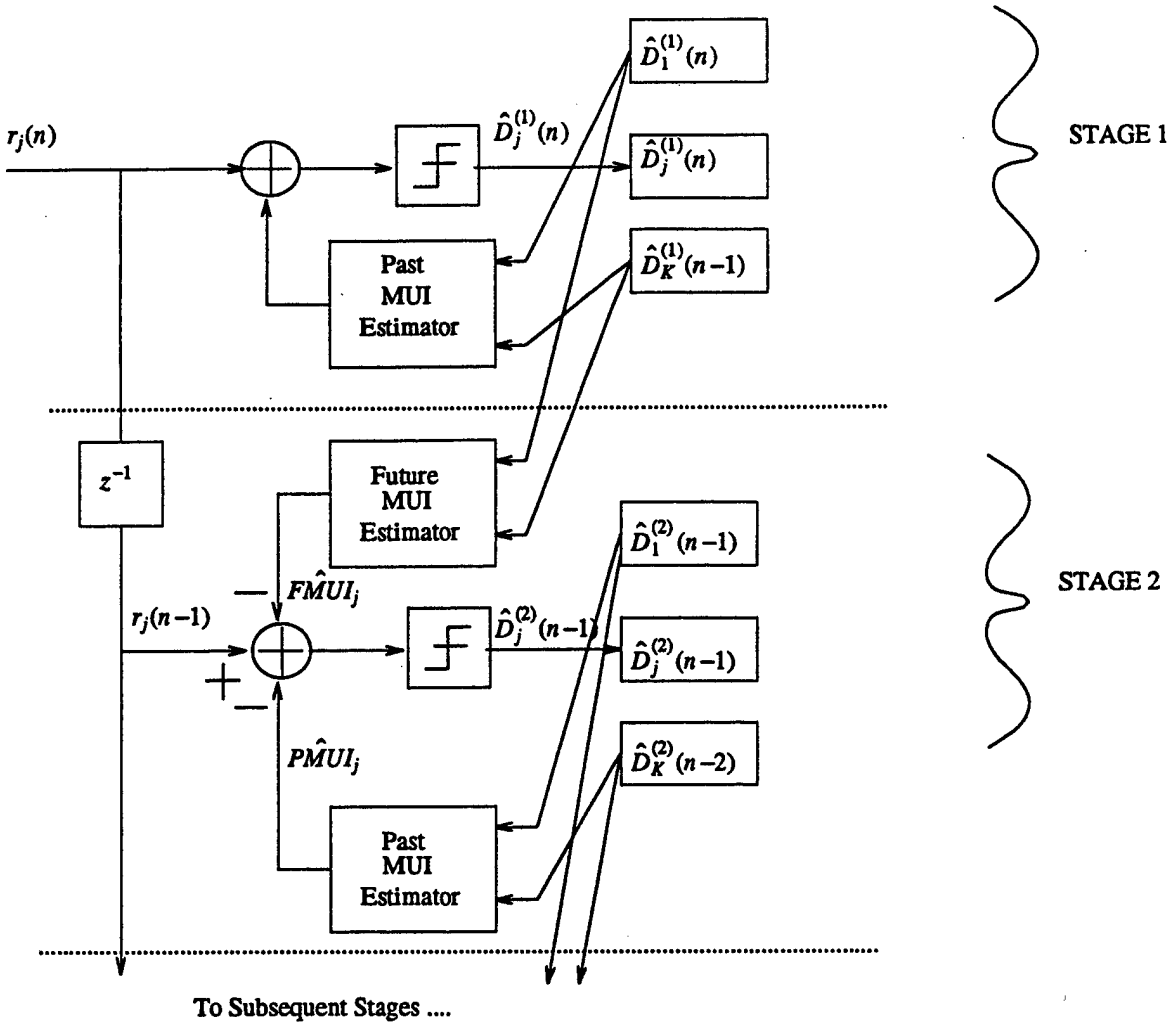

Figure 3.3 A hybrid multistage algorithm with 2 stages shown for estimating user j's bit sequence.

It is assumed in the algorithm above that the delay between each of the user's data bit intervals (ie. $\tau_j - \tau_{j-1}$ for each j) is large enough to allow the computation of equations (3.4) and (3.6) for the $j-1^{st}$ user so that the results can be stored in buffers before they are accessed by the j^{th} user's multistage algorithm. To insure that the proper data bit is used in the computation of the MUI, a status bit could be used to indicate whether the data residing in the latch holding the data bit of interest is the desired data bit or that from one symbol period earlier, which would be the case if the computation has not yet been completed for user $j-1$. The j^{th} user's multistage algorithm should then wait until the status bit for the $j-1^{st}$ user's data shows that the data is ready before computing the MUI estimate for the j^{th} user at that stage. In this way, assuming that the computation of each user's data bit at each stage takes less than T/K seconds, where T is the bit period for each user and K is the number of users, the DFE will be able to operate in real time.

This hybrid algorithm combines the best parts of each DFE, namely Varanasi's multistage flexibility, and Xie's breaking up of the MUI into future and past portions which allows the past half of the MUI to be estimated by more reliable i^{th} stage data estimates at the i^{th} stage. The distinguishing feature of the hybrid multistage algorithm is the first-stage which attempts to cancel half of the MUI terms as opposed to the conventional first-stages of both of the other equalizers.

3.2 Simulation Results

In this work, the various receivers were simulated for a four-user system. The values of the cross-correlations were exaggerated to simulate a highly bandwidth efficient CDMA network. Figure 3.4 shows two sets of signature sequences for a four-user system (the complex envelopes of the signals are shown assuming a carrier phase of zero). The resulting crosscorrelation structure is also shown in this figure. There are many signature sets and delays, in general, which yield the same crosscorrelation structure, and so the signature sets which are shown are provided only to illustrate that the set

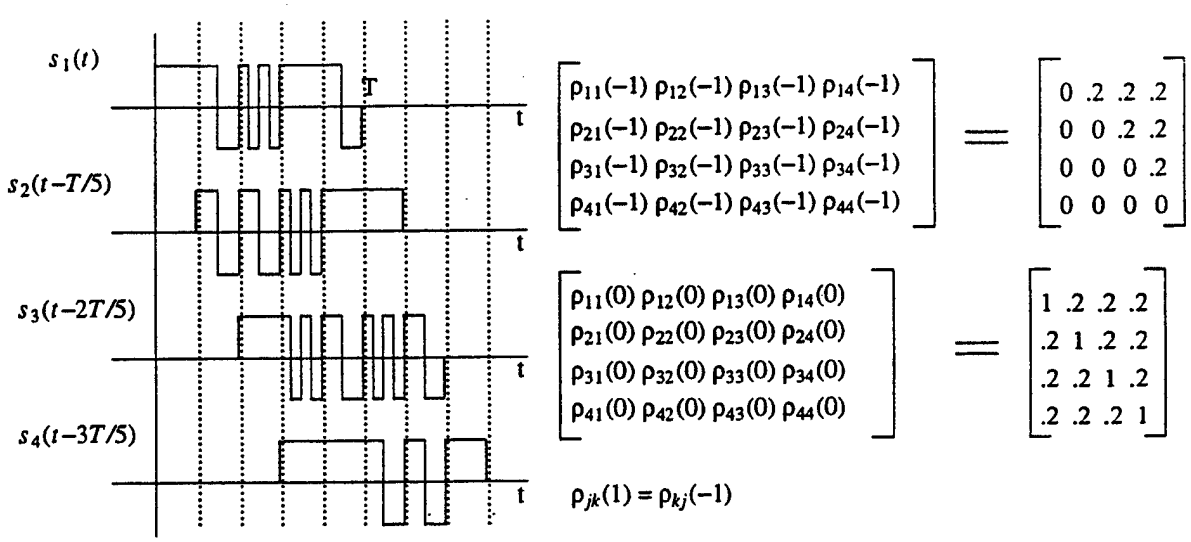

$$\begin{bmatrix} \rho_{11}(-1) & \rho_{12}(-1) & \rho_{13}(-1) & \rho_{14}(-1) \\ \rho_{21}(-1) & \rho_{22}(-1) & \rho_{23}(-1) & \rho_{24}(-1) \\ \rho_{31}(-1) & \rho_{32}(-1) & \rho_{33}(-1) & \rho_{34}(-1) \\ \rho_{41}(-1) & \rho_{42}(-1) & \rho_{43}(-1) & \rho_{44}(-1) \end{bmatrix} = \begin{bmatrix} 0 & .2 & .2 & .2 \\ 0 & 0 & .2 & .2 \\ 0 & 0 & 0 & .2 \\ 0 & 0 & 0 & 0 \end{bmatrix}$$

$$\begin{bmatrix} \rho_{11}(0) & \rho_{12}(0) & \rho_{13}(0) & \rho_{14}(0) \\ \rho_{21}(0) & \rho_{22}(0) & \rho_{23}(0) & \rho_{24}(0) \\ \rho_{31}(0) & \rho_{32}(0) & \rho_{33}(0) & \rho_{34}(0) \\ \rho_{41}(0) & \rho_{42}(0) & \rho_{43}(0) & \rho_{44}(0) \end{bmatrix} = \begin{bmatrix} 1 & .2 & .2 & .2 \\ .2 & 1 & .2 & .2 \\ .2 & .2 & 1 & .2 \\ .2 & .2 & .2 & 1 \end{bmatrix}$$

Figure 3.4a An example set of signature waveforms and delays which yield the correlation structure shown.

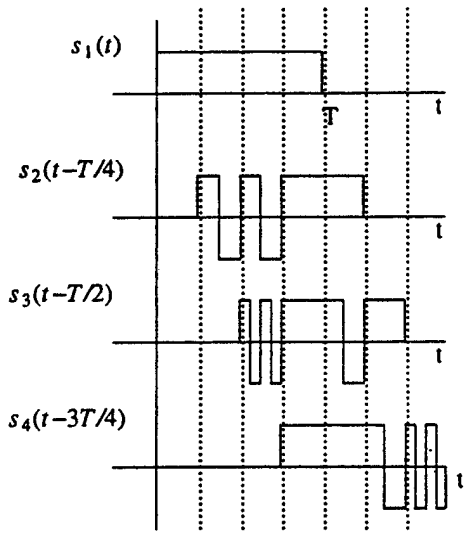

$$\begin{bmatrix} \rho_{11}(-1) & \rho_{12}(-1) & \rho_{13}(-1) & \rho_{14}(-1) \\ \rho_{21}(-1) & \rho_{22}(-1) & \rho_{23}(-1) & \rho_{24}(-1) \\ \rho_{31}(-1) & \rho_{32}(-1) & \rho_{33}(-1) & \rho_{34}(-1) \\ \rho_{41}(-1) & \rho_{42}(-1) & \rho_{43}(-1) & \rho_{44}(-1) \end{bmatrix} = \begin{bmatrix} 0 & .25 & .25 & .25 \\ 0 & 0 & 0 & .25 \\ 0 & 0 & 0 & .25 \\ 0 & 0 & 0 & 0 \end{bmatrix}$$

$$\begin{bmatrix} \rho_{11}(0) & \rho_{12}(0) & \rho_{13}(0) & \rho_{14}(0) \\ \rho_{21}(0) & \rho_{22}(0) & \rho_{23}(0) & \rho_{24}(0) \\ \rho_{31}(0) & \rho_{32}(0) & \rho_{33}(0) & \rho_{34}(0) \\ \rho_{41}(0) & \rho_{42}(0) & \rho_{43}(0) & \rho_{44}(0) \end{bmatrix} = \begin{bmatrix} 1 & .25 & .25 & .25 \\ .25 & 1 & .25 & .5 \\ .25 & .25 & 1 & .25 \\ .25 & .5 & .25 & 1 \end{bmatrix}$$

Figure 3.4b A second set of signature waveforms and delays which yield the more severe correlation structure show

of crosscorrelations simulated are achievable. (It is possible to construct correlation matrices which are not in the range of achievable values.) Both signature sets shown are constructed to provide a high level of MUI which is fairly balanced between the users. This choice of signature waveforms does not necessarily represent an intelligent choice of waveforms for this particular chip-to-symbol rate ratio. It is also probably safe to say that if the MUI was much more severe than that simulated in these examples, then the dominating problem would most likely be that of the initial acquisition of the local oscillators and code sequence generators at the front end of the receiver rather than the performance of the multiuser detectors if synchronization is achieved.

The simulations were performed in the MATLAB environment using the Monte Carlo simulation technique and twenty thousand transmitted bits for each user. The transmitted bits were a random sequence of binomial random variables with a probability of each value being a half (note that sending the all +1's sequence or all -1's sequence does not produce realistic MUI for the other users). The noises were colored properly by generating multidimensional scaled Gaussian random variables for each subinterval of the bit period delineated by the dotted lines in Figure 3.4, and then projecting the random variables onto the subsections of each waveform and finally summing up the projections. It was verified that this method yielded properly colored noise.

Figure 3.5 illustrates the performance of the various DFE structures, and the maximum likelihood sequence estimator (MLSE) for the channel of Figure 3.4a. In this graph, all four users have the same energy level and the performance shown is the average of all of the user's performances. Also, the performance of a single-user system is shown. As expected, Xie's DFE slightly outperforms the second-stage of Varanasi's multistage algorithm due to the decomposition of the MUI into future and past parts. The the hybrid algorithm is able to outperform both of the other DFE approaches.

Figure 3.6 shows the performance of user 1 in a case where E_j/E_1 = 10 dB for $j = 2,3,4$ and the channel of Figure 3.4b. In this case the three-stage hybrid algorithm

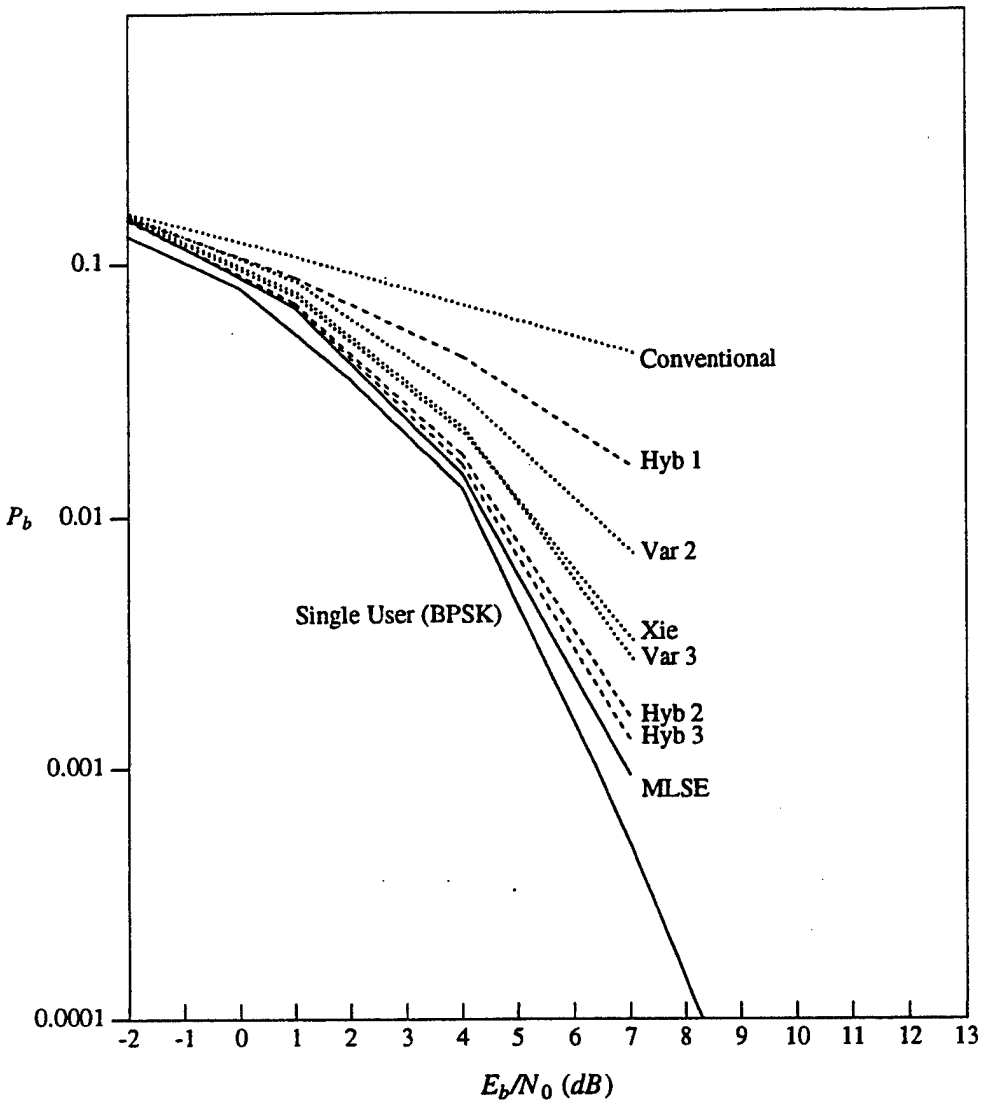

Figure 3.5 Performance curves for a single-user system, a conventional CDMA receiver, the Varanasi multistage algorithm, the Xie DFE, the optimal MLSE and the hybrid algorithm in the 4-user channel shown in Figure 3.4a. Varanasi's Multistage and Xie's DFE are shown as dotted lines, the single-user system and the Verdu MLSE are shown as solid lines, and the hybrid DFE is shown with a dashed line. All users have the same energy.

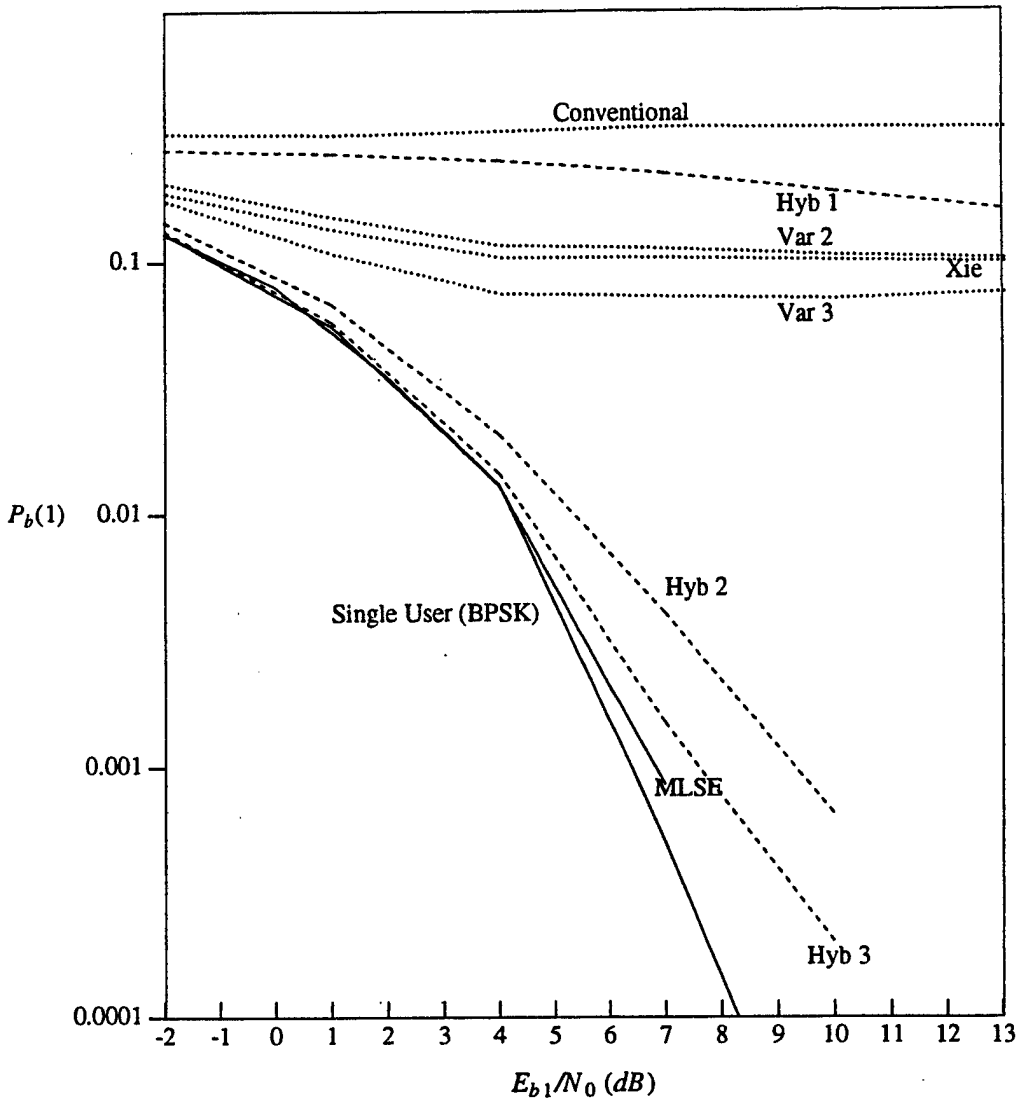

Figure 3.6 Performance curves for a single-user system, a conventional CDMA receiver, the Varanasi multistage algorithm, the Xie DFE, the MLSE and the hybrid algorithm for the 4-user channel of Figure 3.4b with $E_j/E_1 = 10\,dB$ (for all $j \neq 1$). Varanasi's Multistage and the Xie DFE are shown as dotted lines, the MLSE is shown as a solid line and the hybrid DFE is shown with a dashed line.

nearly perfectly cancels the MUI while the other multistage algorithms are hardly able to perform better than the conventional decoder.

Figure 3.7 shows the performance of user 1 for the channel of Figure 3.4b as the energy of the interfering users is varied and E_1/N_0 is fixed at 4 dB. The interesting feature of the graph is that both the optimal sequence estimator and the two and three-stage hybrid DFE's are resistant to the near-far problem on this channel, while the Varanasi and Xie DFE's are not. This implies that for this case, the MLSE and hybrid DFE achieves the single user performance level for sufficiently weak and sufficiently strong interference while the Varanasi and Xie DFE structures only achieve it for sufficiently weak interference. This is due to the fact that as the energy of users 2,3 and 4 becomes large with respect to the energy of user 1 and the noise, user 2's and 4's conventional first-stage has a decision statistic which is dominated by MUI (the MUI term is larger than the desired signal term). Thus as $E_j/E_1 \rightarrow \infty$ and correspondingly $E_j/N_0 \rightarrow \infty, j=2,3,4$, the probability of error for users 2 and 4 does not approach zero and so there will always be some interference doubling for user 1's decision statistic due to incorrect feedback. (Recall that when the feedback is incorrect, the interference is doubled, rather than being cancelled.) Because in this regime, $E_j \gg E_1$, any incorrect feedback of one bit decision will lead to an error with probability 1/2. This implies that the probability of error for user 1 must be greater than the the probability of error that user 1 would have in the absence of MUI.

In the less severe channel of Figure 3.4a, the Varanasi and Xie versions of the DFE are able to acheive the single-user performance level for both sufficiently strong and sufficiently weak interference. This is illustrated in Figure 3.8.

The bottom line in all of these simulations is that the hybrid algorithm outperforms the other algorithms in situations where the conventional first-stages of the Xie and Varanasi DFE's perform badly. In addition, the performance of the hybrid DFE is near that of the optimal MLSE over a wider range of MUI levels than for the other DFE's.

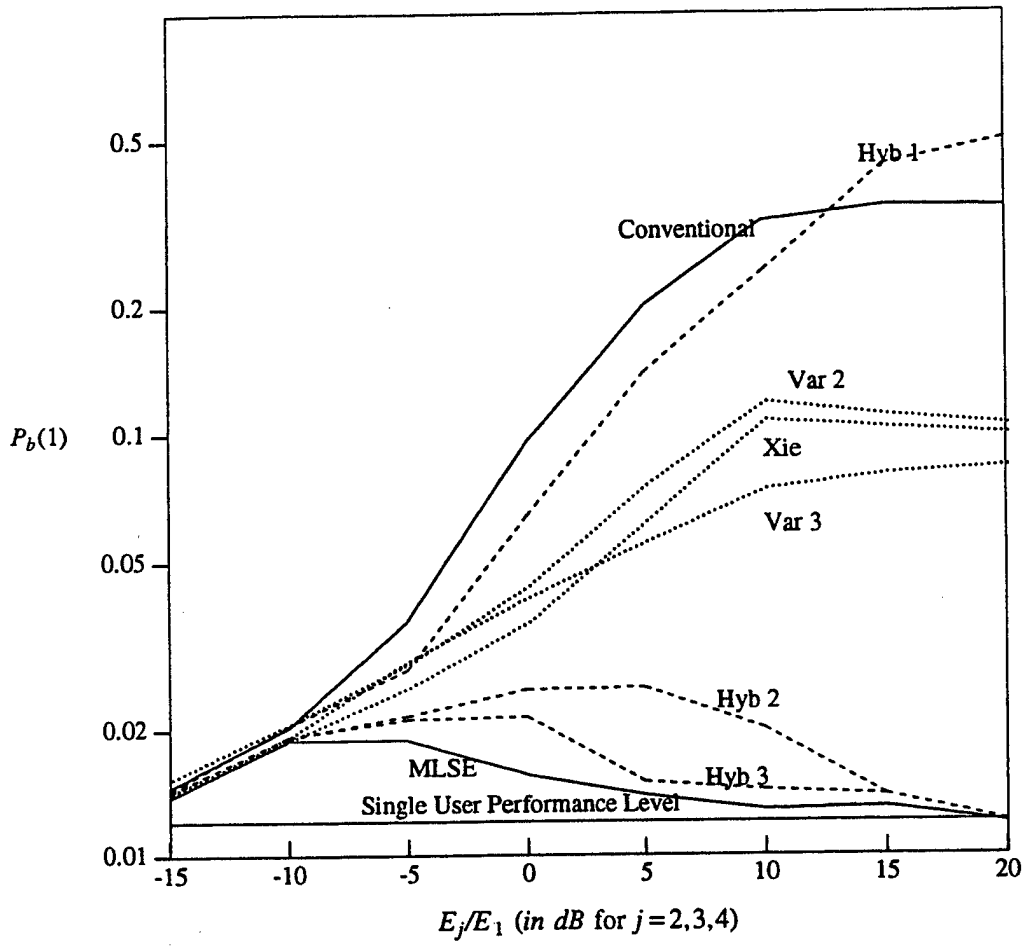

Figure 3.7 Probability of bit error for user one in a 4-user system with $E_b/N_0 = 4$ *dB* for user one and the $\rho = 0.25$ channel of Figure 3.4b plotted versus the energy ratio.

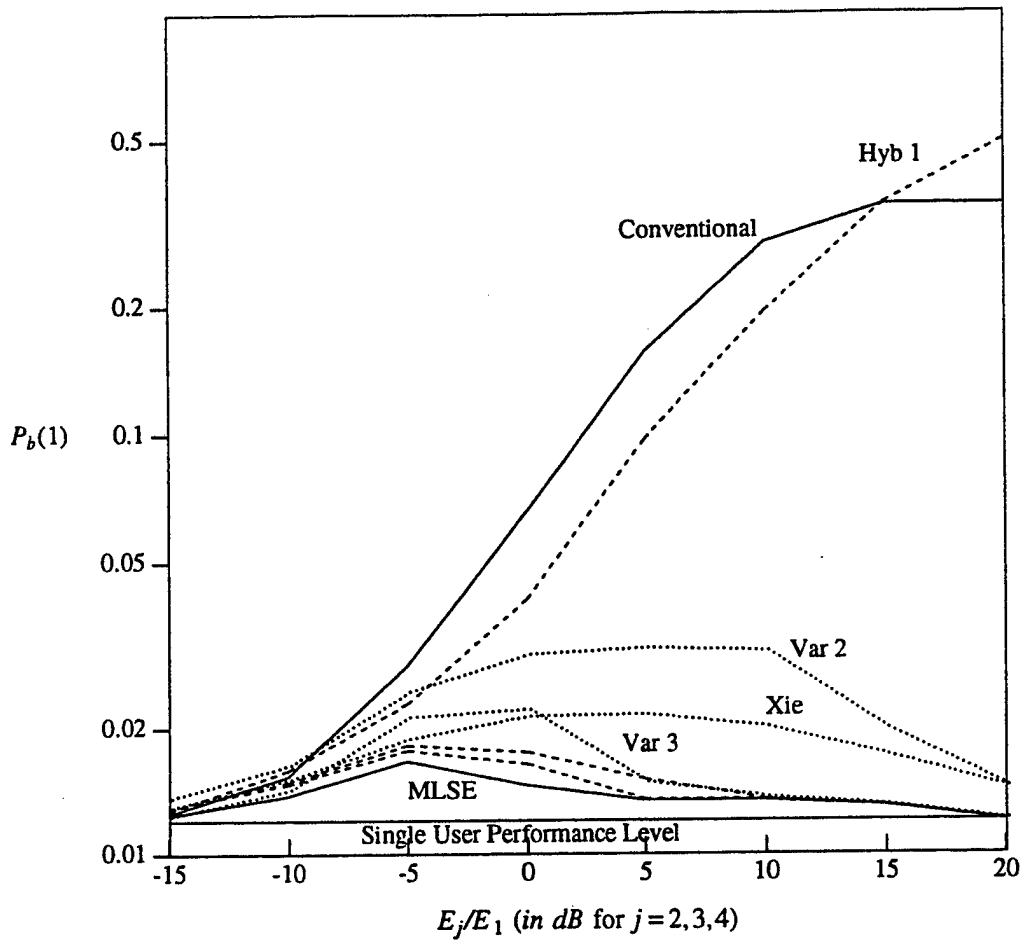

Figure 3.8 Probability of bit error for user one in a 4-user system with $E_b/N_0 = 4$ *dB* for user one and the $\rho = 0.2$ channel of Figure 3.4a plotted versus the energy ratio.

Because the complexity of the hybrid DFE is not much greater than that of the other DFE's (one additional "past MUI estimator" and an adder are necessary for each user), and because the the typical desired operating region for a CDMA network is that with many users, and thus severe MUI, the hybrid DFE is an attractive approach. A nice feature of all of the DFE's discussed here is that they may be implemented in a parallel fashion easily, since it is possible to use multiple processors with a common memory to realize the algorithms. This feature will allow the DFE's to be applied to systems with many users.

3.3 Extensions

The two nonlinear DFE's that have been proposed for CDMA networks led to the development of a hybrid DFE which outperformed the others in all of the situations simulated. We considered only nonlinear DFE's, although it is also possible to combine these DFE's with linear equalizers to form a variety of additional approaches. In [7] and [28], the idea of replacing the conventional first-stage of the Varanasi DFE with a decorrelating filter was considered, and significant performance gains were achieved. In [22] - [24], among other ideas, the idea of replacing the conventional first-stage of the Xie DFE with a decorrelator was considered along with some modifications to the way in which second-stage decisions were formed. These approaches carry with them the added complexity of the decorrelator, but they suggest an obvious extension to the hybrid DFE, namely, that a linear section could be added to the first-stage of the hybrid multistage DFE. This linear section would attempt to eliminate the future MUI from the first-stage's decision statistic either by an inverse filtering approach like that in the DFE in [22] and [23], or by adopting the minimum mean squared error criterion for the future MUI cancellation and using an LMS or RLS approach to adapt the feedforward matrix filter taps. Related ideas were examined in [24].

In [22] -[24], the idea of ordering the users according to their energies rather than their delays was considered. This modification implies that the "future MUI" would take on the meaning of weaker MUI and the "past MUI" would take on the meaning of stronger MUI. It is possible that this modification, when applied to the hybrid would provide better performance. This modification would also mean that the standard hybrid's first-stage would be roughly equivalent to the successive cancellation approaches in [34]. The term successive cancellation refers to approaches wherein the strongest user's signal is decoded first and then remodulated and subtracted from the next strongest user's signal and so on. Thus the hybrid with the users ordered according to energy is a multistage generalization of the successive cancellation schemes.

Another variation of the basic Varanasi DFE is considered in [28]. In this paper, soft decision approaches are employed such as the use of a linear clipper in place of the threshold detector in each stage. These modifications are shown in [28] to provide gains in terms of the asymptotic multiuser efficiency for the two-user case. It is quite reasonable to expect that if these modifications are applied to the Xie DFE or the hybrid DFE, similar gains would be obtained.

Thus in this chapter we have formulated a hybrid DFE which is capable of incorporating the best features of virtually every other DFE that has been proposed. This hybrid DFE shows that the previously proposed approaches have features which are not mutually exclusive, but instead, their features may be combined into a common architecture which outperforms all of the others.

In chapter 5, multiuser receivers which are appropriate for a convolutionally coded CDMA system are proposed which are based on the various DFE's of this chapter. In that chapter, we will see that the DFE category of multiuser receiver is again an attractive approach, in that it has a high performance level and a moderately low complexity. Before examining DFE's for coded links, however, we will first want to consider the optimum sequence estimator in the next chapter to provide a baseline for the best that the

suboptimum approaches of chapter 5 can hope to achieve.

Chapter 4 The Multiuser ML Sequence Estimator for Convolutionally Coded CDMA Links

Now that, among other things, we have reviewed the various types of multiuser receivers that have been proposed for uncoded CDMA systems with additive white Gaussian noise, we are prepared to begin a study of the possible multiuser receiver approaches for coded links. We will begin this study by formulating the optimal sequence estimator in this chapter. An asymptotic analysis and computer simulations will be used to show that this receiver is able to significantly outperform the conventional receiver which was illustrated in Figure 2.6. Furthermore, we will see that the ML sequence estimator is able to achieve a single-user performance level in many situations.

4.1 Optimum Sequence Estimator For Rate-1/2 Convolutional Codes

The optimal MLSE will now be derived for the special case in which each user in the network is employing a rate-1/2 convolutional code with a constraint length W (or memory-order $W-1$), so $T_s = T_b = 2T$. Our limitation to this special case will facilitate considerably the derivation of the decoder, and it will then be outlined how the optimal decoder can be derived in a similar way for a general rate-P/Q convolutional code case.

To begin, it is important to note that the optimal sequence estimator or equalizer for multiple-user uncoded signals operates in a "round-robin" fashion among all K users in the system, [1]. This Viterbi algorithm traverses one trellis stage per channel bit observed per user. The optimal sequence estimator for decoding the rate-1/2 code for one of the users in a single user environment, however, is a Viterbi algorithm which requires two channel observations from the user to move ahead one stage in the trellis. [62] The fact that the equalizer and decoder operate in a fundamentally different way suggests that a slightly different view of the problem is required. The following view of the problem will be adopted in order to bypass this issue. The rate-1/2 convolutional code can be

viewed not as a code which produces two binary bits per information bit period, T_b, but as an equivalent trellis code which produces one 4-ary coded waveform every T_b seconds. By formulating the equalization problem at the receiver with respect to this super-code-symbol view of the received signal, we can accomplish both the tasks of equalization and decoding in the same Viterbi algorithm. Because there is only one 4-ary super-symbol received for each information bit that must be decided, the decoder can be formulated in basically the same fashion as was used in [1] for the MUI problem or [61] for the ISI problem.

We begin by defining the following notation.

$$g_1(t) = \begin{cases} 1 & t \in [0,T) \\ 0 & otherwise \end{cases} \tag{4.1}$$

$$g_2(t) = \begin{cases} 1 & t \in [T,2T) \\ 0 & otherwise \end{cases} \tag{4.2}$$

Next, the following function may be defined

$$\tilde{D}_k(t-nT_b-\tilde{\tau}_k) = D_k^{(1)}(n)\,g_1(t-nT_b-\tilde{\tau}_k) + D_k^{(2)}(n)\,g_2(t-nT_b-\tilde{\tau}_k) \tag{4.3}$$

where, as in Chapter 2, $D_k^{(q)}(n)$ is the k^{th} user's code bit q in the time interval n. Two of the signature-carrier waveforms can likewise be concatenated to form a super-signature waveform.

$$\tilde{s}_k(t-nT_b-\tilde{\tau}_k) = s_k(t-nT_b-\tilde{\tau}_k) + s_k(t-(n+\tfrac{1}{2})T_b-\tilde{\tau}_k) \tag{4.4}$$

This again presumes that the signature sequence repeats every code symbol period. The received waveform may now be written in terms of these waveforms of duration T_b:

$$r(t) = \sum_{n=-\infty}^{\infty} \sum_{k=1}^{K} \tilde{D}_k(t-nT_b-\tilde{\tau}_k)\,\tilde{s}_k(t-nT_b-\tilde{\tau}_k)\sqrt{E_k} + z(t) \tag{4.5}$$

where $z(t)$ is the additive white Gaussian noise with a two-sided spectral density of $N_0/2$. This signal may be viewed as a four-valued super-code symbol, $\{D_k^{(1)}(n), D_k^{(2)}(n)\}$, modulating a pair of orthonormal basis functions through the

procedure defined above. The basis functions in this new view of the waveform are

$$\phi_{1k}(t) = g_1(t)\,\tilde{s}_k(t) \tag{4.6}$$

and

$$\phi_{2k}(t) = g_2(t)\,\tilde{s}_k(t) \tag{4.7}$$

appropriately synchronized with the information bit periods. Thus, this equivalent view of the coding process suggests that the information bits are mapped by the encoder onto waveforms in a space defined by $\phi_{1k}(t)$ and $\phi_{2k}(t)$. Note that although the bases defined in (4.6) and (4.7) are orthonormal, they are not, in general, orthogonal to $\phi_{1j}(t)$ and $\phi_{2j}(t)$ which are the basis set for another user in the system, user j, since $s_k(t)$ and $s_j(t)$ are not orthogonal in general. The result when the received signal is a sum of K component signals is MUI. We now define four parameters which are a measure of the degree of correlation between the basis functions of the different users.

$$\tilde{U}_{jk}(l) = \int_{-\infty}^{\infty} \phi_{1j}(t-\tilde{\tau}_j)\,\phi_{1k}(t-lT_b-\tilde{\tau}_k)dt \tag{4.8}$$

$$\tilde{V}_{jk}(l) = \int_{-\infty}^{\infty} \phi_{2j}(t-\tilde{\tau}_j)\,\phi_{2k}(t-lT_b-\tilde{\tau}_k)dt \tag{4.9}$$

$$\tilde{W}_{jk}(l) = \int_{-\infty}^{\infty} \phi_{1j}(t-\tilde{\tau}_j)\,\phi_{2k}(t-lT_b-\tilde{\tau}_k)dt \tag{4.10}$$

$$\tilde{X}_{jk}(l) = \int_{-\infty}^{\infty} \phi_{2j}(t-\tilde{\tau}_j)\,\phi_{1k}(t-lT_b-\tilde{\tau}_k)dt \tag{4.11}$$

These parameters play the same role in the super-symbol view of the coded signal that $\rho_{jk}(l)$ plays for the standard view of the signal. In fact, $\tilde{U}$, $\tilde{V}$, $\tilde{W}$ and $\tilde{X}$ can be related to ρ directly by substituting (4.4) into (4.6) and (4.7) and then into (4.8) through (4.11).

$$\tilde{U}_{jk}(l) = \rho_{jk}(2l+m_k-m_j) \tag{4.12}$$

$$\tilde{V}_{jk}(l) = \rho_{jk}(2l+m_k-m_j) \tag{4.13}$$

$$\tilde{W}_{jk}(l) = \rho_{jk}(2l+1+m_k-m_j) \tag{4.14}$$

$$\tilde{X}_{jk}(l) = \rho_{jk}(2l-1+m_k-m_j) \tag{4.15}$$

(Recall that $\tilde{\tau}_k = m_k T+\tau_k$, $\tau_k \in [0,T)$, and $m_k \in \{0,...,Q-1\}$.) Note that $\tilde{U}_{jk}(l) = \tilde{V}_{jk}(l) = \tilde{W}_{jk}(l) = \tilde{X}_{jk}(l) = 0$ for $|l|>1$; this fact will play an important role in determining the proper state description of the system for the optimal sequence estimator. Some other useful properties of the correlation parameters are $\tilde{U}_{jk}(l) = \tilde{U}_{kj}(-l)$, $\tilde{V}_{jk}(l) = \tilde{V}_{kj}(-l)$ and $\tilde{X}_{jk}(l) = \tilde{W}_{kj}(-l)$.

Beginning with equation (4.5), note that by performing a modulo-K decomposition of the index i, namely $i = \alpha(i)K+\beta(i)-1$, we can write

$$r(t) = \sum_{i=-M}^{M} \tilde{D}_{\beta(i)}(t-\alpha(i)T_b-\tilde{\tau}_{\beta(i)})\,\tilde{s}_{\beta(i)}(t-\alpha(i)T_b-\tilde{\tau}_{\beta(i)})\sqrt{E_{\beta(i)}} + z(t) \tag{4.16}$$

This assumes that the K users transmit $(2M+1)/K$ information bits each in the time interval of interest and that the signal is zero outside of this interval. We now further simplify the notation by defining the following terms,

$$E^{(i)} = E_{\beta(i)} \tag{4.17}$$

$$D_i^{(q)} = D_{\beta(i)}^{(q)}(\alpha(i)) \tag{4.18}$$

$$\tilde{U}_{im} = \tilde{U}_{\beta(i)\beta(m)}(\alpha(m)-\alpha(i)) \tag{4.19}$$

$$\tilde{V}_{im} = \tilde{V}_{\beta(i)\beta(m)}(\alpha(m)-\alpha(i)) \tag{4.20}$$

$$\tilde{W}_{im} = \tilde{W}_{\beta(i)\beta(m)}(\alpha(m)-\alpha(i)) \tag{4.21}$$

$$\tilde{X}_{im} = \tilde{X}_{\beta(i)\beta(m)}(\alpha(m)-\alpha(i)) \tag{4.22}$$

We have now laid the foundation for the derivation of the MLSE. This development will closely follow the derivation of the optimal MLSE in [61] and [64] for the uncoded ISI channel.

By expanding (4.16) with a Karhunen-Loeve expansion and letting the number of basis functions grow to infinity, we obtain the following waveform metric:

$$\Lambda(\bar{D}_M) = -\int_{-\infty}^{\infty} \Big(r(t) - \sum_{i=-M}^{M} D_i^{(1)} \phi_{1\beta(i)}(t-\alpha(i)T_b-\tilde{\tau}_{\beta(i)})\sqrt{E^{(i)}} + D_i^{(2)} \phi_{2\beta(i)}(t-\alpha(i)T_b-\tilde{\tau}_{\beta(i)})\sqrt{E^{(i)}} \Big)^2 dt \quad (4.23)$$

We next define

$$r_i^{(1)} = r_{\beta(i)}^{(1)}(\alpha(i)) = \int_{-\infty}^{\infty} r(t)\phi_{1\beta(i)}(t-\alpha(i)T_b-\tilde{\tau}_{\beta(i)})dt \quad (4.24)$$

and

$$r_i^{(2)} = r_{\beta(i)}^{(2)}(\alpha(i)) = \int_{-\infty}^{\infty} r(t)\phi_{2\beta(i)}(t-\alpha(i)T_b-\tilde{\tau}_{\beta(i)})dt \quad (4.25)$$

which represent the outputs of a pair of matched filters or correlators for the basis functions for user $\beta(i)$ at time $t = (\alpha(i)+1)T_b + \tilde{\tau}_{\beta(i)}$. By expanding (4.23), and then collecting the appropriate terms we get the following metric.

$$\Lambda(\bar{D}_i) = \Lambda(\bar{D}_{i-1}) + 2\Big[D_i^{(1)}\sqrt{E^{(i)}} \Big(r_i^{(1)} - \sum_{l=1}^{L} \{ D_{i-l}^{(1)} \tilde{U}_{i\,i-l} + D_{i-l}^{(2)} \tilde{W}_{i\,i-l} \}\sqrt{E^{(i-l)}} \Big) + D_i^{(2)}\sqrt{E^{(i)}} \Big(r_i^{(2)} - \sum_{l=1}^{L} \{ D_{i-l}^{(1)} \tilde{X}_{i\,i-l} + D_{i-l}^{(2)} \tilde{V}_{i\,i-l} \}\sqrt{E^{(i-l)}} \Big) \Big] \quad (4.26)$$

where $\bar{D}_i$ represents the multiuser code-symbol sequence up to time interval i, and L is the smallest integer such that for every $L' > L$ we have $\tilde{U}_{jk}(\alpha(L')) = \tilde{V}_{jk}(\alpha(L')) = \tilde{W}_{jk}(\alpha(L')) = \tilde{X}_{jk}(\alpha(L')) = 0$. We have already seen that the correlation parameters are zero when $|\alpha(L')| > 1$, so $L = K-1$.

There are a number of important observations that can be made from the path metric given in equation (4.26). First of all, the i^{th} stage metric depends only on the code symbols in the set

$$\Xi = \{ D_i^{(1)}, D_i^{(2)}, D_{i-1}^{(1)}, D_{i-1}^{(2)}, \ldots, D_{i-K+1}^{(1)}, D_{i-K+1}^{(2)} \}, \quad (4.27)$$

along with the matched filter outputs, $r_i^{(1)}$ and $r_i^{(2)}$, as well as the signal energies and correlations. It is possible to estimate the crosscorrelations using the local oscillators and

code generators which are assumed to be synchronized to the K components of the incoming signal. We can also estimate the energies, $\{E^{(i)}\}$ by averaging the squared outputs of the matched filters for a number of bits. (The number over which they would be averaged would depend on the rate at which the relative strengths of the users is varying.)

For any user, k, the convolutional encoder defines a mapping rule from the input information symbol and present state of the encoder to the code bits, $D_k^{(1)}(n)$ and $D_k^{(2)}(n)$. If we define $h(\cdot)$ as the mapping rule from the input information symbol and state to the 4-ary super-code symbol, $\{D_k^{(1)}(n), D_k^{(2)}(n)\}$ then by substituting the information symbols that define the state of the encoder in for the state, the following expression may be written:

$$\{D_k^{(1)}(n), D_k^{(2)}(n)\} = h\left(I_k(n), I_k(n-1),..., I_k(n-W+1)\right) \tag{4.28}$$

Thus, in this form, it is clear that the 4-ary super-code symbol depends on only W information symbols. Using this information, it is easy to redefine the set Ξ which was defined in equation (4.27) in terms of the information symbols which affect the i^{th} stage metric.

$$\tilde{\Xi} = \{I_i, \sigma_i\} \tag{4.29}$$

$$\sigma_i = \{I_{i-1}, I_{i-2}, \ldots, I_{i-WK+1}\} \tag{4.30}$$

where $I_i = I_{\beta(i)}(\alpha(i))$. Thus it is now apparent that the system may be described in terms of 2^{WK-1} states, since the information symbols are binary. Furthermore, the maximum likelihood sequence estimator can be implemented with a Viterbi algorithm operating on a trellis with 2^{WK-1} states and two branches per state. This trellis will be cyclically time-varying as in the uncoded case, [1]. Furthermore, it is clear that this trellis reduces to the trellis derived in [1] when the constraint length of the code is one (uncoded transmission for each user). Obviously, the number of states in the MLSE grows very quickly with both the number of users in the system and the constraint length, W, of the codes being used. In fact, for a simple 4-user case where each user uses a $W = 3$, or 4-state code, the MLSE requires a Viterbi algorithm operating on a trellis with 2048 states!

The time complexity per bit decoded for the multiuser MLSE is $TCB = O(2^{WK})$ since there are $2 \cdot 2^{WK-1}$ metrics which must be computed at each stage of the trellis and one information bit is decided at each stage. Note that for the case of $W = 1$, the TCB calculated in [1] is again obtained.

Now that the MLSE has been derived for the rate-1/2 case, it is straightforward to generalize to the case of rate-P/Q convolutional codes. The function $\tilde{D}_k(t)$ will again have to be constructed from a set of orthogonal basis functions. One reasonable choice would be a set of Q non-overlapping pulses, each of duration T. Again, the function $\tilde{s}_k(t)$ would be constructed from concatenations of Q versions of $s_k(t)$. The metric derivation could then proceed in the same fashion as in the rate-1/2 case. There are 2^P input hypotheses to test in each T_s for each user, so the overall trellis will have 2^P branches per state. Furthermore, the state of the system will be specified by $(\kappa+P)(K-1)+\kappa$ information bits, so it will have $2^{\kappa K+PK-P}$ states, where $\kappa = \log_2 S$ and S is the number of states in the single user's encoder. This will result in a $TCB = O(2^{\kappa K+PK}/P)$. Because the metrics grow with K as well, the number of arithmetic operations which must be performed for each decoded bit is $O(K\,2^{\kappa K+PK}/P)$. This complexity measure will be used throughout Chapter 5 to compare the complexity of the various receivers as well as the TCB.

Clearly the exponential dependence of the TCB on the number of users, the number of states in each of the user's codes and P makes the use of the optimal decoder prohibitive for a realistic system. It is, however, an important receiver because it represents the best that can be achieved in terms of sequence error probability, and it will provide a good baseline by which to judge the quality of suboptimal schemes. This receiver also raises the possibility of using a variety of sparse searching algorithms like a sequential decoder as was used in [14] for the uncoded case, or reduced state sequence estimation techniques like the ones proposed in [8] and [56] for the uncoded MUI equalization problem or [47] for the combined equalization and decoding problem for single-user links

suffering from ISI.

4.2 Performance of the Optimal Sequence Estimator

To illustrate the derivation of some performance bounds for the MLSE, we will again use the rate 1/2 code example. In this analysis we will fairly closely follow the analysis which appeared in [1] and [61]. In keeping with [1], we consider the decoding window to range from the index $-M$ to the index M. The goal of this section is to estimate the performance of the optimal sequence estimator by bounding the finite and infinite horizon error probabilities for the k^{th} user in the system, denoted $P_k^M(n)$ and $P_k = \lim_{M\to\infty} P_k^M(n)$.

Consider the transmission of the sequence of super-code symbols, $\bar{D} = \{D_i^{(1)}, D_i^{(2)}\}_{i=-M}^{M}$, and a competing sequence in the trellis $\bar{D}+2\bar{e}$ corresponding to the sequence $\{D_i^{(1)}+2e_i^{(1)}, D_i^{(2)}+2e_i^{(2)}\}_{i=-M}^{M}$ where $\bar{e} = \{e_i^{(1)}, e_i^{(2)}\}_{i=-M}^{M}$ is a sequence of code error symbols. Each $e_i^{(q)}$ can take on values in the set $G = \{0, \pm 1\}$. Next, define the following sets:

$$B = \{\, \bar{e}: e_i^{(q)} \in G,\ i=-M,\ldots,M,\ q=1,2,\ e_i^{(q)} \neq 0 \text{ for } \textit{some } i,q \,\} \tag{4.31}$$

$$A(\bar{D}) = \{\, \bar{e}: \bar{e} \in B,\ \bar{D}+2\bar{e} \in C \,\} \tag{4.32}$$

$$C = \{\, \bar{D}: \bar{D} \in h(\{\bar{I}\})\} \tag{4.33}$$

We see above that B is the set of error sequences which have a nonzero element somewhere in the sequence, $A(\bar{D})$ is the set of error sequences in B which have the property that $\bar{D}+2\bar{e}$ is a valid code bit sequence, and C is the set of valid code sequences. Finally, $h(\cdot)$ is the mapping rule defined by the code from an information sequence, $\bar{I}$, to a sequence of super-code symbols, $\bar{D}$, as in (4.28). Since this mapping rule is a one-to-one function, it has an inverse. If we define the information error sequence

$$\bar{\psi} = h^{-1}(\bar{D}+2\bar{e}) - \bar{I} \tag{4.34}$$

which is the information bit error sequence corresponding to $\bar{D}+2\bar{e}$ such that if $\bar{D}=h(\bar{I})$, then $\bar{D}+2\bar{e}=h(\bar{I}+\bar{\psi})$. This allows us to define

$$A_k^M(\bar{D},n)=\{\bar{e}:\bar{e}\in A(\bar{D}),\ \psi_k(n)\neq 0\} \tag{4.35}$$

so $A_k^M(\bar{D},n)$ is the set of admissible error sequences which affect the n^{th} information bit of the k^{th} user. From these definitions, it follows that the probability of error for the n^{th} bit of the k^{th} user is given by

$$P_k^M(n)=\sum_{\bar{D}\in C} P\left[\bigcup_{\bar{e}\in A_k^M(\bar{D},n)}\{\Lambda(\bar{D}+2\bar{e})>\Lambda(\bar{D})\mid \bar{D}\ sent\}\right]\cdot P^M(\bar{D}\ sent) \tag{4.36}$$

As is the usual approach, we choose to bound (4.36) with a union bound.

$$P_k^M(n)\le \sum_{\bar{D}\in C}\ \sum_{\bar{e}\in A_k^M(\bar{D},n)} P(\Lambda(\bar{D}+2\bar{e})>\Lambda(\bar{D})\mid \bar{D}\ sent)\cdot P^M(\bar{D}\ sent) \tag{4.37}$$

The event $\Lambda(\bar{D}+2\bar{e})>\Lambda(\bar{D})$ may now be written by expanding equation (4.23) and substituting

$$r_i^{(1)}=r_{\beta(i)}^{(1)}(\alpha(i))=\sum_{j=i-K+1}^{i+K-1}(D_j^{(1)}\sqrt{E^{(j)}}\,\tilde{U}_{ij}+D_j^{(2)}\sqrt{E^{(j)}}\,\tilde{W}_{ij})+z_i^{(1)} \tag{4.38}$$

and

$$r_i^{(2)}=r_{\beta(i)}^{(2)}(\alpha(i))=\sum_{j=i-K+1}^{i+K-1}(D_j^{(1)}\sqrt{E^{(j)}}\,\tilde{X}_{ij}+D_j^{(2)}\sqrt{E^{(j)}}\,\tilde{V}_{ij})+z_i^{(2)} \tag{4.39}$$

for $r_i^{(1)}$ and $r_i^{(2)}$ respectively, where $z_i^{(1)}$ and $z_i^{(2)}$ are the noise variates at the output of the matched filters for the basis functions $\phi_{1\beta(i)}$ and $\phi_{2\beta(i)}$ respectively for the interval $\alpha(i)$. After some algebra, the following expression for the event $\Lambda(\bar{D}+2\bar{e})>\Lambda(\bar{D})$ is obtained.

$$\sum_{i=-M}^{M}\sum_{m=-M}^{M}(e_i^{(1)}e_m^{(1)}\tilde{U}_{im}+e_i^{(2)}e_m^{(2)}\tilde{V}_{im}+e_i^{(1)}e_m^{(2)}\tilde{W}_{im}+e_i^{(2)}e_m^{(1)}\tilde{X}_{im})\sqrt{E^{(i)}E^{(m)}}$$

$$<\sum_{i=-M}^{M}\sqrt{E^{(i)}}(e_i^{(1)}z_i^{(1)}+e_i^{(2)}z_i^{(2)}) \tag{4.40}$$

Let $\Delta^2(\bar{e})$ represent the left side of equation (4.40). The right side of equation (4.40) is a

linear combination of Gaussian random variables, $z_i^{(1)}$ and $z_i^{(2)}$. It is not difficult to show that $E[z_i^{(1)}] = E[z_i^{(2)}] = 0$ and also that

$$E\left[\begin{bmatrix} z_i^{(1)} \\ z_i^{(2)} \end{bmatrix} (z_m^{(1)}\ z_m^{(2)})\right] = \frac{N_0}{2} \cdot \begin{bmatrix} \tilde{U}_{im} & \tilde{W}_{im} \\ \tilde{X}_{im} & \tilde{V}_{im} \end{bmatrix} \tag{4.41}$$

As a result, if we define γ to be the right side of equation (4.40), then it is not difficult to show that $E[\gamma]=0$ and $Var[\gamma]= \Delta^2(\bar{e}) \cdot N_0/2$.

Next, the two-sequence error probability, or the probability of the event given in equation (4.40), becomes the probability that the Gaussian random variable, γ, is larger than the threshold, $\Delta^2(\bar{e})$. We next define the following efficiency parameter for the pair of sequences differing by the code symbol error sequence $\bar{e}$, as

$$\eta_k^M(\bar{e}) = \frac{\Delta^2(\bar{e})}{2E_k} = \frac{\Delta^2(\bar{e})}{E_{bk}}. \tag{4.42}$$

where $E_{bk} = 2E_k$ is the energy per information bit for user k. This allows us to write

$$P(\Lambda(\bar{D}+2\bar{e}) > \Lambda(\bar{D}) \mid \bar{D}\ sent) = Q\left[\sqrt{\frac{2E_{bk}}{N_0}\eta_k^M(\bar{e})}\right] \tag{4.43}$$

so $\eta_k^M(\bar{e})$ is the asymptotic efficiency relative to uncoded BPSK transmission for the k^{th} user for the pair of sequences $\bar{D}$ and $\bar{D}+2\bar{e}$. This can be shown to reduce to the form of the distance measure in [1] for the uncoded system, because in [1], $\Delta^2(\bar{e})$ may also be expressed as the L_2 norm of the signal generated by modulating the error sequence.

$$S(\bar{e},t) = \sum_{i=-M}^{M} e_i^{(1)}\phi_{1\beta(i)}(t-\alpha(i)T_b-\tilde{\tau}_\beta(i))\sqrt{E^{(i)}} + e_i^{(2)}\phi_{2\beta(i)}(t-\alpha(i)T_b-\tilde{\tau}_\beta(i))\sqrt{E^{(i)}} \tag{4.44}$$

has energy

$$\|S(\bar{e},t)\|^2 = \int_{-\infty}^{\infty} |S(\bar{e},t)|^2 dt = \Delta^2(\bar{e}) \tag{4.45}$$

This implies that an alternate way to express the efficiency parameter defined in (4.42)

for the pair of sequences $\bar{D}$ and $\bar{D}+\bar{e}$ is

$$\eta_k^M(\bar{e}) = \frac{||S(\bar{e},t)||^2}{E_{bk}} \tag{4.46}$$

which is analogous to the form of the distance measure in [1] for the uncoded system.

In order to construct a lower bound on the probability of error for user k, we define the following minimum efficiency as

$$\eta_{k,min}^M(n) = \inf_{\bar{D}\in C} \inf_{\bar{e}\in A_k^M(D,n)} \eta_k^M(\bar{e}) \tag{4.47}$$

so that

$$P_k^M(n) \geq P[\eta_k^M(\bar{e}) = \eta_{k,min}^M(n)] \cdot Q\left[\sqrt{\frac{2E_{bk}}{N_0}\eta_{k,min}^M(n)}\right] \tag{4.48}$$

Thus we now have a lower bound expression for $P_k^M(n)$ given in (4.48). When (4.43) is substituted into equation (4.37) we have an upper bound on $P_k^M(n)$.

To obtain bounds for the infinite horizon error probabilities $P_k = \lim_{M\to\infty} P_k^M(i)$, we may use the same argument used in [1], as it applies equally well to the coded case. Namely for any error sequence $\bar{e}$ such that $e_j=e_n\neq 0$ for $j\neq n$, the sequence

$$\bar{e}' = \begin{cases} e_m & m\leq j \\ e_{m+n-j} & m>j \end{cases} \tag{4.49}$$

satisfies $\Delta^2(\bar{e}')\leq\Delta^2(\bar{e})$ or equivalently $\eta_k^M(\bar{e}')\leq\eta_k^M(\bar{e})$, else it would be possible to construct a sequence with a negative energy. Thus, we may conclude exactly as in [1] that the infinite horizon efficiencies $\eta_k(\bar{e})$ and $\eta_{k,min}$ are achieved by finite length error sequences. As a result, the infinite horizon error probability for the k^{th} user may be lower bounded by

$$P_k \geq P[\eta_k(\bar{e}) = \eta_{k,min}] \cdot Q\left[\sqrt{\frac{2E_{bk}}{N_0}\eta_{k,min}}\right] \tag{4.50}$$

Similarly, by passing (4.37) to the limit as M approaches infinity

$$P_k \le \sum_{\bar{D}\in C} \sum_{\bar{e}\in A_k(\bar{D},n)} P(\bar{D}\ sent)\cdot Q\left[\sqrt{\frac{2E_{bk}}{N_0}\eta_k(\bar{e})}\right], \tag{4.51}$$

where $A_k(\bar{D},n) = \lim_{M\to\infty} A_k^M(\bar{D},n)$. We must note that (4.51) may not converge for all noise levels. In [1], the convergence region was increased by limiting the inner sum to the set of indecomposable sequences. This solution perhaps would be of use here as well to obtain a tighter upper bound, however, we will not focus on this issue here because the convergence of the upper bound will not affect the rest of our analysis.

In the high signal-to-noise ratio regime, the terms in (4.51) with the minimum efficiency will dominate the asymptotic behavior of the receiver. As a result, we will refer to the minimum efficiency, $\eta_{k,min}$ as the *asymptotic multiuser coding gain* for user k (*AMCG*). The *AMCG* is an efficiency parameter which is a measure of the energy gain or loss of the system relative to an uncoded BPSK system operating alone with an energy per information bit of E_{bk}. Observe that $\eta_{k,min}$ depends on the crosscorrelations and relative energies of the users as well as the properties of the code.

In the limiting cases where there is only $K = 1$ user in the system, or when there are K users in the system with perfectly orthogonal super-signature sequences, then $\eta_{k,min}$ is the asymptotic coding gain (*ACG*) of a single-user system operating with the same code. In the special case where the users do not employ coding, $\eta_{k,min}$ is equivalent to the asymptotic multiuser efficiency (*AME*) obtained in [1] for the optimal multiuser receiver for the uncoded system. Thus the asymptotic multiuser coding gain unifies the asymptotic coding gain and the asymptotic multiuser efficiency parameters.

$\eta_k(\bar{e})$ may be rewritten as a quadratic form,

$$\eta_k(\bar{e}) = \frac{1}{2E_k}\bar{e}_\Gamma^T \bar{E}_\Gamma^T \bar{H}_\Gamma \bar{E}_\Gamma \bar{e}_\Gamma. \tag{4.52}$$

To do this, we define the vector $\bar{e}_\Gamma$ to be the subvector of the infinite length error

sequence $\bar{e}$ which consists of all of the nonzero components of $\bar{e}$ and all zero components of $\bar{e}$ which are surrounded by nonzero components. If we assume that the dimension of the vector $\bar{e}_\Gamma$ is $2\Gamma x\, 1$, and

$$\bar{e}_\Gamma = (e_{i_0}^{(1)}, e_{i_0}^{(2)}, e_{i_0+1}^{(1)}, e_{i_0+1}^{(2)}, \ldots, e_{i_0+\Gamma-1}^{(1)}, e_{i_0+\Gamma-1}^{(2)})^T \tag{4.53}$$

then the matrix $\bar{H}_\Gamma$ is defined as $\bar{H}_\Gamma = [\bar{H}_{jk}]_{j,k=i_0}^{i_0+\Gamma-1}$ where the sub matrices are given by

$$\bar{H}_{jk} = \begin{bmatrix} \tilde{U}_{jk} & \tilde{W}_{jk} \\ \tilde{X}_{jk} & \tilde{V}_{jk} \end{bmatrix} . \tag{4.54}$$

Thus, $\bar{H}_\Gamma$ has dimensions $2\Gamma x\, 2\Gamma$. Also, $\bar{E}_\Gamma$ is a diagonal energy matrix with diagonal elements $E_{jj} = (E_{\beta(j)})^{1/2}$.

As an example, consider the 2-user case with each user employing a rate 1/2, 4-state convolutional code, as is shown in Figure 4.2. If user 1 sends an all-zeros sequence, and user 2 sends all-zeros except for stage i_0, where a 1 is sent, then a valid error sequence is

$$\bar{e}_6 = (-1\ -1\ 1\ 1\ 0\ -1\ 0\ 1\ -1\ -1\ 1\ 1)^T. \tag{4.55}$$

For this case, assuming that $m_1 = m_2 = 0$ so that $\tilde{\tau}_1 = \tau_1$ and $\tilde{\tau}_2 = \tau_2$, the $\bar{H}_6$ matrix takes the form

$$\bar{H}_6 = \begin{bmatrix}
1 & 0 & \rho_{21}(0) & 0 & 0 & 0 & 0 & 0 & 0 & 0 & 0 & 0 \\
0 & 1 & \rho_{21}(1) & \rho_{21}(0) & 0 & 0 & 0 & 0 & 0 & 0 & 0 & 0 \\
\rho_{21}(0) & \rho_{21}(1) & 1 & 0 & 0 & 0 & 0 & 0 & 0 & 0 & 0 & 0 \\
0 & \rho_{21}(0) & 0 & 1 & \rho_{21}(1) & 0 & 0 & 0 & 0 & 0 & 0 & 0 \\
0 & 0 & 0 & \rho_{21}(1) & 1 & 0 & \rho_{21}(0) & 0 & 0 & 0 & 0 & 0 \\
0 & 0 & 0 & 0 & 0 & 1 & \rho_{21}(1) & \rho_{21}(0) & 0 & 0 & 0 & 0 \\
0 & 0 & 0 & 0 & \rho_{21}(0) & \rho_{21}(1) & 1 & 0 & 0 & 0 & 0 & 0 \\
0 & 0 & 0 & 0 & 0 & \rho_{21}(0) & 0 & 1 & \rho_{21}(1) & 0 & 0 & 0 \\
0 & 0 & 0 & 0 & 0 & 0 & 0 & \rho_{21}(1) & 1 & 0 & \rho_{21}(0) & 0 \\
0 & 0 & 0 & 0 & 0 & 0 & 0 & 0 & 0 & 1 & \rho_{21}(1) & \rho_{21}(0) \\
0 & 0 & 0 & 0 & 0 & 0 & 0 & 0 & \rho_{21}(0) & \rho_{21}(1) & 1 & 0 \\
0 & 0 & 0 & 0 & 0 & 0 & 0 & 0 & 0 & \rho_{21}(0) & 0 & 1
\end{bmatrix}$$

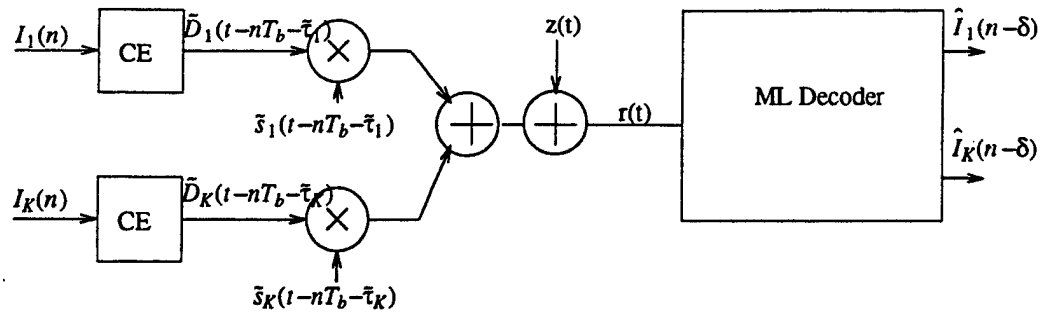

Figure 4.1 Maximum Likelihood Sequence Estimator for a convolutionally encoded CDMA system. CE: Convolutional encoder.

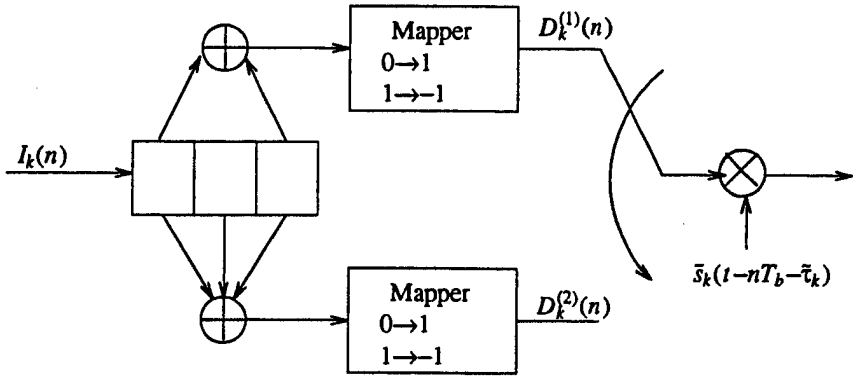

Figure 4.2 Rate 1/2, 4-state convolutional code.

and if the users have equal energy, then the effective efficiency for this error sequence is

$$\eta_1(\bar{e}) = \tfrac{1}{2}\,\bar{e}_6^T\,\bar{H}_6\,\bar{e}_6 = 5 - 5\rho_{21}(0) - 3\rho_{21}(1) \tag{4.57}$$

This implies that for this particular case, a necessary condition for the MLSE to have an asymptotic loss relative to a single-user system is

$$\eta_1(\bar{e}) = 5 - 5\rho_{21}(0) - 3\rho_{21}(1) < d_f/2 \tag{4.58}$$

implying that, because the free distance of the code in use is $d_f = 5$, if

$$\rho_{21}(0) + \frac{3}{5}\rho_{21}(1) > \frac{1}{2} \tag{4.59}$$

then the MLSE decoder **will not** achieve a single-user performance level as $N_0/2 \to 0$.

In the same case, if the user's energies are not equal,

$$\eta_1(\bar{e}_6) = \frac{5}{2} + \frac{5E_2}{2E_1} - \left[\frac{E_2}{E_1}\right]^{1/2}\left[\frac{10}{2}\rho_{21}(0) + \frac{6}{2}\rho_{21}(1)\right]. \tag{4.60}$$

This may be considered an upper bound on $\eta_{1,min}$ since the minimum over all valid error sequences is no larger than the $\eta_k(\bar{e})$ for a particular valid error sequence.

In general an interesting result is obtained when we examine $\eta_k(\bar{e})$ for $\bar{e}$ sequences involving only *single–user* errors. Note that for every $\bar{e} \in A_k(\bar{D},n)$ such that every nonzero element of $\bar{e}$ corresponds to user k, (in other words, only user k is involved in the error event)

$$\eta_k(\bar{e}) = \frac{1}{2E_k}\bar{e}_\Gamma^T\bar{E}_\Gamma^T\bar{H}_\Gamma\bar{E}_\Gamma\bar{e}_\Gamma = \frac{1}{2E_k}\cdot E_k \cdot wt[\bar{e}] = \frac{wt_k[\bar{e}]}{2} \tag{4.61}$$

where $wt[\bar{e}]$ is the weight or number of nonzero elements of $\bar{e}$ (or equivalently $\bar{e}_\Gamma$), and $wt_k[\bar{e}]$ is the weight of user k's subsequence of $\bar{e}$. (User k's subsequence is the set of all $\{e_i^{(1)}, e_i^{(2)}\}$ in $\bar{e}$ such that $\beta(i) = k$.) Because

$$\min_{\substack{\bar{e}\in A_k(\bar{D},n)\\ \bar{D}\in C}} \frac{wt_k[\bar{e}]}{2} = \frac{d_f}{2} \tag{4.62}$$

we have the result that $\eta_k(\bar{e}) \geq d_f/2$ for every $\bar{e} \in A_k(\bar{D},n)$ such that every nonzero element of $\bar{e}$ is contained in user k's subsequence.

This result is important because it implies that single-user error events are not responsible if the AMCG is less than the ACG of a single user system. We thus must examine multiple-user error events to find $\eta_k(\bar{e}) < d_f/2$, (Recall that $d_f/2$ is the ACG for a rate 1/2 convolutional code).

In general, the computation of $\eta_{k,min}$ involves a search over all $\bar{e} \in A_k(\bar{D},n)$ for each $\bar{D} \in C$ reference sequence. Rather than attacking this problem directly, we will lower bound the worst-case efficiency for the 2-user situation, and will then illustrate some nice properties of the MLSE using this bound.

By studying the $\bar{H}_\Gamma$ matrix for this 2-user case, we can obtain a lower bound on the result of equation (4.52) in the following way. Every nonzero element of $\bar{e}_\Gamma$ will multiply its corresponding element of $\bar{e}_\Gamma^T$, the corresponding diagonal element of $\bar{H}_\Gamma$ and be weighted by the energy for that element. We thus have as a part of the result of (4.52) the weight of user 1's error subsequence multiplied by E_1 plus the weight of user 2's error subsequence multiplied by E_2. The remaining terms in the result of (4.52) are due to the product of elements of $\bar{e}_\Gamma$ with other elements of $\bar{e}_\Gamma^T$, weighted by the off-diagonal elements of $\bar{H}_\Gamma$ and $(E_1E_2)^{1/2}$. If we lower bound the addition of these off diagonal terms by a number that is smaller than is achievable by the actual off-diagonal terms, then we have a lower bound on equation (4.52). One possible lower bound on the off diagonal terms leads to the following expression which is only a function of the weight of the error sequences. It turns out that this expression is, in most situations, a somewhat loose lower bound on $\eta_k(\bar{e})$. We will focus on the performance of user 1 without any loss in generality.

$$\eta_1(\bar{e}) \geq \min\left\{ f\left[\left[\frac{E_2}{E_1}\right]^{1/2}, wt_1[\bar{e}], wt_2[\bar{e}], \zeta\right], d_f/2 \right\} \tag{4.63}$$

where

$$f\left(\left[\frac{E_2}{E_1}\right]^{1/2}, wt_1[\bar{e}], wt_2[\bar{e}], \zeta\right) = \tfrac{1}{2}\left(wt_1[\bar{e}] + \frac{E_2}{E_1} wt_2[\bar{e}] - \left[\frac{E_2}{E_1}\right]^{1/2} (2\min\{wt_1[\bar{e}], wt_2[\bar{e}]\}+2)\zeta\right) \tag{4.64}$$

and where $\zeta = |\rho_{21}(0)| + |\rho_{21}(1)|$. The function $f(\cdot)$ is a lower bound on $\eta_1(\bar{e})$ as long as $\bar{e}$ has $wt_1[\bar{e}] > 0$ and $wt_2[\bar{e}] > 0$. We have already seen from (4.61) and (4.62) that $d_f/2$ is a lower bound on $\eta_1(\bar{e})$ when $wt_2[\bar{e}] = 0$, so the smaller of these two expressions is less than $\eta_1(\bar{e})$ for all $\bar{e} \in A_k(\bar{D}, n)$.

For a fixed set of crosscorrelations and signal energies, thus a constant ζ and constant $\sqrt{E_2/E_1}$, the function $f(\sqrt{E_2/E_1}, wt_1[\bar{e}], wt_2[\bar{e}], \zeta)$ describes a family of parabolas, one for each value of $wt_1[\bar{e}]$ and $wt_2[\bar{e}]$. It is easy to show that

$$\min_{\substack{wt_1(\bar{e}) \in \{d_f, d_f+1, \ldots\} \\ wt_2(\bar{e}) \in \{d_f, d_f+1, \ldots\}}} f\left(\left[\frac{E_2}{E_1}\right]^{1/2}, wt_1[\bar{e}], wt_2[\bar{e}], \zeta\right) = f\left(\left[\frac{E_2}{E_1}\right]^{1/2}, d_f, d_f, \zeta\right) \tag{4.65}$$

This result implies that

$$\eta_{1,min} \geq F\left(\left[\frac{E_2}{E_1}\right]^{1/2}, \zeta, d_f\right) = \min\left\{f\left(\left[\frac{E_2}{E_1}\right]^{1/2}, d_f, d_f, \zeta\right), d_f/2\right\} \tag{4.66}$$

which means that we have lower-bounded the AMCG by a function which depends only on the **user's energies, crosscorrelations** and the **free distance of the code.** This bound on $\eta_{1,min}$ is valid only for the 2-user, rate 1/2 code case, but it will illustrate some very important features of the performance of the MLSE which should remain true for the general K-user, rate P/Q code cases as well. This bound will illustrate these performance features without requiring a solution to the NP-hard problem of searching for the actual error sequence, $\bar{e}$, and corresponding reference sequence, $\bar{D}$, which achieve the actual $\eta_{1,min}$.

The first feature of the bound in (4.66) may be noted by examining the plot of $F(\cdot)$ as a function $(E_2/E_1)^{1/2}$ shown in Figure 4.3 for $\zeta = 0.6$ and $d_f = 5$. As the interfering

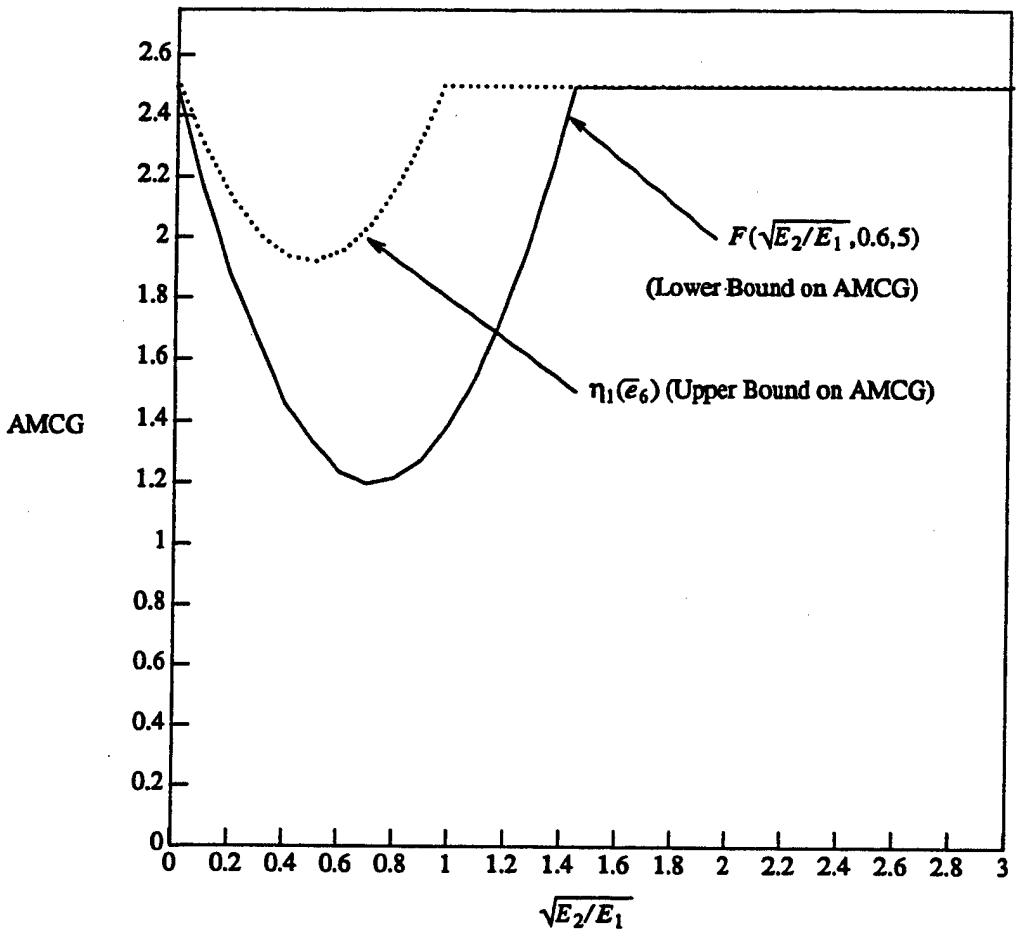

Figure 4.3 Plot of lower bound on $\eta_{1,min}$ for the 2-user, $\rho_{21}(0) = \rho_{21}(1) = 0.3$ case with each user employing the code shown in Figure 2. Also shown is the actual $\eta_1(\bar{e})$ for the specific error event given in equation (4.55).

signal strength, E_2 becomes small relative to E_1, $F(\cdot)$ approaches the ACG of the single user system. Also, as E_2 becomes large relative to E_1, $F(\cdot)$ again reaches the ACG of a single user. In fact, for

$$\left[\frac{E_2}{E_1}\right]^{1/2} > 2\zeta \cdot \frac{d_f+1}{d_f} \tag{4.67}$$

the MLSE necessarily will have the same asymptotic performance as that of a single-user system. In fact, because $F(\cdot)$ is only a lower bound on the AMCG of the receiver, the actual energy ratio above which single-user performance is achieved may be significantly lower than the threshold given in (4.67). This point may be illustrated by the dashed line in Figure 4.3 which is the upper bound given in equation (4.60). Without performing the search for $\eta_{1,min}$, we do not know whether the $\eta_1(\bar{e})$ shown for that particular $\bar{e}$ is the minimum, but if it is, then the actual threshold for $(E_2/E_1)^{1/2}$ above which single-user asymptotic performance is achieved would be 0.96.

Another interesting feature of the bound in equation (4.66) is that it provides a lower bound on the near-far resistance of the MLSE, which is defined as the infimum of $\eta_{k,min}$ over the energies of the interfering users. [4] This infimum for the function $F(\cdot)$ is

$$\inf_{(E_2/E_1)^{1/2} \in [0,\infty)} \eta_{k,min} \geq \inf_{(E_2/E_1)^{1/2} \in [0,\infty)} F\left(\left[\frac{E_2}{E_1}\right]^{1/2}, \zeta, d_f\right) = \frac{d_f}{2} - \frac{\zeta^2}{2d_f}(d_f+1)^2 \tag{4.68}$$

which is positive for

$$\zeta = |\rho_{21}(0)| + |\rho_{21}(1)| < \frac{d_f}{d_f+1} \tag{4.69}$$

A strictly positive near-far resistance implies that the receiver will have a performance that goes to zero at the same exponential rate as a single-user system operating with an energy penalty of $\eta_{1,min}$.

It is also interesting to note that as the code which is employed becomes more powerful, or as d_f increases, the conditions on the crosscorrelations of the users become

progressively less restrictive to achieve near-far resistance. In other words, a stronger code allows the MLSE to remain near-far resistant on a channel with more severe MUI than would be possible with a weaker code. Again, however, because $F(\cdot)$ is simply a lower bound on $\eta_{k,min}$, the actual AMCG may be positive when the minimum of $F(\cdot)$ is not. Nonetheless, the fact that (4.69) implies a positive lower bound is an interesting feature of the bound in (4.66).

4.3 Simulation Results

To provide some direct comparisons between the performance of the MLSE and the conventional receiver in terms of bit error rate at moderate to low E_b/N_0, we will use a computer simulation for some two-user cases. Figure 4.4 shows the results of a simulation of a two-user system where each user employs a 4-state rate 1/2 convolutional code. The resulting super-trellis used by the MLSE has 32 states. Figure 4.4 illustrates a fairly severe MUI environment where $\rho_{12}(0) = 0.3$ and $\rho_{12}(-1) = 0.3$. In this case, the MLSE is able to recoup almost all of the loss that the conventional decoder suffers when compared with the performance in the single-user environment. In Figure 4.5, the same 0.3 channel is simulated for a varying near-far energy ratio. This figure shows that the MLSE approach achieves a single-user performance level for sufficiently strong or sufficiently weak interference. This result is supported by the asymptotic performance suggested by the bound in Figure 4.3. In addition, equation (4.68) suggests that the MLSE is near-far resistant for this case, since $\zeta = 0.6$ and $d_f = 5$. Also, the upper bound on the AMCG in Figure 4.3 suggests that there is not necessarily an asymptotic loss for the MLSE relative to the single-user performance level in the equal-energy case since the AMCG is upper bounded by 2.5 at an energy ratio of one. This is supported by the simulation in Figure 4.4.

Figures 4.6, 4.7 and 4.8 show the performance curves for a more severe two-user channel with $\rho_{12}(0) = 0.4$ and $\rho_{12}(-1) = 0.4$ and the same code. In all of these graphs,

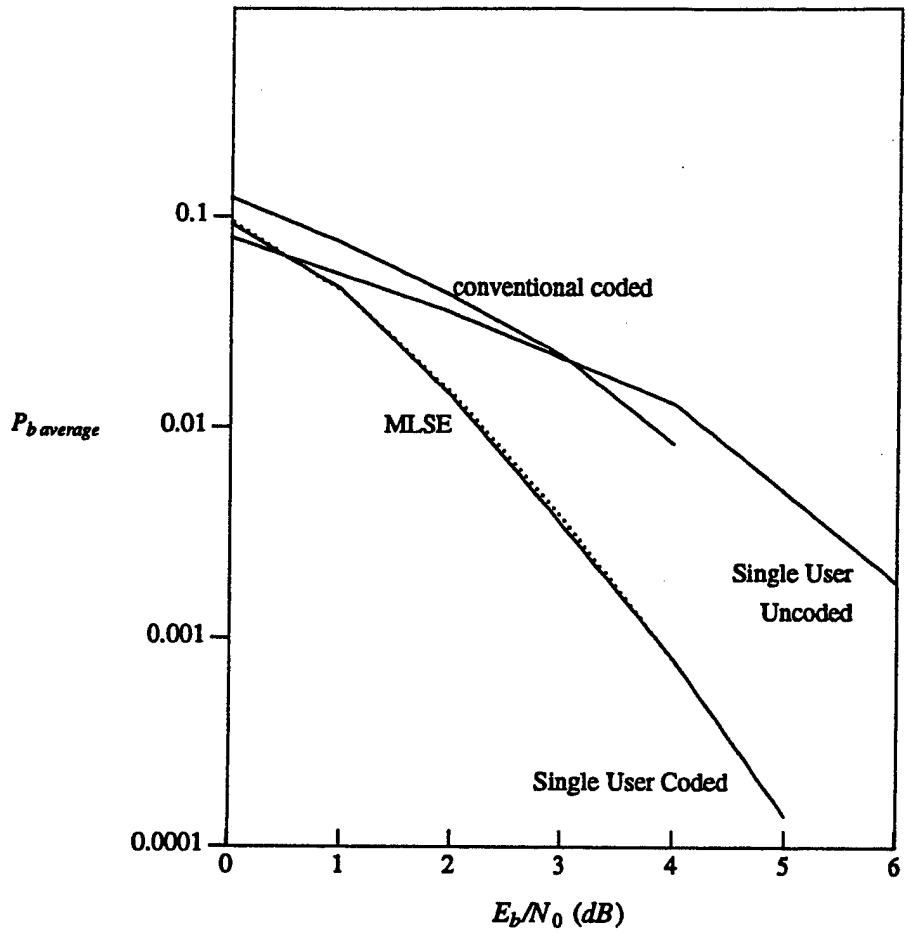

Figure 4.4 Performance curves of the MLSE (dotted line) for a 2-user channel with $\rho_{12}(0) = 0.3$ and $\rho_{12}(-1) = 0.3$ and equal energies. The solid lines show a single-user system (no MUI) with and without the rate-1/2 4-state convolutional code and also a multiuser system with a conventional receiver.

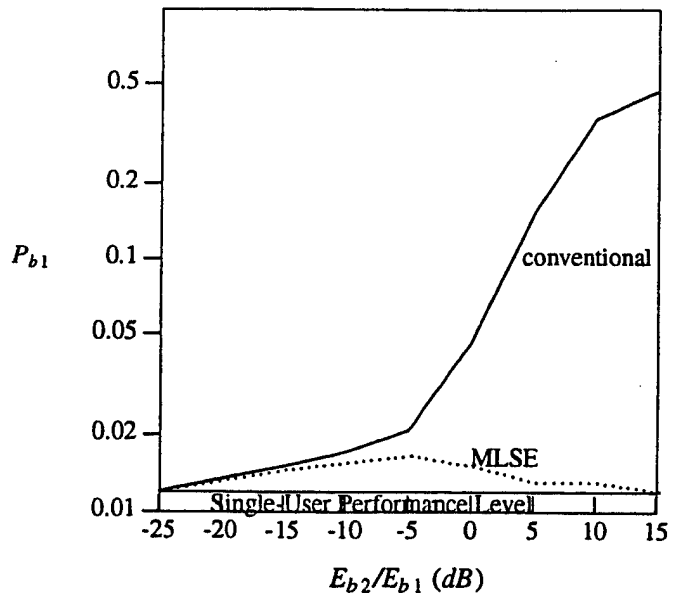

Figure 4.5 Near-far ratio performance curves of the MLSE on a 2-user channel with $\rho_{12}(0) = 0.3$ and $\rho_{12}(-1) = 0.3$ at $E_{b1}/N_0 = 2\ dB$. The single-user system performance level (no MUI) with the rate-1/2 4-state convolutional code is shown as a solid line and the MLSE performance is shown as a dotted line.

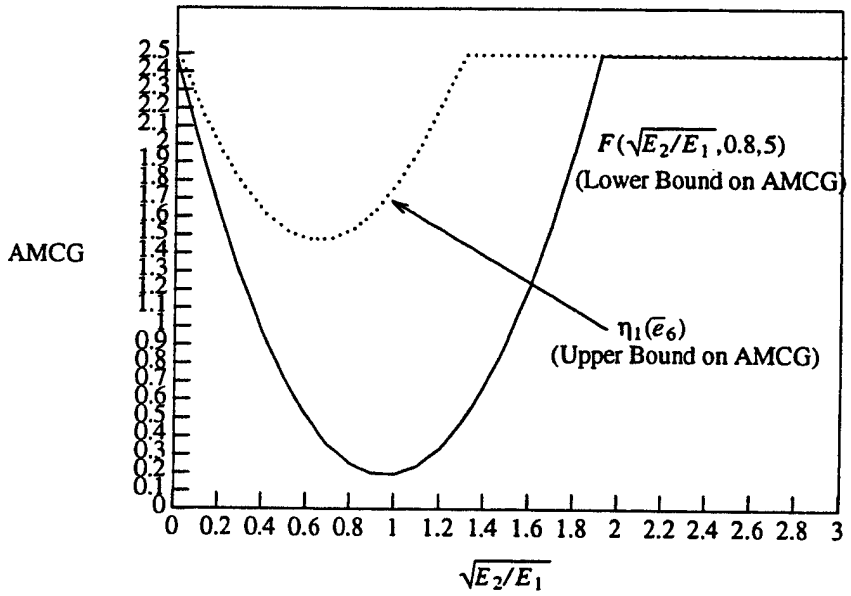

Figure 4.6 Plot of lower bound on $\eta_{1,min}$ for the 2-user, $\rho_{21}(0) = \rho_{21}(1) = 0.4$ case with each user employing the code shown in Figure 2. Also shown is the actual $\eta_1(\bar{e})$ for the specific error event given in equation (4.55).

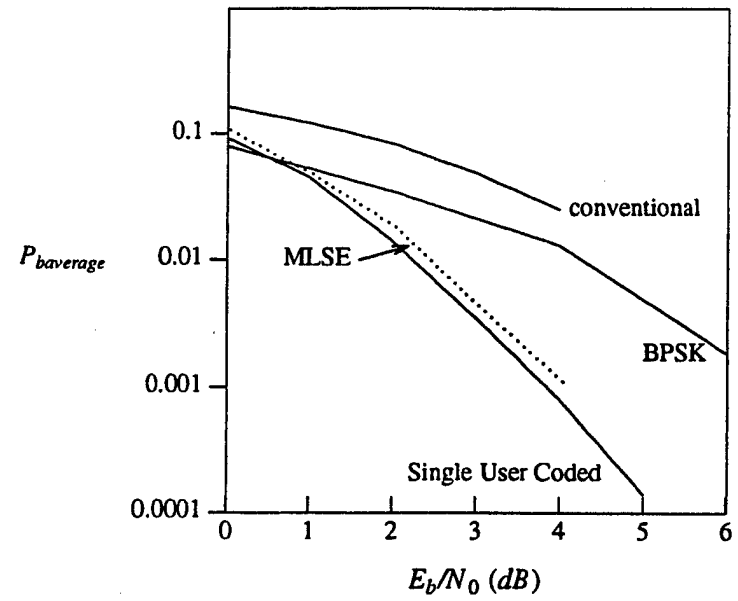

Figure 4.7 Performance curve of the MLSE for a 2-user channel with $\rho_{12}(0) = 0.4$ and $\rho_{12}(-1) = 0.4$ and equal energies. The solid lines show a single user system (no MUI) with and without the rate-1/2 4-state convolutional code.

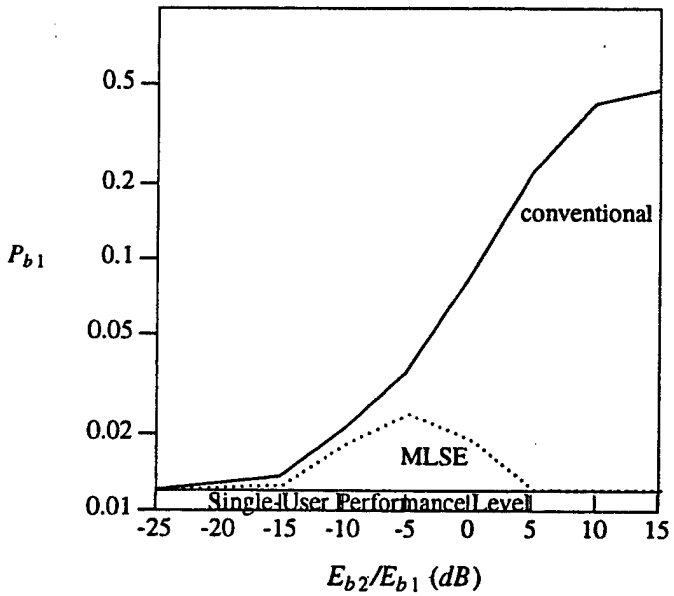

Figure 4.8 Near-far ratio performance curve of the MLSE a 2-user channel with $\rho_{12}(0) = 0.4$ and $\rho_{12}(-1) = 0.4$ at $E_{b1}/N_0 = 2$ dB for the rate-1/2 4-state convolutional code case.

we see that the performance is worse than in the corresponding figures for the 0.3 channel, but again the MLSE is near-far resistant.

It is worth noting that all of the performance analysis in this chapter has been based upon the metric for the case where each user in the system employs rate-1/2 convolutional codes. The expression for the distance and asymptotic multiuser coding gain will be more complicated in the general rate-P/Q code case, but the derivation procedure will be the same. Thus the work in this chapter is meant to illustrate the general procedure for the error analysis of the more complex general code rate case.

In conclusion, in this chapter the maximum likelihood sequence estimator was formulated for CDMA systems where each user employs a convolutional code to improve its performance. It was shown that the complexity of the MLSE has an exponent given by the **product** of W and K (in the rate 1/2 code case). This high complexity points to the use of suboptimal approaches to attempt to attain high performance levels with a more reasonable complexity. In the next chapter we will pursue this goal by introducing a number of suboptimum receiver architectures that are appropriate for coded CDMA links.

Chapter 5 Suboptimum Multiuser Receivers for Convolutionally Coded CDMA Links

In the last chapter, the ML sequence estimator was introduced and we saw that its performance was significantly better than the conventional receiver's, however its complexity was prohibitively high. Motivated by the need for low complexity receivers with a performance level that is similar to the optimal sequence estimator's, we search in this chapter for low-complexity suboptimal receivers. Figure 5.1 outlines the various approaches that will be examined in this chapter.

Through an asymptotic analysis and simulation, it will be shown that these multiuser detection techniques are able to significantly improve the performance of the conventional basestation architecture. In the last chapter, an important performance measure, named the *asymptotic multiuser coding gain* (AMCG), was introduced. This parameter may be defined, in general, as the required energy of a binary antipodal single-user receiver which achieves the same performance as the multiuser receiver (as the noise power approaches zero), divided by the required energy of a *single-user* binary antipodal receiver for an *uncoded* link. Recall that this parameter reduces to the familiar asymptotic multiuser efficiency (AME) parameter for the uncoded multiuser case, and to the asymptotic coding gain (ACG) in the single-user coded case. Several of the decision feedback approaches which will be studied in this chapter do not lend themselves to an analysis in terms of AMCG. As a result, these approaches will be compared with the important baseline architectures via a computer simulation.

Rather than introducing the suboptimum receivers of Figure 5.1 in the order that they appear in the figure, it will be preferable to first discuss the partitioned approaches, and then to discuss the combined equalization and decoding approaches afterwards. This presentation will provide a unified view of the various approaches.

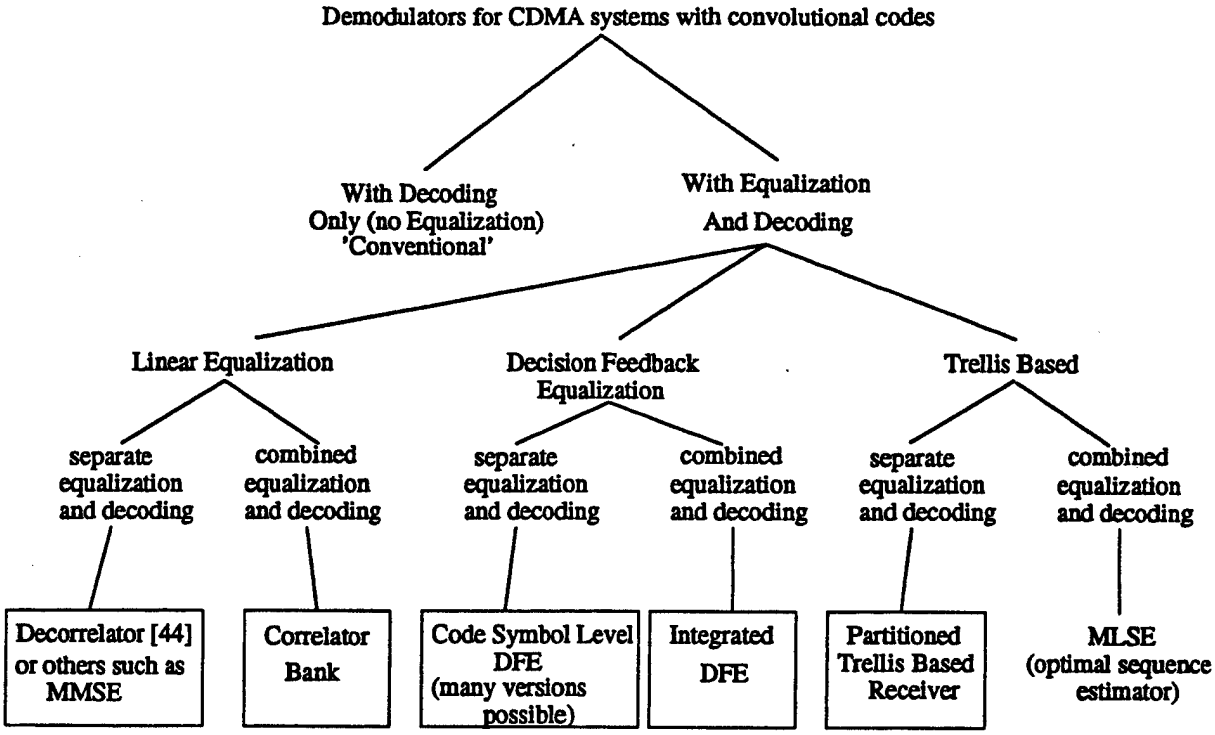

Figure 5.1: Tree diagram of the possible receiver structures for CDMA systems operating with convolutional codes. All of the partitioned approaches (separate equalization and decoding) can be implemented in a hard or soft decision form.
(The approaches in boxes will be discussed in this chapter)

5.1 Hard-Decision Partitioned Approaches

The broad class of multiuser receiver architectures which treat equalization of the MUI and decoding of the code separately as shown in Figure 5.2 will be referred to as *partitioned* multiuser receivers. Within this class of partitioned approaches are those which use a hard-decision multiuser receiver to supply hard decisions from the inner channel to a bank of outer Viterbi decoders, and those which use soft decision multiuser receivers to supply soft-decisions to the outer decoders. For the hard-decision case, sufficient interleaving can provide the outer decoders with statistics which can be accurately modeled as the outputs of a bank of K binary symmetric channels. This level of sufficient interleaving will typically be achieved with a block interleaver which has a width equal to the release depth of the outer Viterbi algorithms (roughly five times the constraint length, W), and a depth greater than the average length of an error event (which is only a few code symbols at high SNR).

Before analyzing the performance of a hard-decision partitioned multiuser receiver, it will be useful to first consider the performance of a hard-decision receiver operating on a coded link with no interferers. Consider, without any loss in generality, the performance of user k operating in isolation. For this case, the crossover probability for the binary symmetric channel is

$$p_k = Q\left[\sqrt{\frac{2E_k}{N_0}}\right] = Q\left[\sqrt{\frac{2E_{bk}}{N_0} R_c}\right] \tag{5.1}$$

since $E_k = R_c E_{bk}$. The first-event error probability in the Viterbi decoder can be bounded by

$$P_e \leq \sum_{d=d_f}^{\infty} a_d P_2(d) \tag{5.2}$$

where a_d is the multiplicity of paths with a distance d from the desired path and $P_2(d)$ is the probability of confusing two sequences which are d Hamming units apart. The bit

error probability can be bounded by a similar sum. If we define

$$t = \left\lfloor \frac{d_f - 1}{2} \right\rfloor \tag{5.3}$$

where the function $\lfloor x \rfloor$ gives the next integer smaller than or equal to x. As $N_0/2 \to 0$, the first-event error probability becomes dominated by the leading term in the series (5.2), namely

$$P_e \approx a_{d_f} P_2(d_f) = a_{d_f} p_k^{t+1} \qquad as\ N_0/2 \to 0 \tag{5.4}$$

This term may be upper-bounded using (5.1) and the asymptotically tight upper bound $Q(x) \leq \frac{1}{2} exp(-x^2/2)$.

$$a_{d_f} p_k^{t+1} \leq a_{d_f} (\tfrac{1}{2})^{t+1} \exp\left[-\frac{E_{bk}}{N_0} R_c (t+1) \right] \tag{5.5}$$

It follows from (5.4) and (5.5) that the ACG for this hard-decision receiver is

$$ACG = R_c (t+1) = R_c \left[\left\lfloor \frac{d_f - 1}{2} \right\rfloor + 1 \right] \tag{5.6}$$

in terms of an absolute ratio, and in terms of decibels as $ACG_{dB} = 10 \log(ACG)$.

With this single-user case as a foundation, we may proceed to analyze the AMCG for a partitioned hard-decision multiuser receiver. Consider again the receiver illustrated by Figure 5.2. If the interleaving is perfect, in the sense that it has an adequate depth to provide a memoryless inner channel for the outer decoders, then the overall channel may be modeled as a bank of K binary symmetric channels. The crossover probability for the k^{th} user's binary symmetric channel is then given by

$$p_k \leq \sum_{\eta \geq \eta_{k,min}^{(inner)}} b_\eta Q\left[\sqrt{\frac{2E_{bk}}{N_0} R_c \eta} \right] \tag{5.7}$$

where $\eta_{k,min}^{(inner)}$ is the AME of the k^{th} user's multiuser receiver which operates on the sequence of code symbols as though they were uncoded symbols, and b_η is the effective

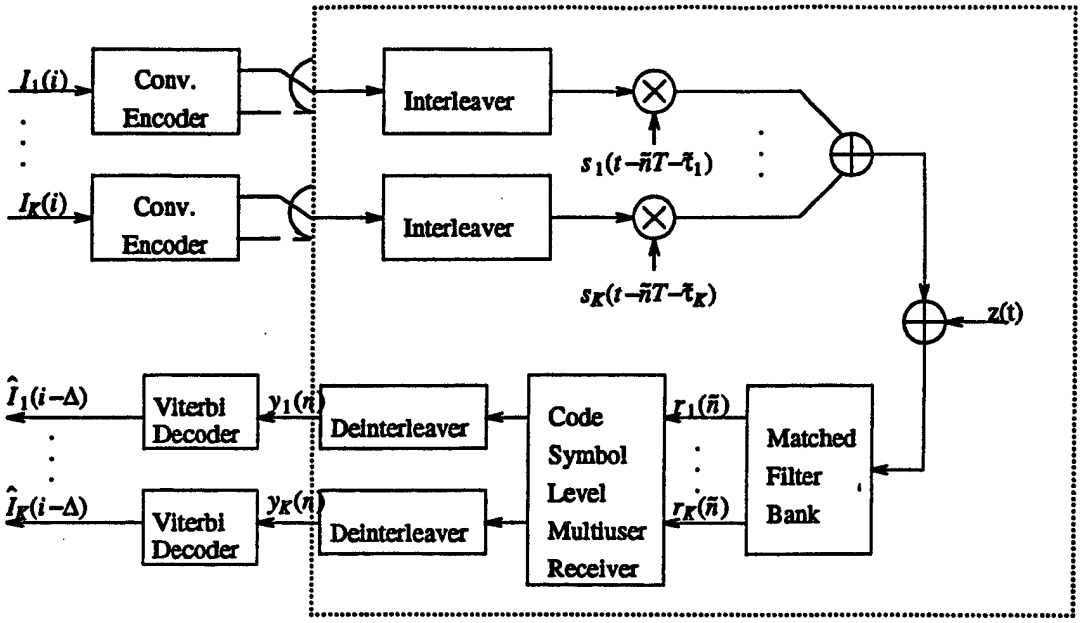

Figure 5.2 CDMA link with a partitioned receiver. If the interleaving can successfully break up the inner channel's memory, then the link within the dotted box may be accurately modeled as K parallel BSCs in the hard-decision multiuser receiver case.
($\bar{n} = n$ if there is no interleaving on the link)

multiplicity of competing sequences of distance η. Equation (5.2) again gives the first-event error probability and the first term of this series will again dominate for low noise situations.

$$P_e \approx a_{d_f} P_2(d_f) \approx a_{d_f} \cdot \left[b_{\eta_{k,min}^{(inner)}} Q\left[\sqrt{\frac{2E_{bk}}{N_0} \cdot R_c \eta_{k,min}^{(inner)}} \right] \right]^{t+1} \qquad as\ N_0/2 \rightarrow 0 \qquad (5.8)$$

As in (5.5), this leading term may be upper bounded as follows

$$a_{d_f} (b_{\eta_{k,min}^{(inner)}})^{t+1} p_k^{t+1} \leq a_{d_f} (\tfrac{1}{2})^{t+1} (b_{\eta_{k,min}^{(inner)}})^{t+1} \exp\left[-\frac{E_{bk}}{N_0} R_c \eta_{k,min}^{(inner)} (t+1) \right] \qquad (5.9)$$

Because this bound is asymptotically tight, we have

$$AMCG_k = \eta_{k,min} = \left[\left\lfloor \frac{d_f - 1}{2} \right\rfloor + 1 \right] \cdot R_c \cdot \eta_{k,min}^{(inner)} \qquad (5.10)$$

as long as the interleaving is perfect.

This is an important result, because it is a simple relation for the AMCG of the overall hard-decision partitioned multiuser receiver in terms of 1) the code rate, 2) the free distance of the code and 3) the AME of the multiuser receiver which is employed for making code bit decisions. The AME has been computed for many multiuser receivers on uncoded links, and so using those results from the literature, we may easily compute the AMCG for the perfectly interleaved hard-decision partitioned receiver of interest.

We now state some of the AME expressions from the literature and use these results to compute the AMCG using (5.10). In [2] and [3], the AME for user one in a two-user system is given for the optimum sequence estimator as

$$\eta_{1,min}^{O} = 1 - \sqrt{\frac{E_2}{E_1}} \left\{ \max\left[0, 2\left|\rho_{21}(0)\right| - \sqrt{\frac{E_2}{E_1}} \right] + \max\left[0, 2\left|\rho_{21}(1)\right| - \sqrt{\frac{E_2}{E_1}} \right] \right\} \qquad (5.11)$$

In [4], the AME for user one in a two-user system is given for the decorrelator with an infinite horizon as

$$\eta^{d}_{1,min} = \sqrt{[1-(\rho_{21}(0)+\rho_{21}(1))^2][1-(\rho_{21}(0)-\rho_{21}(1))^2]} \tag{5.12}$$

In [2] the AME of the conventional receiver was derived for the 2-user case, and the result was

$$\eta^{c}_{1,min} = \begin{cases} 1-2\zeta\sqrt{\frac{E_2}{E_1}}+\zeta^2\frac{E_2}{E_1} & \text{for } \sqrt{\frac{E_2}{E_1}} < \zeta^{-1} \\ 0 & \text{for } \sqrt{\frac{E_2}{E_1}} \geq \zeta^{-1} \end{cases} \tag{5.13}$$

where as in Chapter 4, $\zeta = |\rho_{21}(0)| + |\rho_{21}(1)|$. Finally, in [29], an expression for the AME of the 2-stage Varanasi multistage DFE is given. This expression will not be repeated here for the sake of brevity, but instead the interested reader can refer to [29].

Using all of these expressions and (5.10), we may plot the AMCG for a hard-decision partitioned receiver in a 2-user system with a conventional inner receiver, a decorrelator, and a ML sequence estimator. In Figures 5.3, 5.4, 5.5 and 5.6, the AMCG for user 1 is plotted versus $\sqrt{E_2/E_1}$ for some specific codes and channel conditions. In Figure 5.3, the curves are plotted for the case where both users employ a rate 1/2 4-state code with $d_f = 5$, and $\rho_{21}(0) = \rho_{21}(1) = 0.2$. For this code, by equation (5.6) we know that the ACG for user one operating in isolation is $ACG = 1.5$, or $10\log(1.5)$ dB. Figures 5.4 and 5.5 show the AMCG versus near-far energy ratio again for the same code with $d_f = 5$, but this time with $\rho_{21}(0) = \rho_{21}(1) = 0.3$ in Figure 5.4 and $\rho_{21}(0) = \rho_{21}(1) = 0.4$ in Figure 5.5. These figures illustrate that as the channel cross-correlations become greater, the achievable multiuser coding gain for the partitioned receivers drops, although the benefits of coding remain the same. Figure 5.6 shows the same curves for the case where the codes employed are rate 1/2 64-state codes which have $d_f = 10$, again with $\rho_{21}(0) = \rho_{21}(1) = 0.3$. From this figure and equation (5.10), it is clear that a stronger code is able to improve the achievable multiuser coding gain given the same channel conditions. (compare with Figure 5.4)

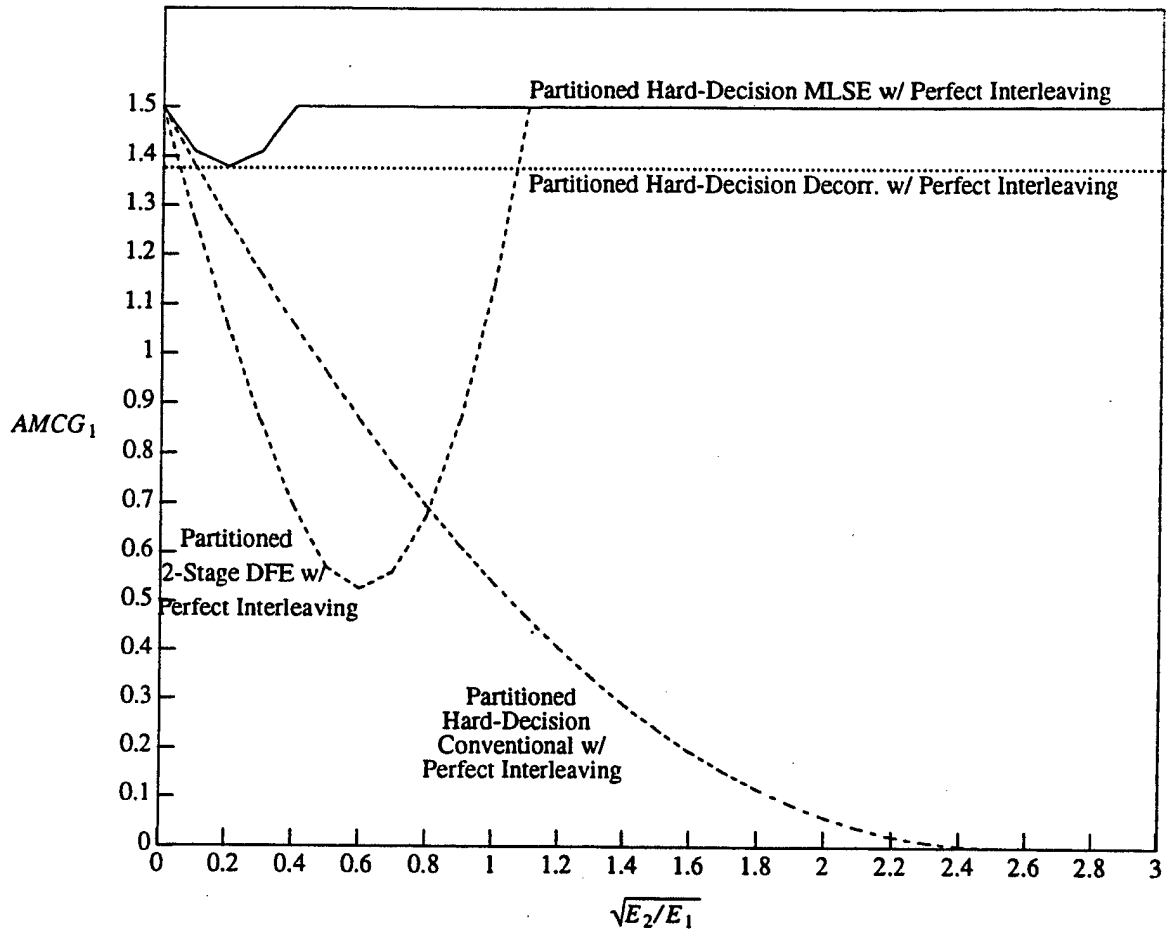

Figure 5.3 Plot of AMCG for the 2-user, $\rho_{21}(0) = \rho_{21}(1) = 0.2$ case where both users employ a rate 1/2 4-state code with $d_f = 5$. The ACG for a single-user system using this code is 10 log (1.5) dB for a hard-decision decoder.

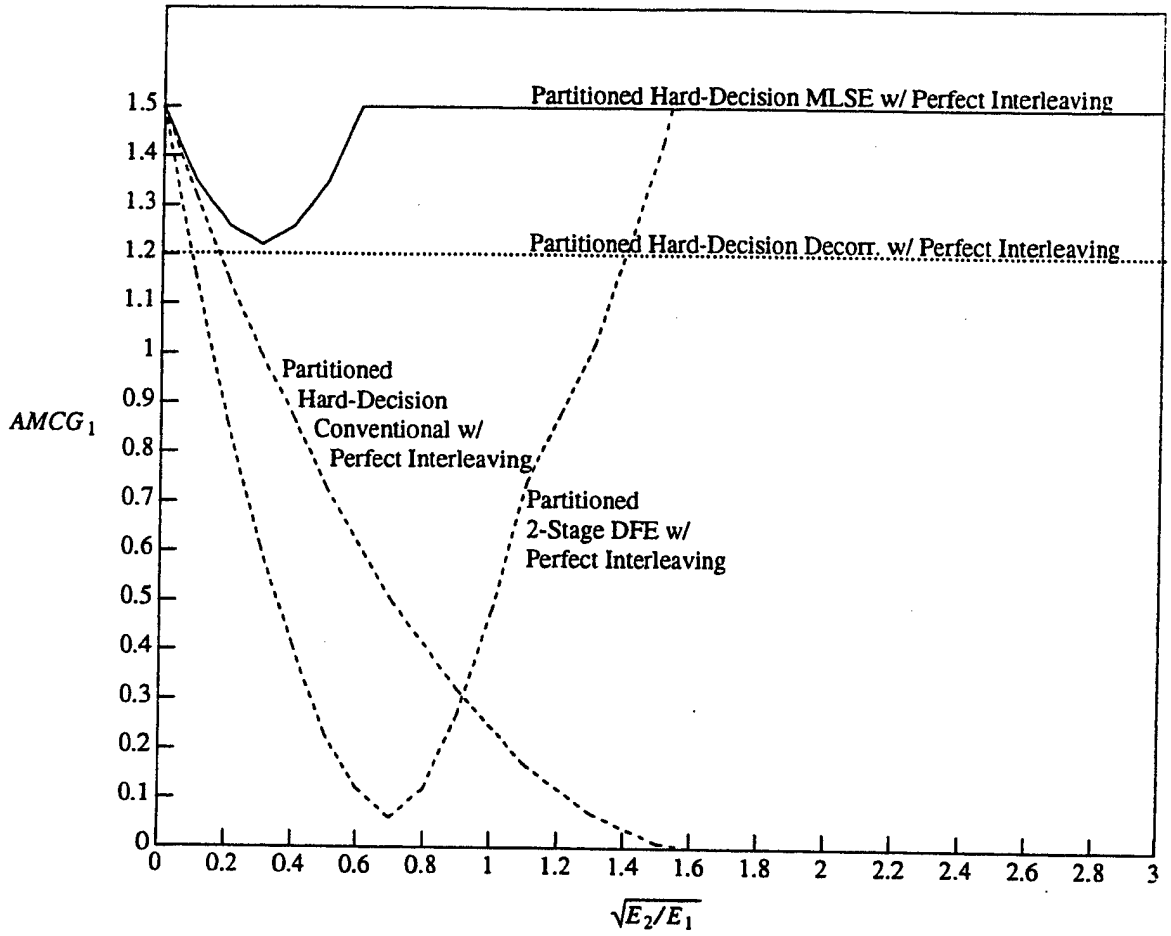

Figure 5.4 Plot of AMCG for the 2-user, $\rho_{21}(0) = \rho_{21}(1) = 0.3$ case where both users employ a rate 1/2 4-state code with $d_f = 5$. The ACG for a single-user system using this code is 10 log (1.5) dB for a hard-decision decoder.

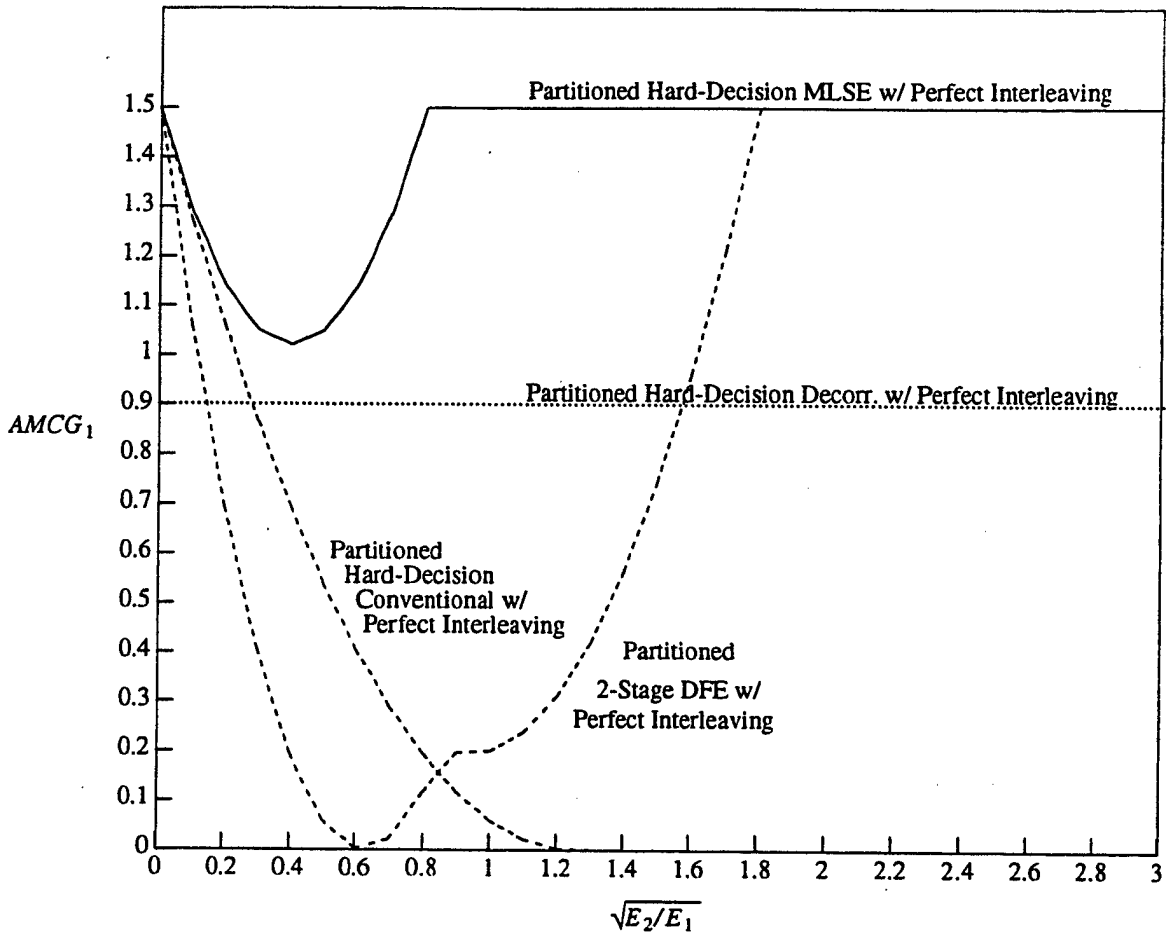

Figure 5.5 Plot of AMCG for the 2-user, $\rho_{21}(0) = \rho_{21}(1) = 0.4$ case where both users employ a rate 1/2 4-state code with $d_f = 5$. The ACG for a single-user system using this code is 10 log (1.5) dB for a hard-decision decoder.

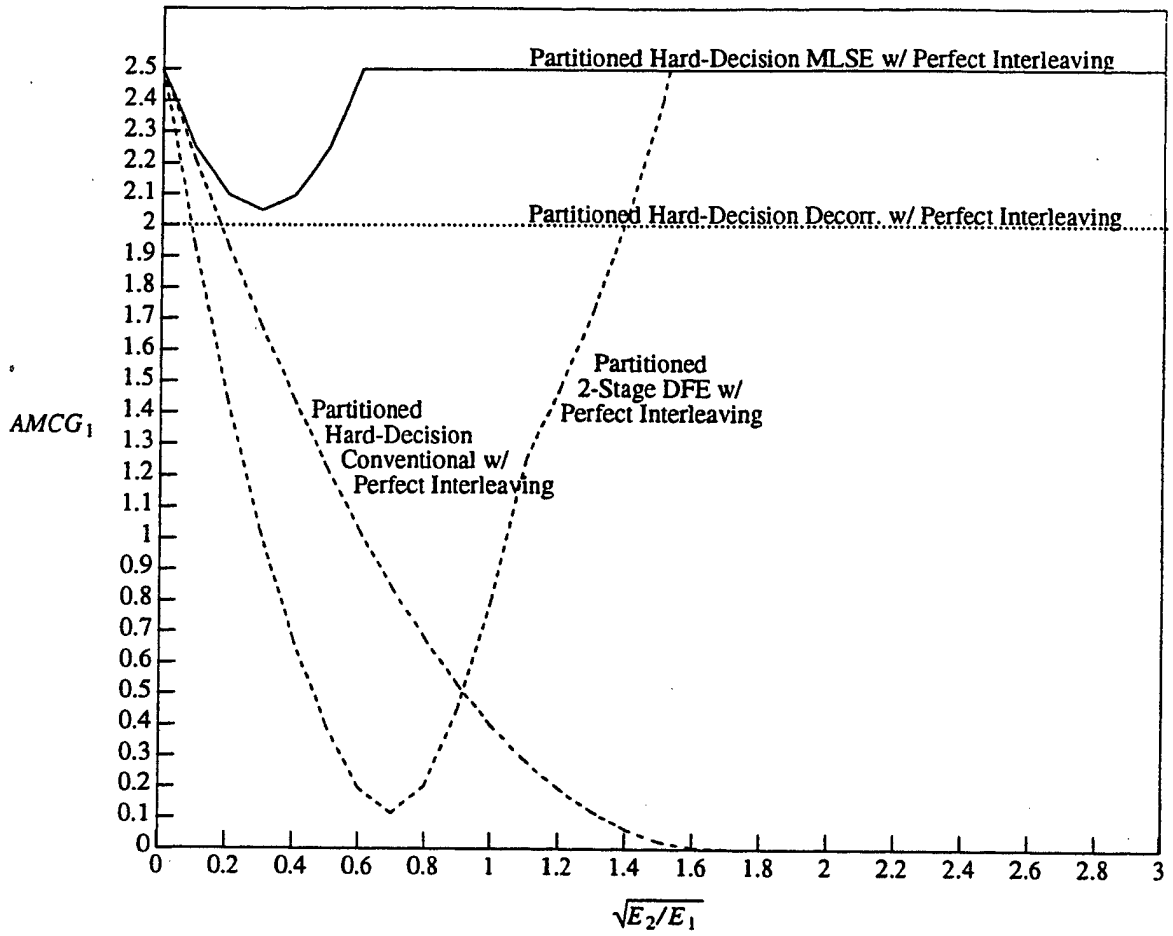

Figure 5.6 Plot of AMCG for the 2-user, $\rho_{21}(0) = \rho_{21}(1) = 0.3$ case where both users employ a rate 1/2 64-state code with $d_f = 10$. The ACG for a single-user system using this code is 10 log (2.5) dB for a hard-decision decoder.

The complexity of the various receivers may be measured with the time complexity per decoded bit. The overall TCB will be the sum of the TCB of the outer Viterbi decoders and Q times the TCB of the inner multiuser receiver since Q code bits must be decided for every stage of the outer decoders. If we assume that the code is a rate P/Q code and has a binary memory order of κ bits, then the outer Viterbi algorithms will have a TCB = $O(2^{\kappa+P}/P)$. (Note that if code puncturing is used to obtain a rate P/Q code from a rate $1/Q$ code, then the complexity of the outer Viterbi algorithms will be TCB = $O(2^{\kappa+1})$ since there are 2^{κ} states and 2 branches per state.) Furthermore, the conventional inner receiver will have $TCB_{conv.} = O(1)$, the MLSE inner receiver will have $TCB_{MLSE} = O(2^{K})$ and the J-stage DFE inner receiver will have $TCB_{DFE} = O(J)$ assuming that the complexity of one MUI calculation is roughly equivalent to a metric calculation (which it often is not). It may be more useful to compare the rough number of arithmetic operations (or multiplications) per decoded bit to make a comparison with the decorrelator. For the MLSE this is $O(K\,2^{K})$, and for the J-stage DFE this is $O(JK)$. We know from Section 2.1.2 that the decorrelator requires roughly $O(\delta K)$ operations per decoded bit if δ is the impulse response truncation depth of a decorrelator which is implemented with an FIR matrix filter. It follows that the overall number of arithmetic operations per decoded information bit for the hard decision partitioned receivers is on the order of $OP_{conv} \approx O(2^{\kappa+P}/P)$ for the conventional inner receiver, $OP_{MLSE} \approx O([QK2^{K}+2^{\kappa+P}]/P)$ for the MLSE inner receiver, $OP_{JDFE} \approx O([QKJ+2^{\kappa+P}]/P)$ for the J-stage DFE inner receiver and $OP_{dec.} \approx O([QK\delta+2^{\kappa+P}]/P)$ for the decorrelator inner receiver.

Another consideration in the choice of receiver architecture might be the decoding delay for the receiver. The overall decoding delay for a partitioned receiver will be the sum of the decoding delay of the inner receiver with that of the deinterleaver with that of the outer Viterbi decoder. The decoding delay of the outer Viterbi decoders will typically be a few times the constraint length, W, of the code in use. We may assume for

comparison's sake that this delay is $\Delta_{VA} = 5WT_s$ seconds. The decoding delay for the conventional inner receiver will be zero, except for maybe the delay associated with the quantization process, (which will be negligible). A J-stage DFE will have a decoding delay of $\Delta_{JDFE} = (J-1)T_s/Q$. An MLSE which has a release depth of $5K$ stages will have a delay of roughly $\Delta_{MLSE} = 5KT/K = 5T_s/Q$ seconds. A decorrelator or MMSE linear inner receiver with an impulse response truncation depth of δ taps will have a decoding delay of $\Delta_{dec.} = \delta T/2 = T_s\delta/2Q$ seconds. This implies that if we neglect the deinterleaver's delay since it will presumably be the same for all receivers, we get the following overall delays for the hard-decision partitioned receivers: $\Delta_{P\,|conv} \approx 5WT_s$ for the conventional inner receiver, $\Delta_{P\,|MLSE} \approx 5T_s/Q + 5WT_s$ for the MLSE inner receiver, $\Delta_{P\,|JDFE} \approx (J-1)T_s/Q + 5WT_s$ for the J-stage DFE inner receiver and $\Delta_{P\,|dec.} \approx \delta T_s/2Q + 5WT_s$ for the decorrelating inner receiver. It is worth noting that all of these decoding delays are roughly the same.

5.2 Soft-Decision Partitioned Approaches

The computation of the AMCG for the soft-decision partitioned approaches is more difficult than for the hard-decision case. We will have to write expressions for the decision statistics at the outer Viterbi decoders for the various inner multiuser receivers, and then upper bound the worst-case values of these decision statistics to obtain lower bound expressions for the AMCG of the overall receivers. It is interesting and important to note that the conventional receiver may be viewed as a member of the class of soft-decisioned partitioned receivers with a degenerate multiuser receiver which simply passes the matched filter outputs to the outer Viterbi algorithms without altering them. As a result, by analyzing the multiuser receivers in this class, we will also be analyzing the important conventional receiver's performance.

Before analyzing the soft-decision partitioned multiuser receivers in detail, however, it will again be useful to first consider the single-user case. To analyze the ACG for

a soft-decision receiver operating in isolation, we begin by bounding the first-event error probability:

$$P_e \leq \sum_{d=d_f}^{\infty} a_d P_2(d) \tag{5.14}$$

where $P_2(d)$ is the probability of confusing two sequences which are a distance d Hamming units apart. The bit error probability will be bounded by a sum which is similar to (5.14). On a standard additive white Gaussian noise channel, the two sequence error probability is given by

$$P_2(d) = Q\left[\sqrt{\frac{2E_{bk}}{N_0} d \cdot R_c}\right] \tag{5.15}$$

Thus using the asymptotically tight bound $Q(x) \leq \frac{1}{2} \exp(-x^2/2)$, we have

$$P_e \leq \sum_{d=d_f} \frac{a_d}{2} \exp\left[-\frac{E_{bk}}{N_0} d R_c\right] \tag{5.16}$$

As $N_0/2 \rightarrow 0$, the first event error probability becomes dominated by the leading term in the series. Thus

$$P_e \approx \frac{a_{d_f}}{2} \exp\left[-\frac{E_{bk}}{N_0} d_f R_c\right] \qquad as\ N_0/2 \rightarrow 0 \tag{5.17}$$

and we may recognize the asymptotic coding gain from (5.17) as

$$ACG = d_f R_c \tag{5.18}$$

which is usually expressed as $ACG_{dB} = 10\log(ACG)$ dB. When this is compared to the hard-decision result in equation (5.10), we see that the soft-decision decoder has between 2 and 3 dB better performance than the hard-decision decoder. This is a familiar result. (See [64] or [67])

With the single-user ACG clearly defined, we may now move on to examine the AMCG for soft-decision partitioned multiuser receivers. Consider the system shown in

Figure 5.2 again. If the deinterleaved outputs of the multiuser receiver are now considered to be soft outputs denoted by $y_k^{(q)}(n)$ for the k^{th} user's code bit q in the n^{th} interval, then the first question to be asked is, "What is the structure of the optimal subsequent decoders?" If $y_k^{(q)}(n)$ is conditionally Gaussian given the information bit sequence for user k, then the appropriate decoding strategy for sequences over a decoding window $n = i_0$ to $i_0 + \Gamma$ is to use a Viterbi algorithm with the following correlation metric

$$\Lambda(\bar{y}_k \mid \bar{D}_k) = \sum_{n=i_0}^{i_0+\Gamma} \sum_{q=1}^{Q} y_k^{(q)}(n) \cdot D_k^{(q)}(n) \tag{5.19}$$

where $\bar{y}_k$ is the deinterleaved sequence of soft decision outputs of user k's multiuser receiver, $\bar{D}_k$ is the sequence of transmitted code symbols for user k. Note that to maintain consistency with the "horizon" used in Chapter 4, $i_0 = \alpha(-M)$ and $\Gamma = \alpha(M) - i_0$.

The notation used in equation (5.19) is going to become overly complex later and so we will simplify this equation by defining a modulo Q decomposition of an index, j, in the same way that we defined the modulo K decomposition in Chapter 4. In this way, we can write (5.19) with a single sum which accumulates all Q of the code bits for each interval, n, for user k.

$$\Lambda(\bar{y}_k \mid \bar{D}_k) = \sum_{j=i_0}^{i_0+Q\Gamma} y_{kj} D_{kj} \tag{5.20}$$

In this equation, $y_{kj} = y_k^{(\alpha(j))}(\beta(j))$, $D_{kj} = D_k^{(\alpha(j))}(\beta(j))$, and $j = \alpha(j)Q + \beta(j) - 1$. (Note that we assume that $i_0 = \beta(i_0)$ without a loss in generality)

The metric for any competing sequence in the trellis $\bar{D}_k + 2\bar{e}_k$ will be

$$\Lambda(\bar{y}_k \mid \bar{D}_k + 2\bar{e}_k) = \sum_{j=i_0}^{i_0+Q\Gamma} y_{kj}[D_{kj} + 2e_{kj}] \tag{5.21}$$

where $\bar{e}_k$ is user $k's$ subsequence of $\bar{e}$ from Chapter 4, and $e_{kj} = e_k^{(\alpha(j))}(\beta(j))$. It thus follows that the two-sequence error probability will be given by

$$P_2(\bar{e}_k) = P[\Lambda(\bar{y}_k \mid \bar{D}_k + 2\bar{e}_k) > \Lambda(\bar{y}_k \mid \bar{D}_k)] = P[\sum_{j=i_0}^{i_0+Q\Gamma} y_{kj} e_{kj} > 0] \tag{5.22}$$

where $P_2(\bar{e}_k)$ denotes the two-sequence error probability for sequences differing by $\bar{e}_k$, and it is assumed that the nonzero portion of the error sequence $\{e_{kj}\}$ occurs in the region $i_0 \le j \le i_0 + Q\Gamma$.

To proceed, we need to be able to characterize y_{kj}. To do this, let

$$y_{kj} = D_{kj}\sqrt{E_k} + N_{kj} \tag{5.23}$$

where N_{kj} is the noise (or perturbation in general) for user k's code bit $\alpha(j)$ in the $\beta(j)^{th}$ interval after deinterleaving the soft-decision multiuser receiver outputs. The characteristics of the noise will depend on the inner multiuser receiver in use.

5.2.1 The Conventional Receiver

With this generic description of the inputs to the outer Viterbi decoders, we may now consider a number of special cases for specific soft-decision multiuser inner receivers. One of the most important special cases of the soft-decision partitioned receiver is the conventional receiver. This receiver essentially uses a degenerate multiuser receiver which simply passes the matched filter outputs on to the outer Viterbi algorithms without altering them in any way, except possibly descrambling them in a deinterleaver. For the conventional receiver, each input to the outer Viterbi algorithms corresponds to a desired part, $D_{kj}\sqrt{E_k}$, and a noise part, corresponding to

$$N_{kj} = RMUI_{kj} + \tilde{z}_{kj} = MUI_{kj} + z_{kj} \tag{5.24}$$

$RMUI_{kj}$ denotes the residual MUI, which for the conventional receiver is equal to the MUI on the matched filter output, and $\tilde{z}_{kj}$ denotes the Gaussian portion of the noise. It is worth noting that this overall noise is not Gaussian, and so the use of the correlation metric in the outer Viterbi decoders is not optimum. The noise is Gaussian conditioned on the signal plus interference, however the outer Viterbi algorithms do not condition on the interference due to the other users. An interesting research topic might be to derive the metric for the outer decoders which is optimal for the noise due to the sum of the

Gaussian noise and the interference. We will not proceed in this direction, but will simply note the suboptimality of the adopted metric. It is worth noting that it is common to appeal to the Central Limit Theorem to claim that the noise is approximately Gaussian. This leads to the claim that the correlation metric is appropriate for the outer decoders. The Central Limit Theorem leads to misleading and overly optimistic conclusions in many cases, however.

Because the noise statistic in (5.24) will be Gaussian conditioned on a given sequence of the desired user and the interferers, we could obtain a performance estimate by averaging with respect to all possible sequences. This performance will be asymptotically determined by the worst-case interference case. As a result, we may bound the residual MUI by its effective worst case value for completely unconstrained interferers to obtain a lower bound on the AMCG of the conventional receiver. The worst case value of $RMUI_{kj}$ when the constraints on the other user's transmitted code sequences are taken into account will be no greater than (and most often lower than) the value assuming unconstrained sequences. If interleaving is used on the link, then the interference patterns will be closer to unconstrained interference patterns since the interleaving will effectively break up the code's constraints. Another point worth noticing is that according to (5.24), the noise on the receiver outputs is the same as the noise on the matched filter outputs, albeit potentially scrambled from the deinterleaving process. The noise sequence $\{z_{kj}\}_{j=1}^{\infty}$ is white, and the deinterleaving will not affect this.

With this characterization of y_{kj}, we may proceed to substitute (5.24) and (5.23) into (5.22).

$$P_2(\overline{e}_k) = P[\sum_{j=i_0}^{i_0+Q\Gamma} e_{kj}z_{kj} > -\sum_{j=i_0}^{i_0+Q\Gamma} e_{kj}(D_{kj}\sqrt{E_k} + MUI_{kj})] \tag{5.25}$$

Next define

$$\beta = \sum_{j=i_0}^{i_0+Q\Gamma} e_{kj}z_{kj} \tag{5.26}$$

Note that whenever $e_{kj} \neq 0$, then $e_{kj} = -D_{kj}$ (since $D_{kj} + 2e_{kj}$ must be a valid error sequence). Making these substitutions we get

$$P_2(\bar{e}_k) = P[\beta > \sum_{j=i_0}^{i_0+Q\Gamma} (e_{kj})^2 \sqrt{E_k} - e_{kj} MUI_{kj}] \tag{5.27}$$

Next, replace $e_{kj} \cdot MUI_{kj}$ by its largest possible value for completely unconstrained interferers,

$$e_{kj}\, MUI_{kj} \leq (e_{kj})^2 \left[\sum_{m=1}^{k-1} |\rho_{km}(1)| \sqrt{E_m} + \sum_{m \neq k} |\rho_{km}(0)| \sqrt{E_m} + \sum_{m=k+1}^{K} |\rho_{km}(-1)| \sqrt{E_m} \right] \tag{5.28}$$

Thus

$$P_2(\bar{e}_k) \leq P[\beta > \sum_{j=i_0}^{i_0+Q\Gamma} (e_{kj})^2 \sqrt{\tilde{E}_k}] \tag{5.29}$$

where

$$\gamma_k = \sqrt{E_k} - \left[\sum_{m=1}^{k-1} |\rho_{km}(1)| \sqrt{E_m} + \sum_{m \neq k} |\rho_{km}(0)| \sqrt{E_m} + \sum_{m=k+1}^{K} |\rho_{km}(-1)| \sqrt{E_m} \right] \tag{5.30}$$

We may next note that

$$wt[\bar{e}_k] = \sum_{j=i_0}^{i_0+Q\Gamma} (e_{kj})^2 \tag{5.31}$$

so (5.29) becomes

$$P_2(\bar{e}_k) \leq P[\beta > wt[\bar{e}_k]\gamma_k] \tag{5.32}$$

Because β is a linear combination of white Gaussian random variables of zero mean and variance $N_0/2$, it is not difficult to show that $E[\beta] = 0$, and $E[\beta^2] = wt[\bar{e}_k] \cdot N_0/2$. It follows that

$$P_2(\bar{e}_k) \leq Q\left[\sqrt{\frac{2E_{bk}}{N_0} \cdot \frac{\gamma_k^2}{E_{bk}} \cdot wt[\bar{e}_k]} \right] \quad \text{for } \gamma_k \geq 0 \tag{5.33}$$

which implies that

$$\eta_k^c(\bar{e}_k) \geq \frac{\gamma_k^2}{E_{bk}} \cdot wt[\bar{e}_k] \qquad \text{for } \gamma_k \geq 0 \tag{5.34}$$

Since γ_k, which was defined in (5.30), may be negative, we may generalize the bound in (5.34) to be

$$\eta_k^c(\bar{e}_k) \geq \max^2\{\, 0,\, \gamma_k (wt[\bar{e}_k]/E_{bk})^{1/2} \tag{5.35}$$

Finally, since $E_{bk} = E_k / R_c$, we note that

$$\eta_k^c \geq \inf_{\bar{e}_k \text{ valid}} \eta_k^c(\bar{e}_k) \geq \max^2\{\, 0,\, \gamma_k (d_f R_c / E_k)^{1/2} \,\} \tag{5.36}$$

Stated in a different form we have the final bound

$$\eta_{k,min}^c \geq \max^2\{\, 0, (d_f R_c)^{1/2} [1 - \sum_{m=1}^{k-1} |\rho_{km}(1)| \left[\frac{E_m}{E_k}\right]^{1/2} - \sum_{m \neq k} |\rho_{km}(0)| \left[\frac{E_m}{E_k}\right]^{1/2} - \sum_{m=k+1}^{K} |\rho_{km}(-1)| \left[\frac{E_m}{E_k}\right]^{1/2}]\}$$

For the 2-user, $R_c = 1/2$ case, this bound takes the form

$$\eta_{1,min}^c > \begin{cases} \frac{d_f}{2}\left[1 - \zeta\sqrt{\frac{E_2}{E_1}}\right]^2 & \text{if } \sqrt{\frac{E_2}{E_1}} < 1/\zeta \\ 0 & \textit{otherwise} \end{cases} \tag{5.38}$$

(recall that $\zeta = |\rho_{21}(0)| + |\rho_{21}(1)|$) This lower bound on the AMCG for the conventional receiver is potentially loose if the coding imposes severe restrictions on the allowable interfering sequences. This is due to the fact that the worst-case allowable interfering sequence may be much less severe than the unconstrained worst case sequence. Nonetheless, with good interleaving, we believe that it will be a reasonable approximation.

The bound in (5.38) is plotted in Figures 5.7, 5.8 and 5.9 for the $\zeta =$ 0.4, 0.6 and 0.8 cases respectively. From these figures, we see that as the energy of the interferer grows, the AMCG of user 1's conventional receiver drops to zero. This zero AMCG typically implies that the receiver will have a performance floor.

The TCB and decoding delay of the conventional receiver with soft-decisions will be the same as those of the partitioned hard-decision receiver with a conventional inner receiver.

5.2.2 Soft-Decision Partitioned Receiver With A Linear Multiuser Receiver

Another interesting class of partitioned receivers is those with a linear inner multiuser receiver, [44]. The most well known members of the class of linear multiuser receivers are the decorrelator, [4] and the minimum mean squared error (MMSE) receivers [17], [21], [24] and [13]. In addition, there are a number of other linear receivers that have appeared in the literature, including the optimal near-far resistant linear receiver in [4].

In this section, we will focus on the decorrelator as a representative of this class because it leads to a tractable analysis. This multiuser receiver has the property that $RMUI_{kj} = 0$ at the decorrelator output, but the variance of $\tilde{z}_{kj}$ will generally be larger than that of z_{kj} due to this receiver's noise enhancement property. For this receiver, we may write the two-sequence error probability as

$$P_2(\bar{e}_k) = P[\sum_{j=i_0}^{i_0+Q\Gamma} e_{kj}\cdot(D_{kj}\sqrt{E_k} + \tilde{z}_{kj}) > 0\,] \tag{5.39}$$

$$= P[\sum_{j=i_0}^{i_0+Q\Gamma} e_{kj}\tilde{z}_{kj} > -\sum_{j=i_0}^{i_0+Q\Gamma} e_{kj}D_{kj}\sqrt{E_k}\,] \tag{5.40}$$

If we next notice that $D_{kj} = -e_{kj}$ whenever $e_{kj} \neq 0$, use (5.31), and redefine β for this section in the same fashion as in (5.26) to now be

$$\beta = \sum_{j=i_0}^{i_0+Q\Gamma} e_{kj}\,\tilde{z}_{kj}\,, \tag{5.41}$$

then we rewrite (5.40) as

$$P_2(\bar{e}_k) = P[\beta > wt[\bar{e}_k]\sqrt{E_k}\,]\,. \tag{5.42}$$

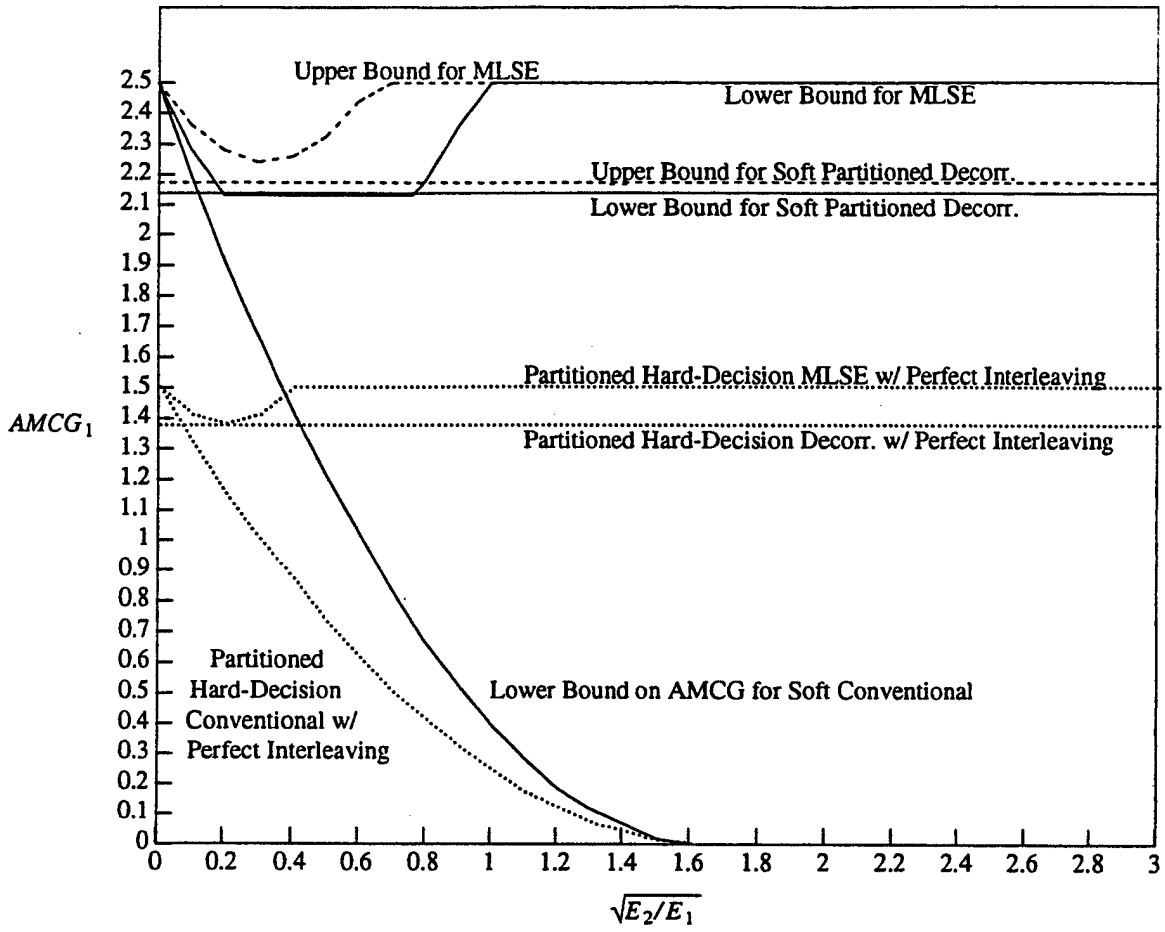

Figure 5.7 Plot of AMCG for the 2-user, $\rho_{21}(0) = \rho_{21}(1) = 0.2$ case where both users employ a rate 1/2 4-state code with $d_f = 5$. The ACG for a single-user system using this code is 10 log (1.5) dB for a hard-decision decoder and 10 log (2.5) dB for a soft-decision decoder. Lower bounds are shown as solid lines, upper bounds as dashed lines, and the partitioned hard-decision approaches are shown as dotted lines for comparison (from Figure 5.3).

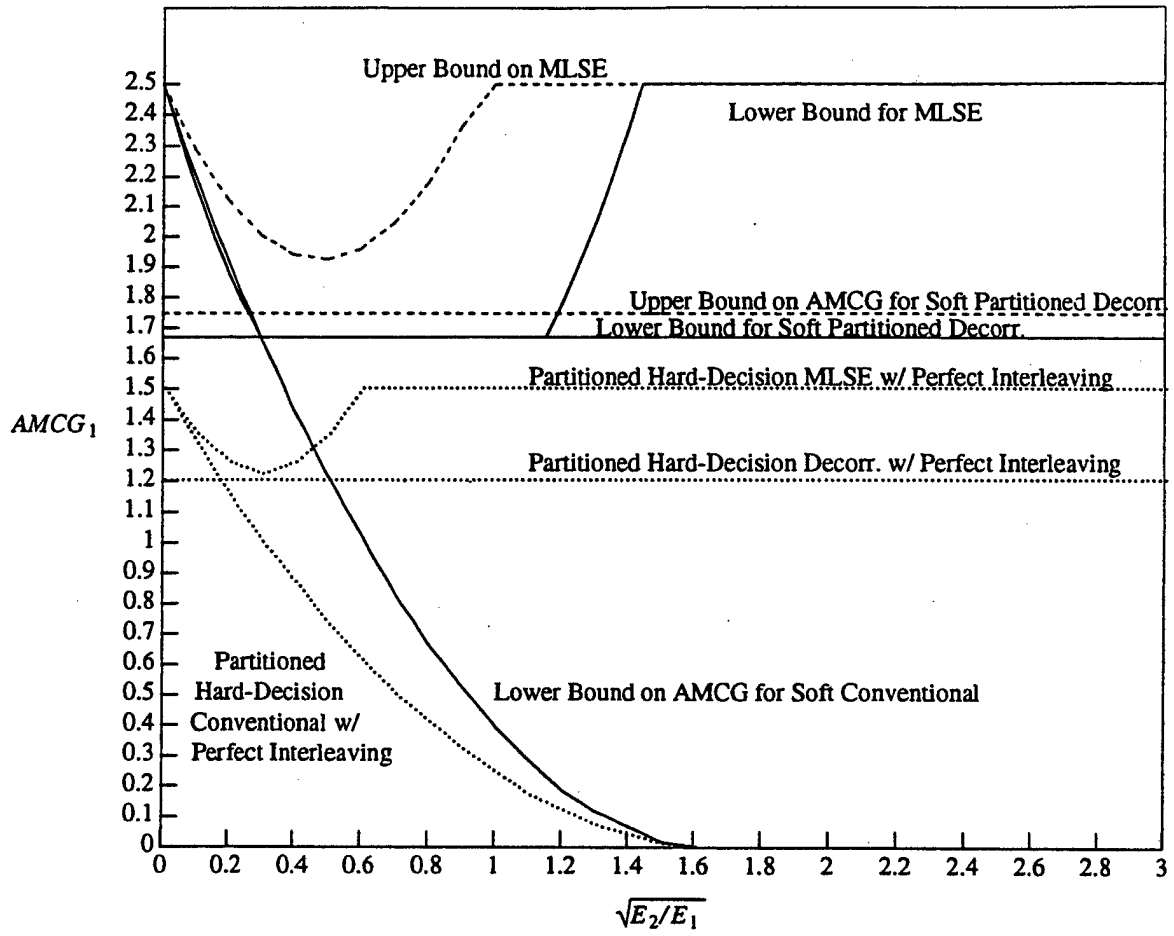

Figure 5.8 Plot of AMCG for the 2-user, $\rho_{21}(0) = \rho_{21}(1) = 0.3$ case where both users employ a rate 1/2 4-state code with $d_f = 5$. The ACG for a single-user system using this code is 10 log (1.5) dB for a hard-decision decoder and 10 log (2.5) dB for a soft-decision decoder. Lower bounds are shown as solid lines, upper bounds as dashed lines, and the partitioned hard-decision approaches are shown as dotted lines for comparison (from Figure 5.4).

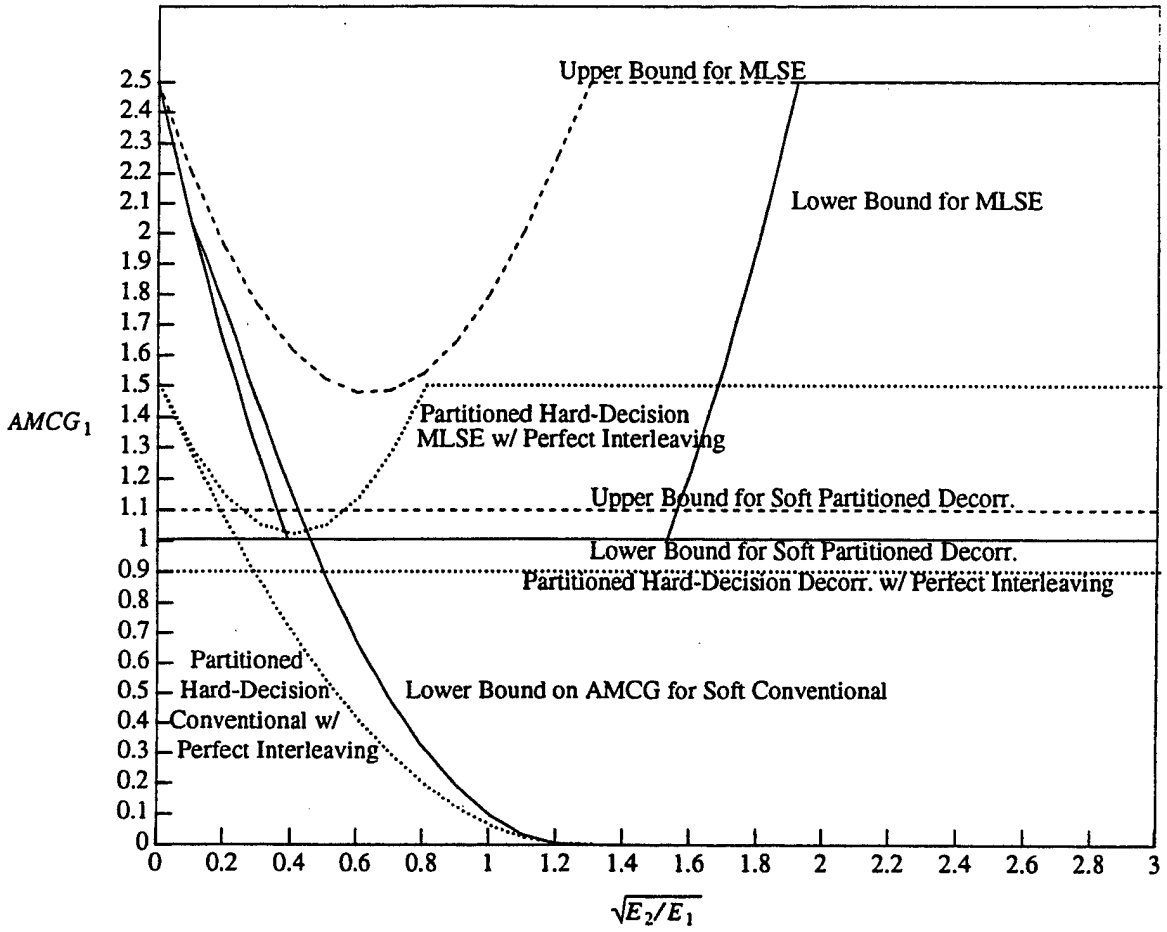

Figure 5.9 Plot of AMCG for the 2-user, $\rho_{21}(0) = \rho_{21}(1) = 0.4$ case where both users employ a rate 1/2 4-state code with $d_f = 5$. The ACG for a single-user system using this code is 10 log (1.5) dB for a hard-decision decoder and 10 log (2.5) dB for a soft-decision decoder. Lower bounds are shown as solid lines, upper bounds as dashed lines, and the partitioned hard-decision approaches are shown as dotted lines for comparison (from Figure 5.5).

β is a linear combination of $\tilde{z}_{kj}$'s which are each, in turn, a linear combination of the matched filter output noises, $\{z_{kj}\}$. It is easy to show that $E[\beta] = 0$. The computation of the second moment of β requires more work, however.

$$E[\beta^2] = E[\sum_{j=i_0}^{i_0+Q\Gamma} e_{kj}\tilde{z}_{kj} \sum_{p=i_0}^{i_0+Q\Gamma} e_{kp}\tilde{z}_{kp}] \tag{5.43}$$

$$= \sum_{j=i_0}^{i_0+Q\Gamma} \sum_{p=i_0}^{i_0+Q\Gamma} e_{kj}e_{kp}E[\tilde{z}_{kj}\tilde{z}_{kp}] \tag{5.44}$$

Next, define

$$E[\tilde{z}_{kj}\tilde{z}_{kp}] = \frac{N_0}{2}\Phi_{kk}(p-j) \tag{5.45}$$

Using this nomenclature, we may proceed to rewrite (5.42) as

$$P_2(\bar{e}_k) = Q\left[\sqrt{\frac{E_k \cdot wt[\bar{e}_k]^2}{E[\beta^2]}}\right] \tag{5.46}$$

$$= Q\left[\sqrt{\frac{2E_{bk}}{N_0} \cdot \frac{R_c wt[\bar{e}_k]^2}{\sum_j \sum_p e_{kj}e_{kp}\Phi_{kk}(p-j)}}\right] \tag{5.47}$$

so it is easy to see from (5.47) that

$$\eta_k^d(\bar{e}_k) = \frac{R_c wt[\bar{e}_k]^2}{\sum_j \sum_p e_{kj}e_{kp}\Phi_{kk}(p-j)} \tag{5.48}$$

$$= \frac{R_c wt[\bar{e}_k]^2}{wt[\bar{e}_k]\Phi_{kk}(0) + 2\sum_{j=i_0}^{i_0+Q\Gamma} \sum_{l=1}^{Q\Gamma} e_{kj}e_{kj-l}\Phi_{kk}(l)} \tag{5.49}$$

Now, all that remains to be done to obtain numerical results is to evaluate $\Phi_{kk}(l)$. We will do this for the 2-user case. If $\bar{\rho}(z)$ denotes the multiuser system channel transfer function matrix (see Section 2.1.2), and so $\bar{\rho}^{-1}(z)$ denotes the decorrelator's transfer function matrix, then for the 2-user case we have, [4]

$$\bar{\rho}^{-1}(z) = \frac{1}{1-\rho_{12}^2-\rho_{21}^2-\rho_{12}\rho_{21}z-\rho_{12}\rho_{21}z^{-1}} \begin{bmatrix} 1 & -(-\rho_{12}+\rho_{21}z^{-1}) \\ -(\rho_{12}+\rho_{21}z) & 1 \end{bmatrix} \quad (5.50)$$

so

$$\rho_{kk}^{-1}(z) = \frac{1}{1-\rho_{12}^2-\rho_{21}^2-\rho_{12}\rho_{21}z-\rho_{12}\rho_{21}z^{-1}} \qquad \text{for } k \in \{1,2\} \quad (5.51)$$

Taking the inverse Z-transform of this polynomial, we obtain

$$\Phi_{kk}(l) = ZT^{-1}[\rho_{kk}^{-1}(z)] = \frac{(1-\rho_{12}^2-\rho_{21}^2-\sqrt{[1-(\rho_{12}+\rho_{21})^2][1-(\rho_{12}-\rho_{21})^2]})^{|l|}}{(2\rho_{12}\rho_{21})^{|l|}\sqrt{[1-(\rho_{12}+\rho_{21})^2][1-(\rho_{12}-\rho_{21})^2]}} \quad (5.52)$$

where $\rho_{12} = \rho_{21}(0)$, and $\rho_{21} = \rho_{21}(1)$. [4]

We may write the denominator of (5.48) as a matrix quadratic form

$$\eta_k^d(\bar{e}_k) = \frac{R_c \cdot wt[\bar{e}_k]}{\bar{e}_k^T \bar{\Phi}_{kk} \bar{e}_k} \quad (5.53)$$

where $\bar{\Phi}_{kk}$ is a positive-definite Toeplitz matrix with elements

$$[\bar{\Phi}_{kk}]_{ij} = \Phi_{kk}(i-j) \quad (5.54)$$

Next, if we note that the Rayleigh product may be upper bounded by the largest eigenvalue of $\bar{\Phi}_{kk}$, namely $\lambda_{\max}$,

$$\frac{\bar{e}_k^T \bar{\Phi}_{kk} \bar{e}_k}{\bar{e}_k^T \bar{e}_k} \le \lambda_{\max} \quad (5.55)$$

and we note that $\bar{e}_k^T \bar{e}_k = wt[\bar{e}_k]$, then we obtain the following lower bound

$$\eta_k^d(\bar{e}_k) \ge \frac{R_c \cdot wt[\bar{e}_k]}{\lambda_{\max}} \quad (5.56)$$

A lower bound on the AMCG would then be the following

$$\eta_{k,min}^d \ge \min_{wt[\bar{e}_k] \in \{d_f, d_f+1, \ldots\}} \frac{R_c \cdot wt[\bar{e}_k]}{\lambda_{\max}} = \frac{R_c d_f}{\lambda_{\max}} \quad (5.57)$$

Because $\lambda_{\max}$ depends on the dimensions of $\bar{e}_k$ and $\bar{\Phi}_{kk}$, we must note that this

eigenvalue increases as the dimension of $\bar{e}_k$ and $\bar{\Phi}_{kk}$ increases. It thus follows that the tightest bound will be obtained by using the eigenvalue corresponding to the smallest permissible dimension, which is 6 for the rate 1/2 4-state code we are considering as our example. This leads to $\lambda_{max} = 0.5228$ for the case where $\rho_{21}(1) = \rho_{21}(0) = 0.3$. For this case, equation (5.57) yields the bound $\eta_1^d \geq 1.6417$.

We may obtain a slightly tighter lower bound on the AMCG via the following procedure. Note that $\Phi_{kk}(l)$ has the property that $\Phi_{kk}(0) > \Phi_{kk}(1) > \Phi_{kk}(2) > \ldots$ so the second term in the denominator of (5.49) may be upper bounded as follows

$$2\sum_{j=i_0}^{i_0+Q\Gamma}\sum_{l=1}^{Q\Gamma} e_{kj}e_{kj-l}\Phi_{kk}(l) \leq 2\Big[\sum_{l=1}^{wt[\bar{e}_k]-1}\Phi_{kk}(l)(wt[\bar{e}_k]-l)\Big] \tag{5.58}$$

and this allows us to bound the expression in (5.49) by

$$\eta_k^d(\bar{e}_k) \geq \frac{R_c wt[\bar{e}_k]^2}{wt[\bar{e}_k]\Phi_{kk}(0) + 2\sum_{l=1}^{wt[\bar{e}_k]-1}\Phi_{kk}(l)(wt[\bar{e}_k]-l)} = g(R_c, wt[\bar{e}_k], \rho_{12}, \rho_{21}) \tag{5.59}$$

This is a bound on $\eta_k^d(\bar{e}_k)$ which is only a function of $wt[\bar{e}_k]$ rather than the actual error sequence $\bar{e}_k$. Using the fact that this expression is monotonically increasing with $wt[\bar{e}_k]$, we can obtain a lower bound on the AMCG for this partitioned receiver.

$$\eta_{k,min}^d \geq \min_{wt[\bar{e}_k]\in\{d_f, d_f+1, \ldots\}} g(R_c, wt[\bar{e}_k], \rho_{12}, \rho_{21}) = \frac{R_c d_f^2}{d_f\Phi_{kk}(0) + 2\sum_{l=1}^{d_f-1}\Phi_{kk}(l)(d_f-l)} \tag{5.60}$$

As an example, for the case where $\rho_{21}(1) = \rho_{21}(0) = 0.3$ we get $\eta_1^d \geq 1.67$. This result is tighter than the bound which used the eigenvalue bound on the Rayleigh product and it is plotted in Figure 5.8. The results for $\rho_{21}(0) = \rho_{21}(1) = 0.2$ and 0.4 are plotted in Figures 5.7 and 5.9 respectively.

Another interesting result of (5.60) is that it provides a tightening of the lower bound on the AMCG of the MLSE of Chapter 4. This is due to the fact that the MLSE,

which is the optimal sequence estimator, will have a higher AMCG than the partitioned soft-decision decorrelator, which is a suboptimal sequence estimator. This tightening of the bound on the MLSE's AMCG is incorporated into Figures 5.7 - 5.9.

An upper bound on the AMCG for the soft-decision partitioned decorrelator may be obtained by performing a non-exhaustive search over the set of possible valid $\bar{e}_k$ sequences. One valid error vector for the standard four-state rate 1/2 code is the following, $\bar{e}_k$ = (110111). This error vector gives the smallest result of equation (5.53) of those tested. Because the actual minimum of equation (5.53) over the set of all valid error sequences must be no larger than the minimum of (5.53) over the small set of sequences that we tested, we have an upper bound on the AMCG. This upper bound turns out to be quite close to the lower bound we have already obtained, so we have a very accurate picture of the partitioned decorrelator's performance. This upper bound is also plotted in Figures 5.7 - 5.9.

The complexity of the soft-decision and hard-decision partitioned receivers with a decorrelating inner receiver will be the same, as will the decoding delay. This is a result of the fact that the only difference between the two is that the soft-decision version does not make a hard decision on the decision statistics before passing them to the outer Viterbi decoders, and the outer decoder metrics will differ but be of the same complexity order.

5.2.3 Soft-Decision Partitioned Receiver with a Trellis-Based or Tree-Based Inner Receiver

A third approach which potentially will have the highest performance of any partitioned approach is the one which uses a soft-decision trellis-based or tree-based receiver as the inner multiuser receiver. There are a number of possible trellis-based receivers, the most important of which are the ML sequence estimator, [1], and the reduced state sequence estimator (RSSE), [8], [56]. As an example of a tree-based receiver, see [14].

In their standard form, each of these receivers output hard-decisions, and so the techniques of [51] and [52] must be applied to allow the inner receiver to supply soft outputs to the outer Viterbi decoders.

This approach has recently been proposed by two research groups, [53], and [16]. Both groups cite the prohibitive complexity of the full ML sequence estimator, and examine RSSE and sequential decoding alternatives.

The computation of the AMCG for these approaches remains an open problem. The AMCG of the soft-decision partitioned receiver with an ML sequence estimator should have a higher AMCG than any other partitioned receiver, since the ML sequence estimator is the optimum inner receiver in the sequence error probability sense. It follows that RSSE and sequential decoding approaches which do not suffer significantly in performance relative to the MLSE will also have a high AMCG. The interested reader is referred to [16] and [53] for more detail on these particular approaches.

5.2.4 Soft-Decision Partitioned Receiver With a DFE Inner Receiver

In this approach, a multistage DFE operates on the set of matched filter outputs, by making tentative decisions and feeding these decisions back to make estimates of the MUI which will be subtracted from other matched filter outputs. The key in the *soft code symbol DFE* (SCS-DFE) approach is that at the final stage, the MUI estimate will again be subtracted from the delayed matched filter output, but no hard-decision making will be performed. Instead, the modified matched filter output will be passed straight to the Viterbi decoder.

At this point, we have not committed to a particular type of multistage DFE. As discussed in Chapter 3, there have been at least six architectures proposed in the literature for asynchronous CDMA links, [6], [13], [22]-[24], [34], [20] and [45], and there has also been some work on improving the decision making procedure of the algorithms, [28]. The improved decision making procedures in [28] can easily be applied to any of

the basic architectures.

The performance of this class of approaches is difficult to evaluate analytically, due to the presence of error propagation. Expressions for the AME of the Varanasi DFE have recently been reported in [29], but the approaches used to get those AME expressions do not easily generalize to the coded link case. It is possible to evaluate the AMCG under the assumption of correct feedback. However this implies that as long as the correlation parameters and energies have been perfectly estimated, $RMUI = 0$. Since there is no residual interference if the feedback is correct, and there is no noise enhancement, as in the case of the decorrelator, we obtain the result that the AMCG is that of a single-user system. Clearly, the presence of error propagation degrades the AMCG by some amount, so the computation of the actual AMCG remains an open question. Consequently, simulation will be the performance evaluation technique for this class of receiver.

Because the structure of the integrated DFE which will be discussed in Section 5.3 is most like the Varanasi style uncoded link multistage decoder, it is interesting to compare the integrated DFE with the Varanasi style SCS-DFE. In addition, because it was shown in Chapter 3 that in most cases, the Hybrid DFE outperforms the other two architectures on an uncoded link, it is an obvious candidate for use in an SCS-DFE structure. Thus, the structures that were simulated were the Hybrid and Varanasi versions of the SCS-DFE. The modifications to the decision making devices in each preliminary stage of the multistage decoders discussed in [28] were not considered here, although those modifications may provide improvements in some cases.

Figure 5.10 shows the performance curves for the "0.2 channel" illustrated by Figure 3.4a. As Figure 5.10 illustrates, the conventional decoder suffers about a 3 dB loss at $P_{b\,average} = 2 \cdot 10^{-3}$ relative to the performance of the same receiver operating in the absence of MUI. For this case, the Hybrid version of the SCS-DFE outperforms the Varanasi version of the SCS-DFE. This is similar to the results obtained on the uncoded link simulated in Chapter 3.

Figure 5.11 shows the performance for the more severe channel illustrated in Figure 3.4b. In this figure, it is evident that all of the decoders perform significantly worse than in the "0.2 channel" due to the more severe MUI. In addition, the hybrid SCS-DFE again outperforms the Varanasi DFE.

Once again, the complexity and decoding delay of the soft-decision partitioned DFE receiver will be of the same order as in the hard-decision case.

5.3 Combined Equalization and Decoding Approaches

In all of the partitioned approaches, regardless of the type, the multiuser receiver operates at the code symbol level as though there were no coding on the link, and then passes its decisions or improved statistics to an outer decoder. The deficiency with this approach is that separating the functions of cancelling the MUI and decoding the message does not take full advantage of the coding on the link. The approaches discussed in this section attempt to alleviate this shortcoming.

5.3.1 Linear Combined Equalization and Decoding Approaches

A linear approach could be defined as any approach which somehow forms decision statistics for the information symbols using a linear method, ie. by linearly combining matched filter outputs, or more generally by performing linear operations on the received waveform without the use of matched filters at all. For any linear receiver, after decision statistics have been formed, a decision must be made to determine the estimated bit. This decision making procedure will typically be nonlinear. One example of decision making procedure would be the comparison of a decision statistic to a threshold and output of a corresponding bit. (i.e. the signum function) Another example would be a decision maker which chooses the largest of a set of decision statistic and outputs the corresponding symbol or symbols.

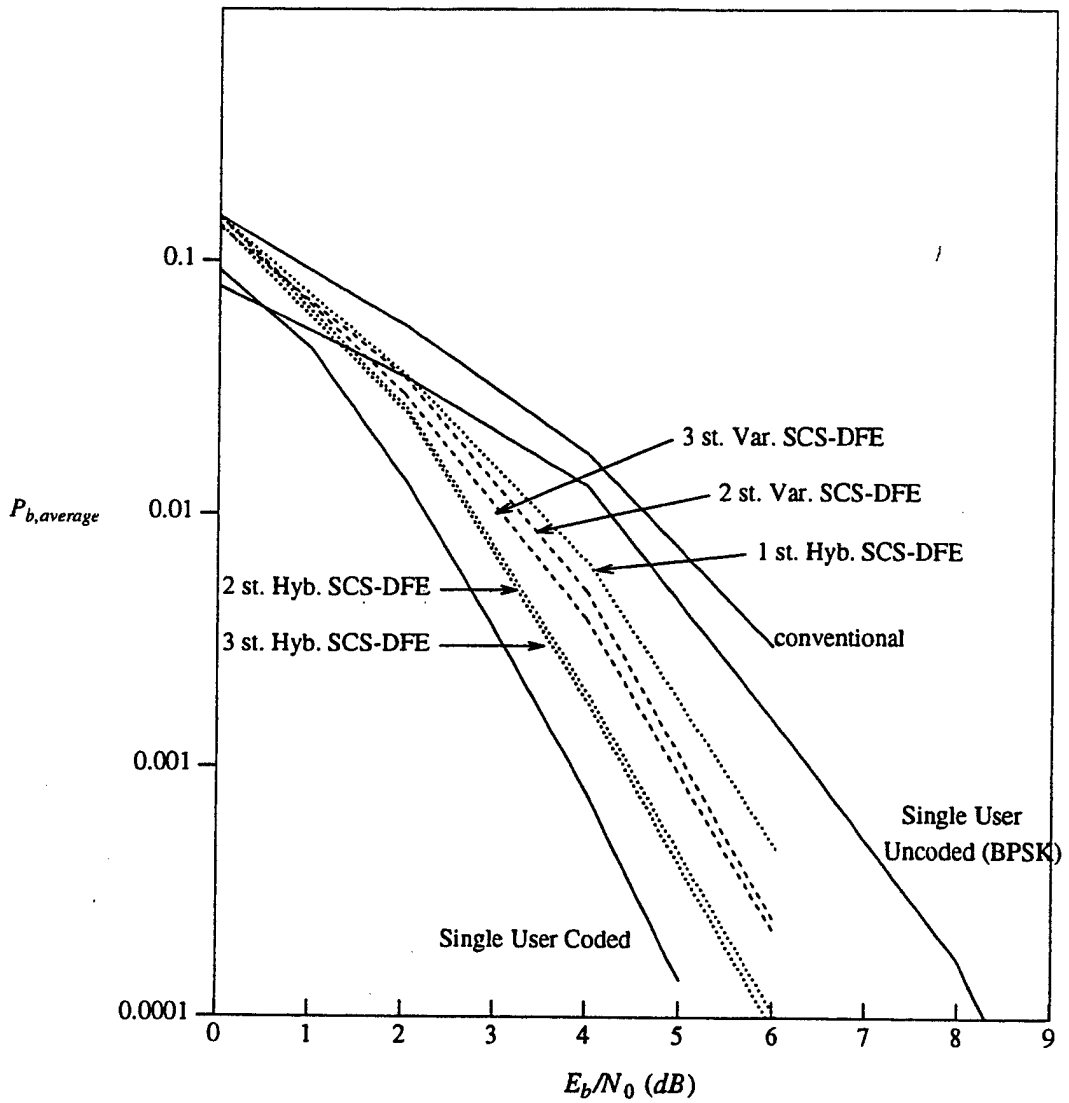

Figure 5.10 Performance curves of the soft-decision partitioned decision feedback receivers for the 4-user 0.2 channel illustrated in Figure 3.4a. The solid lines show a single user system (no MUI) with and without the rate-1/2 4-state convolutional code. Also shown are the one, two and three stage soft code symbol DFEs for both the Varanasi (dashed) and Hybrid (dotted) architectures. Note that the Varanasi style one-stage soft code symbol DFE is equivalent to the conventional receiver.

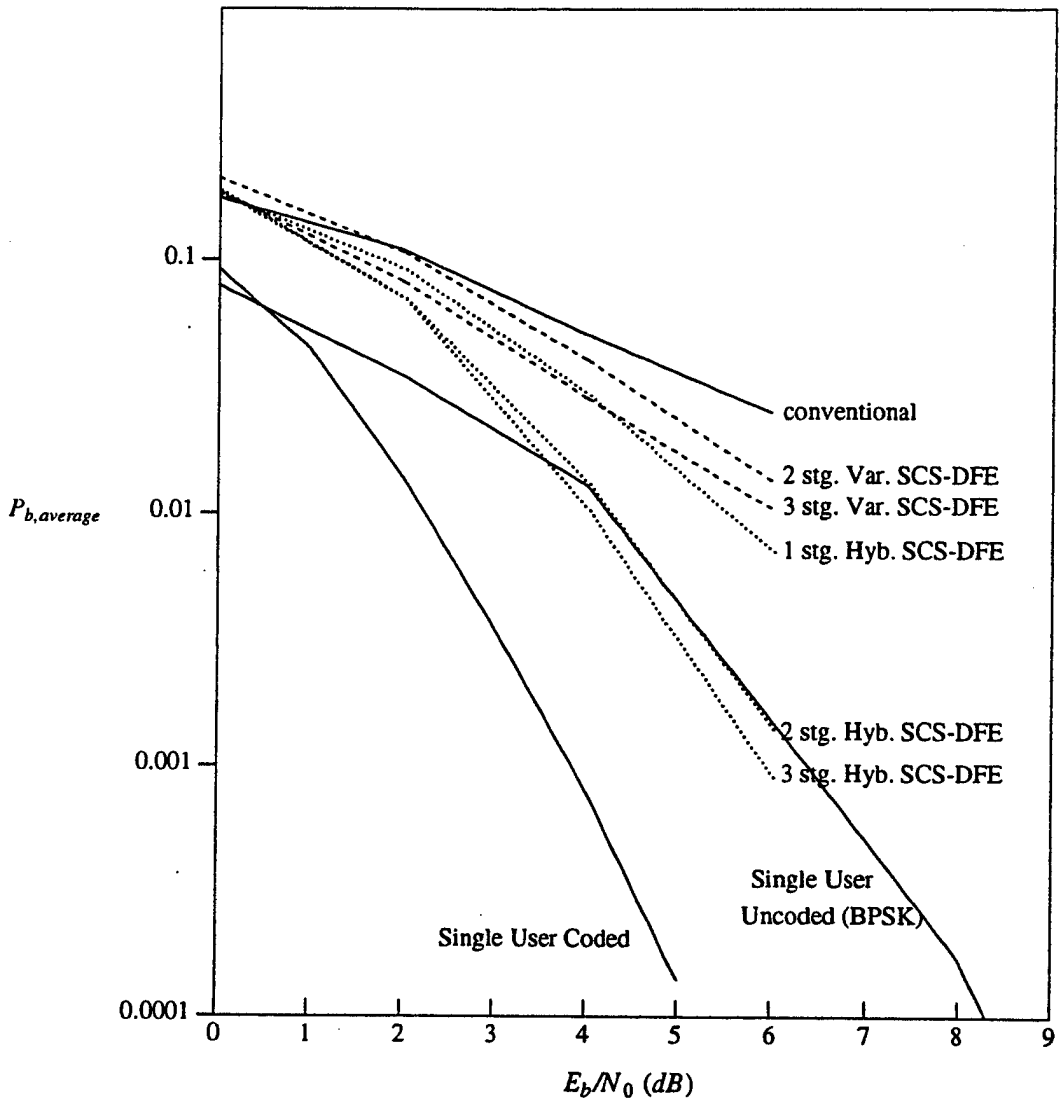

Figure 5.11 Performance curves for the various soft-decision partitioned decision feedback receivers for the more severe 4-user 0.25 channel illustrated in Figure 3.4b. The solid lines show a single user system (no MUI) with and without the rate-1/2 4-state convolutional code. Also shown are the one, two and three stage soft code symbol DFEs of both the Varanasi (dashed) and Hybrid (dotted) architectures.

The optimal receiver in terms of sequence error probability may be implemented in its most general form as a bank of correlators each of which correlates the received sequence with a waveform corresponding to a different transmitted information bit sequence. The decision maker would then simply choose the sequence of information bits for each user which corresponded to the largest correlator output. If the horizon of the transmission is $2M+1$ as in Chapter 4, then there would need to be 2^{2M+1} correlators assuming that each user sends binary data. For even a fairly small horizon, the number of correlators would be prohibitively high. We saw in Chapter 4 that this same ML sequence estimator may be implemented using a trellis-based receiver whose complexity did not depend on the horizon size.

The fact that the ML receiver can be implemented in a linear form, however, is significant because it raises the possibility of forming suboptimum receivers which are linear and have a lower complexity that the optimal linear receiver. The question remains open, however, as to whether the complexity could ever be lowered to an implementable level. Clearly, it would be desirable to develop a linear receiver which linearly combined the matched filter outputs to form its decision statistics, rather than having to build a large number of correlators. The convolutional code used by each of the users is a linear code, and thus may in some cases be invertible using a stable (and maybe even causal) linear receiver. The determination of the exact structure of this combined equalization and decoding linear receiver with a reasonable complexity remains an open question at this point, however.

5.3.2 Trellis-Based and Tree-Based Combined Equalization and Decoding Approaches

The MLSE of Chapter 4 is a trellis-based approach which combines the functions of equalization and decoding into one operation. This approach is the optimal sequence estimator. In this section, we briefly discuss the notion of a suboptimum trellis-based or

tree-based receiver, which was alluded to in Chapter 4.

The MLSE has a prohibitively high number of states, thus it is natural to look to simplify the decoding process by combining states in some fashion. This approach of combining states in some fashion is what is referred to as reduced state sequence estimation (RSSE). There are a number of publications on the application of RSSE to simplify the MLSE for the uncoded case, [8], [56], as well as at least one other on the application of RSSE to simplify the process of equalizing and decoding a coded signal on a single-user dispersive link, [47]. It is undoubtedly possible to apply these techniques to the problem at hand to obtain a performance versus complexity tradeoff.

Just as in [14], it is also presumably possible to use sequential decoding approaches to lower the complexity of the MLSE for the coded link case. Sequential decoding would also provide the opportunity to tradeoff performance versus complexity.

One problem with the trellis-based and tree-based approaches, however, is that they are apparently not as robust to mismatch (a misestimation of the correlation or energy parameters) as some of the simpler approaches like the partitioned decorrelator and DFE approaches. In [27], it was shown that the uncoded link MLSE was not as robust as a Varanasi DFE to mismatch, in the sense that for even small values of mismatch, the suboptimum DFE outperformed the MLSE. This high sensitivity of the optimal approach to mismatch is a very undesirable feature, and it may very well carry over to suboptimal approaches which are based on the MLSE like the RSSE and sequential approaches. Nonetheless, given no mismatch, the trellis-based and tree-based approaches have the potential to perform nearly as well as the MLSE, possibly with a significantly decreased complexity.

5.3.3 The Decision Feedback Combined Equalization and Decoding Approach: The Integrated DFE

The idea in the approach we will refer to as the *integrated DFE* is that the MUI can be more reliably estimated by exploiting the coding. Thus, instead of using a hard-decision device in the first stage of a multistage DFE, like that of [6], we may decode the message using a soft-decision Viterbi algorithm which operates on the stream of matched filter outputs in the j^{th} channel, and then re-encodes the decoded bits to form estimates of the code bits. These code bit estimates can then be used to estimate the MUI in other user's channels. Again, as in the uncoded case, the decision feedback may be performed for as many stages as is desired. (See Figure 5.12) The performance of this approach is difficult to evaluate analytically, again due to the presence of incorrect feedback. As a result, simulation will be the performance evaluation technique in this section.

A characteristic of convolutional codes, or most codes for that matter, is that at very low signal to noise ratios, the coded link may perform worse than an uncoded link. When the signal to noise ratio is in this regime, it is possible that the Viterbi decoder whose outputs are re-encoded to form the ML estimate of the code bit sequence, may perform worse than a simple hard-decision device operating on the code bits without regard to the coding. As a result of this characteristic, it is important that the combination of the thermal noise and MUI is not so strong that the re-encoded Viterbi output sequence is worse than the estimated code bits of a simple threshold detector for the integrated DFE to outperform an SCS-DFE. Basically, the structure which provides better estimates of the code bit sequence will have a better estimate of the MUI in the other channel's multistage decoders. In general, because coding generally allows better estimates of the transmitted sequence, it is reasonable to expect the integrated DFE to outperform an SCS-DFE of a similar architecture like a SCS-DFE with a Varanasi DFE.

Figure 5.13 shows performance of the integrated DFE and the various SCS-DFE approaches on the "0.2 channel" illustrated by Figure 3.4a. In this environment, the

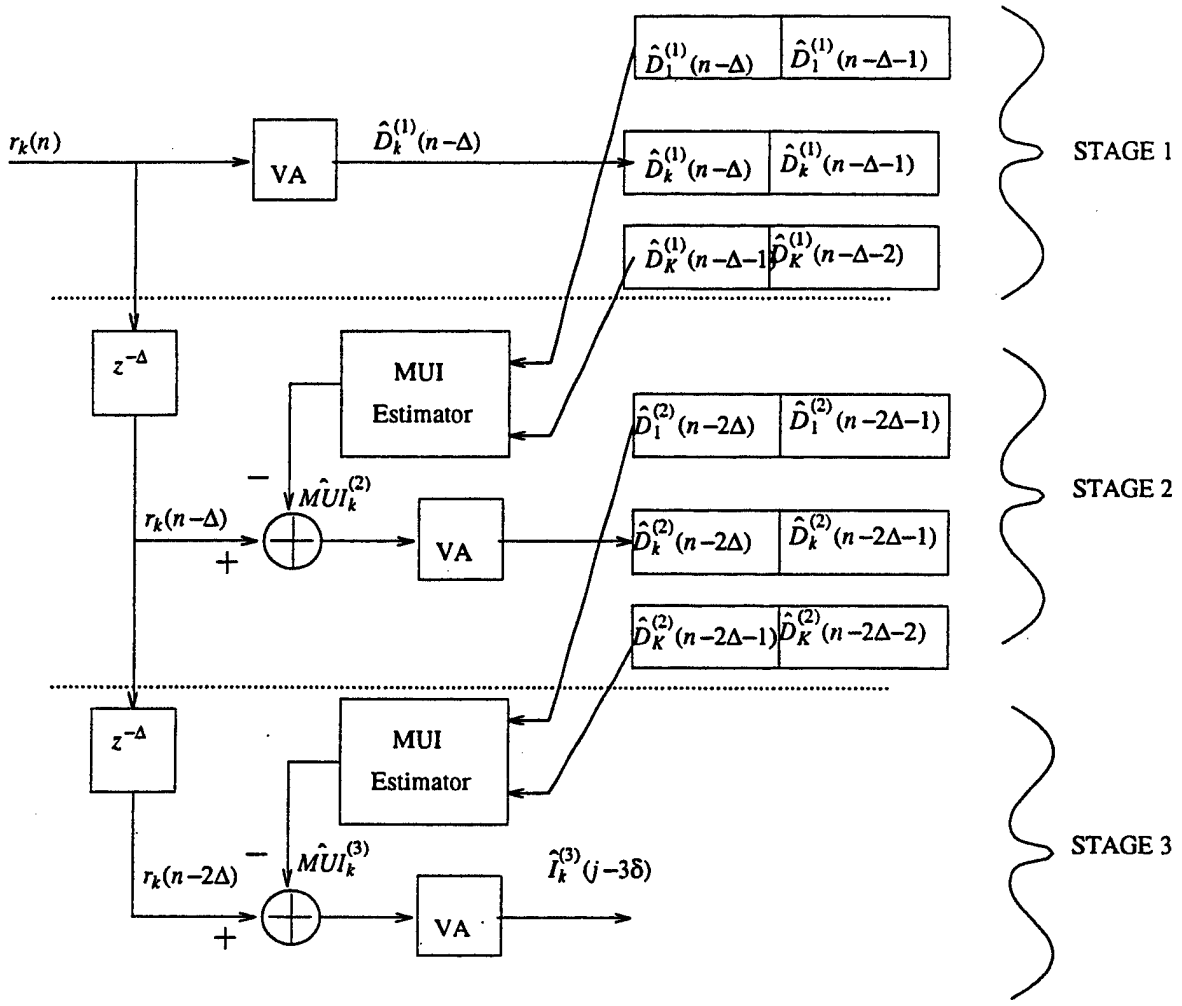

Figure 5.12 The structure of a 3-stage integrated DFE for the k^{th} user with Viterbi algorithms (denoted VA) at each stage. Δ is the maximum delay in code bit periods corresponding to δ information bit periods

integrated DFE is able to nearly recoup all of this loss, while the various SCS-DFEs are able to only recoup some of the loss. It may thus be concluded that the thermal noise and MUI are weak enough to be operating in the regime where a receiver which exploits the coding performs better than one which does not.

Figure 5.14 shows the performance on the more severe channel illustrated in Figure 3.4b. The integrated DFE still uniformly outperforms the Varanasi version of the SCS-DFE. For these particular channel characteristics, however, the hybrid SCS-DFE is able to outperform the integrated DFE at larger values of E_b/N_0. While this may seem surprising at first, it is simply due to the fact that even though the hybrid SCS-DFE performs separate equalization and decoding, it has a high quality first stage which is able to provide better code symbol estimates to the second stage MUI estimator than the conventional Viterbi algorithm operating in the first stage of the integrated DFE. This case illustrates that when the MUI is strong enough, the integrated DFE will not always outperform a well designed SCS-DFE, although it does in most cases.

To compute the TCB for the integrated DFE, we again assume that the computation of the MUI in each stage of the DFE structures is roughly equivalent in complexity to the computation of one metric in the Viterbi decoder. Thus adopting this convention, we may conclude that for a link with rate $1/Q$ and constraint length W codes, the J-stage integrated DFE has a time complexity of roughly TCB = $O((J-1)Q+J2^W)$. This is significantly higher than that of the SCS-DFE, although it is far less than that of the MLSE of Chapter 4. In the general rate P/Q code case, if again, $\kappa = \log_2 S$ where S is the number of states in each user's encoder, the integrated DFE has TCB = $O([(J-1)Q+J2^{\kappa+P}]/P)$. Again, because each MUI computation grows in complexity with K, we may say that the number of operations per decoded bit is on the order of $OP_{IDFE} = O([(J-1)QK+J2^{\kappa+P}]/P)$.

If it is assumed again that the Viterbi decoders used operate with a decoding delay which is typically on the order of $5W$, then the overall decoding delay of the J-stage

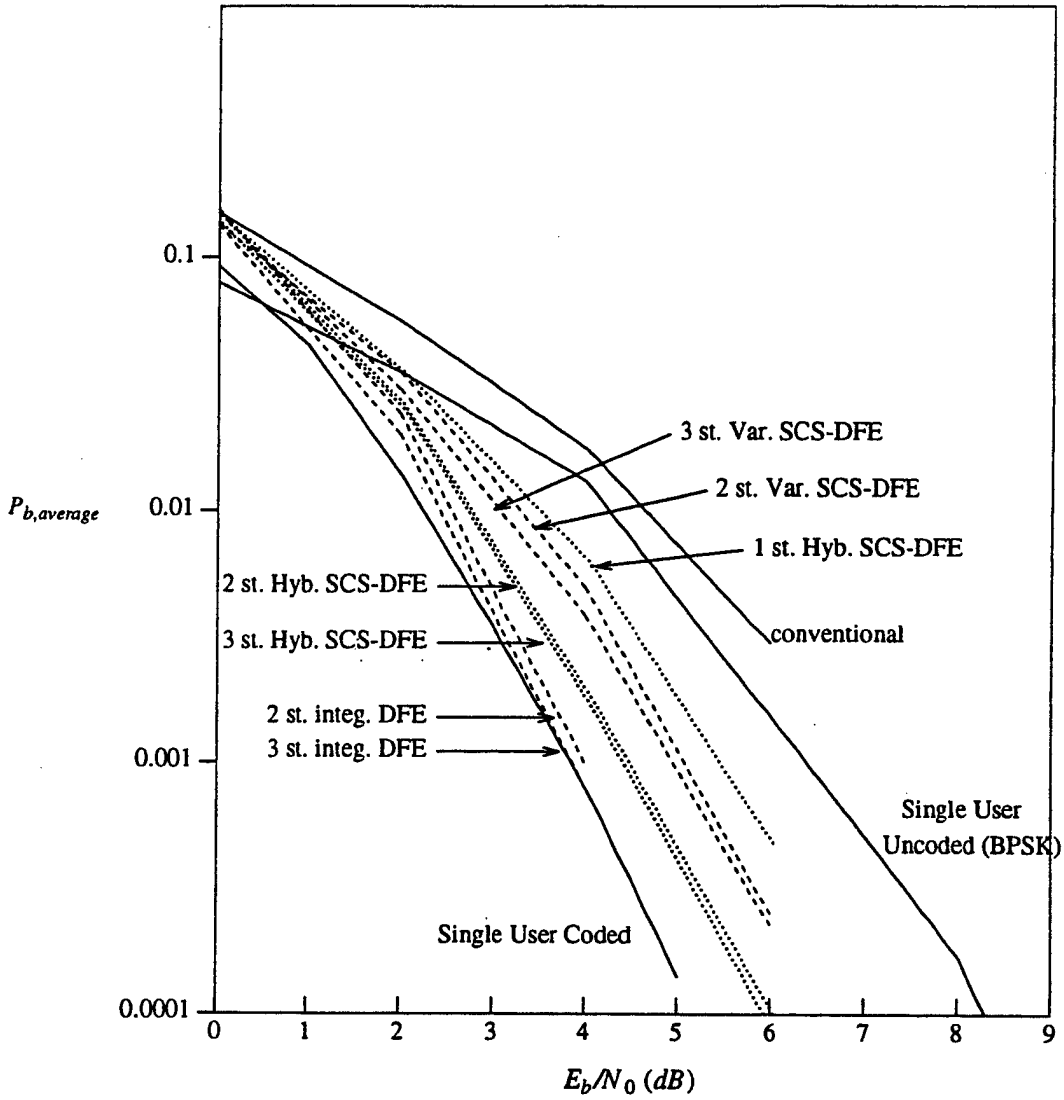

Figure 5.13 Performance curves of the various decision feedback receivers for the 4-user 0.2 channel illustrated in Figure 3.4a. The solid lines show a single user system (no MUI) with and without the rate-1/2 4-state convolutional code. Also shown are the one, two and three stage soft code symbol DFEs for both the Varanasi (dashed) and Hybrid (dotted) architectures, and a one, two and three stage integrated DFE (dashed lines). Note that the Varanasi style one-stage soft code symbol DFE and the one-stage integrated DFE are both equivalent to the conventional receiver.

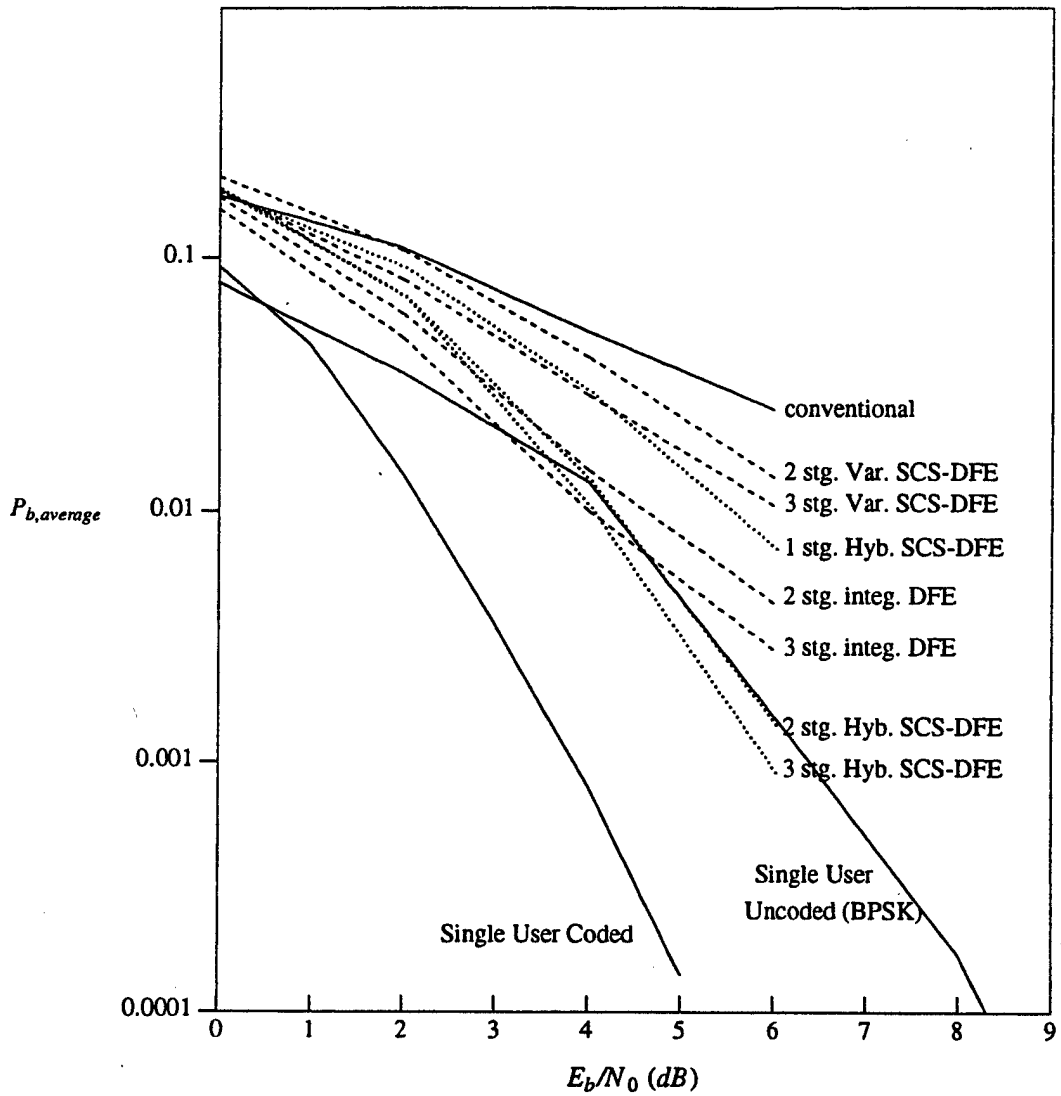

Figure 5.14 Performance curves of the various decision feedback receivers for the more severe 4-user 0.25 channel illustrated in Figure 3.4b. The solid lines show a single user system (no MUI) with and without the rate-1/2 4-state convolutional code. Also shown are the one, two and three stage soft code symbol DFEs of both the Varanasi (dashed) and Hybrid (dotted) architectures, and a one, two and three stage integrated DFE (dashed lines). Note that the Varanasi style one-stage soft code symbol DFE and the one-stage integrated DFE are both equivalent to the conventional receiver.

integrated DFE is roughly $5JW$.

We may thus conclude that the integrated DFE has a larger TCB, and a longer decoding delay than any of the SCS-DFE approaches, but its performance is better in most cases. As a result, the appropriate choice of receiver configuration will depend on the expected severity of the channel and the complexity and delay constraints on the receiver. As we have seen in Figure 5.14, however, even the integrated DFE does not perform well when the MUI becomes too strong.

5.4 Comparison of the Suboptimum Approaches

In this chapter, a large number of approaches have been discussed (see Figure 5.1). The approaches can be categorized as linear, DFE and trellis-based, as in Figure 5.1, or they may be categorized as partitioned and combined approaches as they were presented in this chapter.

The determination of which approach is the best for a specific situation is not trivial, because there are a number of factors which must be considered. Throughout this chapter, the number of arithmetic operations per decoded bit was used as a measure of the complexity of the receivers. Figure 5.15 shows a table comparing the complexity for some of the approaches discussed for two specific cases, a 2-user 2-state code case and a 100-user 64-state code case. It is clear that for a large number of users and large codes, the MLSE and Partitioned MLSE are too complex to be used. Most of the other approaches are, however, fairly reasonable.

The decoding delay is another factor which will be of importance in some applications, such as voice communications. Figure 5.16 shows a table comparing the decoding delay of some of the approaches discussed for the same two cases as were used in Figure 5.15. The interesting feature of this table is that most of the approaches have about the same decoding delay, with the exception of the Integrated DFE approaches. Even the very complex MLSE has a decoding delay that is the same as the conventional receiver,

Approximate Number of Operations Per Decided Bit		
receiver	2-user, 2-state case	100-user, 64-state case
MLSE	32	5E212
Partitioned MLSE	20	1.27E32
3-stg. integrated DFE	20	784
2-stg. integrated DFE	12	456
3-stg. SCS-DFE	16	728
2-stg. SCS-DFE	12	528
Partitioned Decor.	24	1128
Conventional	4	128

Figure 5.15 Complexity comparison for two specific rate 1/2 code cases. The partitioned decorrelator approach assumes an impulse response truncation depth of $\delta = 5$.

Decoding Delay		
receiver	2-user, 2-state case	100-user, 64-state case
MLSE	10Ts	35Ts
Partitioned MLSE	12.5Ts	37.5Ts
3-stg. integrated DFE	30Ts	105Ts
2-stg. integrated DFE	20Ts	70Ts
3-stg. SCS-DFE	11Ts	36Ts
2-stg. SCS-DFE	10.5Ts	35.5Ts
Partitioned. Decor.	11.25Ts	36.25Ts
Conventional	10Ts	35Ts

Figure 5.16 Decoding delay comparison for the same cases as in Figure 5.15.

assuming that all of the decoding operations can be completed in real time. (which they typically can not)

In all cases, the performance is a very important factor in the determination of which approach is the best. Throughout this chapter, the various approaches were compared using the AMCG performance measure whenever possible. When the receivers did not lend themselves to an AMCG analysis, as in the case of the DFE's, computer simulations were used to compare their performance to the important baselines, the single-user bound, the MLSE's performance and the conventional receiver's performance. In some cases, no performance analysis was given at all, but the receivers were discussed briefly anyway, for the sake of completeness. For these receivers, the interested reader was either referred to references which discussed their performance, as in the case of the soft-decision partitioned trellis-based/tree-based approaches, or a performance analysis has simply not been done yet. For most of the receivers in this chapter, however, the tools have been developed for comparing the various options.

An examination of the figures of this chapter illustrates that the MLSE of Chapter 4 has the highest performance. The worst performance of any receiver considered was the hard-decision conventional followed by the soft-decision conventional. The soft-decision partitioned approaches with a decorrelator or DFE inner receiver provide reasonable performance and have a fairly low complexity. If a higher complexity and decoding delay is tolerable, the integrated DFE will usually provide the best compromise of performance and complexity.

Thus the basestation architecture which is most appropriate will depend on a number of different factors and there is no single correct solution for every situation. This dissertation has presented the pros and cons of each approach, however, so that the options may be compared in light of the constraints of a given application.

Chapter 6 Conclusions

In this final chapter, the important results of this dissertation will be summarized. The merits and drawbacks of the proposed basestation architectures will be discussed. Finally this chapter will conclude with some thoughts on questions that remain open and may warrant additional research in the future.

6.1 Summary of Results

In this thesis, we considered direct sequence asynchronous CDMA systems with and without coding on a nondispersive AWGN channel. The notion of multiuser detection, wherein a receiver jointly demodulates all of the users in a CDMA system, was first reviewed and then extended to CDMA systems with coding. In Chapter 2, after defining the concept of multiuser detection, a survey of the literature on the topic was presented. The review of the optimal receiver for the uncoded case led to the study of a wide variety of suboptimum approaches for the uncoded case which have already been proposed. These approaches may be broadly categorized as trellis/tree based approaches, linear approaches and decision feedback approaches.

The review of the decision feedback approaches was deferred to Chapter 3, because the discussion of the nonlinear DFE approaches in [6] and [13] led to a new hybrid DFE approach. This hybrid DFE was shown through simulations to greatly outperform the approaches in [6] and [13] in most cases. It was next seen that the approaches discussed in [7], [22] - [24] and [28] could be incorporated into the hybrid design to provide a DFE which used the best features of each approach. Even the approach discussed in [34] could be viewed as special case of the hybrid architecture. Thus the major contribution of Chapter 3 is the unification of the different decision feedback approaches into a common architecture, and the illustration that the ideas used in each of the previous DFE's are not mutually exclusive.

We next proceeded to begin a study of receiver architectures for CDMA links with convolutional coding. It was natural to begin the study with the optimal receiver (optimal in the sequence error probability sense). For the sake of simplicity, this maximum likelihood sequence estimator was derived for the case where each user employed the same rate 1/2 code. This derivation generalizes easily to the case where the users employ rate P/Q codes and also the case where each user employs a different code. After the metric was derived for the rate 1/2 case, it was shown that the decoder may be implemented using a Viterbi algorithm which operates on a time-varying trellis with 2^{WK-1} states (recall that W is the constraint length of the codes and K is the number of users in the system). The time complexity per decoded bit and rough number of arithmetic operations per decoded bit were then determined for this receiver and were seen to be exponential in both K and W. In the general rate P/Q code case, the complexity was exponential in P, K, and κ, which is the binary memory order of the code.

A performance analysis was then undertaken for the MLSE and an upper and lower bound on the asymptotic efficiency of this receiver relative to an uncoded coherent BPSK receiver was determined. This asymptotic efficiency was given the name asymptotic multiuser coding gain (AMCG). It was seen that the AMCG unifys the asymptotic coding gain parameter and the asymptotic multiuser efficiency parameter which are traditional figure of merit parameters for single-user coded systems and multiuser uncoded systems respectively. The bounding procedure on the AMCG was used to avoid having to solve the NP-hard problem of searching for the valid error sequence which minimizes the efficiency equation (4.42) over the infinite set of all valid error sequences. Finally, some simulations were presented to illustrate the performance of the MLSE at moderate and low bit error rates.

The very high complexity of the MLSE illustrated the need for suboptimum basestation architectures which perform nearly as well as the MLSE with a lower complexity. Chapter 5 examined a large number of possible receiver architectures which attempt to

satisfy this need.

The first architectures examined were the partitioned receivers, which treat the equalization of the MUI and the decoding of the code separately. These approaches may be subdivided into hard and soft decision partitioned receivers. In the hard-decision partitioned approach, an inner multiuser receiver operates on the received code symbol sequence without regard to the coding and then supplies hard-decisions to a bank of outer Viterbi decoders. In the soft-decision approach, the inner multiuser receivers are modified to supply soft-decisions to the outer Viterbi decoders. These approaches were analyzed in terms of AMCG, TCB, arithmetic operations per decoded bit and decoding delay for various inner receivers. Because the soft-decision partitioned receiver with a DFE as the inner receiver did not lend itself to an AMCG analysis, a computer simulation was used to compare it to the important baseline approaches.

The next family of suboptimum approaches which were examined were those which combine the operations of equalization and decoding into a single operation. The integrated DFE was introduced as a DFE which estimates the MUI by exploiting the coding on the link. This approach was shown to perform better than the partitioned DFE approaches in most cases. If the interference and noise were so severe so as to cause the Viterbi decoder to provide a worse sequence estimate than a simple symbol-by-symbol detector which does not consider the coding, then the integrated DFE does not perform as well as a well designed partitioned DFE. Again because of the presence of error propagation, the integrated DFE's performance was estimated using a computer simulation. Also, short discussions were given for suboptimum combined equalization and decoding approaches which were linear and trellis/tree based. Chapter 5 concluded with a brief comparison of the complexities and decoding delays of the various receivers.

There is no single clear winning approach, as each provides advantages and disadvantages in different situations. If an unlimited amount of processing power is available, the optimal solution is the clear winner. Furthermore, for a network with only a few users

and small codes, the complexity of the optimal receiver may be tolerable, however this situation will probably be very uncommon in practice. If the processing power of the receiver is very limited, it may only be possible to use a conventional receiver. The conventional receiver will typically provide the lowest performance of any approach studied, however. For situations where there is enough processing power to implement an intermediate approach, we have examined a range of options in Chapter 5. The partitioned approaches with soft-decision inner receivers will provide a relatively low complexity and high performance in many situations. If the processing power is high enough, a combined equalization and decoding approach will generally outperform a partitioned approach. In many situations, the integrated DFE seemed to provide the best performance of the approaches considered, however its time complexity per decoded bit and decoding delay are higher than many of the other approaches. The integrated DFE's complexity as measured in terms of the number of arithmetic operations per decoded bit is comparable to many of the partitioned approaches, however. The partitioned SCS-DFE approaches, particularly with a hybrid DFE inner multiuser receiver, are also probably a good compromise in many situations.

This dissertation has provided an introduction to a large number of approaches and their performance and complexity.

6.2 Future Research Possibilities

There are many possibilities for future research in this area. This work was concerned with CDMA links wherein convolutional coding is employed. Convolutional codes are a logical choice of codes for this situation, but there may be links where trellis coded modulation (TCM) or block coding is used instead. The extension to the TCM case will not be particularly difficult. Formulating the optimal receiver for the block coding case may be more difficult, although many of the suboptimal approaches will easily generalize to this case.

Some work has been done recently to develop expressions for the asymptotic multiuser efficiency (AME) of the Varanasi DFE, [29]. This work does not extend easily to the analysis of the AME of the hybrid DFE, however the development of AME expressions for the hybrid DFE would be a big contribution. Furthermore, it would also be worthwhile to develop expressions for the AMCG of the DFE approaches discussed in Chapter 5. This would allow a direct comparison with the other approaches via the AMCG performance measure.

Another interesting extension of this work is to consider dispersive channels. There has been a significant amount of work recently on the design of multiuser receivers for dispersive uncoded CDMA systems, [9], [31] - [33]. Because many cellular channels are somewhat dispersive, it would be worthwhile to unify the work in [9], [31] - [33] with that in this dissertation.

Finally, by no means has this dissertation proposed every possible multiuser receiver for coded links. There are most likely other solutions which have not yet been developed which may produce robust, low-complexity, high performance basestations. This dissertation has addressed many multiuser receiver architectures, but there may be some sophisticated new solutions waiting to be discovered still.

In conclusion, it is hoped that this dissertation has opened the door to the field of multiuser detection for coded CDMA systems. We have seen that there exists great potential for multiuser receivers to significantly improve upon the performance of the conventional basestation architecture. In the future, this work will undoubtably lead to a significant improvement of the capacity of CDMA networks and should help illustrate that CDMA is a very attractive and worthwhile technique for allowing many users to share the crowded spectrum.

References

[1] S. Verdu, "Minimum Probability of Error for Asynchronous Gaussian Multiple Access Channels," *IEEE Trans. Inform. Theory*, vol. IT-32, Jan. 1986, pp 85-96.

[2] S. Verdu, "Optimum Multiuser Asymptotic Efficiency," *IEEE Trans. on Comm.*, vol.34, no.9, May 1991, pp. 890-897.

[3] S. Verdu, "Recent Progress in Multiuser Detection," *Advances in Communications and Control Systems, ComCon '88*, Lecture Notes in Control and Information Science Series, NY, Springer-Verlag, 1989.

[4] R. Lupas and S. Verdu, "Near-Far Resistance of Multiuser Detectors in Asynchronous Channels," *IEEE Trans. on Comm.*, vol.38, no.4, April 1990, pp 496-508.

[5] H.V. Poor, S. Verdu, "Single-User Detectors for Multiuser Channels," *IEEE Trans. on Comm.*, vol. 36, no. 1, Jan. 1988, pp.50-60.

[6] M. Varanasi and B. Aazhang, "Multistage Detection in Asynchronous CDMA Communications," *IEEE Trans. on Comm.*, vol.38, no.4, pp 509-519, April 1990.

[7] M. Varanasi and B. Aazhang, "Near-Optimum Detection in Synchronous Code-Division Multiple-Access Systems," *IEEE Trans. on Comm.*, vol.39, no.5, May 1991, pp 725-736.

[8] M.K. Varanasi "Reduced State Sequence Detection for Asynchronous Gaussian Multiple-Access Channels", *Proceedings of ISIT*, San Antonio, Texas, January, 1993, pp. 42.

[9] S. Vasudevan, M.K. Varanasi, "Multiuser Detection over CDMA Fading Channels with Memory," *Proc. of GLOBECOM'93*, Houston, TX, December, 1993.

[10] B. Aazhang, B.P. Paris, and G.C. Orsak, "Neural Networks for Multiuser Detection in Code-Division Multiple-Access Communications," *IEEE Trans. on Comm.*, vol.40, no.7, July 1992, pp 1212-1222.

[11] U. Fawer, B Aazhang, "A Multiuser Receiver for Code Division Multiple Access Communications over Multipath Channels," submitted to *IEEE Trans. on Comm.*.

[12] B. DeCleene, *The Simulation of a Multistage Receiver* for *CDMA Cellular Communications*, Senior Thesis, Dept. of Electrical Engineering, Univ. of Virginia, March 1992.

[13] Z. Xie, R.T. Short and C.K. Rushforth, "A Family of Suboptimum Detectors for Coherent Multiuser Communications," *IEEE Journ. on Select. Areas in Comm.*, vol.8, no.4, May 1990, pp 683-690.

[14] Z. Xie, C.K. Rushforth, R.T. Short, "Multiuser Signal Detection Using Sequential Decoding," *IEEE Trans. on Comm.*, vol. 38, no. 5, May 1990, pp. 578-583.

[15] Z. Xie, C.K. Rushforth, R.T. Short, T.K. Moon, "Joint Signal Detection and Parameter Estimation in Multiuser Communications," *IEEE Trans. on Comm.*, vol.41, Aug 1993, pp 1208-1216.

[16] C.K. Rushforth, M. Nasiri-Kinari, A. Abbaszadeh, "A Reduced-Complexity Sequence Detector With Soft Outputs for Partial-Response Channels," *Proc. of GLOBECOM'93*, Houston, TX, December, 1993.

[17] A. Kajiwara and M. Nakagawa, "Crosscorrelation Cancellation in SS/DS Block Demodulator," *IEICE Trans.*, vol. E 74, no.9, pp 2596-2601, Sept. 1991.

[18] R. Kohno, H. Imai, M. Hatori, and S. Pasupathy, "An Adaptive Canceller of Cochannel Interference for Direct-Sequence Spread-Spectrum Multiple-Access Communication Networks in a Power Line," *IEEE Journ. on Select. Areas in Comm.*, vol.8, no.4, May 1990, pp 691-699.

[19] Kohno et. al., "Combination of an Adaptive Array Antenna and a Canceller of Interference for Direct-Sequence Spread-Spectrum Multiple-Access Systems," *IEEE Journ. on Select. Areas in Comm.*, vol.8, no.4, May 1990, pp 675-681.

[20] Y.C. Yoon, R. Kohno, "A Spread-Spectrum Multiaccess System with Cochannel Interference Cancellation for Multipath Fading Channels," *IEEE Journ. on Select. Areas in Comm.*, vol. 11, no. 7, Sept. 1993.

[21] A. Duel-Hallen, "Equalizers for Multiple Input/Multiple Output Channels and PAM Systems with Cyclostationary Input Sequences," *IEEE Journ. on Select. Areas in Comm.*, vol.10, no.3, April 1992, pp 630-639.

[22] A. Duel-Hallen, "On Suboptimal Detection for Asynchronous Code-Division Multiple-Access Channels," Proceedings of the 1992 Conference on Information Science and Systems, Princeton, NJ, pp. 838-843.

[23] A. Duel-Hallen, "A Family of Multiuser Decision-Feedback Detectors for Asynchronous Code-Division Multiple-Access Channels," to be published in *IEEE Trans. on Comm.*.

[24] A. Duel-Hallen, "Multiuser MMSE and Zero-Forcing Decision Feedback Detectors for Asynchronous CDMA," *Proc. of GLOBECOM'93*, Houston, TX, December, 1993.

[25] K.S. Schneider, "Optimum Detection of Code Division Multiplexed Signals," *IEEE Trans. on Aerospace* and *Electronic Systems*, vol.AES-15, no. 1, Jan. 1979, pp. 181-185.

[26] W.V. Etten, "Maximum Likelihood Receiver for Multiple Channel Transmission Systems," *IEEE Trans. on Comm.*, Feb. 1976, pp. 276-283.

[27] M. Kocic, D. Brady, "Asymptotic Multiuser Efficiency of the Maximum Likelihood Sequence Detector with Channel Mismatch," *Proceedings of CISS'93*.

[28] X. Zhang, D. Brady, "Soft-Decision Multistage Detectors for Asynchronous AWGN Channels," *Proceedings of the Thirty-First Allerton Conference on*

Communication Control and *Computing*, October, 1993.

[29] X. Zhang, D. Brady, "Asymptotic Multiuser Efficiency for M-Stage Detection," submitted to the *IEEE Trans. on Info. Theory.*

[30] S.D. Gray, D. Brady, "The Asymptotic Multiuser Efficiency of Two-Stage Detection in Mismatched AWGN Channels," submitted to CTMC at GLOBECOM '93.

[31] Z. Zvonar, D. Brady, "Multiuser Detection in Single-Path Fading Channels", to appear in *IEEE Trans. on Comm.*.

[32] Z. Zvonar, D. Brady, "Optimum Detection in Asynchronous Multiple-Access Multipath Rayleigh Fading Channels," submitted to *IEEE Trans. on Comm.*.

[33] Z. Zvonar, D. Brady, "Differentially Coherent Multiuser Detection in Asynchronous CDMA Flat Rayleigh Fading Channels," submitted to *IEEE Trans. on Comm.*.

[34] P.Patel, J. Holtzman, "Analysis of a DS/CDMA Interference Cancellation Scheme Using Correlations," *Proc. of GLOBECOM'*93, Houston, TX, December, 1993.

[35] R. Singh, "Suppressing Multiple-Access Interference In DS/CDMA Communication Systems," *CISS'*92?, pp. 832-837.

[36] N. Suehiro, "Elimination Filter for Co-Channel Interference in Asynchronous SSMA Systems," *Proc. of* 1991 *IEEE International Symposium on Info. Theory*, Budapest, Hungary, June, 1991, pp.322.

[37] M. Abdulrahman, D.D. Falconer, A.U.H. Sheikh, "Equalization For Interference Cancellation In Spread Spectrum Multiple Access Systems," *Proc. of IEEE Vehicular Technology Conference '*92.

[38] G.D. Boudreau, D.D. Falconer, S.A. Mahmoud, "A Comparison of Trellis Coded Versus Convolutionally Coded Spread-Spectrum Multiple-Access Systems," *IEEE Journ. on Select. Areas in Comm.*, vol.8, no.4, May 1990, pp 628-640.

[39] T.R. Giallorenzi, S.G. Wilson, "Decision Feedback Techniques for CDMA System Equalization," submitted to *IEEE Trans. on Comm.*.

[40] T.R. Giallorenzi, S.G. Wilson, "Decision Feedback Multiuser Receivers for Asynchronous CDMA Systems," *Proceedings of GLOBECOM'*93, Houston, TX.

[41] T.R. Giallorenzi, S.G. Wilson, "Trellis-Based Multiuser Receivers for Convolutionally Coded CDMA Systems," *Proceedings of the Thirty–First Allerton Conference on Communication Control* and *Computing*, October, 1993.

[42] T.R. Giallorenzi, S.G. Wilson, "CDMA System Equalization Techniques," *Technical Report UVA/*538341*/EE*93/101, Communication Systems Laboratory, Dept. of Elec. Engineering, University of Virginia, August, 1992.

[43] T.R. Giallorenzi, S.G. Wilson, "Multistage Decision Feedback and Trellis-Based Multiuser Receivers for Convolutionally Coded CDMA Systems," *Technical Report UVA/538341/EE 93/102*, Communication Systems Laboratory, Dept. of Elec. Engineering, University of Virginia, May, 1993.

[44] S.S.H. Wijayasuriya, G.H. Norton, J.P. McGeehan, "A Sliding Window Decorrelating Algorithm for DS-CDMA Receivers," *Electronics Letters*, vol. 28, no. 17, August, 1992, pp.1596-1598.

[45] A.J. Viterbi, "Very Low Rate Convolutionl Codes for Maximum Theoretical Performance of Spread-Spectrum Multiple-Access Channels," *IEEE Journ. on Select. Areas in Comm.*, vol.8, no.4, May 1990, pp 641-649.

[46] R. Giubilei, "Efficiency of Asynchronous CDMA Systems," *Electronics Letters*, vol. 27, no. 4, 14th February, 1991, pp. 343-345.

[47] P.R. Chevillat, E. Eleftheriou, "Decoding of Trellis-Encoded Signals in the Presence of Intersymbol Interference and Noise," *IEEE Trans. on Comm.*, vol. 37, no. 7, July 1989, pp. 669-676.

[48] K. Wesolowski, "Efficient Digital Receiver Structure for Trellis-Coded Signals Transmitted Through Channels With Intersymbol Interference," *Electronics Letters*, vol. 23. no. 24, November 1987, pp. 1265-1267.

[49] L.B. Milstein, "Interference Rejection Techniques in Spread Spectrum Communications," *Proc. of the IEEE*, vol. 76, no. 6, June, 1988, pp.657-671.

[50] H.V. Poor, "Signal Processing for Wideband Communications," *IEEE Info. Society Newsletter*, vol. 42, no. 2, June, 1992.

[51] J. Hagenauer, P. Hoeher, "A Viterbi Algorithm with Soft-Decision Outputs and its Applications," *Proceedings of GLOBECOM '89*, Dallas, Texas, Nov. 1989, pp. 1680-1686.

[52] P. Hoeher, "Advances in Soft-Output Decoding", *Proc. of GLOBECOM'93*, Houston, TX, December, 1993.

[53] P. Hoeher, "On Channel Coding and Multiuser Detection for DS-CDMA," *Proc. IEEE ICUPC '93*, Ottowa, Canada, October, 1993, pp.641-646.

[54] M.B. Pursley, D.V. Sawarte, and W.E. Stark, "Error Probability for Direct-Sequence Spread-Spectrum Multiple-Access Communications- Part I: Upper and Lower Bounds," *IEEE Trans. on Comm.*, vol. COM-30, May 1982, pp.975-984.

[55] E.A. Geraniotis, M.B. Pursley, "Error Probability for Direct-Sequence Spread-Spectrum Multiple-Access Communications- Part II: Approximations," *IEEE Trans. on Comm.*, vol. COM-30, May 1982, pp.985-995.

[56] S.K. Wilson, J.M. Cioffi, "Equalization Techniques for Direct Sequence Code-Division Multiple Access Systems in Multipath Channels" *Proc. of ISIT'93*, San Antonio, TX.

[57] M.V. Eyuboglu, S.U.H. Qureshi, "Reduced-State Sequence Estimation with Set Partitioning and Decision Feedback," *IEEE Trans. on Comm.*, vol. 36, Jan. 1988, pp.13-20.

[58] M.V. Eyuboglu, S.U.H. Qureshi, "Reduced-State Sequence Estimation for Coded Modulation on Intersymbol Interference Channels."*IEEE Journ. on Select. Areas in Comm.*, vol.7, no.6, Aug. 1989, pp 989-995.

[59] J.B. Anderson, E. Offer, "Reduced-State Sequence Detection with Convolutional Codes," *Technical Report TR*–92–5, Rensselaer Polytechnic Institute, July, 1992.

[60] W. Sheen, G.L. Stuber, "Error Probability for Reduced-State Sequence Estimation," *IEEE Journ. on Select. Areas in Comm.*, vol.10, no.3, April 1992, pp 571-578.

[61] G. Ungerboeck, "Adaptive Maximum-Likelihood Receiver for Carrier-Modulated Data-Transmission Systems," *IEEE Trans. on Comm.*, vol. 22, no. 5, May 1974, pp. 624-636.

[62] G.D. Forney, "The Viterbi Algorithm," *Proceedings of the IEEE*, vol. 61, no. 3, March 1973, pp. 268-278.

[63] G.D. Forney, "Maximum-Likelihood Sequence Estimation of Digital Sequences in the Presence of Intersymbol Interference," *IEEE Trans. Inform. Theory*, vol. IT-18, no. 3, May 1972, pp 363-378.

[64] J.G. Proakis, Digital Communications, New York: McGraw-Hill, 1988.

[65] R.C. Dixon, Spread Spectrum Systems, New York: John Wiley and Sons, 1976.

[66] M.K. Simon, J.K. Omura, R.A. Scholtz, B.K. Levitt, Spread Spectrum Communications, Computer Science Press, 1985.

[67] S.G. Wilson, Digital Modulation and Coding, to be published by Prentice-Hall.

APPENDIX

Technical Papers:

The Multiuser ML Sequence Estimator for Convolutionally Coded Asynchronous CDMA Systems

Suboptimum Multiuser Receivers for Convolutionally Coded Asynchronous CDMA Systems

Suboptimum Multiuser Receivers for Convolutionally Coded Asynchronous CDMA Systems

T.R. Giallorenzi
Unisys Corporation
640 North 2200 West
Salt Lake City, Utah 84116-2988
(no work phone # or email assigned yet)
Home Phone: (801) 277-0959

and

S.G. Wilson
Department of Electrical Engineering
Thornton Hall
University of Virginia
(804) 924-6091
sgw@virginia.edu

Abstract

Motivated by the high complexity of the optimal sequence estimator for convolutionally coded asynchronous CDMA systems, which is developed in [25], and the potentially poor performance of the conventional receiver due to multiuser interference and the near-far problem, in this paper we examine relatively simple multiuser receivers which perform nearly as well as the optimal receiver. The multiuser receivers discussed in this paper are of two types. The first set of approaches are partitioned approaches that treat the multiuser interference equalization problem and the decoding problem separately. The second set of approaches are integrated approaches that perform both the equalization and decoding operations together. We study linear, decision feedback and trellis/tree-based approaches in each category. The asymptotic efficiency of this receiver relative to an uncoded coherent BPSK receiver (termed asymptotic multiuser coding gain, or AMCG) is used as a performance criterion throughout. Also, computer simulations are used whenever the computation of the AMCG is not feasible. It is shown that a number of the approaches which are introduced in this paper achieve a high performance level with a moderate complexity.

1. Introduction

There has been a large amount of interest recently in the design of multiuser receivers for CDMA systems. These receivers jointly estimate the transmitted symbols of all of the users in the system, as opposed to estimating them independently. This approach is most appropriate for a base station in a multipoint-to-point network where the receiver must acquire and demodulate all of the signals in the network. Almost all of the multiuser detection work has centered on uncoded links, see for example [1] - [8], [10] - [21]. Only recently has the problem of multiuser detection of coded links been considered, [22] - [26] and [30]. In [26], a sliding window version of the decorrelator, which was introduced in [4], was introduced and the authors alluded to the use of coding on the link as well. In [30], a partitioned soft-decision trellis-based approach was considered wherein the equalization and decoding operations are performed separately.

In [25], the ML sequence estimator was introduced. Its performance was significantly better than the conventional receiver's, however its complexity was prohibitively high. Motivated by the need for low complexity receivers with a performance level that is commensurate with the optimal sequence estimator's, we search in this paper for low-complexity suboptimal receivers. Figure 1 outlines the various approaches that will be examined in this paper.

Through an asymptotic analysis and simulation, it will be shown that these multiuser detection techniques are able to significantly improve the performance of the conventional basestation architecture. In [25], an important performance measure, named the *asymptotic multiuser coding gain* (AMCG), was introduced. This parameter may be defined, in general, as the required energy of a binary antipodal single-user receiver which achieves the same performance as the multiuser receiver (as the noise power approaches zero), divided by the required energy of a *single–user* binary antipodal receiver for an *uncoded* link. This parameter reduces to the familiar asymptotic multiuser efficiency (AME) parameter for the uncoded multiuser case, [2], and to the asymptotic coding gain (ACG) in the single-user coded case. Several of the decision feedback approaches which will be studied in this paper do not lend themselves to an analysis in terms of AMCG. As a result, these approaches will

be compared with the important baseline architectures via a computer simulation.

Rather than introducing the suboptimum receivers of Figure 1 in the order that they appear in the figure, it will be preferable to first discuss the partitioned approaches, and then to discuss the combined equalization and decoding approaches afterwards. This presentation will provide a unified view of the various approaches.

2. Notation

It will be assumed that the CDMA system has K users operating simultaneously on a common frequency in an asynchronous fashion. In general, it will be assumed that each user employs binary convolutional coding on its link. One further assumption in this paper is that each user employs the same convolutional code, although it is not at all difficult to generalize this work to the case where each user employs a different code.

At each time interval of length T_s, the convolutional code is generated for user k by passing P binary information bits, $\bar{I}_k(n) = (I_k^{(1)}(n),..., I_k^{(P)}(n))$, through a shift register consisting of W stages with Q modulo-2 adders. The number of output bits for each P-bit input sequence is Q bits. The rate of the code is $R_c = P/Q$ and the constraint length of the code is W. The output sequence of binary code bits for the interval corresponding to input bits $\bar{I}_k(n)$ is $(D_k^{(1)}(n),...,D_k^{(Q)}(n))$. Note that for $W = 1$ and $P = Q = 1$, we have the *uncoded* case, so in that case $D_k(n) = I_k(n)$.

In the time interval $[nT_s+(q-1)T+\tilde{\tau}_k, nT_s+qT+\tilde{\tau}_k)$, user k transmits data bit $D_k^{(q)}(n)$, where $\tilde{\tau}_k$ represents the time shift of the k^{th} user relative to some reference time, thus accounting for the asynchronism of the users relative to each other. T represents the code bit period and $T_b = T/R_c$ is the information bit duration, thus $T_s = QT = PT_b$. Let $\tilde{\tau}_k = m_k T+\tau_k$, $\tau_k \in [0,T)$, and $m_k \in \{0,...,Q-1\}$. Thus $m_k T$ is a coarse time shift and τ_k is a fine time shift for user k.

Each user in the system is assigned a particular signature sequence, and it will be assumed that this signature sequence has a duration equal to the code bit interval, although this assumption can be relaxed with a change of the notation. We will combine the carrier and signature sequence into a single signal, thus the k^{th} carrier multiplied by the binary (± 1) signature sequence, $PN_k(t)$, will be denoted by

$$s_k(t) = \begin{cases} \sqrt{2/T}\, PN_k(t)\, cos\,(\omega_c t) & 0 \le t \le T \\ 0 & otherwize \end{cases} \qquad (1)$$

The energy of the k^{th} user's code bit measured at the receiver will be denoted by E_k. It will be assumed that all K users transmit their signals through a common additive white Gaussian noise channel with two-sided noise spectral density $N_0/2$, and so the received signal will have the following form

$$r(t) = \sum_{n=-\infty}^{\infty} \sum_{k=1}^{K} \sum_{q=1}^{Q} D_k^{(q)}(n) \sqrt{E_k}\, s_k(t - nT_s - (q-1)T - \tilde{\tau}_k) + z(t) \tag{2}$$

where $z(t)$ denotes the noise.

Next we define the partial cross-correlation of the known signature sequences j and k to be

$$\rho_{jk}(l) = \int_{-\infty}^{\infty} s_j(t - \tau_j)\, s_k(t - lT - \tau_k)\, dt \ . \tag{3}$$

It is worth noting that $\rho_{jj}(0) = 1$ and $\rho_{jk}(l) = \rho_{kj}(-l)$.

As in the uncoded case, there are a number of ways in which a multiuser receiver can operate to improve upon the performance of the conventional basestation which makes decisions on each user's data using only the sequence of matched filter outputs for that user. In the next two sections, we will begin by studying hard-decision and soft-decision partitioned multiuser receivers which treat the equalization and decoding problems separately.

3. Hard-Decision Partitioned Approaches

The broad class of multiuser receiver architectures which treat equalization of the MUI and decoding of the code separately as shown in Figure 2 will be referred to as *partitioned* multiuser receivers. Within this class of partitioned approaches are those which use a hard-decision multiuser receiver to supply hard decisions from the inner channel to a bank of outer Viterbi decoders, and those which use soft decision multiuser receivers to supply soft-decisions to the outer decoders. For the hard-decision case, sufficient interleaving can provide the outer decoders with statistics which can be accurately modeled as the outputs of a bank of K binary symmetric channels. This level of sufficient interleaving will typically be achieved with a block interleaver which has a width equal to the release depth of the outer Viterbi algorithms (roughly five times the constraint length, W), and a depth greater than the average length of an error event (which is only a few code symbols at high SNR).

The crossover probability for the k^{th} user's binary symmetric channel may be written as

$$p_k \leq \sum_{\eta \geq \eta_{k,min}^{(inner)}} b_\eta Q\left[\sqrt{\frac{2E_{bk}}{N_0} R_c \eta}\right] \tag{4}$$

where $\eta_{k,min}^{(inner)}$ is the AME (introduced in [2]) of the k^{th} user's multiuser receiver which operates on the sequence of code symbols as though they were uncoded symbols, and b_η is the effective multiplicity of competing sequences of distance η. The first-event error probability is given by

$$P_e \leq \sum_{d=d_f}^{\infty} a_d P_2(d) \tag{5}$$

where a_d is the multiplicity of paths with a distance d from the desired path and $P_2(d)$ is the probability of confusing two sequences which are d Hamming units apart. The first term of this series will dominate for low noise situations:

$$P_e \simeq a_{d_f} P_2(d_f) \simeq a_{d_f} \cdot \left[b_{\eta_{k,min}^{(inner)}} Q\left[\sqrt{\frac{2E_{bk}}{N_0} \cdot R_c \eta_{k,min}^{(inner)}}\right]\right]^{t+1} \qquad as\ N_0/2 \rightarrow 0 \tag{6}$$

where

$$t = \left\lfloor \frac{d_f - 1}{2} \right\rfloor \tag{7}$$

The leading term in (6) may be upper bounded using the asymptotically tight bound $Q(x) \leq \frac{1}{2} exp(-x^2/2)$ as follows

$$a_{d_f} (b_{\eta_{k,min}^{(inner)}})^{t+1} p_k^{t+1} \leq a_{d_f} (b_{\eta_{k,min}^{(inner)}}/2)^{t+1} \exp\left[-\frac{E_{bk}}{N_0} R_c \eta_{k,min}^{(inner)} (t+1)\right] \tag{8}$$

Because this bound is asymptotically tight, we have

$$AMCG_k = \eta_{k,min} = \left[\left\lfloor \frac{d_f - 1}{2} \right\rfloor + 1\right] \cdot R_c \cdot \eta_{k,min}^{(inner)} \tag{9}$$

as long as the interleaving is perfect.

This is an important result, because it is a simple relation for the AMCG of the overall hard-decision partitioned multiuser receiver in terms of 1) the code rate, 2) the free distance of the code and 3) the AME of the multiuser receiver which is employed for making code bit decisions. It is not difficult to show that the asymptotic coding gain for a hard-decision

receiver operating in isolation is

$$ACG = R_c\,(t+1) = R_c\left(\left\lfloor \frac{d_f - 1}{2} \right\rfloor + 1\right) \tag{10}$$

thus the AMCG is actually the product of the AME of the inner receiver and the ACG of a hard-decision receiver operating in isolation using the same code. The AME has been computed for many multiuser receivers on uncoded links, and so using those results from the literature, we may easily compute the AMCG for the perfectly interleaved hard-decision partitioned receiver of interest.

Using the expressions for the AME of the inner multiuser receivers from [2], [3], [4], and [17], we may plot the AMCG for a hard-decision partitioned receiver in a 2-user system with a conventional inner receiver, a decorrelator, and a ML sequence estimator. versus $\sqrt{E_2/E_1}$ for specific codes and channel conditions. In Figure 3, the AMCG is plotted versus $\sqrt{E_2/E_1}$ for user one and the case where both users employ a rate 1/2 4-state code with $d_f = 5$, and $\rho_{21}(0) = \rho_{21}(1) = 0.2$. For this code, by equation (10) we know that the ACG for user one operating in isolation is $ACG = 1.5$, or $10\log(1.5)$ dB. Figure 4 shows the AMCG versus near-far energy ratio again for the same code with $d_f = 5$, but this time with $\rho_{21}(0) = \rho_{21}(1) = 0.3$. These figures illustrate that as the channel cross-correlations become higher, the achievable multiuser coding gain for the partitioned receivers drops. Figure 5 shows the same curves for the case where the codes employed are rate 1/2 64-state codes which have a $d_f = 10$ and again $\rho_{21}(0) = \rho_{21}(1) = 0.3$. From this figure and equation (9), it is clear that a stronger code is able to improve the achievable multiuser coding gain given the same channel conditions. (compare with Figure 4)

The complexity of the various receivers may be measured with the time complexity per decoded bit. The overall TCB will be the sum of the TCB of the outer Viterbi decoders and Q times the TCB of the inner multiuser receiver since Q code bits must be decided for every stage of the outer decoders. If we assume that the code is a rate P/Q code and has a binary memory order of κ bits, then the outer Viterbi algorithms will have a TCB = $O(2^{\kappa+P}/P)$. (Note that if code puncturing is used to obtain a rate P/Q code from a rate $1/Q$ code, then the complexity of the outer Viterbi algorithms will be TCB = $O(2^{\kappa+1})$ since there are 2^{κ} states and 2 branches per state.) Furthermore, the conventional inner receiver will have $TCB_{conv.} = O(1)$, the MLSE inner receiver will have $TCB_{MLSE} = O(2^K)$ and the J-stage DFE inner receiver will have roughly $TCB_{DFE} = O(J)$ assuming that the complexity of one MUI

calculation is roughly equivalent to a metric calculation (which it often is not). It may be more useful to compare the rough number of arithmetic operations (or multiplications) per decoded bit to make a more fair comparison. For the MLSE this is roughly $O(K\,2^K)$, and for the J-stage DFE this is approximately $O(JK)$. The decorrelator requires roughly $O(\delta K)$ operations per decoded bit if δ is the impulse response length truncation depth of a decorrelator which is implemented with an FIR matrix filter. It follows that the overall number of arithmetic operations per decoded information bit for the hard decision partitioned receivers is on the order of $OP_{conv} \approx O(2^{\kappa+P}/P)$ for the conventional inner receiver, $OP_{MLSE} \approx O([QK2^K+2^{\kappa+P}]/P)$ for the MLSE inner receiver, $OP_{JDFE} \approx O([QKJ+2^{\kappa+P}]/P)$ for the J-stage DFE inner receiver and $OP_{dec.} \approx O([QK\delta+2^{\kappa+P}]/P)$ for the decorrelator inner receiver.

4. Soft-Decision Partitioned Approaches

The computation of the AMCG for the soft-decision partitioned approaches is more difficult than for the hard-decision case. We will have to write expressions for the decision statistics at the outer Viterbi decoders for the various inner multiuser receivers, and then upper bound the worst-case values of these decision statistics to obtain lower bound expressions for the AMCG of the overall receivers. It is interesting and important to note that the conventional receiver may be viewed as a member of the class of soft-decisioned partitioned receivers with a degenerate multiuser receiver which simply passes the matched filter outputs to the outer Viterbi algorithms without altering them. As a result, by analyzing the multiuser receivers in this class, we will also be analyzing the important conventional receiver's performance.

Consider the system shown in Figure 2 again. If the deinterleaved outputs of the multiuser receiver are now considered to be soft outputs denoted by $y_k^{(q)}(n)$ for the k^{th} user's code bit q in the n^{th} interval, then the first question to be asked is, "What is the structure of the optimal subsequent decoders?" If $y_k^{(q)}(n)$ is conditionally Gaussian, then the appropriate decoding strategy for sequences over a decoding window $n = i_0$ to $i_0+\Gamma$ is to use a Viterbi algorithm with the following correlation metric

$$\Lambda(\overline{y}_k \mid \overline{D}_k) = \sum_{n=i_0}^{i_0+\Gamma} \sum_{q=1}^{Q} y_k^{(q)}(n) \cdot D_k^{(q)}(n) \tag{11}$$

where $\overline{y}_k$ is the deinterleaved sequence of soft decision outputs of user k's multiuser receiver,

and $\bar{D}_k$ is the sequence of transmitted code symbols for user k. Note that if we wish to maintain consistency with the "horizon" used in [25], $i_0 = \alpha(-M)$ and $\Gamma = \alpha(M) - i_0$.

The notation used in equation (11) is going to become overly complex later and so we will simplify this equation by defining a modulo Q decomposition of an index, j, in the same way that the modulo K decomposition was defined in [1] and [25]. In this way, we can write (11) with a single sum which accumulates all Q of the code bits for each interval, n, for user k.

$$\Lambda(\bar{y}_k \mid \bar{D}_k) = \sum_{j=i_0}^{i_0+Q\Gamma} y_{kj} D_{kj} \tag{12}$$

In this equation, $y_{kj} = y_k^{(\alpha(j))}(\beta(j))$, $D_{kj} = D_k^{(\alpha(j))}(\beta(j))$, and $j = \alpha(j)Q + \beta(j) - 1$. (Note that we assume that $i_0 = \beta(i_0)$ without a loss in generality)

The metric for any valid competing sequence in the trellis $\bar{D}_k + 2\bar{e}_k$ will be

$$\Lambda(\bar{y}_k \mid \bar{D}_k + 2\bar{e}_k) = \sum_{j=i_0}^{i_0+Q\Gamma} y_{kj}[D_{kj} + 2e_{kj}] \tag{13}$$

where $\bar{e}_k$ is user k's error sequence, and $e_{kj} = e_k^{(\alpha(j))}(\beta(j))$. It thus follows that the two-sequence error probability for sequences differing by $\bar{e}_k$ will be given by

$$P_2(\bar{e}_k) = P[\Lambda(\bar{y}_k \mid \bar{D}_k + 2\bar{e}_k) > \Lambda(\bar{y}_k \mid \bar{D}_k)] = P[\sum_{j=i_0}^{i_0+Q\Gamma} y_{kj} e_{kj} > 0] \tag{14}$$

where it is assumed that the nonzero portion of the error sequence $\{e_{kj}\}$ occurs in the region $i_0 \le j \le i_0 + Q\Gamma$.

To proceed, we need to be able to characterize y_{kj}. To do this, let

$$y_{kj} = D_{kj}\sqrt{E_k} + N_{kj} \tag{15}$$

where N_{kj} is the noise for user k's code bit $\alpha(j)$ in the $\beta(j)^{th}$ interval after deinterleaving the soft-decision multiuser receiver outputs. The characteristics of the noise will depend on the inner multiuser receiver in use.

4.1 The Conventional Receiver

With this generic description of the inputs to the outer Viterbi decoders, we may now consider a number of special cases for specific soft-decision multiuser inner receivers. One of the most important special cases of the soft-decision partitioned receiver is the

conventional receiver. This receiver essentially uses a degenerate multiuser receiver which simply passes the matched filter outputs on to the outer Viterbi algorithms without altering them in any way, except possibly unscrambling them in a deinterleaver. For the conventional receiver, each input to the outer Viterbi algorithms corresponds to a desired part, $D_{kj}\sqrt{E_k}$, and a noise part, corresponding to

$$N_{kj} = RMUI_{kj} + \tilde{z}_{kj} = MUI_{kj} + z_{kj} \tag{16}$$

$RMUI_{kj}$ denotes the residual MUI, which for the conventional receiver is equal to the MUI on the matched filter output, and $\tilde{z}_{kj}$ denotes the Gaussian portion of the noise. It is worth noting that this overall noise is not Gaussian, and so the use of the correlation metric in the outer Viterbi decoders is not optimum. The noise is Gaussian, conditioned on the signal plus interference; however the outer Viterbi algorithms do not condition on the interference due to the other users. It is worth noting that it is common to appeal to the Central Limit Theorem to claim that the noise in equation (16) is approximately Gaussian. This leads to the claim that the correlation metric is appropriate for the outer decoders. The Central Limit Theorem leads to misleading and overly optimistic conclusions in many cases, however.

Because the noise statistic in (16) will be Gaussian conditioned on a given sequence of the desired user and the interferers, we could obtain a performance estimate by averaging with respect to all possible sequences. This performance will be asymptotically determined by the worst-case interference case. As a result, we may bound the residual MUI by its effective worst case value for completely unconstrained interferers to obtain a lower bound on the AMCG of the conventional receiver. The worst case value of $RMUI_{kj}$ when the constraints on the other user's transmitted code sequences are taken into account will be no greater than (and most often lower than) the value assuming unconstrained sequences. If interleaving is used on the link, then the interference patterns will be closer to unconstrained interference patterns since the interleaving will effectively break up the code's constraints. Another point worth noticing is that according to (16), the noise on the receiver outputs is the same as the noise on the matched filter outputs, albeit potentially scrambled from the deinterleaving process. The noise sequence $\{z_{kj}\}_{j=1}^{\infty}$ is white, and the deinterleaving will not affect this.

With this characterization of y_{kj}, we may proceed to substitute (15) and (16) into (14).

$$P_2(\overline{e_k}) = P[\sum_{j=i_0}^{i_0+Q\Gamma} e_{kj}z_{kj} > -\sum_{j=i_0}^{i_0+Q\Gamma} e_{kj}(D_{kj}\sqrt{E_k} + MUI_{kj})] \tag{17}$$

Next define

$$\beta = \sum_{j=i_0}^{i_0+Q\Gamma} e_{kj} z_{kj} \tag{18}$$

Note that whenever $e_{kj} \neq 0$, then $e_{kj} = -D_{kj}$ (since $D_{kj} + 2e_{kj}$ must be a valid error sequence). Making these substitutions we get

$$P_2(\bar{e}_k) = P\left[\beta > \sum_{j=i_0}^{i_0+Q\Gamma} (e_{kj})^2 \sqrt{E_k} - e_{kj} MUI_{kj}\right] \tag{19}$$

Next, replace $e_{kj} MUI_{kj}$ by its largest possible value for completely unconstrained interferers,

$$e_{kj} MUI_{kj} \leq (e_{kj})^2 \left[\sum_{m=1}^{k-1} |\rho_{km}(1)| \sqrt{E_m} + \sum_{m \neq k} |\rho_{km}(0)| \sqrt{E_m} + \sum_{m=k+1}^{K} |\rho_{km}(-1)| \sqrt{E_m}\right] \tag{20}$$

Thus

$$P_2(\bar{e}_k) \leq P\left[\beta > \sum_{j=i_0}^{i_0+Q\Gamma} (e_{kj})^2 \gamma_k\right] \tag{21}$$

where

$$\gamma_k = \sqrt{E_k} - \left[\sum_{m=1}^{k-1} |\rho_{km}(1)| \sqrt{E_m} + \sum_{m \neq k} |\rho_{km}(0)| \sqrt{E_m} + \sum_{m=k+1}^{K} |\rho_{km}(-1)| \sqrt{E_m}\right] \tag{22}$$

We may next note that

$$wt[\bar{e}_k] = \sum_{j=i_0}^{i_0+Q\Gamma} (e_{kj})^2 \tag{23}$$

so (21) becomes

$$PSUB2(\bar{e}_k) \leq P[\beta > wt[\bar{e}_k]\gamma_k] \tag{24}$$

Because β is a linear combination of independent Gaussian random variables of zero mean and variance $N_0/2$, it is not difficult to show that $E[\beta] = 0$, and $E[\beta^2] = wt[\bar{e}_k] \cdot N_0/2$. It follows that

$$P_2(\bar{e}_k) \leq Q\left[\sqrt{\frac{2E_{bk}}{N_0} \cdot \frac{\gamma_k^2}{E_{bk}} \cdot wt[\bar{e}_k]}\right] \quad \text{for } \gamma_k \geq 0 \tag{25}$$

which implies that

$$\eta_k^c(\bar{e}_k) \geq \frac{\gamma_k^2}{E_{bk}} \cdot wt[\bar{e}_k] \quad \text{for } \gamma_k \geq 0 \tag{26}$$

Since γ_k, which was defined in (22), may be negative, we may generalize the bound in (26) to be

$$\eta_k^c(\bar{e}_k) \geq \max^2\{\, 0,\, \gamma_k(wt[\bar{e}_k]/E_{bk})^{1/2} \,\} \tag{27}$$

Finally, since $E_{bk} = E_k/R_c$, we note that

$$\eta_{k,min}^c \geq \inf_{\bar{e}_k \text{ valid}} \eta_k^c(\bar{e}_k) \geq \max^2\{\, 0,\, \gamma_k(d_f R_c/E_k)^{1/2} \,\} \tag{28}$$

Stated in a different form we have the final bound

$$\eta_{k,min}^c \geq \max^2\{\, 0,(d_f R_c)^{1/2}\,[1 - \sum_{m=1}^{k-1} |\rho_{km}(1)| \left[\frac{E_m}{E_k}\right]^{1/2} - \sum_{m\neq k} |\rho_{km}(0)| \left[\frac{E_m}{E_k}\right]^{1/2} - \sum_{m=k+1}^{K} |\rho_{km}(-1)| \left[\frac{E_m}{E_k}\right]^{1/2}\,]\,\}$$

For the 2-user, $R_c = 1/2$ case, this bound takes the form

$$\eta_{1,min}^c > \begin{cases} \frac{d_f}{2}\left[1 - \zeta\sqrt{\frac{E_2}{E_1}}\right]^2 & \text{if } \sqrt{\frac{E_2}{E_1}} < 1/\zeta \\ 0 & \textit{otherwise} \end{cases} \tag{30}$$

(recall that $\zeta = |\rho_{21}(0)| + |\rho_{21}(1)|$) This lower bound on the AMCG for the conventional receiver is potentially loose if the coding imposes severe restrictions on the allowable interfering sequences. This is due to the fact that the worst-case allowable interfering sequence may be much less severe than the unconstrained worst case sequence. Nonetheless, with good interleaving, we believe that it will be a reasonable approximation.

The bound in (30) is plotted in Figures 6 and 7 for the $\zeta = 0.4$ and 0.6 cases respectively. From these figures, we see that as the energy of the interferer grows, the AMCG of user 1's conventional receiver drops to zero. This zero AMCG typically implies that the receiver will have a performance floor.

The TCB of the conventional receiver with soft-decisions will be the same as those of the partitioned hard-decision receiver with a conventional inner receiver.

4.2 Soft-Decision Partitioned Receiver With A Linear Multiuser Receiver

Another interesting class of partitioned receivers is those with a linear inner multiuser receiver, [26]. The most well known members of the class of linear multiuser receivers are the decorrelator, [4] and the minimum mean squared error (MMSE) receivers [7] and [14].

In this section, we will focus on the decorrelator from [4] as a representative of this class because it leads to a tractable analysis. This multiuser receiver has the property that $RMUI_{kj} = 0$ at the decorrelator output, but the variance of $\tilde{z}_{kj}$ will generally be larger than that of z_{kj} due to this receiver's noise enhancement property (see equation (16)). For this receiver, we may write the two-sequence error probability as

$$P_2(\overline{e}_k) = P[\sum_{j=i_0}^{i_0+Q\Gamma} e_{kj}(D_{kj}\sqrt{E_k} + \tilde{z}_{kj}) > 0] \tag{31}$$

$$= P[\sum_{j=i_0}^{i_0+Q\Gamma} e_{kj}\tilde{z}_{kj} > -\sum_{j=i_0}^{i_0+Q\Gamma} e_{kj}D_{kj}\sqrt{E_k}] \tag{32}$$

If we next notice that $D_{kj} = -e_{kj}$ whenever $e_{kj} \neq 0$, use (23), and redefine β for this section in the same fashion as in (18) to now be

$$\beta = \sum_{j=i_0}^{i_0+Q\Gamma} e_{kj}\,\tilde{z}_{kj}\,, \tag{33}$$

then we rewrite (32) as

$$P_2(\overline{e}_k) = P[\beta > wt[\overline{e}_k]\sqrt{E_k}]\,. \tag{34}$$

β is a linear combination of $\tilde{z}_{kj}$'s which are each, in turn, a linear combination of the matched filter output noises, $\{z_{kj}\}$. It is easy to show that $E[\beta] = 0$. The computation of the second moment of β requires more work, however.

$$E[\beta^2] = E[\sum_{j=i_0}^{i_0+Q\Gamma} e_{kj}\tilde{z}_{kj} \sum_{p=i_0}^{i_0+Q\Gamma} e_{kp}\tilde{z}_{kp}] \tag{35}$$

$$= \sum_{j=i_0}^{i_0+Q\Gamma} \sum_{p=i_0}^{i_0+Q\Gamma} e_{kj}e_{kp}E[\tilde{z}_{kj}\tilde{z}_{kp}] \tag{36}$$

Next, define

$$E[\tilde{z}_{kj}\tilde{z}_{kp}] = \frac{N_0}{2}\Phi_{kk}(p-j) \tag{37}$$

Using this nomenclature, we may proceed to rewrite (34) as

$$P_2(\overline{e}_k) = Q\left[\sqrt{\frac{E_k \cdot wt[\overline{e}_k]^2}{E[\beta^2]}}\right] \tag{38}$$

$$= Q\left[\sqrt{\frac{2E_{bk}}{N_0}\cdot\frac{R_c wt[\bar{e}_k]^2}{\sum_j\sum_p e_{kj}e_{kp}\Phi_{kk}(p-j)}}\right] \tag{39}$$

so it is easy to see from (39) that

$$\eta_k^d(\bar{e}_k) = \frac{R_c wt[\bar{e}_k]^2}{\sum_j\sum_p e_{kj}e_{kp}\Phi_{kk}(p-j)} \tag{40}$$

$$= \frac{R_c wt[\bar{e}_k]^2}{wt[\bar{e}_k]\Phi_{kk}(0) + 2\sum_{j=i_0}^{i_0+Q\Gamma}\sum_{l=1}^{Q\Gamma} e_{kj}e_{kj-l}\Phi_{kk}(l)} \tag{41}$$

Now, all that remains to be done to obtain numerical results is to evaluate $\Phi_{kk}(l)$. We will do this for the 2-user case. If $\bar{\rho}(z)$ denotes the multiuser system channel transfer function matrix, and so $\bar{\rho}^{-1}(z)$ denotes the decorrelator's transfer function matrix, then for the 2-user case we have, [4]

$$\bar{\rho}^{-1}(z) = \frac{1}{1-\rho_{12}^2-\rho_{21}^2-\rho_{12}\rho_{21}z-\rho_{12}\rho_{21}z^{-1}}\begin{bmatrix} 1 & -(-\rho_{12}+\rho_{21}z^{-1}) \\ -(\rho_{12}+\rho_{21}z) & 1 \end{bmatrix} \tag{42}$$

so

$$\rho_{kk}^{-1}(z) = \frac{1}{1-\rho_{12}^2-\rho_{21}^2-\rho_{12}\rho_{21}z-\rho_{12}\rho_{21}z^{-1}} \qquad \text{for } k\in\{1,2\} \tag{43}$$

Taking the inverse Z-transform of this polynomial, we obtain

$$\Phi_{kk}(l) = ZT^{-1}[\rho_{kk}^{-1}(z)] = \frac{(1-\rho_{12}^2-\rho_{21}^2-\sqrt{[1-(\rho_{12}+\rho_{21})^2][1-(\rho_{12}-\rho_{21})^2]})^{|l|}}{(2\rho_{12}\rho_{21})^{|l|}\sqrt{[1-(\rho_{12}+\rho_{21})^2][1-(\rho_{12}-\rho_{21})^2]}} \tag{44}$$

where $\rho_{12} = \rho_{21}(0)$, and $\rho_{21} = \rho_{21}(1)$, [4].

We may obtain lower bound on the AMCG via the following procedure. Note that $\Phi_{kk}(l)$ has the property that $\Phi_{kk}(0) > \Phi_{kk}(1) > \Phi_{kk}(2) > \ldots$ so the second term in the denominator of (41) may be upper bounded as follows

$$2\sum_{j=i_0}^{i_0+Q\Gamma}\sum_{l=1}^{Q\Gamma} e_{kj}e_{kj-l}\Phi_{kk}(l) \le 2\Big[\sum_{l=1}^{wt[\bar{e}_k]-1}\Phi_{kk}(l)(wt[\bar{e}_k]-l)\Big] \tag{45}$$

and this allows us to bound the expression in (41) by

$$\eta_k^d(\bar{e}_k) \geq \frac{R_c wt[\bar{e}_k]^2}{wt[\bar{e}_k]\Phi_{kk}(0) + 2\sum_{l=1}^{wt[\bar{e}_k]-1} \Phi_{kk}(l)(wt[\bar{e}_k]-l)} = g(R_c, wt[\bar{e}_k], \rho_{12}, \rho_{21}) \qquad (46)$$

This is a bound on $\eta_k^d(\bar{e}_k)$ which is only a function of $wt[\bar{e}_k]$ rather than the actual error sequence $\bar{e}_k$. Using the fact that this expression is monotonically increasing with $wt[\bar{e}_k]$, we can obtain a lower bound on the AMCG for this partitioned receiver:

$$\eta_{k,min}^d \geq \min_{wt[\bar{e}_k] \in \{d_f, d_f+1, \ldots\}} g(R_c, wt[\bar{e}_k], \rho_{12}, \rho_{21}) = \frac{R_c d_f^2}{d_f \Phi_{kk}(0) + 2\sum_{l=1}^{d_f-1} \Phi_{kk}(l)(d_f-l)} \qquad (47)$$

As an example, for the case where $\rho_{21}(1) = \rho_{21}(0) = 0.3$ we get $\eta_1^d \geq 1.67$ (see Figure 7). The result for $\rho_{21}(0) = \rho_{21}(1) = 0.2$ is plotted in Figure 6.

Another interesting result of (47) is that it provides a tightening of the lower bound on the AMCG of the MLSE of [25]. This is due to the fact that the MLSE, which is the optimal sequence estimator, will have a higher AMCG than the partitioned soft-decision decorrelator, which is a suboptimal sequence estimator. This tightening of the bound on the MLSE's AMCG is incorporated into Figures 6 and 7.

An upper bound on the AMCG for the soft-decision partitioned decorrelator may be obtained by performing a non-exhaustive search over the set of possible valid $\bar{e}_k$ sequences. One valid error vector for the standard four-state rate 1/2 code is the following, $\bar{e}_k$ = (110111). This error vector gives the smallest result of equation (41) of those tested. Because the actual minimum of equation (41) over the set of all valid error sequences must be no larger than the minimum of (41) over the small set of sequences that we tested, we have an upper bound on the AMCG. This upper bound turns out to be quite close to the lower bound we have already obtained, so we have a very accurate picture of the partitioned decorrelator's performance. This upper bound is also plotted in Figures 6 and 7.

The complexity of the soft-decision and hard-decision partitioned receivers with a decorrelating inner receiver will be the same. This is a result of the fact that the only difference between the two is that the soft-decision version does not make a hard decision on the decision statistics before passing them to the outer Viterbi decoders, and the outer decoder metrics will differ but be of the same complexity order.

4.3 Soft-Decision Partitioned Receiver with a Trellis-Based or Tree-Based Inner Receiver

A third approach which potentially will have the best performance of any partitioned approach is the one which uses a soft-decision trellis-based or tree-based receiver as the inner multiuser receiver. There are a number of possible trellis-based receivers, the most important of which are the ML sequence estimator, [1], and the reduced state sequence estimator (RSSE), [6], [31]. As an example of a tree-based receiver, see [8]. In their standard form, each of these receivers output hard-decisions, and so techniques such as those of [29] must be applied to allow the inner receiver to supply soft outputs to the outer Viterbi decoders.

This approach has recently been proposed by two research groups, [9], and [30]. Both groups cite the prohibitive complexity of the full ML sequence estimator, and examine RSSE and sequential decoding alternatives.

The computation of the AMCG for these approaches remains an open problem. The AMCG of the soft-decision partitioned receiver with an ML sequence estimator should have a higher AMCG than any other partitioned receiver, since the ML sequence estimator is the optimum inner receiver in the sequence error probability sense. It follows that RSSE and sequential decoding approaches which do not suffer significantly in performance relative to the MLSE will also have a high AMCG. The interested reader is referred to [9] and [30] for more detail on these particular approaches.

4.4 Soft-Decision Partitioned Receiver With a DFE Inner Receiver

In this approach, a multistage DFE operates on the set of matched filter outputs, by making tentative decisions and feeding these decisions back to make estimates of the MUI which will be subtracted from other matched filter outputs. The key in the *soft code symbol DFE* (SCS-DFE) approach is that at the final stage, the MUI estimate will again be subtracted from the delayed matched filter output, but no hard-decision making will be performed. Instead, the modified matched filter output will be passed straight to the Viterbi decoder.

At this point, we have not committed to a particular type of multistage DFE. As discussed in [21], there have been at least six architectures proposed in the literature for

asynchronous CDMA links, [5], [7], [12 - 14], [19 - 21] and [27], and there has also been some work on improving the decision making procedure of the algorithms, [16].

The performance of this class of approaches is difficult to evaluate analytically, due to the presence of error propagation. Expressions for the AME of the Varanasi DFE have recently been reported in [17], but the approaches used to get those AME expressions do not easily generalize to the coded link case. It is possible to evaluate the AMCG under the assumption of correct feedback. However this implies that as long as the correlation parameters and energies have been perfectly estimated, $RMUI = 0$. Since there is no residual interference if the feedback is correct, and there is no noise enhancement, as in the case of the decorrelator, we obtain the result that the AMCG is that of a single-user system. Clearly, the presence of error propagation degrades the AMCG by some amount, so the computation of the actual AMCG remains an open question. Consequently, simulation will be the performance evaluation technique for this class of receiver.

Because the structure of the integrated DFE which will be discussed in section 5.3 is most like the Varanasi style uncoded link multistage decoder, it is interesting to compare the integrated DFE with the Varanasi style SCS-DFE. In addition, because it was shown in [20 - 21] that in most cases, the Hybrid DFE outperforms the other two architectures on an uncoded link, it is an obvious candidate for use in an SCS-DFE structure. Thus, the structures that were simulated were the Hybrid and Varanasi versions of the SCS-DFE. The modifications to the decision making devices in each preliminary stage of the multistage decoders discussed in [16] were not considered here, although those modifications may provide improvements in some cases.

Figure 9 shows the performance curves for a four-user "0.2 channel". As this figure illustrates, the conventional decoder suffers about a 3 dB loss at $P_{b\ average} = 2 \cdot 10^{-3}$ relative to the performance of the same receiver operating in the absence of MUI. For this case, the Hybrid version of the SCS-DFE outperforms the Varanasi version of the SCS-DFE. This is similar to the results obtained on the uncoded link simulated in [20 - 21].

Figure 10 shows the performance for a more severe channel. In this figure, it is evident that all of the decoders perform significantly worse than in the "0.2 channel" due to the more severe MUI. In addition, the hybrid SCS-DFE again outperforms the Varanasi DFE.

Once again, the complexity of the soft-decision partitioned DFE receiver will be of the same order as in the hard-decision case.

5. Combined Equalization and Decoding Approaches

In all of the partitioned approaches, regardless of the type, the multiuser receiver operates at the code symbol level as though there were no coding on the link, and then passes its decisions or improved statistics to an outer decoder. The deficiency with this approach is that separating the functions of cancelling the MUI and decoding the message does not take full advantage of the coding on the link. The approaches discussed in this section attempt to alleviate this shortcoming.

5.1. Trellis-Based and Tree-Based Combined Equalization and Decoding Approaches

The MLSE of [25] is a trellis-based approach which combines the functions of equalization and decoding into one operation. This approach is the optimal sequence estimator. The MLSE has a prohibitively high number of states, thus it is natural to look to simplify the decoding process by combining states in some fashion. This approach of combining states in some fashion is what is referred to as reduced state sequence estimation (RSSE). There are a number of publications on the application of RSSE to simplify the MLSE for the uncoded case, [6], [31], as well as at least one other on the application of RSSE to simplify the process of equalizing and decoding a coded signal on a single-user dispersive link, [28]. It is undoubtedly possible to apply these techniques to the problem at hand to obtain a performance versus complexity tradeoff.

Just as in [8], it is also presumably possible to use sequential decoding approaches to lower the complexity of the MLSE for the coded link case. Sequential decoding would also provide the opportunity to tradeoff performance versus complexity.

One problem with the trellis-based approaches, however, is that they may not be as robust to mismatch (a misestimation of the correlation or energy parameters) as some of the simpler approaches like the partitioned decorrelator and DFE approaches. In [15], it was shown that the uncoded link MLSE was not as robust as a Varanasi DFE to mismatch, in the sense that for even small values of mismatch, the suboptimum DFE outperformed the MLSE. This high sensitivity of the optimal approach to mismatch is a very undesirable feature, and it may very well carry over to suboptimal approaches which are based on the MLSE like the RSSE and sequential approaches. Nonetheless, given no mismatch, the trellis-based and tree-based approaches have the potential to perform nearly as well as the MLSE, possibly with a significantly decreased complexity.

5.2 The Decision Feedback Combined Equalization and Decoding Approach: The Integrated DFE

The idea in the approach we will refer to as the *integrated DFE* is that the MUI can be more reliably estimated by exploiting the coding. Thus, instead of using a hard-decision device in the first stage of a multistage DFE, like that of [5], we may decode the message using a soft-decision Viterbi algorithm which operates on the stream of matched filter outputs in the j^{th} channel, and then re-encodes the decoded bits to form estimates of the code bits. These code bit estimates can then be used to estimate the MUI in other user's channels. Again, as in the uncoded case, the decision feedback may be performed for as many stages as is desired (see Figure 8) The performance of this approach is difficult to evaluate analytically, again due to the presence of incorrect feedback. As a result, simulation will be the performance evaluation technique in this section.

A characteristic of convolutional codes, or most codes for that matter, is that at very low signal to noise ratios, the coded link may perform worse than an uncoded link. When the signal to noise ratio is in this regime, it is possible that the Viterbi decoder whose outputs are re-encoded to form the ML estimate of the code bit sequence, may perform worse than a simple hard-decision device operating on the code bits without regard to the coding. As a result of this characteristic, it is important that the combination of the thermal noise and MUI is not so strong that the re-encoded Viterbi output sequence is worse than the estimated code bits of a simple threshold detector for the integrated DFE to outperform an SCS-DFE. Basically, the structure which provides better estimates of the code bit sequence will have a better estimate of the MUI in the other channel's multistage decoders. In general, because coding generally allows better estimates of the transmitted sequence, it is reasonable to expect the integrated DFE to outperform an SCS-DFE of a similar architecture like a SCS-DFE with a Varanasi DFE.

Figure 9 shows performance of the integrated DFE and the various SCS-DFE approaches on the "0.2 channel". In this environment, the integrated DFE is able to nearly recoup all of this loss, while the various SCS-DFEs are able to only recoup some of the loss. It may thus be concluded that the thermal noise and MUI are weak enough to be operating in the regime where a receiver which exploits the coding performs better than one which does not.

Figure 10 shows the performance on a more severe channel. The integrated DFE still uniformly outperforms the Varanasi version of the SCS-DFE. For these particular channel characteristics, however, the hybrid SCS-DFE is able to outperform the integrated DFE at larger values of E_b/N_0. While this may seem surprising at first, it is simply due to the fact that even though the hybrid SCS-DFE performs separate equalization and decoding, it has a high quality first stage which is able to provide better code symbol estimates to the second stage MUI estimator than the conventional Viterbi algorithm operating in the first stage of the integrated DFE. This case illustrates that when the MUI is strong enough, the integrated DFE will not always outperform a well designed SCS-DFE, although it does in most cases.

To compute the TCB for the integrated DFE, we again assume that the computation of the MUI in each stage of the DFE structures is roughly equivalent in complexity to the computation of one metric in the Viterbi decoder. Thus adopting this convention, we may conclude that for a link with rate $1/Q$ and constraint length W codes, the J-stage integrated DFE has a time complexity of roughly TCB = $O((J-1)Q+J2^W)$. This is significantly higher than that of the SCS-DFE, although it is far less than that of the MLSE of [25]. In the general rate P/Q code case, if again, $\kappa = \log_2 S$ where S is the number of states in each user's encoder, the integrated DFE has TCB = $O([(J-1)Q+J2^{\kappa+P}]/P)$. Again, because each MUI computation grows in complexity with K, we may say that the number of arithmetic operations per decoded bit is on the order of $OP_{IDFE} = O([(J-1)QK+J2^{\kappa+P}]/P)$. This is of about the same order as for the partitioned SCS-DFE approaches.

We may thus conclude that the integrated DFE has a larger TCB than any of the SCS-DFE approaches, but its complexity as measured in terms of the number of operations required per decoded bit is not necessarily higher and its performance is better in most cases. As a result, the integrated DFE is an attractive approach. As we have seen in Figure 10, however, even the integrated DFE does not perform well when the MUI becomes too strong.

6. Conclusions

In this paper, a large number of approaches have been discussed (see Figure 1). The approaches can be categorized as linear, DFE and trellis-based, as in Figure 1, or they may be categorized as partitioned and combined approaches as they were presented in this paper.

Throughout this paper, the number of arithmetic operations per decoded bit was used as a measure of the complexity of the receivers. It is clear that for a large number of users and

large codes, the MLSE and Partitioned MLSE are too complex to be of use. The conventional approach has the lowest complexity and all of the other approaches have an intermediate complexity (linear with K).

Throughout this paper, the various approaches were compared using the AMCG performance measure whenever possible. When the receivers did not lend themselves to an AMCG analysis, as in the case of the DFE's, computer simulations were used to compare their performance to the important baselines, the single-user bound, the MLSE's performance and the conventional receiver's performance.

An examination of the figures of this paper illustrate that the MLSE of [25] has the best performance. The worst performance of any receiver considered was the hard-decision conventional followed by the soft-decision conventional. The soft-decision partitioned approaches with a decorrelator or DFE inner receiver provide reasonable performance and have a fairly low complexity. Also, the integrated DFE provided a good compromise of performance and complexity in the situations considered.

References

[1] S. Verdu, "Minimum Probability of Error for Asynchronous Gaussian Multiple Access Channels," *IEEE Trans. Inform. Theory*, vol. IT-32, Jan. 1986, pp 85-96.

[2] S. Verdu, "Optimum Multiuser Asymptotic Efficiency," *IEEE Trans. on Comm.*, vol.34, no.9, May 1991, pp. 890-897.

[3] S. Verdu, "Recent Progress in Multiuser Detection," *Advances in Communications and Control Systems, ComCon '88*, Lecture Notes in Control and Information Science Series, NY, Springer-Verlag, 1989.

[4] R. Lupas and S. Verdu, "Near-Far Resistance of Multiuser Detectors in Asynchronous Channels," *IEEE Trans. on Comm.*, vol.38, no.4, April 1990, pp 496-508.

[5] M. Varanasi and B. Aazhang, "Multistage Detection in Asynchronous CDMA Communications," *IEEE Trans. on Comm.*, vol.38, no.4, pp 509-519, April 1990.

[6] M.K. Varanasi "Reduced State Sequence Detection for Asynchronous Gaussian Multiple-Access Channels", *Proceedings of ISIT*, San Antonio, Texas, January, 1993, pp. 42.

[7] Z. Xie, R.T. Short and C.K. Rushforth, "A Family of Suboptimum Detectors for Coherent Multiuser Communications," *IEEE Journ. on Select. Areas in Comm.*, vol.8, no.4, May 1990, pp 683-690.

[8] Z. Xie, C.K. Rushforth, R.T. Short, "Multiuser Signal Detection Using Sequential Decoding," *IEEE Trans. on Comm.*, vol. 38, no. 5, May 1990, pp. 578-583.

[9] C.K. Rushforth, M. Nasiri-Kinari, A. Abbaszadeh, "A Reduced-Complexity Sequence Detector With Soft Outputs for Partial-Response Channels," *Proc. of GLOBECOM'93*, Houston, TX, December, 1993.

[10] R. Kohno, H. Imai, M. Hatori, and S. Pasupathy, "An Adaptive Canceller of Cochannel Interference for Direct-Sequence Spread-Spectrum Multiple-Access Communication Networks in a Power Line," *IEEE Journ. on Select. Areas in Comm.*, vol.8, no.4, May 1990, pp 691-699.

[11] Kohno et. al., "Combination of an Adaptive Array Antenna and a Canceller of Interference for Direct-Sequence Spread-Spectrum Multiple-Access Systems," *IEEE Journ. on Select. Areas in Comm.*, vol.8, no.4, May 1990, pp 675-681.

[12] A. Duel-Hallen, "On Suboptimal Detection for Asynchronous Code-Division Multiple-Access Channels," Proceedings of the 1992 Conference on Information Science and Systems, Princeton, NJ, pp. 838-843.

[13] A. Duel-Hallen, "A Family of Multiuser Decision-Feedback Detectors for Asynchronous Code-Division Multiple-Access Channels," to be published in *IEEE Trans. on Comm.*

[14] A. Duel-Hallen, "Multiuser MMSE and Zero-Forcing Decision Feedback Detectors for Asynchronous CDMA," *Proc. of GLOBECOM'93*, Houston, TX, December, 1993.

[15] M. Kocic, D. Brady, "Asymptotic Multiuser Efficiency of the Maximum Likelihood Sequence Detector with Channel Mismatch," *Proceedings of CISS'93*.

[16] X. Zhang, D. Brady, "Soft-Decision Multistage Detectors for Asynchronous AWGN Channels," *Proceedings of the Thirty–First Allerton Conference on Communication Control and Computing*, October, 1993.

[17] X. Zhang, D. Brady, "Asymptotic Multiuser Efficiency for M-Stage Detection," submitted to the *IEEE Trans. on Info. Theory.*

[18] S.D. Gray, D. Brady, "The Asymptotic Multiuser Efficiency of Two-Stage Detection in Mismatched AWGN Channels," submitted to CTMC at GLOBECOM '93.

[19] P.Patel, J. Holtzman, "Analysis of a DS/CDMA Interference Cancellation Scheme Using Correlations," *Proc. of GLOBECOM'93*, Houston, TX, December, 1993.

[20] T.R. Giallorenzi, S.G. Wilson, "Decision Feedback Techniques for CDMA System Equalization," submitted to *IEEE Trans. on Comm.*.

[21] T.R. Giallorenzi, S.G. Wilson, "Decision Feedback Multiuser Receivers for Asynchronous CDMA Systems," *Proceedings of GLOBECOM'93*, Houston, TX.

[22] T.R. Giallorenzi, S.G. Wilson, "Trellis-Based Multiuser Receivers for Convolutionally Coded CDMA Systems," *Proceedings of the Thirty–First Allerton Conference on Communication Control and Computing*, October, 1993.

[23] T.R. Giallorenzi, S.G. Wilson, "Multistage Decision Feedback and Trellis-Based Multiuser Receivers for Convolutionally Coded CDMA Systems," *Technical Report UVA/538341/EE93/102*, Communication Systems Laboratory, Dept. of Elec. Engineering, University of Virginia, May, 1993.

[24] T.R. Giallorenzi, *Multiuser Receivers for Convolutionally Coded CDMA Systems*, Ph.D. Dissertation, Dept. of Electrical Engineering, University of Virginia, May 1994.

[25] T.R. Giallorenzi, S.G. Wilson, "The Multiuser ML Sequence Estimator for Convolutionally Coded Asynchronous CDMA Systems," submitted to *IEEE Trans. on Comm.* Feb. 1994.

[26] S.S.H. Wijayasuriya, G.H. Norton, J.P. McGeehan, "A Sliding Window Decorrelating Algorithm for DS-CDMA Receivers," *Electronics Letters*, vol. 28, no. 17, August, 1992, pp.1596-1598.

[27] A.J. Viterbi, "Very Low Rate Convolutionl Codes for Maximum Theoretical Performance of Spread-Spectrum Multiple-Access Channels," *IEEE Journ. on Select. Areas in Comm.*, vol.8, no.4, May 1990, pp 641-649.

[28] P.R. Chevillat, E. Eleftheriou, "Decoding of Trellis-Encoded Signals in the Presence of Intersymbol Interference and Noise," *IEEE Trans. on Comm.*, vol. 37, no. 7, July 1989, pp. 669-676.

[29] J. Hagenauer, P. Hoeher, "A Viterbi Algorithm with Soft-Decision Outputs and its Applications," *Proceedings of GLOBECOM '89*, Dallas, Texas, Nov. 1989, pp. 1680-1686.

[30] P. Hoeher, "On Channel Coding and Multiuser Detection for DS-CDMA," *Proc. IEEE ICUPC '93*, Ottowa, Canada, October, 1993, pp.641-646.

[31] S.K. Wilson, J.M. Cioffi, "Equalization Techniques for Direct Sequence Code-Division Multiple Access Systems in Multipath Channels" *Proc. of ISIT'93*, San Antonio, TX.

[32] M.V. Eyuboglu, S.U.H. Qureshi, "Reduced-State Sequence Estimation with Set Partitioning and Decision Feedback," *IEEE Trans. on Comm.*, vol. 36, Jan. 1988, pp.13-20.

[33] M.V. Eyuboglu, S.U.H. Qureshi, "Reduced-State Sequence Estimation for Coded Modulation on Intersymbol Interference Channels."*IEEE Journ. on Select. Areas in Comm.*, vol.7, no.6, Aug. 1989, pp 989-995.

[34] J.B. Anderson, E. Offer, "Reduced-State Sequence Detection with Convolutional Codes," *Technical Report TR-92-5*, Rensselaer Polytechnic Institute, July, 1992.

[35] J.G. Proakis, Digital Communications, New York: McGraw-Hill, 1988.

[36] S.G. Wilson, Digital Modulation and Coding, to be published by Prentice-Hall.

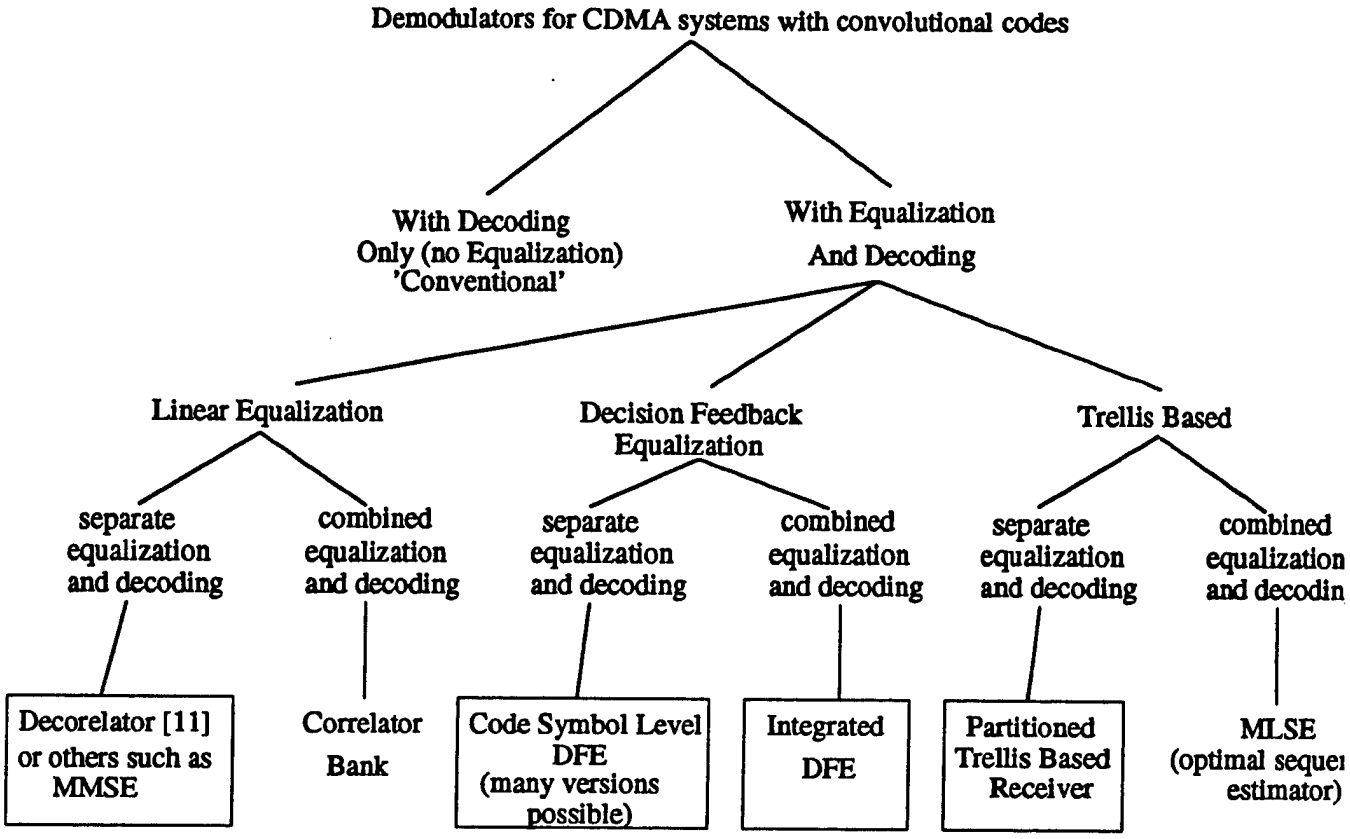

Figure 1: Tree diagram of the possible receiver structures for CDMA systems operating with convolutional codes
All of the partitioned approaches (separate equalization and decoding) can be implemented in a hard or soft decision form.
(The approaches in boxes will be discussed in this paper)

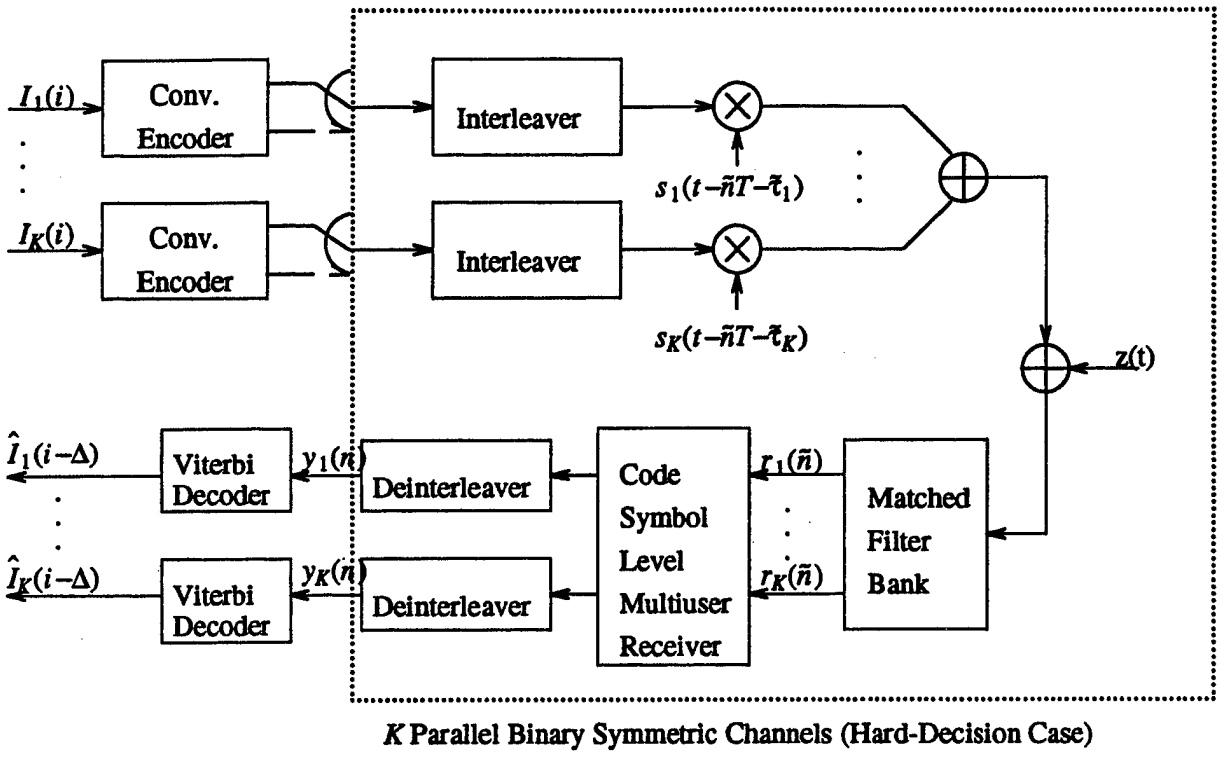

Figure 2 CDMA link with a partitioned receiver. If the interleaving can successfully break up the inner channel's memory, then the link within the dotted box may be accurately modeled as K parallel BSCs in the hard-decision multiuser receiver case.
($\tilde{n} = n$ if there is no interleaving on the link)

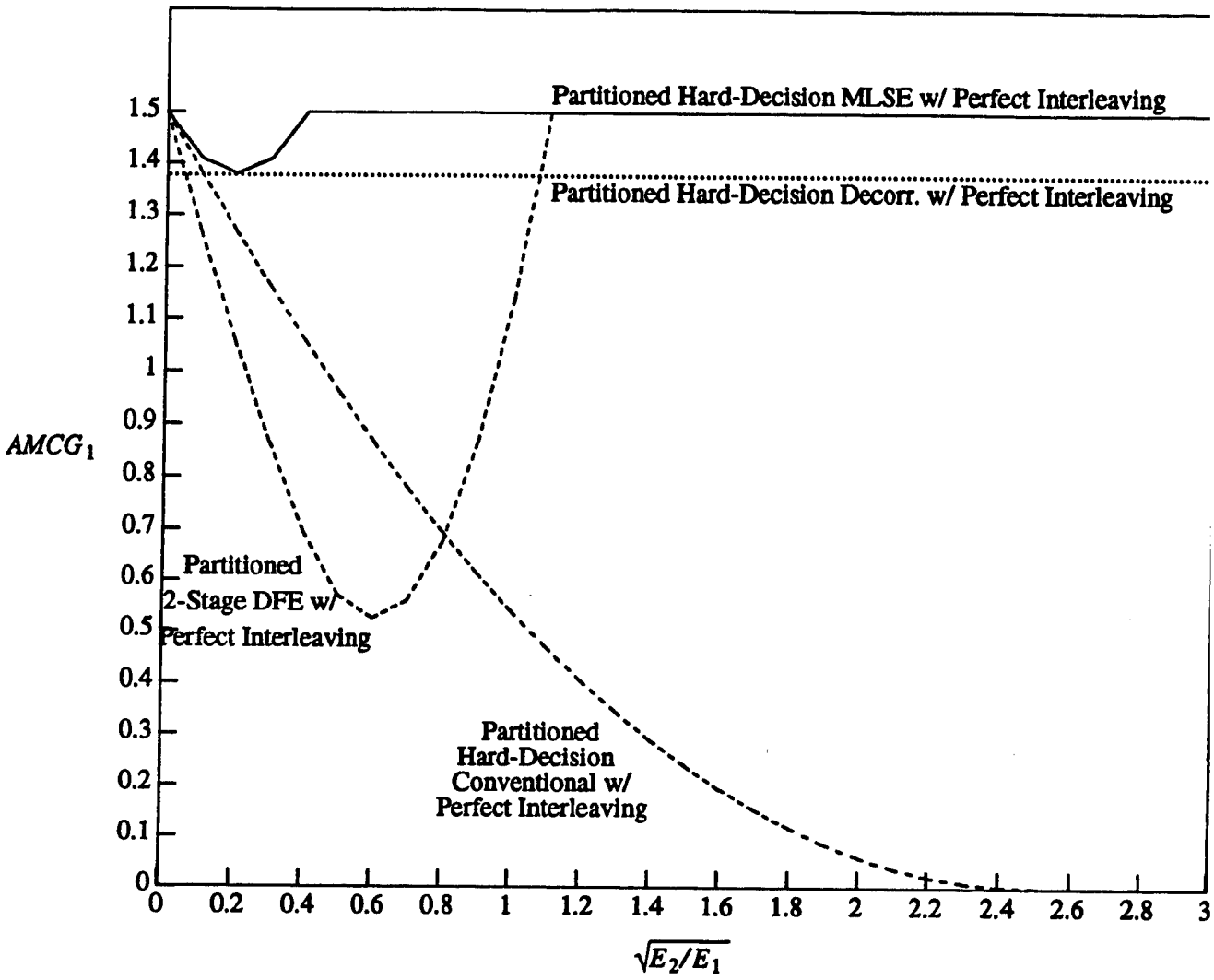

Figure 3: Plot of AMCG for the 2-user, $\rho_{21}(0) = \rho_{21}(1) = 0.2$ case where both users employ a rate 1/2 4-state code with $d_f = 5$. The ACG for a single-user system using this code is 10 log (1.5) dB for a hard-decision decoder.

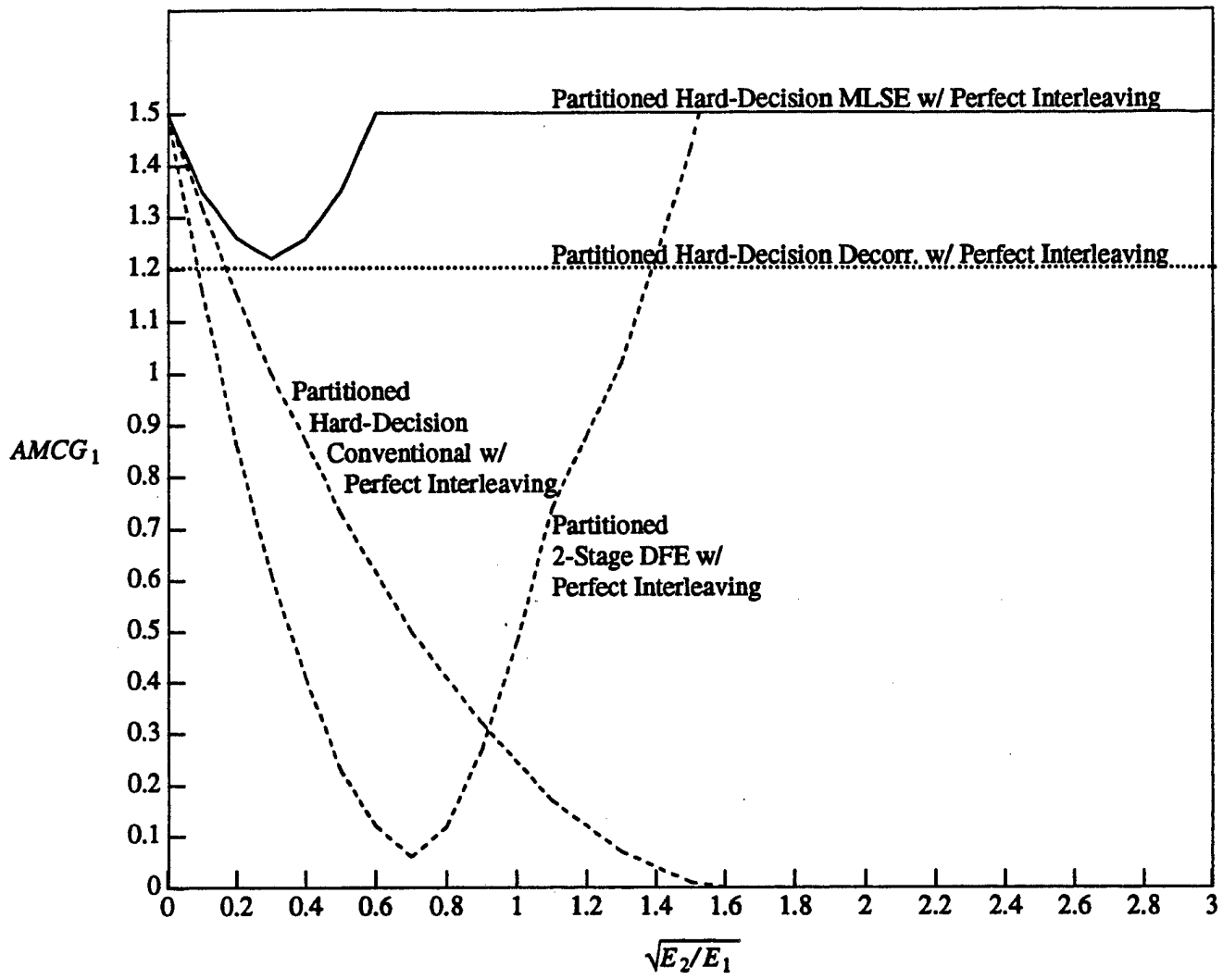

Figure 4: Plot of AMCG for the 2-user, $\rho_{21}(0) = \rho_{21}(1) = 0.3$ case where both users employ a rate 1/2 4-state code with $d_f = 5$. The ACG for a single-user system using this code is 10 log (1.5) dB for a hard-decision decoder.

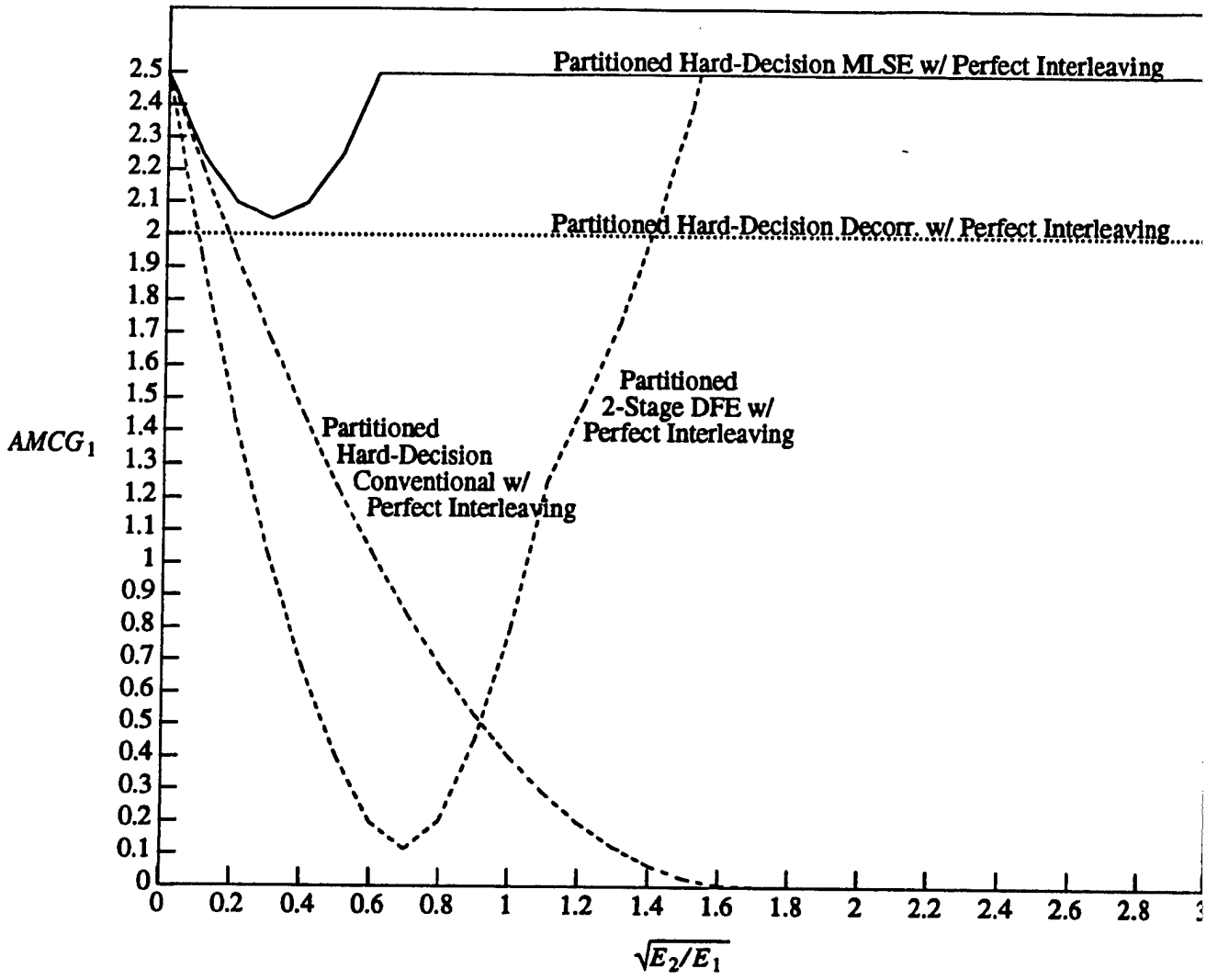

Figure 5: Plot of AMCG for the 2-user, $\rho_{21}(0) = \rho_{21}(1) = 0.3$ case where both users employ a rate 1/2 64-state code with $d_f = 10$. The ACG for a single-user system using this code is 10 log (2.5) dB for a hard-decision decoder.

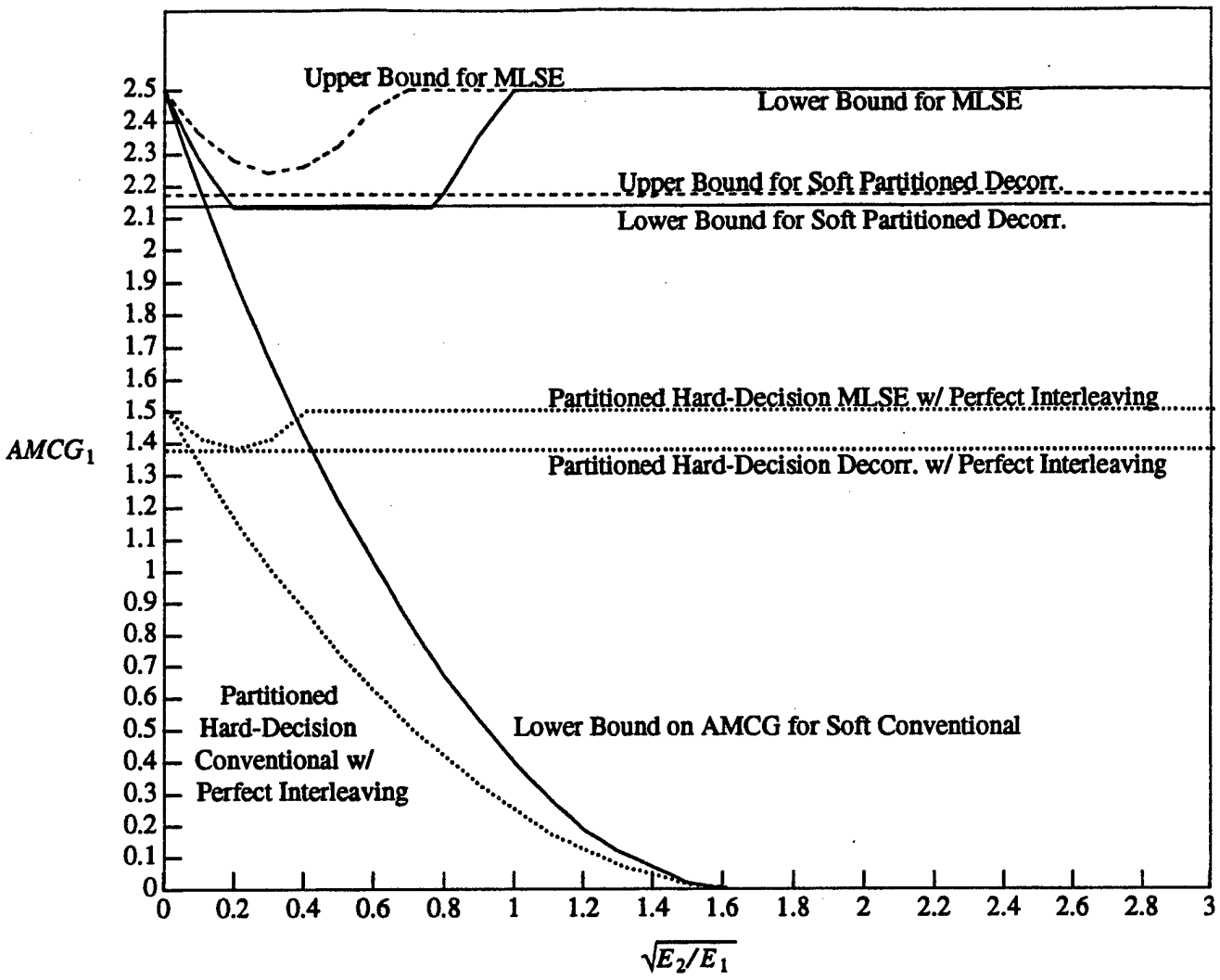

Figure 6: Plot of AMCG for the 2-user, $\rho_{21}(0) = \rho_{21}(1) = 0.2$ case where both users employ a rate 1/2 4-state code with $d_f = 5$. The ACG for a single-user system using this code is 10 log (1.5) dB for a hard-decision decoder and 10 log (2.5) dB for a soft-decision decoder. Lower bounds are shown as solid lines, upper bounds as dashed lines, and the partitioned hard-decision approaches are shown as dotted lines for comparison (from Figure 3).

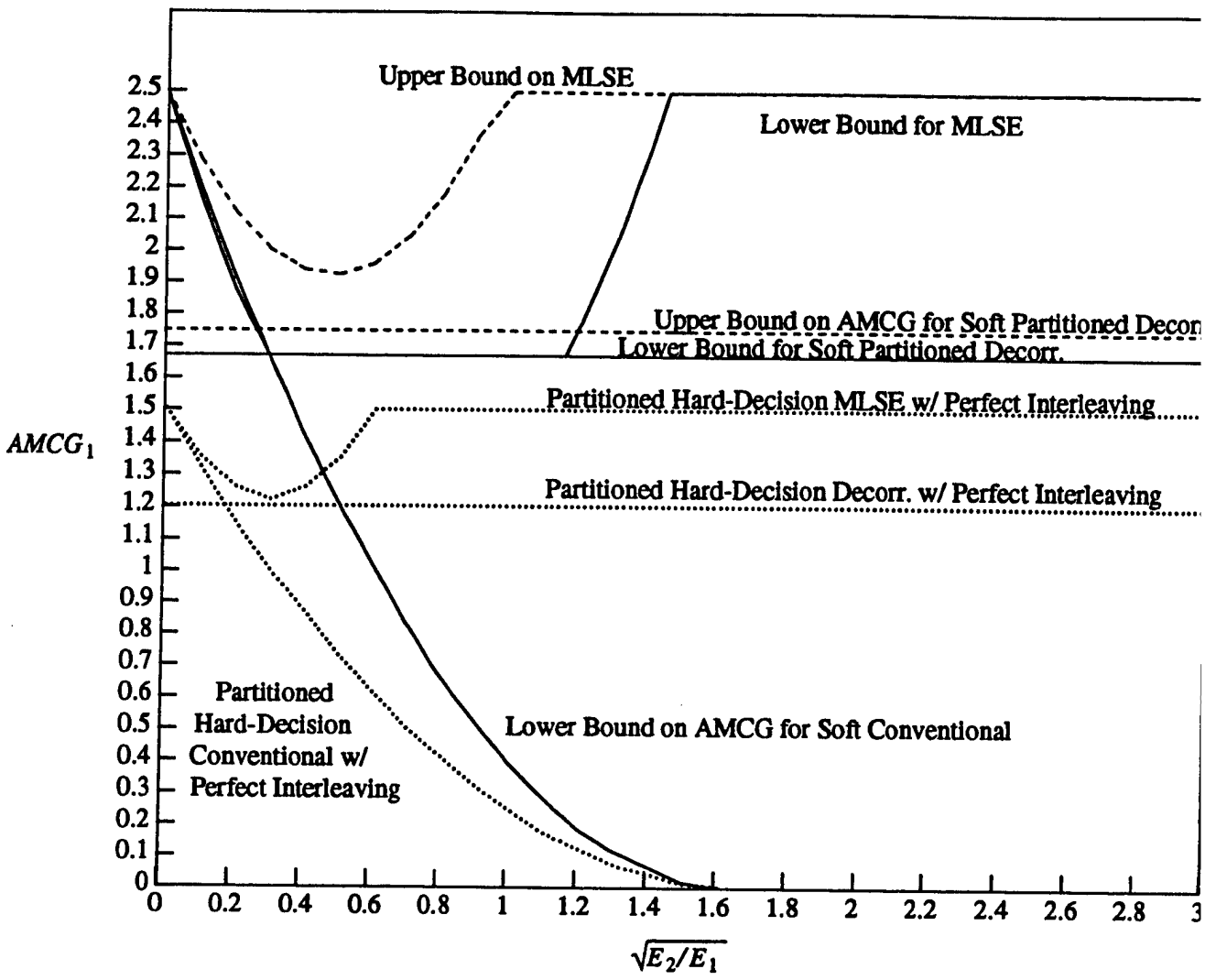

Figure 7: Plot of AMCG for the 2-user, $\rho_{21}(0) = \rho_{21}(1) = 0.3$ case where both users employ a rate 1/2 4-state code with $d_f = 5$. The ACG for a single-user system using this code is 10 log (1.5) dB for a hard-decision decoder and 10 log (2.5) dB for a soft-decision decoder. Lower bounds are shown as solid lines, upper bounds as dashed lines, and the partitioned hard-decision approaches are shown as dotted lines for comparison (from Figure 4).

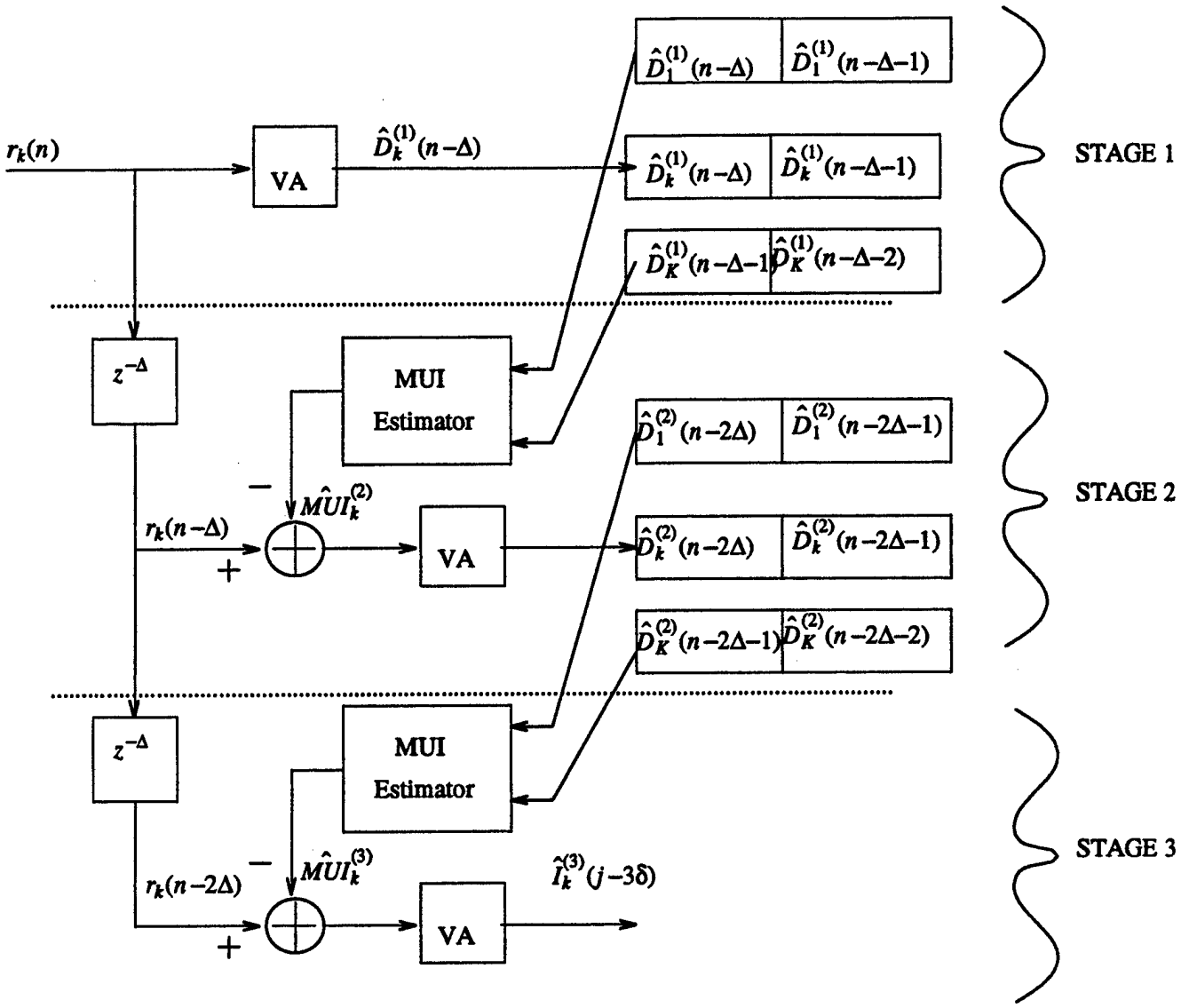

Figure 8: The structure of a 3-stage integrated DFE for the k^{th} user with Viterbi algorithms (denoted VA) at each stage. Δ is the maximum delay in code bit periods corresponding to δ information bit periods

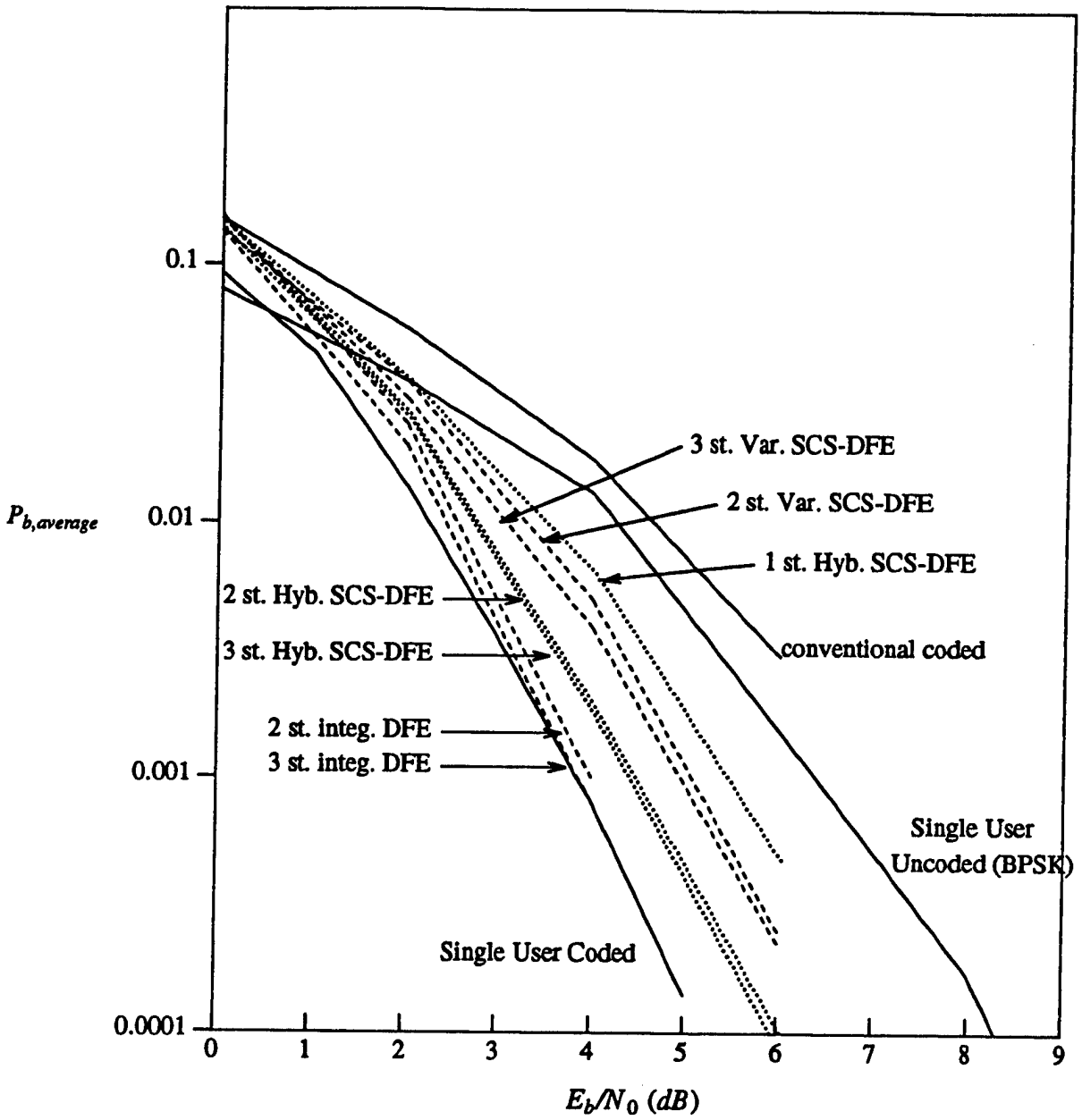

Figure 9: Performance curves of the various decision feedback receivers for a 4-user channel with $\rho_{jk}(l) = 0.2$ for all overlapping bits. The solid lines show a single user system (no MUI) with and without the rate-1/2 4-state convolutional code and a multiuser conventional receiver. Also shown are the one, two and three stage soft code symbol DFEs for both the Varanasi (dashed) and Hybrid (dotted) architectures, and a one, two and three stage integrated DFE (dashed lines). Note that the Varanasi style one-stage soft code symbol DFE and the one-stage integrated DFE are both equivalent to the conventional receiver.

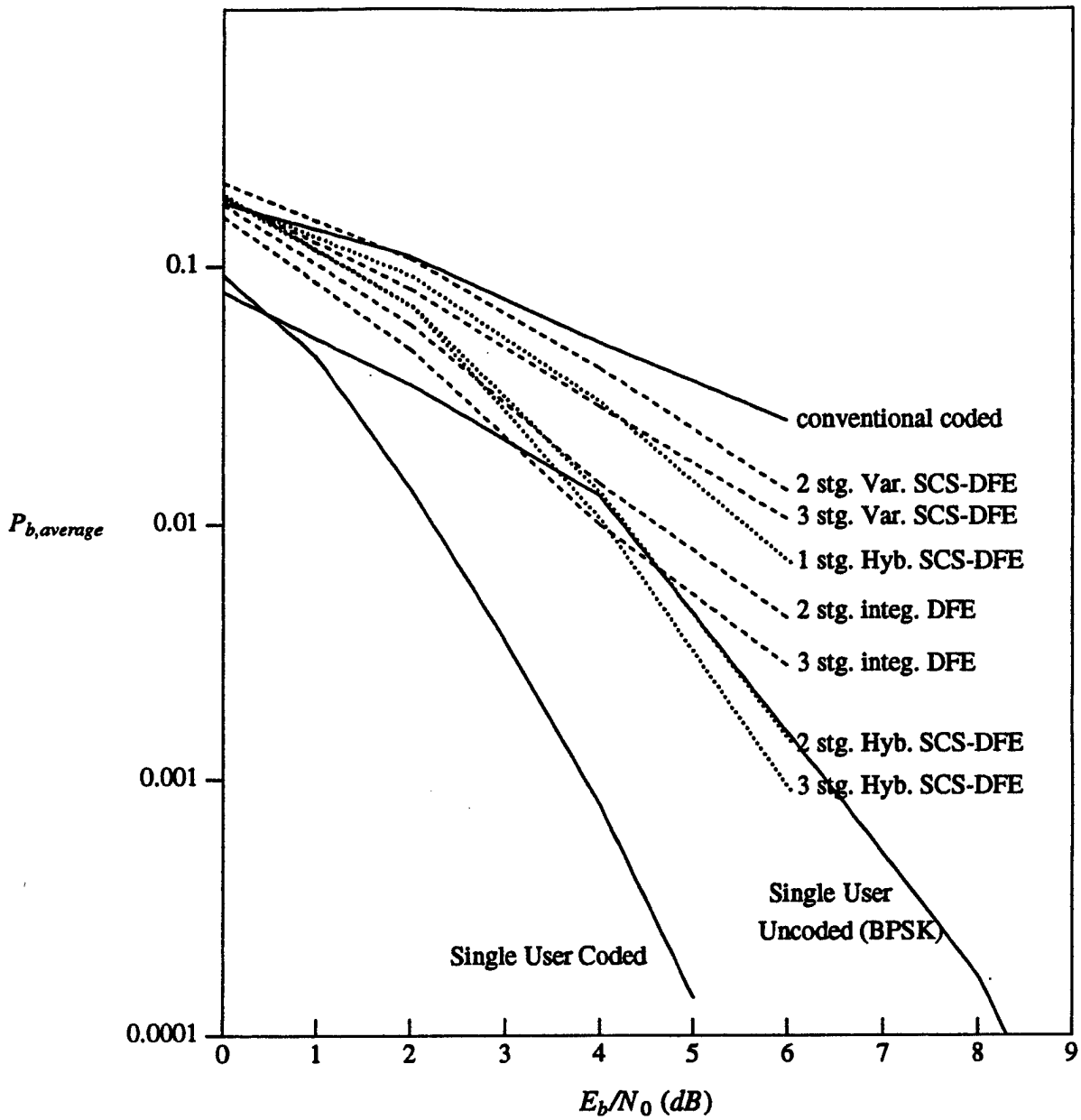

Figure 10: Performance curves of the various decision feedback receivers for a more severe 4-user channel. (See correlation matrices below) The solid lines show a single user system (no MUI) with and without the rate-1/2 4-state convolutional code and a multiuser conventional receiver. Also shown are the one, two and three stage soft code symbol DFEs of both the Varanasi (dashed) and Hybrid (dotted) architectures, and a one, two and three stage integrated DFE (dashed lines). Note that the Varanasi style one-stage soft code symbol DFE and the one-stage integrated DFE are both equivalent to the conventional receiver.

$$\bar{\rho}(0) = \begin{bmatrix} 1 & .25 & .25 & .25 \\ .25 & 1 & .25 & .5 \\ .25 & .25 & 1 & .25 \\ .25 & .5 & .25 & 1 \end{bmatrix}$$

$$\bar{\rho}(-1) = \begin{bmatrix} 0 & .25 & .25 & .25 \\ 0 & 0 & 0 & .25 \\ 0 & 0 & 0 & .25 \\ 0 & 0 & 0 & 0 \end{bmatrix}$$

The Multiuser ML Sequence Estimator for Convolutionally Coded Asynchronous CDMA Systems

T.R. Giallorenzi
Unisys Corporation
640 North 2200 West
Salt Lake City, Utah 84116-2988
(no work phone # or email assigned yet)
Home Phone: (801) 277-0959

and

S.G. Wilson
Department of Electrical Engineering
Thornton Hall
University of Virginia
(804) 924-6091
sgw@virginia.edu

Abstract

The optimal multiuser sequence estimator is formulated for an asynchronous direct-sequence CDMA system where each user employs convolutional coding to improve its performance on a non-dispersive AWGN channel. It is shown that the decoder may be implemented efficiently using a Viterbi algorithm which operates on a time-varying trellis with a number of states which is exponential in the product of the number of users in the system and the constraint length of the codes used (for the rate 1/2 code case). The asymptotic efficiency of this receiver relative to an uncoded coherent BPSK receiver (termed asymptotic multiuser coding gain, or AMCG) is then upper and lower bounded. The AMCG parameter unifies the asymptotic coding gain parameter and the asymptotic multiuser efficiency parameter which are traditional figure of merit parameters for single-user coded systems and multiuser uncoded systems respectively. Finally, some simulations are presented to illustrate the performance of the MLSE at moderate and low bit error rates.

1. Introduction

In code division multiple access (CDMA) systems, multiple users transmit, often asynchronously, over a common communication channel, typically using the direct sequence spread spectrum technique. The receiver operating in the AWGN environment receives a signal which is the sum of all of the transmitted signals in noise, and the receiver must synchronize to the desired signal and estimate the desired user's transmitted data. Often, in an attempt to improve performance, error control coding will be used on each of the links as well.

The traditional method of coherently demodulating direct sequence CDMA signals is to synchronize a local code generator and oscillator to the signal of interest and then to make decisions on the received signal as though the desired signal is the only one present. The traditional decoder's structure is that of a correlator or matched filter which is matched to the desired signal, followed by a decoder if coding is used on the link. The performance of the traditional decoder suffers for two major reasons. First, the signature sequences of the different users will not be orthogonal to each other, giving rise to multi-user interference, or MUI, and second, in the common situation where all of the signals arriving at the receiver are of different strengths the strong signals tend to overwhelm the weak signals, even with reasonably good signature sequences. This second problem is referred to as the *near–far* problem.

There has been a large amount of interest recently in the design of multiuser receivers for CDMA systems. These receivers jointly estimate the transmitted symbols of all of the users in the system, as opposed to estimating them independently. This approach is most appropriate for a base station in a multipoint-to-point network where the receiver must acquire and demodulate all of the signals in the network. Almost all of the multiuser detection work has centered on uncoded links, see for example [1] - [5]. Only recently has the problem of multiuser detection of coded links been considered, [6], [11] - [13] and [15].

In this paper, the multiuser maximum likelihood receiver will be formulated for convolutionally coded nondispersive AWGN links. We will see that this receiver performs both

the functions of equalization of the MUI and decoding of the code together. Section 2 of this paper will outline some of the notation that will be used, and will also define the problem in more precise terms. In section 3, we formulate the ML receiver using the rate 1/2 code case as an example, and then analyze its performance.

2. Notation

It will be assumed that the CDMA system has K users operating simultaneously on a common frequency in an asynchronous fashion. In general, it will be assumed that each user employs binary convolutional coding on its link. While it is quite conceivable that block codes could be used effectively on a CDMA link, convolutional codes have the advantage that they operate in a sequential fashion. Because the decoders that will be studied in this work are sequential in nature, the convolutional codes are a much better match to the decoders than block codes. One further assumption in this paper is that each user employs the same convolutional code, although it is not at all difficult to generalize this work to the case where each user employs a different code.

At each time interval of length T_s, the convolutional code is generated for user k by passing P binary information bits, $\bar{I}_k(n) = (I_k^{(1)}(n),..., I_k^{(P)}(n))$, through a shift register consisting of W stages with Q modulo-2 adders. The number of output bits for each P-bit input sequence is Q bits. The rate of the code is $R_c = P/Q$ and the constraint length of the code is W. The output sequence of binary code bits for the interval corresponding to input bits $\bar{I}_k(n)$ is $(D_k^{(1)}(n),...,D_k^{(Q)}(n))$. Note that for $W = 1$ and $P = Q = 1$, we have the *uncoded* case, so in that case $D_k(n) = I_k(n)$.

In the time interval $[nT_s+(q-1)T+\tilde{\tau}_k, nT_s+qT+\tilde{\tau}_k)$, user k transmits data bit $D_k^{(q)}(n)$, where $\tilde{\tau}_k$ represents the time shift of the k^{th} user relative to some reference time, thus accounting for the asynchronism of the users relative to each other. T represents the code bit period and $T_b = T/R_c$ is the information bit duration, thus $T_s = QT = PT_b$. Let $\tilde{\tau}_k = m_k T+\tau_k$, $\tau_k \in [0,T)$, and $m_k \in \{0,...,Q-1\}$. Thus $m_k T$ is a coarse time shift and τ_k is a fine time shift for user k.

Each user in the system is assigned a particular signature sequence, and it will be assumed that this signature sequence has a duration equal to the code bit interval, although

this assumption can be relaxed with a change of the notation. We will combine the carrier and signature sequence into a single signal, thus the k^{th} carrier multiplied by the binary (± 1) signature sequence, $PN_k(t)$, will be denoted by

$$s_k(t) = \begin{cases} \sqrt{2/T}\, PN_k(t)\cos(\omega_c t) & 0 \le t \le T \\ 0 & otherwise \end{cases} \tag{1}$$

The energy of the k^{th} user's code bit measured at the receiver will be denoted by E_k. It will be assumed that all K users transmit their signals through a common additive white Gaussian noise channel with two-sided noise spectral density $N_0/2$ W/Hz, and so the received signal will have the following form

$$r(t) = \sum_{n=-\infty}^{\infty} \sum_{k=1}^{K} \sum_{q=1}^{Q} D_k^{(q)}(n)\sqrt{E_k}\, s_k(t - nT_s - (q-1)T - \tilde{\tau}_k) + z(t) \tag{2}$$

where $z(t)$ denotes the noise.

Next we define the partial cross-correlation of the known signature sequences j and k to be:

$$\rho_{jk}(l) = \int_{-\infty}^{\infty} s_j(t-\tau_j)\, s_k(t - lT - \tau_k)\, dt \ . \tag{3}$$

It is worth noting that $\rho_{jj}(0) = 1$ and $\rho_{jk}(l) = \rho_{kj}(-l)$.

The base station that will be referred to as the *conventional* base station on this coded link attempts to estimate the k^{th} user's data using only the matched filter outputs for the k^{th} user. It will be assumed that the Viterbi algorithm operating on each user's observed code symbols is a soft-Viterbi algorithm having a decoding delay of δ information symbols, where generally δ will be several times the constraint length, W, of the code. The time complexity per decoded bit for this receiver may be estimated by considering the number of metric computations per information bit decided. If we define the binary memory order of the encoder to be $\kappa = \log_2 S$ where S is the number of states of each user's encoder, then there are $2^{\kappa+P}$ metrics computed for every P bits decided, so $TCB = O(2^{\kappa+P}/P)$.

As in the uncoded case, there are a number of ways that a multiuser receiver can operate to improve upon the performance of the conventional basestation. In the next section, the optimum maximum likelihood sequence estimator will be derived for this problem

and analyzed. Because this receiver has a very high complexity, in [11] and [13], a partitioned trellis-based approach is be introduced, along with a number of multistage decision feedback approaches which all have a lower complexity than the optimal sequence estimator.

3 Optimum Sequence Estimator For Rate-1/2 Convolutional Codes

The optimal MLSE will now be derived for the special case in which each user in the network is employing a rate-1/2 convolutional code with a constraint length of W, so $T_s = T_b = 2T$. Our limitation to this special case will facilitate considerably the derivation of the decoder, and it will then be outlined how the optimal decoder can be derived in a similar way for a general rate-P/Q convolutional code case.

To begin, it is important to note that the optimal sequence estimator or equalizer for multiple-user uncoded signals operates in a "round-robin" fashion among all K users in the system, [1]. This Viterbi algorithm traverses one trellis stage per channel bit observed. The optimal sequence estimator for decoding the rate-1/2 code for one of the users in a single user environment, however, is a Viterbi algorithm which requires two channel observations from the user of interest to move ahead one stage in the trellis, [14]. The rate-1/2 convolutional code can, however, be viewed not as a code which produces two binary bits per information bit period, T_b, but as an equivalent trellis code which produces one 4-ary coded waveform every T_b seconds. By formulating the equalization problem at the receiver with respect to this super-code-symbol view of the received signal, we can accomplish both the tasks of equalization and decoding in the same Viterbi algorithm. Because there is only one 4-ary super-symbol received for each information bit that must be decided, the decoder can be formulated in basically the same fashion as was used in [1] for the MUI problem or [7] for the ISI problem.

We begin by defining the following notation.

$$g_1(t) = \begin{cases} 1 & t \in [0,T) \\ 0 & otherwise \end{cases} \tag{4}$$

$$g_2(t) = \begin{cases} 1 & t \in [T,2T) \\ 0 & otherwise \end{cases} \tag{5}$$

Next, define a concatenation of coded signals as

$$\tilde{D}_k(t-nT_b-\tilde{\tau}_k) = D_k^{(1)}(n)\, g_1(t-nT_b-\tilde{\tau}_k) + D_k^{(2)}(n)\, g_2(t-nT_b-\tilde{\tau}_k)\ . \tag{6}$$

Two of the signature-carrier waveforms can likewise be concatenated to form a super-signature waveform.

$$\tilde{s}_k(t-nT_b-\tilde{\tau}_k) = s_k(t-nT_b-\tilde{\tau}_k) + s_k(t-(i+\tfrac{1}{2})T_b-\tilde{\tau}_k) \tag{7}$$

This presumes that the signature sequence repeats every code symbol period. The received waveform may now be written in terms of these waveforms of duration T_b:

$$r(t) = \sum_{i=-\infty}^{\infty} \sum_{k=1}^{K} \tilde{D}_k(t-nT_b-\tilde{\tau}_k)\, \tilde{s}_k(t-nT_b-\tilde{\tau}_k)\sqrt{E_k} + z(t) \tag{8}$$

This signal may be viewed as a four-valued super-code symbol, $\{D_k^{(1)}(n), D_k^{(2)}(n)\}$, modulating a pair of orthonormal basis functions through the procedure defined above. The basis functions in this new view of the waveform are

$$\phi_{1k}(t) = g_1(t)\, \tilde{s}_k(t) \tag{9}$$

and

$$\phi_{2k}(t) = g_2(t)\, \tilde{s}_k(t) \tag{10}$$

appropriately synchronized with the information bit periods. Thus, this equivalent view of the coding process suggests that the information bits are mapped by the encoder onto waveforms in a space defined by $\phi_{1k}(t)$ and $\phi_{2k}(t)$. Note that although the bases defined in (9) and (10) are orthonormal, they are not, in general, orthogonal to $\phi_{1j}(t)$ and $\phi_{2j}(t)$ which are the basis set for another user in the system, user j, since $s_k(t)$ and $s_j(t)$ are not orthogonal in general. The result when the received signal is a sum of K component signals is MUI. We now define four parameters which are a measure of the degree of correlation between the basis functions of the different users.

$$\tilde{U}_{jk}(l) = \int_{-\infty}^{\infty} \phi_{1j}(t-\tilde{\tau}_j)\, \phi_{1k}(t-lT_b-\tilde{\tau}_k)dt \tag{11}$$

$$\tilde{V}_{jk}(l) = \int_{-\infty}^{\infty} \phi_{2j}(t-\tilde{\tau}_j)\, \phi_{2k}(t-lT_b-\tilde{\tau}_k)dt \tag{12}$$

$$\tilde{W}_{jk}(l) = \int_{-\infty}^{\infty} \phi_{1j}(t-\tilde{\tau}_j)\, \phi_{2k}(t-lT_b-\tilde{\tau}_k)dt \tag{13}$$

$$\tilde{X}_{jk}(l) = \int_{-\infty}^{\infty} \phi_{2j}(t-\tilde{\tau}_j)\, \phi_{1k}(t-lT_b-\tilde{\tau}_k)dt \tag{14}$$

These parameters play the same role in the super-symbol view of the coded signal that $\rho_{jk}(l)$ plays for the standard view of the signal. In fact, $\tilde{U}$, $\tilde{V}$, $\tilde{W}$ and $\tilde{X}$ can be related to ρ directly by substituting (9) and (10) into (11) through (14).

$$\tilde{U}_{jk}(l) = \rho_{jk}(2l+m_k-m_j) \tag{15a}$$

$$\tilde{V}_{jk}(l) = \rho_{jk}(2l+m_k-m_j) \tag{15b}$$

$$\tilde{W}_{jk}(l) = \rho_{jk}(2l+1+m_k-m_j) \tag{15c}$$

$$\tilde{X}_{jk}(l) = \rho_{jk}(2l-1+m_k-m_j) \tag{15d}$$

Note that $\tilde{U}_{jk}(l) = \tilde{V}_{jk}(l) = \tilde{W}_{jk}(l) = \tilde{X}_{jk}(l) = 0$ for $|l|>1$; this fact will play an important role in determining the proper state description of the system for the optimal sequence estimator. Some other useful properties of the correlation parameters are $\tilde{U}_{jk}(l) = \tilde{U}_{kj}(-l)$, $\tilde{V}_{jk}(l) = \tilde{V}_{kj}(-l)$ and $\tilde{X}_{jk}(l) = \tilde{W}_{kj}(-l)$.

Beginning with equation (8), note that by performing a modulo-K decomposition of the index i, namely $i = \alpha(i)K+\beta(i)-1$, and by assuming that the K users transmit $(2M+1)/K$ information bits each in the time interval of interest and that the signal is zero outside of this interval, we can write

$$r(t) = \sum_{i=-M}^{M} \tilde{D}_{\beta(i)}(t-\alpha(i)T_b-\tilde{\tau}_{\beta(i)})\,\tilde{s}_{\beta(i)}(t-\alpha(i)T_b-\tilde{\tau}_{\beta(i)})\sqrt{E_{\beta(i)}} + z(t) \tag{16}$$

We now further simplify the notation by defining the following terms,

$$E^{(i)} = E_{\beta(i)} \tag{17}$$

$$D_i^{(q)} = D_{\beta(i)}^{(q)}(\alpha(i)) \tag{18}$$

$$\tilde{U}_{im} = \tilde{U}_{\beta(i)\beta(m)}(\alpha(m)-\alpha(i)) \tag{19}$$

$$\tilde{V}_{im} = \tilde{V}_{\beta(i)\beta(m)}(\alpha(m)-\alpha(i)) \tag{20}$$

$$\tilde{W}_{im} = \tilde{W}_{\beta(i)\beta(m)}(\alpha(m)-\alpha(i)) \tag{21}$$

$$\tilde{X}_{im} = \tilde{X}_{\beta(i)\beta(m)}(\alpha(m)-\alpha(i)) \tag{22}$$

We have now laid the foundation for the derivation of the MLSE. This development will closely follow the derivation of the optimal MLSE in [7] and [8] for the uncoded ISI channel.

By expanding (16) with a Karhunen-Loeve expansion and letting the dimensionality of the expansion grow, we obtain the following waveform metric:

$$\Lambda(\bar{D}_M) = -\int_{-\infty}^{\infty} \Big(r(t) - \sum_{i=-M}^{M} D_i^{(1)} \phi_{1\beta(i)}(t-\alpha(i)T_b-\tilde{\tau}_{\beta(i)})\sqrt{E^{(i)}} + D_i^{(2)} \phi_{2\beta(i)}(t-\alpha(i)T_b-\tilde{\tau}_{\beta(i)})\sqrt{E^{(i)}} \Big)^2 dt \quad (23)$$

We next define:

$$r_i^{(1)} = r_{\beta(i)}^{(1)}(\alpha(i)) = \int_{-\infty}^{\infty} r(t)\phi_{1\beta(i)}(t-\alpha(i)T_b-\tilde{\tau}_{\beta(i)})dt \quad (24)$$

and

$$r_i^{(2)} = r_{\beta(i)}^{(2)}(\alpha(i)) = \int_{-\infty}^{\infty} r(t)\phi_{2\beta(i)}(t-\alpha(i)T_b-\tilde{\tau}_{\beta(i)})dt \quad (25)$$

which represent the outputs of a pair of matched filters or correlators for the basis functions for user $\beta(i)$ at time $t = (\alpha(i)+1)T_b + \tilde{\tau}_{\beta(i)}$. By expanding (23), and then collecting the appropriate terms we get the following metric:

$$\Lambda(\bar{D}_i) = \Lambda(\bar{D}_{i-1}) + 2\Big[D_i^{(1)}\sqrt{E^{(i)}} \Big(r_i^{(1)} - \sum_{l=1}^{L} \{ D_{i-l}^{(1)} \tilde{U}_{i\,i-l} + D_{i-l}^{(2)} \tilde{W}_{i\,i-l} \} \sqrt{E^{(i-l)}} \Big)$$

$$+ D_i^{(2)}\sqrt{E^{(i)}} \Big(r_i^{(2)} - \sum_{l=1}^{L} \{ D_{i-l}^{(1)} \tilde{X}_{i\,i-l} + D_{i-l}^{(2)} \tilde{V}_{i\,i-l} \} \sqrt{E^{(i-l)}} \Big) \Big] \quad (26)$$

where $\bar{D}_i$ represents the multiuser code-symbol sequence up to time interval i, and L is the smallest integer such that for every $L' > L$ we have $\tilde{U}_{jk}(\alpha(L')) = \tilde{V}_{jk}(\alpha(L')) = \tilde{W}_{jk}(\alpha(L')) = \tilde{X}_{jk}(\alpha(L')) = 0$. We have already seen that the correlation parameters are zero when $|\alpha(L')| > 1$, so $L = K-1$.

There are a number of important observations that can be made from the path metric given in equation (26). First of all, the i^{th} stage metric depends only on the code symbols in the set

$$\Xi = \{ D_i^{(1)}, D_i^{(2)}, D_{i-1}^{(1)}, D_{i-1}^{(2)}, \ldots, D_{i-K+1}^{(1)}, D_{i-K+1}^{(2)} \}, \quad (27)$$

along with the matched filter outputs, $r_i^{(1)}$ and $r_i^{(2)}$, as well as the signal energies and correlations. It is possible to estimate the crosscorrelations using the local oscillators and code generators which are assumed to be synchronized to the K components of the incoming signal. We can also estimate the energies, $\{E^{(i)}\}$ by averaging the outputs of the matched filters for

a number of bits. (The number over which they would be averaged would depend on the rate at which the relative strengths of the users is varying.)

For any user, k, the convolutional encoder defines a mapping rule from the input information symbol and present state of the encoder to the code bits, $D_k^{(1)}(n)$ and $D_k^{(2)}(n)$. If we define $h(\cdot)$ as the mapping rule from the input information symbol and state to the 4-ary super-code symbol, $\{D_k^{(1)}(n), D_k^{(2)}(n)\}$ then by substituting the information symbols that define the state of the encoder in for the state, the following expression may be written:

$$\{D_k^{(1)}(n), D_k^{(2)}(n)\} = h[I_k(n), I_k(n-1), \ldots, I_k(n-W+1)] \tag{28}$$

Thus, in this form, it is clear that the 4-ary super-code symbol depends on only W information symbols. Using this information, it is easy to redefine the set Ξ which was defined in equation (27) in terms of the information symbols which affect the i^{th} stage metric.

$$\tilde{\Xi} = \{I_i, \sigma_i\} \tag{29}$$

$$\sigma_i = \{I_{i-1}, I_{i-2}, \ldots, I_{i-WK+1}\} \tag{30}$$

where $I_i = I_{\beta(i)}(\alpha(i))$. Thus it is now apparent that the system may be described in terms of 2^{WK-1} states, since the information symbols are binary. Furthermore, the maximum likelihood sequence estimator can be implemented with a Viterbi algorithm operating on a trellis with 2^{WK-1} states and two branches per state. This trellis will be cyclically time-varying as in the uncoded case, [1]. Furthermore, it is clear that this trellis reduces to the trellis derived in [1] when the constraint length of the code is one (uncoded transmission for each user). Obviously, the number of states in the MLSE grows very quickly with both the number of users in the system and the constraint length of the codes being used. In fact, for a simple 4-user case where each user uses a $W = 3$, or 4-state code, the MLSE requires a Viterbi algorithm operating on a trellis with 2048 states!

The time complexity per bit decoded for the multiuser MLSE is $TCB = O(2^{WK})$ since there are $2 \cdot 2^{WK-1}$ metrics which must be computed at each stage of the trellis and one information bit is decided at each stage. Note that for the case of $W = 1$, the TCB calculated in [1] is again obtained.

Now that the MLSE has been derived for the rate-1/2 case, it is straightforward to generalize to the case of rate-P/Q convolutional codes. The function $\tilde{D}_k(t)$ will again have to be

constructed from a set of orthogonal basis functions. One reasonable choice would be a set of Q non-overlapping pulses, each of duration T. Again, the function $\tilde{s}_k(t)$ would be constructed from concatenations of Q versions of $s_k(t)$. The metric derivation could then proceed in the same fashion as in the rate-1/2 case. There are 2^P input hypotheses to test in each T_s for each user, so the overall trellis will have 2^P branches per state. Furthermore, the state of the system will be specified by $(\kappa+P)(K-1)+\kappa$ information bits, so it will have $2^{\kappa K+PK-P}$ states, where $\kappa = \log_2 S$ and S is the number of states in the single user's encoder. This will result in a $TCB = O(2^{\kappa K+PK}/P)$.

Clearly the exponential dependence of the TCB on the number of users, the number of states in each of the user's codes and P makes the use of the optimal decoder prohibitive for a realistic system. It is, however, an important receiver because it represents the best that can be achieved in terms of sequence error probability, and it will provide a good baseline by which to judge the quality of suboptimal schemes. This receiver also raises the possibility of using a variety of sparse searching algorithms like a sequential decoder as was used in [5] for the uncoded case, or reduced state sequence estimation techniques like the one proposed in [4] for the uncoded MUI equalization problem or [9] for the combined equalization and decoding problem for single-user links suffering from ISI.

3.1 Performance of the Optimal Sequence Estimator

To illustrate the derivation of some performance bounds for the MLSE, we will again use the rate 1/2 code example. In this analysis we will fairly closely follow the analysis which appeared in [1] and [7]. In keeping with [1], we consider the decoding window to range from the index $-M$ to the index M. The goal of this section is to estimate the performance of the optimal sequence estimator by bounding the finite and infinite horizon error probabilities for the k^{th} user in the system, denoted $P_k^M(n)$ and $P_k = \lim_{M\to\infty} P_k^M(n)$.

Consider the transmission of the sequence of super-code symbols, $\bar{D} = \{D_i^{(1)}, D_i^{(2)}\}_{i=-M}^{M}$, and a competing sequence in the trellis $\bar{D}+2\bar{e}$ corresponding to the sequence $\{D_i^{(1)}+2e_i^{(1)}, D_i^{(2)}+2e_i^{(2)}\}_{i=-M}^{M}$ where $\bar{e} = \{e_i^{(1)}, e_i^{(2)}\}_{i=-M}^{M}$ is a sequence of code error symbols. Each $e_i^{(q)}$ can take on values in the set $G = \{0, \pm 1\}$. Next, define the following sets:

$$B = \{\, \bar{e}: e_k^{(q)}(n) \in G,\ n = \alpha(-M), \ldots, \alpha(M),$$

$$k = 1, \ldots, K,\ q = 1,2,\ e_k^{(q)}(n) \neq 0 \text{ for } \textit{some } n,k,q \,\} \tag{31}$$

$$A(\bar{D}) = \{\, \bar{e}: \bar{e} \in B,\ \bar{D} + 2\bar{e} \in C \,\} \tag{32}$$

$$C = \{\, \bar{D}: \bar{D} \in h(\{\, \bar{I} \,\})\} \tag{33}$$

where $h(\cdot)$ is the mapping rule defined by the code from an information sequence, $\bar{I}$, to a sequence of super-code symbols, $\bar{D}$, as in (28). Since this mapping rule is a one-to-one function, it has an inverse. If we define the information error sequence

$$\bar{\psi} = h^{-1}(\bar{D} + 2\bar{e}) - \bar{I} \tag{34}$$

which is the information bit error sequence corresponding to $\bar{D} + 2\bar{e}$ such that if $\bar{D} = h(\bar{I})$, then $\bar{D} + 2\bar{e} = h(\bar{I} + \bar{\psi})$. This allows us to define

$$A_k^M(\bar{D}, n) = \{\bar{e}: \bar{e} \in A(\bar{D}),\ \psi_k(n) \neq 0\} \tag{35}$$

so $A_k^M(\bar{D}, n)$ is the set of admissible error sequences which affect the n^{th} information bit of the k^{th} user. From these definitions, it follows that the probability of error for the n^{th} bit of the k^{th} user is given by

$$P_k^M(n) = \sum_{\bar{D} \in C} P\left[\bigcup_{\bar{e} \in A_k^M(\bar{D}, n)} \{\Lambda(\bar{D} + 2\bar{e}) > \Lambda(\bar{D}) \mid \bar{D} \textit{ sent} \} \right] \cdot P^M(\bar{D} \textit{ sent}) \tag{36}$$

As is the usual approach, we choose to bound (36) with a union bound.

$$P_k^M(n) \leq \sum_{\bar{D} \in C} \sum_{\bar{e} \in A_k^M(\bar{D}, n)} P(\Lambda(\bar{D} + 2\bar{e}) > \Lambda(\bar{D}) \mid \bar{D} \textit{ sent}) \cdot P^M(\bar{D} \textit{ sent}) \tag{37}$$

The event $\Lambda(\bar{D} + 2\bar{e}) > \Lambda(\bar{D})$ may now be written by expanding equation (23) and substituting

$$r_i^{(1)} = r_{\beta(i)}^{(1)}(\alpha(i)) = \sum_{j=i-K+1}^{i+K-1} (D_j^{(1)} \sqrt{E^{(j)}}\, \tilde{U}_{ij} + D_j^{(2)} \sqrt{E^{(j)}}\, \tilde{W}_{ij}) + z_i^{(1)} \tag{38}$$

and

$$r_i^{(2)} = r_{\beta(i)}^{(2)}(\alpha(i)) = \sum_{j=i-K+1}^{i+K-1} (D_j^{(1)} \sqrt{E^{(j)}}\, \tilde{X}_{ij} + D_j^{(2)} \sqrt{E^{(j)}}\, \tilde{V}_{ij}) + z_i^{(2)} \tag{39}$$

for $r_i^{(1)}$ and $r_i^{(2)}$ respectively, where $z_i^{(1)}$ and $z_i^{(2)}$ are the noise variates at the output of the matched filters for the basis functions $\phi_{1\beta(i)}$ and $\phi_{2\beta(i)}$ respectively for the interval $\alpha(i)$. After

some algebra, the following expression for the event $\Lambda(\bar{D}+2\bar{e}) > \Lambda(\bar{D})$ is obtained.

$$\sum_{i=-M}^{M}\sum_{m=-M}^{M}(e_i^{(1)}e_m^{(1)}\tilde{U}_{im}+e_i^{(2)}e_m^{(2)}\tilde{V}_{im}+e_i^{(1)}e_m^{(2)}\tilde{W}_{im}+e_i^{(2)}e_m^{(1)}\tilde{X}_{im})\sqrt{E^{(i)}E^{(m)}}$$

$$< \sum_{i=-M}^{M}\sqrt{E^{(i)}}(e_i^{(1)}z_i^{(1)}+e_i^{(2)}z_i^{(2)}) \tag{40}$$

Let $\Delta^2(\bar{e})$ represent the left side of equation (40). The right side of equation (40) is a linear combination of Gaussian random variables, $z_i^{(1)}$ and $z_i^{(2)}$. It is not difficult to show that $E[z_i^{(1)}] = E[z_i^{(2)}] = 0$ and also that

$$E\left[\begin{bmatrix}z_i^{(1)}\\ z_i^{(2)}\end{bmatrix}(z_m^{(1)}\ z_m^{(2)})\right] = \frac{N_0}{2}\cdot\begin{bmatrix}\tilde{U}_{im} & \tilde{W}_{im}\\ \tilde{X}_{im} & \tilde{V}_{im}\end{bmatrix} \tag{41}$$

As a result, if we define γ to be the right side of equation (40), then it is not difficult to show that $E[\gamma]=0$ and $Var[\gamma]=\Delta^2(\bar{e})\cdot N_0/2$.

Next, the two-sequence error probability, or the probability of the event given in equation (40), becomes the probability that the Gaussian random variable, γ, is larger than the threshold, $\Delta^2(\bar{e})$. We next define the following efficiency parameter for the pair of sequences separated by the code symbol error sequence, $\bar{e}$, as

$$\eta_k^M(\bar{e}) = \frac{\Delta^2(\bar{e})}{2E_k} = \frac{\Delta^2(\bar{e})}{E_{bk}}. \tag{42}$$

where $E_{bk} = 2E_k$ is the energy per information bit for user k. This allows us to write

$$P(\Lambda(\bar{D}+2\bar{e}) > \Lambda(\bar{D}) \mid \bar{D}\ sent) = Q\left[\sqrt{\frac{2E_{bk}}{N_0}\eta_k^M(\bar{e})}\right] \tag{43}$$

so $\eta_k^M(\bar{e})$ is the asymptotic efficiency relative to uncoded BPSK transmission for the k^{th} user for the pair of sequences $\bar{D}$ and $\bar{D}+2\bar{e}$. This can be shown to reduce to the form of the distance measure in [1] for the uncoded system, because as in [1], $\Delta^2(\bar{e})$ may also be expressed as the L_2 norm of the signal generated by modulating the error sequence.

In order to construct a lower bound on the probability of error for user k, we define the following minimum efficiency as

$$\eta_{k,min}^M(n) = \inf_{\bar{D}\in C}\ \inf_{\bar{e}\in A_k^M(\bar{D},n)}\ \eta_k^M(\bar{e}) \tag{44}$$

so that

$$P_k^M(n) \geq P\left[\eta_k^M(\bar{e}) = \eta_{k,min}^M(n)\right] \cdot Q\left[\sqrt{\frac{2E_{bk}}{N_0}\eta_{k,min}^M(n)}\right] \tag{45}$$

Thus we now have a lower bound expression for $P_k^M(n)$ given in (45), and when (43) is substituted into equation (37) we have an upper bound on $P_k^M(n)$.

To obtain bounds for the infinite horizon error probabilities we may conclude exactly as in [1] that the infinite horizon efficiencies $\eta_k(\bar{e})$ and $\eta_{k,min}$ are achieved by finite length error sequences. As a result, the infinite horizon error probability for the k^{th} user may be lower bounded by

$$P_k \geq P\left[\eta_k(\bar{e}) = \eta_{k,min}\right] \cdot Q\left[\sqrt{\frac{2E_{bk}}{N_0}\eta_{k,min}}\right] \tag{46}$$

Similarly, by passing (37) to the limit as M approaches infinity

$$P_k \leq \sum_{\bar{D} \in C} \sum_{\bar{e} \in A_k(\bar{D},n)} P(\bar{D}\ sent) \cdot Q\left[\sqrt{\frac{2E_{bk}}{N_0}\eta_k(\bar{e})}\right], \tag{47}$$

where $A_k(\bar{D},n) = \lim_{M \to \infty} A_k^M(\bar{D},n)$. We should note that (47) may not converge for all noise levels. In [1], the convergence region was increased by limiting the inner sum to the set of indecomposable sequences. This solution perhaps would be of use here as well to obtain a tighter upper bound, however, we will not focus on this issue here because the convergence of (47) will not affect the rest of our analysis.

In the high signal-to-noise ratio regime, the terms in (47) with the minimum efficiency will dominate the asymptotic behavior of the receiver. As a result, we will refer to the minimum efficiency, $\eta_{k,min}$ as the *asymptotic multiuser coding gain* for user k (*AMCG*). The *AMCG* is an efficiency parameter which is a measure of the energy gain or loss of the receiver relative to an uncoded BPSK system operating in isolation with an energy per information bit of E_{bk}.

In the limiting cases where there is only $K = 1$ user in the system, or when there are K users in the system with perfectly orthogonal super-signature sequences, then $\eta_{k,min}$ is the asymptotic coding gain (*ACG*) of a single-user system operating with the same code. In the

limiting case where the users do not employ coding, $\eta_{k,min}$ is equivalent to the asymptotic multiuser efficiency (*AME*) obtained in [1] for the optimal multiuser receiver for the uncoded system. Thus the asymptotic multiuser coding gain unifies the asymptotic coding gain and the asymptotic multiuser efficiency parameters.

The equation for $\eta_k(\bar{e})$ may be rewritten in the form of a quadratic form,

$$\eta_k(\bar{e}) = \frac{1}{2E_k} \bar{e}_\Gamma^T \bar{E}_\Gamma^T \bar{H}_\Gamma \bar{E}_\Gamma \bar{e}_\Gamma. \tag{48}$$

To do this, we define the vector $\bar{e}_\Gamma$ to be the subvector of the infinite length error sequence $\bar{e}$ which consists of all of the nonzero components of $\bar{e}$ and all zero components of $\bar{e}$ which are surrounded by nonzero components. If we assume that the dimension of the vector $\bar{e}_\Gamma$ is $2\Gamma x\, 1$, and

$$\bar{e}_\Gamma = (e_{i_0}^{(1)}, e_{i_0}^{(2)}, e_{i_0+1}^{(1)}, e_{i_0+1}^{(2)}, \ldots, e_{i_0+\Gamma-1}^{(1)}, e_{i_0+\Gamma-1}^{(2)})^T \tag{49}$$

then the matrix $\bar{H}_\Gamma$ is defined as $\bar{H}_\Gamma = [\bar{H}_{jk}]_{j,k=i_0}^{i_0+\Gamma-1}$ where the sub matrices are given by

$$\bar{H}_{jk} = \begin{bmatrix} \tilde{U}_{jk} & \tilde{W}_{jk} \\ \tilde{X}_{jk} & \tilde{V}_{jk} \end{bmatrix}. \tag{50}$$

Thus, $\bar{H}_\Gamma$ has dimensions $2\Gamma x\, 2\Gamma$. Also, $\bar{E}_\Gamma$ is a diagonal energy matrix with diagonal elements $E_{jj} = (E_{\beta(j)})^{1/2}$.

As an example, consider the 2-user case where each user employs a rate 1/2, 4-state convolutional code, as is shown in Figure 2. If user 1 sends an all zeros sequence, and user 2 sends all zeros except for stage i_0, where a 1 is sent, then a valid error sequence is

$$\bar{e}_6 = (-1\ -1\ 1\ 1\ 0\ -1\ 0\ 1\ -1\ -1\ 1\ 1)^T. \tag{51}$$

For this case, assuming that $m_1 = m_2 = 0$ so that $\tilde{\tau}_1 = \tau_1$ and $\tilde{\tau}_2 = \tau_2$, the $\bar{H}_6$ matrix takes the form

$$\bar{H}_6 = \begin{bmatrix}
1 & 0 & \rho_{21}(0) & 0 & 0 & 0 & 0 & 0 & 0 & 0 & 0 & 0 \\
0 & 1 & \rho_{21}(1) & \rho_{21}(0) & 0 & 0 & 0 & 0 & 0 & 0 & 0 & 0 \\
\rho_{21}(0) & \rho_{21}(1) & 1 & 0 & 0 & 0 & 0 & 0 & 0 & 0 & 0 & 0 \\
0 & \rho_{21}(0) & 0 & 1 & \rho_{21}(1) & 0 & 0 & 0 & 0 & 0 & 0 & 0 \\
0 & 0 & 0 & \rho_{21}(1) & 1 & 0 & \rho_{21}(0) & 0 & 0 & 0 & 0 & 0 \\
0 & 0 & 0 & 0 & 0 & 1 & \rho_{21}(1) & \rho_{21}(0) & 0 & 0 & 0 & 0 \\
0 & 0 & 0 & 0 & \rho_{21}(0) & \rho_{21}(1) & 1 & 0 & 0 & 0 & 0 & 0 \\
0 & 0 & 0 & 0 & 0 & \rho_{21}(0) & 0 & 1 & \rho_{21}(1) & 0 & 0 & 0 \\
0 & 0 & 0 & 0 & 0 & 0 & 0 & \rho_{21}(1) & 1 & 0 & \rho_{21}(0) & 0 \\
0 & 0 & 0 & 0 & 0 & 0 & 0 & 0 & 0 & 1 & \rho_{21}(1) & \rho_{21}(0) \\
0 & 0 & 0 & 0 & 0 & 0 & 0 & 0 & \rho_{21}(0) & \rho_{21}(1) & 1 & 0 \\
0 & 0 & 0 & 0 & 0 & 0 & 0 & 0 & 0 & \rho_{21}(0) & 0 & 1
\end{bmatrix}$$

and if the users have equal energy, then the effective efficiency for this error sequence is

$$\eta_1(\bar{e}) = \tfrac{1}{2}\,\bar{e}_6^T\,\bar{H}_6\,\bar{e}_6 = 5 - 5\rho_{21}(0) - 3\rho_{21}(1) \tag{53}$$

This implies that for this particular case, a necessary condition for the MLSE to have an **asymptotic loss** relative to a single-user system is

$$\eta_1(\bar{e}) = 5 - 5\rho_{21}(0) - 3\rho_{21}(1) < d_f/2 \tag{54}$$

implying that because the free distance of the code in use is $d_f = 5$, if

$$\rho_{21}(0) + \frac{3}{5}\rho_{21}(1) > \frac{1}{2} \tag{55}$$

then the MLSE **will not** achieve a single-user performance level as $N_0/2 \to 0$.

In the same case, if the user's energies are not equal,

$$\eta_1(\bar{e}_6) = \frac{5}{2} + \frac{5E_2}{2E_1} - \left[\frac{E_2}{E_1}\right]^{1/2}\left[\frac{10}{2}\rho_{21}(0) + \frac{6}{2}\rho_{21}(1)\right]. \tag{56}$$

This may be considered to be an upper bound on $\eta_{1,min}$ since the minimum over all valid error sequences is no larger than the $\eta_k(\bar{e})$ for a particular valid error sequence.

In general an interesting result is obtained when we examine $\eta_k(\bar{e})$ for $\bar{e}$ sequences involving only *single-user* errors. Note that for every $\bar{e} \in A_k(\bar{D},n)$ such that every nonzero element of $\bar{e}$ corresponds to user k, (in other words, only user k is involved in the error event)

$$\eta_k(\bar{e}) = \frac{1}{2E_k}\bar{e}_\Gamma^T\bar{E}_\Gamma^T\bar{H}_\Gamma\bar{E}_\Gamma\bar{e}_\Gamma = \frac{1}{2E_k}\cdot E_k \cdot wt[\bar{e}] = \frac{wt_k[\bar{e}]}{2} \tag{57}$$

where $wt[\bar{e}]$ is the weight or number of nonzero elements of $\bar{e}$ (or equivalently $\bar{e}_\Gamma$), and $wt_k[\bar{e}]$ is the weight of user k's subsequence of $\bar{e}$. (User k's subsequence is the set of all $\{e_i^{(1)}, e_i^{(2)}\}$ in $\bar{e}$ such that $\beta(i) = k$.) Because

$$\min_{\substack{\bar{e}\in A_k(\bar{D},n)\\ \bar{D}\in C}} \frac{wt_k[\bar{e}]}{2} = \frac{d_f}{2} \tag{58}$$

we have the result that $\eta_k(\bar{e}) \geq d_f/2$ for every $\bar{e} \in A_k(\bar{D},n)$ such that every nonzero element of $\bar{e}$ is contained in user k's subsequence.

This result is important because it implies that single-user error events are not responsible if the AMCG is less than the ACG of a single-user system. We thus must examine

multiple-user error events to find $\eta_k(\bar{e}) < d_f/2$, which is the ACG for a rate 1/2 convolutional code.

In general, the computation of $\eta_{k,min}$ involves a search over all $\bar{e} \in A_k(\bar{D},n)$ for each $\bar{D} \in C$ reference sequence. Rather than attacking this problem directly, in this paper we will lower bound the worst-case efficiency for the 2-user situation, and will then illustrate some nice properties of the MLSE using this bound.

By studying the $\bar{H}_\Gamma$ matrix for this 2-user case, we can obtain a lower bound on the result of equation (48) in the following way. Every nonzero element of $\bar{e}_\Gamma$ will multiply its corresponding element of $\bar{e}_\Gamma^T$, the corresponding diagonal element of $\bar{H}_\Gamma$ and be weighted by the energy for that element. We thus have, as a part of the result of (48), the weight of user 1's error subsequence multiplied by E_1 plus the weight of user 2's error subsequence multiplied by E_2. The remaining terms in the result of (48) are due to the product of elements of $\bar{e}_\Gamma$ with other elements of $\bar{e}_\Gamma^T$, weighted by the off-diagonal elements of $\bar{H}_\Gamma$ and $(E_1E_2)^{1/2}$. If we lower bound the sum of these off diagonal terms by a number that is smaller than is achievable by the actual off-diagonal terms, then we have a lower bound on equation (48). One possible lower bound on the off diagonal terms leads to the following expression which is only a function of the weight of the error sequences. It turns out that this expression is, in most situations, a somewhat loose lower bound on $\eta_k(\bar{e})$. We will focus on the performance of user 1 without any loss in generality.

$$\eta_1(\bar{e}) \geq \min\{\, f\left[(E_2/E_1)^{1/2}, wt_1[\bar{e}], wt_2[\bar{e}], \zeta\right],\ d_f/2 \,\} \tag{59}$$

where

$$f\left[(E_2/E_1)^{1/2}, wt_1[\bar{e}], wt_2[\bar{e}], \zeta\right] = \tfrac{1}{2}\Big(wt_1[\bar{e}] + \frac{E_2}{E_1} wt_2[\bar{e}] - (E_2/E_1)^{1/2}(2\min\{wt_1[\bar{e}], wt_2[\bar{e}]\}+2)\zeta\Big) \tag{60}$$

and where $\zeta = |\rho_{21}(0)| + |\rho_{21}(1)|$. The function $f(\cdot)$ is a lower bound on $\eta_1(\bar{e})$ as long as $\bar{e}$ has $wt_1[\bar{e}] > 0$ and $wt_2[\bar{e}] > 0$. We have already seen from (57) and (58) that $d_f/2$ is a lower bound on $\eta_1(\bar{e})$ when $wt_2[\bar{e}] = 0$, so the smaller of these two expressions is less than $\eta_1(\bar{e})$ for all $\bar{e} \in A_k(\bar{D},n)$.

For a fixed set of crosscorrelations and signal energies, thus a constant ζ and constant $\sqrt{E_2/E_1}$, the function $f(\sqrt{E_2/E_1}, wt_1[\bar{e}], wt_2[\bar{e}], \zeta)$ describes a family of parabolas, one for each value of $wt_1[\bar{e}]$ and $wt_2[\bar{e}]$. It is easy to show that

$$\min_{\substack{wt_1(\bar{e})\in\{d_f,d_f+1,\ldots\} \\ wt_2(\bar{e})\in\{d_f,d_f+1,\ldots\}}} f\left\{(E_2/E_1)^{1/2}, wt_1[\bar{e}], wt_2[\bar{e}], \zeta\right\} = f\left\{(E_2/E_1)^{1/2}, d_f, d_f, \zeta\right\} \tag{61}$$

This result implies that

$$\eta_{1,min} \geq F\left[\sqrt{\frac{E_2}{E_1}}, \zeta, d_f\right] = \min\{f\left[\sqrt{\frac{E_2}{E_1}}, d_f, d_f, \zeta\right], d_f/2\} \tag{62}$$

which means that we have lower bounded the AMCG by a function which depends only on the **user's energies, crosscorrelations** and the **free distance of the code.** This bound on $\eta_{1,min}$ is valid only for the 2-user, rate 1/2 code case, but it will illustrate some very important features of the performance of the MLSE which should remain true for the general K-user, rate P/Q code cases as well. This bound will illustrate these performance features without requiring a solution to the NP-hard problem of searching for the actual error sequence, $\bar{e}$, and corresponding reference sequence, $\bar{D}$, which achieve the actual $\eta_{1,min}$.

The first feature of the bound in (62) may be noted by examining the plot of $F(\cdot)$ as a function $\sqrt{E_2/E_1}$ shown in Figure 3 for $\zeta = 0.6$ and $d_f = 5$. As the interfering signal strength, E_2 becomes small relative to E_1, $F(\cdot)$ approaches the ACG of the single user system. Also, as E_2 becomes large relative to E_1, $F(\cdot)$ again reaches the ACG of a single user. In fact, for

$$(E_2/E_1)^{1/2} > 2\zeta \cdot \frac{d_f+1}{d_f} \tag{63}$$

the MLSE necessarily will have the same asymptotic performance as that of a single-user system. In fact, because $F(\cdot)$ is only a lower bound on the AMCG of the receiver, the actual energy ratio above which single-user performance is achieved may be significantly lower than the threshold given in (63). This point may be illustrated by the dotted line in Figure 3 which is the actual plot of $\eta_1(\bar{e})$ for the $\bar{e}$ given in equation (56). Without performing the search for $\eta_{1,min}$, we do not know whether the $\eta_1(\bar{e})$ shown for that particular $\bar{e}$ is the minimum, but if it is, then the actual threshold for $\sqrt{E_2/E_1}$ above which single-user

asymptotic performance is achieved would be 0.96.

Another interesting feature of the bound in equation (62) is that it provides a lower bound on the near-far resistance of the MLSE, which is defined as the infimum of $\eta_{k,min}$ over the energies of the interfering users. [3] This infimum for the function $F(\cdot)$ is

$$\inf_{(E_2/E_1)^{1/2} \in [0,\infty)} \eta_{k,min} \geq \inf_{(E_2/E_1)^{1/2} \in [0,\infty)} F\left[(E_2/E_1)^{1/2}, \zeta, d_f\right] = \frac{d_f}{2} - \frac{\zeta^2}{2d_f}(d_f+1)^2 \qquad (64)$$

which is positive for

$$\zeta = |\rho_{21}(0)| + |\rho_{21}(1)| < \frac{d_f}{d_f+1} \qquad (65)$$

A strictly positive near-far resistance implies that the receiver will have an error rate that goes to zero at the same exponential rate as a single-user system operating with an energy penalty of $\eta_{1,min}$.

It is also interesting to note that as the code which is employed becomes more powerful, or as d_f increases, the conditions on the crosscorrelations of the users becomes progressively less restrictive to achieve near-far resistance. In other words, a stronger code allows the MLSE to remain near-far resistant on a channel with more severe MUI than would be possible with a weaker code. Again, however, because $F(\cdot)$ is simply a lower bound on $\eta_{k,min}$, the actual AMCG may be positive when the minimum of $F(\cdot)$ is not. Nonetheless, the fact that (65) implies a positive lower bound is an interesting feature of the bound in (62).

3.2 Simulation Results

To provide some direct comparisons between the performance of the MLSE and the conventional receiver in terms of bit error rate at a moderate to low E_b/N_0, we will use a computer simulation for some two-user cases. Figure 4 shows the results of a simulation of a two-user system where each user employs a 4-state rate 1/2 convolutional code. The resulting super-trellis used by the MLSE has 32 states. Figure 4 illustrates a severe MUI environment where $\rho_{12}(0) = 0.3$ and $\rho_{12}(-1) = 0.3$. In this case, the MLSE is able to recoup almost all of the loss that the conventional decoder suffers when compared with the performance in the single-user environment. In Figure 5, the same 0.3 channel is simulated for a varying near-far energy ratio. This figure shows that the MLSE approach achieves a single-user

performance level for sufficiently strong or sufficiently weak interference. This result is supported by the asymptotic performance suggested by the bound in Figure 3. In addition, equation (64) suggests that the MLSE is near-far resistant for this case, since $\zeta = 0.6$ and $d_f = 5$. Also, the upper bound on the AMCG in Figure 3 suggests that there is not necessarily an asymptotic loss for the MLSE relative to the single-user performance level in the equal-energy case since the AMCG is upper bounded by 2.5 at an energy ratio of one. This is supported by the simulation in Figure 4.

It is worth noting that all of the performance analysis in this paper has been based upon the metric for the case where each user in the system employs rate-1/2 convolutional codes. The expression for the distance and asymptotic multiuser coding gain will be more complicated in the general rate-P/Q code case, but the derivation procedure will be the same. Thus the work in this paper is meant to illustrate the general procedure for the error analysis of the more complex general code rate case.

4. Conclusions

In this paper, the maximum likelihood sequence estimator was formulated for CDMA systems where each user employs a convolutional code to improve its performance. It was shown that the complexity of the MLSE depends exponentially on the number of users in the system, the number of states in each user's encoder and the number of input information bits, P. This high complexity points to the use of suboptimal approaches to attempt to attain high performance levels with a more reasonable complexity, such as reduced state sequence estimation approaches [15], sequential decoding approaches (currently under investigation by the authors of [16]), linear approaches, [6] and [13], or multistage decision feedback approaches, [11] and [13].

5. References

[1] S. Verdu, "Minimum Probability of Error for Asynchronous Gaussian Multiple Access Channels," *IEEE Trans. Inform. Theory*, vol. IT-32, Jan. 1986, pp. 85-96.

[2] S. Verdu, "Optimum Multiuser Asymptotic Efficiency," *IEEE Trans. on Comm.*, vol.34, no.9, May 1991, pp. 890-897.

[3] R. Lupas and S. Verdu, "Near-Far Resistance of Multiuser Detectors in Asynchronous Channels," *IEEE Trans. on Comm.*, vol.38, no.4, April 1990, pp 496-508.

[4] M.K. Varanasi, "Reduced State Sequence Detection for Asynchronous Gaussian Multiple-Access Channels", *Proceedings of ISIT*, San Antonio, Texas, January, 1993, pp. 42.

[5] Z. Xie, C.K. Rushforth, R.T. Short, "Multiuser Signal Detection Using Sequential Decoding," *IEEE Trans. on Comm.*, vol. 38, no. 5, May 1990, pp. 578-583.

[6] S.S.H. Wijayasuriya, G.H. Norton, J.P. McGeehan, "A Sliding Window Decorrelating Algorithm for DS-CDMA Receivers," *Electronics Letters*, vol. 28, no. 17, August, 1992, pp.1596-1598.

[7] G. Ungerboeck, "Adaptive Maximum-Likelihood Receiver for Carrier-Modulated Data-Transmission Systems," *IEEE Trans. on Comm.*, vol. 22, no. 5, May 1974, pp. 624-636.

[8] J.G. Proakis, *Digital Communications*, New York: McGraw-Hill, 1989.

[9] P.R. Chevillat, E. Eleftheriou, "Decoding of Trellis-Encoded Signals in the Presence of Intersymbol Interference and Noise," *IEEE Trans. on Comm.*, vol. 37, no. 7, July 1989, pp. 669-676.

[11] T.R. Giallorenzi, S.G. Wilson, "Multistage Decision Feedback and Trellis-Based Multiuser Receivers for Convolutionally Coded CDMA Systems," *Technical Report UVA/538341/EE93/102*, University of Virginia, May 1993.

[12] T.R. Giallorenzi, S.G. Wilson, "Trellis-Based Multiuser Receivers for Convolutionally Coded CDMA Systems," *Proceedings of the* 31st *Annual Allerton Conference on Communications Controls* and *Computing.*

[13] T.R. Giallorenzi, S.G. Wilson, "Suboptimum Multiuser Receivers for Convolutionally Coded Asynchronous CDMA Systems," submitted to *IEEE Trans. on Comm.* in February 1994.

[14] G.D. Forney, "The Viterbi Algorithm," *Proceedings of the IEEE*, vol. 61, no. 3, March 1973, pp. 268-278.

[15] P. Hoeher, "On Channel Coding and Multiuser Detection for DS-CDMA," *Proc. IEEE ICUPC '93*, Ottowa, Canada, October, 1993, pp.641-646.

[16] C.K. Rushforth, M. Nasiri-Kinari, A. Abbaszadeh, "A Reduced-Complexity Sequence Detector With Soft Outputs for Partial-Response Channels," *Proc. of GLOBECOM'93*, Houston, TX, December, 1993.

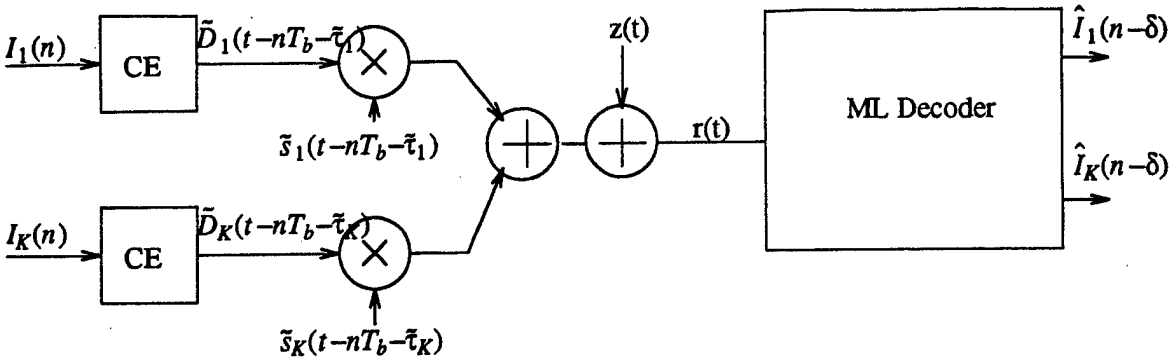

Figure 1 Maximum Likelihood Sequence Estimator for a convolutionally encoded CDMA system.

(CE: convolutional encoder)

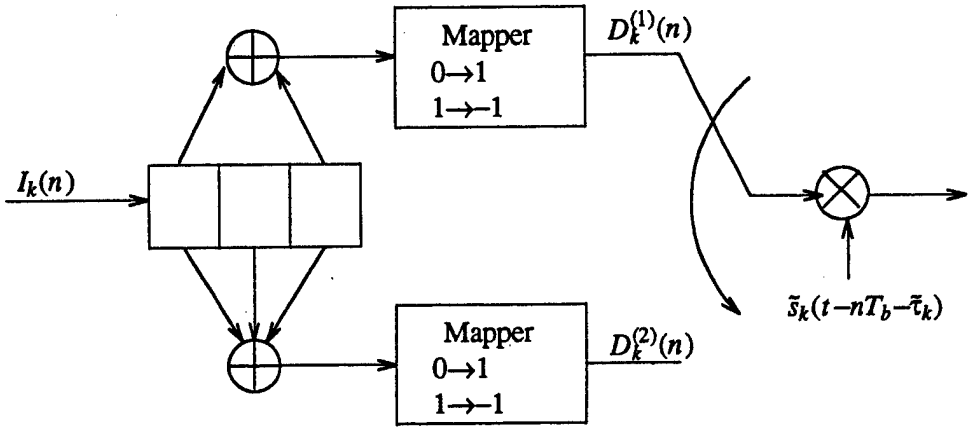

Figure 2 Rate 1/2, 4-state convolutional code.

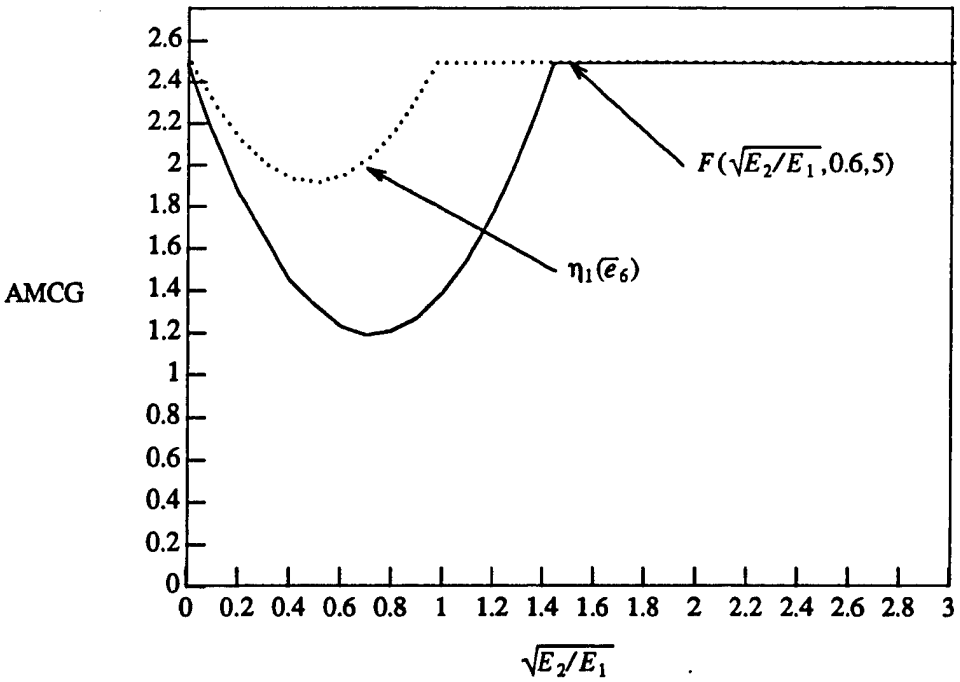

Figure 3 Plot of lower bound on $\eta_{1,min}$ for the 2-user, $\rho_{21}(0) = \rho_{21}(1) = 0.3$ case with each user employing the code shown in Figure 2. Also shown is the actual $\eta_1(\bar{e})$ for the specific error event given in equation (51).

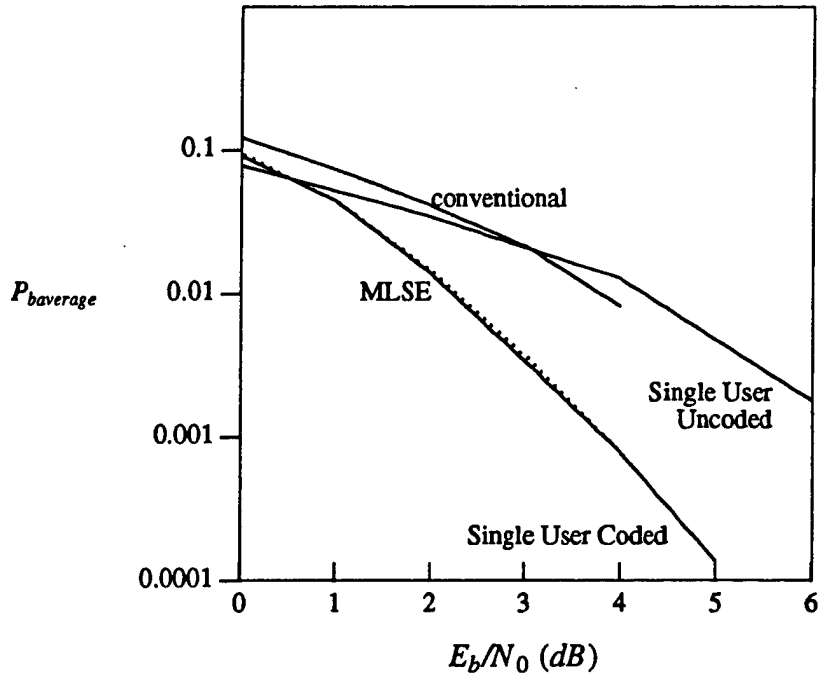

Figure 4 Performance curves of the MLSE (dotted line) for a 2-user channel with $\rho_{12}(0) = 0.3$ and $\rho_{12}(-1) = 0.3$ and equal energies. The solid lines show a single user system (no MUI) with and without the rate-1/2 4-state convolutional code.

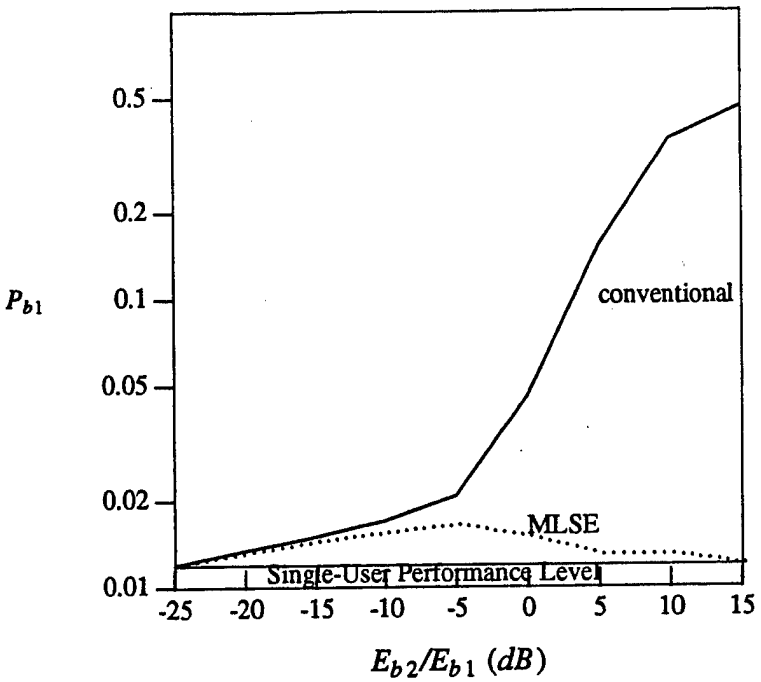

Figure 5 Near-far ratio performance curves of the MLSE on a 2-user channel with $\rho_{12}(0) = 0.3$ and $\rho_{12}(-1) = 0.3$ at $E_{b1}/N_0 = 2\,dB$. The single-user system performance level (no MUI) with the rate-1/2 4-state convolutional code is shown as a solid line and the MLSE performance is shown as a dotted line.

DISTRIBUTION LIST

1 - 3	Warren D. Peele, Program Director Southeastern Center for Electrical Engineering Education Management Office, Central Florida Facility 11th & Massachusetts Avenue St. Cloud, FL 34769
*	SEAS Postaward Administration
4 - 5	S. G. Wilson
6 - 7	F. O'Bryant
8	SEAS Preaward Administration Files

*Cover letter

JO#5640:ph